

**EGE UNIVERSITY GRADUATE SCHOOL OF NATURAL AND
APPLIED SCIENCES**

(DOCTORATE THESIS)

**TREATMENT OF INDUSTRIAL WASTEWATERS BY
UTILIZING IN ENERGY (CH₄/H₂) PRODUCTION VIA
HYDROTHERMAL GASIFICATION**

Nihal CENGİZ

Supervisor: Prof. Dr. Levent BALLICE

Co-Supervisor: Prof. Dr. Mehmet SAĞLAM

Department of Chemical Engineering

Presentation Date: 15.12.2017

Bornova-İZMİR

2017

Nihal CENGİZ tarafından doktora tezi olarak sunulan “Endüstriyel Atıksuların Hidrotermal Gazlaştırma İle Enerji (CH₄/H₂) Üretiminde Değerlendirilerek Arıtılması” başlıklı bu çalışma EÜ Lisansüstü Eğitim ve Öğretim Yönetmeliği ile EÜ Fen Bilimleri Enstitüsü Eğitim ve Öğretim Yönergesi'nin ilgili hükümleri uyarınca tarafımızdan değerlendirilerek savunmaya değer bulunmuş ve 15.12.2017 tarihinde yapılan tez savunma sınavında aday oybirliği/oyçokluğu ile başarılı bulunmuştur.

Jüri Üyeleri:

Jüri Başkanı : Prof. Dr. Levent BALLICE

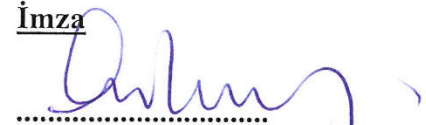




Raportör Üye : Prof. Dr. Nalan KABAY

Üye : Prof. Dr. Kadir YURDAKOÇ

Üye : Prof. Dr. Müşerref ARDA

Üye : Prof. Dr. Erol ŞEKER

İmza


.....

.....

.....

.....

.....

EGE ÜNİVERSİTESİ FEN BİLİMLERİ ENSTİTÜSÜ

ETİK KURALLARA UYGUNLUK BEYANI

EÜ Lisansüstü Eğitim ve Öğretim Yönetmeliğinin ilgili hükümleri uyarınca Yüksek Lisans Tezi / Doktora Tezi olarak sunduğum “Endüstriyel Atıksuların Hidrotermal Gazlaştırma İle Enerji (CH₄/H₂) Üretiminde Değerlendirilerek Arıtılması” başlıklı bu tezin kendi çalışmam olduğunu, sunduğum tüm sonuç, doküman, bilgi ve belgeleri bizzat ve bu tez çalışması kapsamında elde ettiğimi, bu tez çalışmasıyla elde edilmeyen bütün bilgi ve yorumlara atıf yaptığımı ve bunları kaynaklar listesinde usulüne uygun olarak verdiğimi, tez çalışması ve yazımı sırasında patent ve telif haklarını ihlal edici bir davranışımın olmadığını, bu tezin herhangi bir bölümünü bu üniversite veya diğer bir üniversitede başka bir tez çalışması içinde sunmadığımı, bu tezin planlanmasından yazımına kadar bütün safhalarda bilimsel etik kurallarına uygun olarak davrandığımı ve aksinin ortaya çıkması durumunda her türlü yasal sonucu kabul edeceğimi beyan ederim.

15 / 12 / 2017



Nihal CENGİZ

ÖZET**ENDÜSTRİYEL ATIKSULARIN HİDROTERMAL GAZLAŞTIRMA
İLE ENERJİ (CH₄/H₂) ÜRETİMİNDE DEĞERLENDİRİLEREK
ARITILMASI**

CENGİZ, Nihal

Doktora Tezi, Kimya Mühendisliği Anabilim Dalı

Tez Danışmanı: Prof. Dr. Levent BALLİCE

İkinci Danışman: Mehmet SAĞLAM

Ekim, 2017, 223 sayfa

Tez kapsamında, arıtıma karşı dirençli olan Afyon Alkaloidleri Fabrikası atıksuyunun hidrotermal gazlaştırma (HTG) yöntemi ile kimyasal oksijen ihtiyacının ve içeriğindeki kirleticilerin ne ölçüde giderilebileceği araştırılmıştır. HTG ile organik karbon içeriği yüksek bu atıksuyun önemli ölçüde arıtımı sağlanırken, yüksek oranlarda H₂ ve CH₄ içeren ve temiz enerji kaynağı olarak değerlendirilebilecek bir gaz ürün oluşmaktadır.

En uygun reaksiyon koşullarını belirlemek amacıyla fabrikadan temin edilen atıksu ile 300, 400, 500 ve 600°C reaksiyon sıcaklıklarında ve 200, 275, 350 ve 425 bar basınç seviyelerinde (500 ve 600°C'de) gazlaştırma denemeleri gerçekleştirilmiştir. En uygun katalizör miktarı ise farklı miktarlarda K₂CO₃ varlığında yapılan denemeler ile saptanmıştır. Laboratuvarında sentezlediğimiz aktifleştirilmiş kırmızı çamur katalizörleri, NaOH, KOH, Na₂CO₃, Raney Nikel 4200, Raney Nikel 2800, Aktif Nikel, Nikel-Silis/Aluminyum ile de katalizör tipinin etkisi incelenmiştir. Reaksiyon sıcaklığının artması gazlaşma ile H₂ ve CH₄ verimlerini arttırmıştır. Basıncın artması ise gazlaşma verimi ile H₂ miktarını düşürmüş, CH₄ oluşumunu hafifçe arttırmıştır. Katalizör kullanımı gazlaşmayı arttırırken, gaz ürün kompozisyon ve veriminde değişikliklere sebep olmuştur.

Anahtar Sözcükler: Biyokütle, atıksu, kritiküstü gazlaştırma, hidrojen, metan.

ABSTRACT**TREATMENT OF INDUSTRIAL WASTEWATERS BY
UTILIZING IN ENERGY (CH₄/H₂) PRODUCTION VIA
HYDROTHERMAL GASIFICATION**

CENGİZ, Nihal

PhD in Chemical Engineering

Supervisor: Prof. Dr. Levent BALLİCE

Co-supervisor: Mehmet SAĞLAM

October, 2017, 223 pages

Within the scope of the thesis, it has been investigated how much the chemical oxygen demand and the pollutants in Opium Alkaloids Plant wastewater, which is resistant to treatment can be removed by the Hydrothermal Gasification (HTG) method. This wastewater with high organic carbon content is treated to a significant extent by HTG, while a gaseous product rich in H₂ and CH₄ is also produced which can be utilized as clean energy sources.

Gasification experiments were carried out at the reaction temperatures of 300, 400, 500 and 600°C and at the pressure levels of 200, 275, 350 and 425 bar (500 and 600°C) with the wastewater supplied from the factory to determine the most appropriate reaction conditions. The most favorable amount of catalyst was determined by adding different amounts of K₂CO₃. The effect of catalyst type was examined with activated red mud catalysts synthesized in the laboratory, NaOH, KOH, Na₂CO₃, Raney Nickel 4200, Raney Nickel 2800, Activated Nickel, Nickel-Silica/Aluminum. The increase in reaction temperature increased H₂ and CH₄ yields and gasification efficiency (CGE). Higher pressures decreased the yields of H₂ and CGE, and slightly increased the formation of CH₄. Catalyst use increases gasification and causes changes in gas product composition and yield.

Keywords: Biomass, wastewater, supercritical gasification, hydrogen, methane.

ACKNOWLEDGEMENTS

Firstly, I would like to express my sincere gratitude to my advisors Prof. Dr. Mehmet SAĞLAM and Prof. Dr. Levent Ballice for the continuous support of my Ph. D study and related research, for their patience, motivation, and immense knowledge. I am very grateful to my master thesis supervisor, Prof Dr. Mithat Yüksel, who motivated me to start MSc. for his guidance and support during Ph. D studies, also. I could not have imagined having better advisors and mentors for my MSc. and Ph. D studies, project works, and papers. The day I have met them was a new life for me, I felt their support as a family during all my academic life and in improving myself.

Besides my advisors, I would like to thank the rest of my thesis committee: Prof. Dr. Kadir YURDAKOÇ and Prof. Dr. Nalan KABAY, for their insightful comments and encouragement, but also for the hard question which incited me to widen my research from various perspectives. I would like to offer special thanks to Prof. Dr. Erol ŞEKER and Prof. Dr. Müşerref ARDA not only for their time and patience, but for their intellectual contributions while evaluating of my thesis.

I would like to acknowledge Dr. Tülay Güngören Madenoğlu for her valuable contributions and guidance and I also thank to Gürsel Serin and Asst. Prof. Murat Sert for their supports. I gratefully appreciate for the financial support of Ege University - Aliye Üster Vakfı and Ege University-EBILTEM (Projects No: 15 MÜH 055 and 16 MÜH 133) and TÜBİTAK (Project No: 114Y500).

Last but not the least, I would like to thank my family: my daughter, and my husband, who support me spiritaully throughout writing this thesis and my life with patience. Thanks to my parents and best friends for every kind of supports and for being with me in all my life.



TABLE OF CONTENTS

	Page
ÖZET	vii
ABSTRACT	ix
ACKNOWLEDGEMENTS.....	xi
LIST OF FIGURES	xvii
LIST OF TABLES.....	xxvii
LIST OF SYMBOLS AND ABBREVIATIONS.....	xxxv
1. INTRODUCTION	1
2. GENERAL INFORMATION	5
2.1 Industrial Wastewater	5
2.1.1 Treatment Methods Applied To Industrial Wastewaters.....	7
2.2 Opium Alkaloid Manufacturing	10
2.3 Opium Alkaloid Plant In Turkey	12
2.3.1 Extraction Unit.....	12
2.3.2 Derivatives Unit.....	13
2.4 Production Of Alkaloids In Afyonkarahisar Plant.....	14
2.5 Alkaloid Wastewater	15
2.6 Supercritical Fluids.....	18
2.6.1 Applications Of Supercritical Fluids	19
2.7 Supercritical Water	22
2.7.1 Density.....	22
2.7.2 Dielectric Constant, E (Relative Permittivity).....	23
2.7.2 Ionic Product, Kw.....	25
2.7.4 Dynamic Viscosity (μ) And Diffusivity (D).....	27

TABLE OF CONTENTS (CONTINUED)

	Page
2.8 SCW in Chemical Reactions.....	29
2.8.1 Water as Reactant, Product and Catalyst	29
2.8.2 Supercritical Water Oxidation (SCWO) Reactions	31
2.8.3 Supercritical Water Gasification (SCWG) Reactions	32
3. LITERATURE REVIEW.....	33
3.1 Hydrothermal Gasification Studies.....	33
3.2 Hydrothermal Gasification of Various Wastewaters	34
3.3 Treatment Studies of Opium Alkaloid Wastewater	37
4. MATERIAL AND METHOD	40
4.1 Feedstock	40
4.1.1 Characterization of wastewater.....	40
4.2 Experimental set-up	43
4.3 Catalysts.....	45
4.3.1 Catalyst preparation procedure from red mud:	45
4.4 Experimental procedure	50
4.5 Analysis equipments	51
4.5.1 Gaseous product analysis:.....	51
4.5.2 Liquid product analysis:.....	53
4.6 Experimental studies completed	54
5. RESULTS AND DISCUSSION	57
5.1. Influence Of Temperature and Catalyst amount on Gasification of Opium Alkaloid Wastewater.....	57

TABLE OF CONTENTS (CONTINUED)

	Page
5.1.1 Carbon gasification efficiencies (CGE, %), and amount of produced gas (mol gas/kg C in wastewater)	65
5.1.2 The composition and yields of the gaseous product.....	67
5.1.3 Variation of TOC and COD values and removal efficiencies	70
5.2 Influence of Pressure on Gasification of Opium Alkaloid Wastewater	72
5.2.1 CGE, CLE and amount of produced gas in the absence/presence of K_2CO_3	82
5.2.2 Gaseous product distribution and yields.....	83
5.2.3. Variation of TOC and COD removal efficiencies	86
5.3 Influence of Catalysts on Gasification of Opium Alkaloid Wastewater	87
5.3.1 Influence Of Red Mud Catalysts On Gasification Of Opium Alkaloid Wastewater	87
5.3.2 Influence of Alkali Catalysts on Gasification Of Opium Alkaloid Wastewater	172
5.3.3 Influence of Nickel based Catalysts on Gasification of Opium Alkaloid Wastewater	184

TABLE OF CONTENTS (CONTINUED)

	Page
5.4 Characterization analysis of raw alkaloid wastewater	188
6. CONCLUSION.....	196
REFERENCES.....	202
CURRICULUM VITAE	
APPENDICES	
APPENDIX I.....	
APPENDIX II	
APPENDIX III.....	

LIST OF FIGURES

Figure	Page
Figure 2-1. Total anhydrous morphine alkaloid contained in all poppy straw varieties: production in main producing countries, in morphine equivalent, 2006-2015 (International Narcotics Control Board, 2016).	12
Figure 2-2. Extraction unit.....	13
Figure 2-3. Derivatives Unit.....	14
Figure 2-4. Process flow diagram for an opium alkaloid industry (Ersahin, 2011)	15
Figure 2-5. Alkaloid production process equipments (Turkish Atomic Energy Authority, 2011,).....	15
Figure 2-6. Pressure-temperature phase diagram of the matter (Blaber M., 1996)	19
Figure 2-7. Variation of density of water with temperature and pressure ((Pioro and Duffey, 2007).....	23
Figure 2-8. Dependence of dielectric constant of water on temperature and pressure (H. Iwamura et al., 2016).....	24
Figure 2-9. Variation of properties of water (He et al. 2014).....	24
Figure 2-10. Dependence of ion product constant of water (K_w) on temperature and pressure (Iwamura et al., 2016).....	26
Figure 2-11. Properties of Water in Subcritical, Near-Critical, and Supercritical Conditions, Adapted from (Zhang et al., 2010).	27

LIST OF FIGURES (CONTINUED)

Figure	Page
Figure 2-12. Variation of diffusivity of water on temperature and pressure (Madenoglu, 2011).....	28
Figure 2-13. Variation of dynamic viscosity of water on temperature and pressure (Pioro and Duffey, 2007)..	28
Figure 2-14. Reaction mechanism of organic compounds over RuO ₂ catalyst (Park and Tomiyasu 2003).....	30
Figure 2-15. Typical reaction routes in supercritical water gasification of biomass (Reddy et al. 2014). Catalysts A (e.g., Ni, Ru, Rh, Pt, Pd, Ni/Al ₂ O ₃ , Ni/C, Ru/Al ₂ O ₃ , Ru/C and Ru/TiO ₂); Catalysts B (e.g., Ni, Ru, Pt and activated carbon); Catalysts C (e.g., Ni, Rh, Ru, Pt and activated carbon) and Catalysts D (e.g., Ni, Ru, NaOH, KOH, K ₂ CO ₃ and Trona).....	32
Figure 4-1 LC/MS-MS instrument.....	43
Figure 4-2 Batch SCWG system.....	44
Figure 4-3 Batch autoclave reactor photograph and schematic representation	44
Figure 4-4 Schematic representation of red mud activation procedure	49
Figure 4-5 Batch autoclave reactors while the experiments are being performed.....	50
Figure 4-6 Gas Chromatography (AGILENT, GC 7890A) Gas Chromatography (AGILENT, GC 7890A)	52
Figure 4-7 Total Organic Carbon Analyzer (SHIMADZU TOC-VCPH, JAPAN)...	53

LIST OF FIGURES (CONTINUED)

Figure	Page
Figure 4-8 COD analysis equipments (thermo-reactor and spectrophotometer)...	54
Figure 5-1. Temperature and catalyst effects (0.5 g of K_2CO_3) on the gaseous product composition in hydrothermal gasification of alkaloid wastewater.	57
Figure 5-2. Temperature and catalyst effects (0.5 g of K_2CO_3) on the gaseous product yields (mol/kg organic carbon in wastewater) composition in hydrothermal gasification of alkaloid wastewater.	58
Figure 5-3. The effects of the catalyst amount on the gaseous product composition in hydrothermal gasification of alkaloid wastewater at various reaction temperatures (a) 300°C, (b) 400°C, (c) 500°C, and (d) 600°C).	58
Figure 5-4. The effects of the catalyst amount on the gaseous product yields in hydrothermal gasification of alkaloid wastewater at various reaction temperatures (a) 300°C, and (b) 400°C.	60
Figure 5-5. The effects of the catalyst amount on the gaseous product yields in hydrothermal gasification of alkaloid wastewater at various reaction temperatures (b) 500°C, and (c) 600°C.	61
Figure 5-6. The effects of temperature and catalyst (0.5g K_2CO_3) on TOC values and TOC removal efficiencies (a) and COD values and COD removal efficiencies (b) in hydrothermal gasification of alkaloid wastewater at various reaction temperatures 300, 400°C, 500°C, and 600°C.....	64
Figure 5-7. The effects of various amount of catalyst on TOC and COD values in hydrothermal gasification of alkaloid wastewater at various reaction temperatures 400°C, 500°C, and 600°C.	65

LIST OF FIGURES (CONTINUED)

Figure	Page
Figure 5-8. Effect of various operating pressures on gaseous product distribution in hydrothermal gasification of alkaloid wastewater at 500°C without catalyst.	73
Figure 5-9. Effect of various operating pressures on gaseous product yields [mol/kg organic carbon in wastewater] in hydrothermal gasification of alkaloid wastewater at 500°C without catalyst.	73
Figure 5-10. Effect of various catalysts on gaseous product distribution in hydrothermal gasification of alkaloid wastewater at 600°C without catalyst.	74
Figure 5-11. Effect of various catalysts on gaseous product yields in [mol/kg organic carbon in wastewater] in hydrothermal gasification of alkaloid wastewater at 600°C without catalyst.	75
Figure 5-12. Effect of various operating pressures on gaseous product distribution in hydrothermal gasification of alkaloid wastewater at 500°C with K ₂ CO ₃ catalyst.....	76
Figure 5-13. Effect of various operating pressures on gaseous product gaseous product yields in [mol/kg organic carbon in wastewater] in hydrothermal gasification of alkaloid wastewater at 500°C with K ₂ CO ₃ catalyst	76
Figure 5-14. Effect of various operating pressures on gaseous product distribution in hydrothermal gasification of alkaloid wastewater at 600°C with K ₂ CO ₃ catalyst.....	77
Figure 5-15. Effect of various operating pressures on gaseous product yields [mol/kg organic carbon in wastewater] in hydrothermal gasification of alkaloid wastewater at 600°C with K ₂ CO ₃ catalyst.	78

LIST OF FIGURES (CONTINUED)

Figure	Page
Figure 5-16. Comparison of the gaseous product yields [mole/kg Organic Carbon] in hydrothermal gasification of alkaloid wastewater at various operating pressures and with and without catalyst.	79
Figure 5-17. Reaction mechanisms depending on the conditions (Basu and Mettanant 2009).	84
Figure 5-18. Gaseous product distribution in hydrothermal gasification of alkaloid wastewater in the presence of A-group catalysts.	88
Figure 5-19. The effect of catalyst type on gaseous product yields in hydrothermal gasification of alkaloid wastewater in the presence of A-group catalysts.	89
Figure 5-20. The effect of catalyst type on gaseous product distribution in hydrothermal gasification of alkaloid wastewater in the presence of B-group catalysts.	98
Figure 5-21. The effect of catalyst type on gaseous product yields in hydrothermal gasification of alkaloid wastewater in the presence of B-group catalysts.	99
Figure 5-22. Effect of catalyst type of gaseous product distribution in hydrothermal gasification of alkaloid wastewater at 500°C in the presence of AK-group catalysts.	106
Figure 5-23. The effect of catalyst type on gaseous product yields in hydrothermal gasification of alkaloid wastewater in the presence of AK-group catalysts.	106
Figure 5-24. Effect of Nickel impregnation in non-reduced A group catalysts on yields of of CH ₄ and H ₂	112

LIST OF FIGURES (CONTINUED)

Figure	Page
Figure 5-25. Effect of Nickel impregnation in non-reduced A group catalysts on CGE, TOC _{RE} and COD _{RE}	112
Figure 5-26. Effect of Nickel impregnation in reduced A group catalysts on CGE and yields of CH ₄ and H ₂	113
Figure 5-27. Effect of Nickel impregnation in reduced A group catalysts on CGE, TOC _{RE} and COD _{RE}	113
Figure 5-28. Effect of reduction and Nickel impregnation in all catalysts on CH ₄ yields.	114
Figure 5-29. Effect of reduction and Nickel impregnation in all catalysts on H ₂ yields.	114
Figure 5-30. Effect of reduction and Nickel impregnation in all catalysts on CGE	115
Figure 5-31. Effect of reduction and Nickel impregnation in all catalysts on COD Removal Efficiency.....	115
Figure 5-32. Effect of reduction and Nickel impregnation in all catalysts on TOC Removal Efficiency.....	115
Figure 5-33. Effect of K ₂ CO ₃ addition and Nickel impregnation in A group catalysts on CGE.....	116
Figure 5-34. Effect of K ₂ CO ₃ addition and Nickel impregnation in A group catalysts on COD _{RE} and TOC _{RE}	116
Figure 5-35. General electron image (a) and spectrum (b) of A2 catalyst.....	118
Figure 5-36. Electron image (a) and elemental mapping (b)	120

LIST OF FIGURES (CONTINUED)

Figure	Page
Figure 5-37. General electron image (a) and spectrum (b) of A21 catalyst	122
Figure 5-38. Electron image (a) and elemental mapping (b) of A21 catalyst	123
Figure 5-39. General electron image (a) and spectrum (b) of A3 catalyst.	125
Figure 5-40. Electron image (a) and elemental mapping (b) of A3 catalyst	126
Figure 5-41. General electron image (a) and spectrum (b) of A31 catalys	128
Figure 5-42. Electron image (a) and elemental mapping (b) of A31 catalyst.	129
Figure 5-43. General electron image (a) and spectrum (b) of A4 catalysts.....	131
Figure 5-44. Electron image (a) and elemental mapping (b) of A4 catalyst	132
Figure 5-45. General electron image (a) and spectrum (b) of A41 catalysts.....	134
Figure 5-46. Electron image (a) and elemental mapping (b) of A41 catalyst.	135
Figure 5-47. General electron image (a) and spectrum (b) of B2 catalyst	137
Figure 5-48 Electron image (a) and elemental mapping (b) of B2 catalyst.....	138
Figure 5-49. General electron image (a) and spectrum (b) of B21 catalyst	140
Figure 5-50. Electron image (a) and elemental mapping (b) of B21 catalyst.....	141
Figure 5-51. General electron image (a) and spectrum (b) of B3 catalysts.....	143
Figure 5-52. Electron image (a) and elemental mapping (b) of B3 catalyst.....	145
Figure 5-53. General electron image (a) and spectrum (b) of B31 catalysts.....	147

LIST OF FIGURES (CONTINUED)

Figure	Page
Figure 5-54. Electron image (a) and elemental mapping (b) of B31 catalyst.....	148
Figure 5-55. General electron image (a) and spectrum (b) of B4 catalysts.	150
Figure 5-56. Electron image (a) and elemental mapping (b) of B4 catalyst.	152
Figure 5-57. XRD analysis of A2 catalyst	155
Figure 5-58. A21. XRD, phase analysis results	156
Figure 5-59. B2. XRD, phase analysis results	157
Figure 5-60. XRD analysis of B21 catalyst	158
Figure 5-61. X-ray diffraction (XRD) pattern of dry red mud (Ribeiro et al. 2012)	160
Figure 5-62. X-ray pattern of red mud (Nath and Sahoo 2014).....	160
Figure 5-63. Nickel nanoparticles XRD pattern (El-Kemary et al. 2013)	161
Figure 5-64. Nickel nanoparticles (a) and NiO (b) structures (Park et al. 2005)..	161
Figure 5-65. Plot of intensity versus degree (2θ) within NiO peak in XRD pattern of B2 catalyst for FWHM calculation with Origin software.....	163
Figure 5-66. Plot of intensity versus degree (2θ) within NiO peak in XRD pattern of A21 catalyst for FWHM calculation with Origin software.	163
Figure 5-67. Multipoint BET plot for surface area determination for A2.	165
Figure 5-68. Multipoint BET plot for surface area determination for A21.	166

LIST OF FIGURES (CONTINUED)

Figure	Page
Figure 5-69. Multipoint BET plot for surface area determination for B2.	167
Figure 5-70. Multipoint BET plot for surface area determination for B21.	168
Figure 5-71. Volume versus P/P_0 graph of A2 and A21 catalysts.....	170
Figure 5-72. Volume versus P/P_0 graph of B2 and B21 catalysts	171
Figure 5-73. Effect of various catalysts on gaseous product distribution in hydrothermal gasification of alkaloid wastewater at 300°C.....	174
Figure 5-74. Effect of various catalysts on gaseous product distribution in hydrothermal gasification of alkaloid wastewater at 400°C.....	174
Figure 5-75. Effect of various alkali catalysts on gaseous product distribution in hydrothermal gasification of alkaloid wastewater at 500°C.....	175
Figure 5-76. Effect of various alkali catalysts on gaseous product distribution in hydrothermal gasification of alkaloid wastewater at 600°C.....	175
Figure 5-77. Effect of various alkali catalysts on gaseous product yields [mole/kg Organic Carbon] in hydrothermal gasification of alkaloid wastewater at 300°C.	176
Figure 5-78. Effect of various catalysts on gaseous product yields [mole/kg Organic Carbon] in hydrothermal gasification of alkaloid wastewater at 400°C..	177
Figure 5-79. Effect of various catalysts on gaseous product yields [mole/kg Organic Carbon] in hydrothermal gasification of alkaloid wastewater at 500°C..	178
Figure 5-80. Effect of various catalysts on gaseous product yields [mole/kg Organic Carbon] in hydrothermal gasification of alkaloid wastewater at 600°C..	179

LIST OF FIGURES (CONTINUED)

Figure	Page
Figure 5-81. Effect of various catalysts and temperatures on gaseous product yields [mole/kg Organic Carbon] in hydrothermal gasification of alkaloid wastewater at all studied conditions.....	180
Figure 5-82. Comparison of the gaseous product composition in hydrothermal gasification of alkaloid wastewater with various catalysts at 500°C.	185
Figure 5-83. Comparison of the gaseous product yields [mole/kg Organic Carbon] in hydrothermal gasification of alkaloid wastewater with various catalysts at 500°C.....	185
Figure 5-84. HPLC chromatogram of raw wastewater “Sample 1” in BIORAD column.....	191
Figure 5-85. HPLC chromatogram of raw wastewater “Sample 2” in BIORAD column.....	192
Figure 5-86. HPLC chromatogram of raw wastewater “Sample 1” in MACHEREY NAGEL COLUMN column.....	194
Figure 5-87. HPLC chromatogram of raw wastewater “Sample 2” in MACHEREY NAGEL COLUMN column.....	195

LIST OF TABLES

Table	Page
1-1. Comparison of COD contents and obtained COD Removal Efficiencies (COD _{RE}) in treatability studies of opium alkaloid wastewater with conventional techniques and by HTG method.	4
2-1. Substances present in industrial effluents (Bond & Straub, 1974).....	6
2-2. The most important alkaloids in the opium poppy.....	11
2-3. Technical specifications taken from the authorities of the wastewater treatment plant (Oral interview).....	16
2-4. Comparison of the wastewater characterization results of the researchers and treatment plant.....	17
2-5. Discharge limits for opium alkaloid production plants (WPCR, 2004).....	18
2-6. Critical parameters of selected fluids (Pioro and Duffey, 2007).....	19
2-7. Properties of water in various conditions	22
2-8. Ion product of water at various conditions (Xu 2014)	26
4-1. HPLC Operating Conditions for Biorad Aminex HPX-87H column	42
4-2. HPLC Operating Conditions for Nucleogel sugar Pb column	42
4-3. Technical features and operating conditions of LC/MS-MS.....	43
4-4. Equipments used in the analysis of alkaloid wastewater and hydrothermal gasification studies.	51

LIST OF TABLES (CONTINUED)

Table	Page
4-5. Technical features and operating conditions of HP GC 7890A gas chromatography.....	52
4-6. Non-catalytic and catalyst amount optimization with K_2CO_3	54
4-7. Pressure effect experiments	55
4-8. Activated red mud catalyst experiments.....	55
4-9. Activated red mud catalyst (A group) with K_2CO_3 experiments.....	56
4-10. Experiments with alkali and Nickel-based catalysts.	56
5-1. Reaction conditions and experimental results in the presence of various amounts of K_2CO_3 and at 300 & 400°C.	62
5-1. Reaction conditions and experimental results in the presence of various amounts of K_2CO_3 and at 300 & 400°C.	62
5-2. Reaction conditions and experimental results in the presence of various amounts of K_2CO_3 and at 500 & 600°C.	63
5-3. Reaction conditions, CGE, produced gas amount and TOC values of hydrothermal gasification of alkaloid wastewater in the absence of catalyst and at various reaction pressures.	72
5-4. Reaction conditions, CGE, produced gas amount and TOC values of hydrothermal gasification of alkaloid wastewater with K_2CO_3 catalyst and at various reaction pressures.....	72

LIST OF TABLES (CONTINUED)

Table	Page
5-5. The effect of various operating pressures on gaseous product yields [mol/kg carbon in wastewater] in hydrothermal gasification of alkaloid wastewater at 500°C without catalyst.	74
5-6. The effect of various operating pressures on gaseous product yields [mol/kg organic carbon in wastewater] in hydrothermal gasification of alkaloid wastewater at 600°C without catalyst	75
5-7 The effect of various operating pressures on gaseous product yields [mol/kg organic carbon in wastewater] in hydrothermal gasification of alkaloid wastewater at 600°C without catalyst.	77
5-8. Effect of various operating pressures on gaseous product yields [mol/kg organic carbon in wastewater] in hydrothermal gasification of alkaloid wastewater at 600°C with K ₂ CO ₃ catalyst	78
5-9. COD analysis results and COD removal efficiencies of the SCWG of Alkaloid wastewater absence of catalyst and in the presence of K ₂ CO ₃ (KC) catalysts at various pressure and temperatures.	80
5-10. TOC analysis results and TOC removal efficiencies of the SCWG of Alkaloid wastewater absence of catalyst and in the presence of K ₂ CO ₃ (KC) catalysts at various pressure and temperatures.	81
5-11. Reaction conditions, CGE, produced gas amount and TOC values of hydrothermal gasification of alkaloid wastewater at 500°C with the effect of catalyst type in the presence of A-group catalysts.	88
5-12. The effect of catalyst type on gaseous product distribution in the detailed form in hydrothermal gasification of alkaloid wastewater in the presence of A-group catalysts.....	89

LIST OF TABLES (CONTINUED)

Table	Page
5-13. The effect of catalyst type on gaseous product yields [mole gas/kg C in wastewater] in the detailed form in hydrothermal gasification of alkaloid wastewater in the presence of A-group catalysts.....	90
5-14. COD results and COD removal efficiencies of the SCWG of Alkaloid wastewater in the absence of catalyst (NC) and in the presence of Red Mud (RM) and A-group catalysts.	91
5-15. TOC analysis results and TOC removal efficiencies of the SCWG of Alkaloid wastewater absence of catalyst (NC) and in the presence of Red Mud (RM) and A-group catalysts.	92
5-16. Reaction conditions, CGE, produced gas amount and TOC values of hydrothermal gasification of alkaloid wastewater at 500°C with the effect of catalyst type in the presence of B-group catalysts.....	98
5-17. The effect of catalyst type on gaseous product distribution in the detailed form in hydrothermal gasification of alkaloid wastewater in the presence of B-group catalysts.	99
5-18. The effect of catalyst type on gaseous product yields [mole gas/kg C in wastewater] in the detailed form in hydrothermal gasification of alkaloid wastewater in the presence of B-group catalysts.....	100
5-19. COD results and COD removal efficiencies of the SCWG of Alkaloid wastewater in the absence of catalyst (NC) and in the presence of B group catalyst.....	103
5-20. TOC analysis results and TOC removal efficiencies of the SCWG of Alkaloid wastewater in the presence of B group catalyst.....	104

LIST OF TABLES (CONTINUED)

Table	Page
5-21. Reaction conditions, CGE, produced gas amount and TOC values of hydrothermal gasification of alkaloid wastewater at 500°C with the effect of catalyst type in the presence of B-group catalysts.	105
5-22. The effect of catalyst type on gaseous product distribution in the detailed form in hydrothermal gasification of alkaloid wastewater in the presence of AK group catalysts	107
5-23. The effect of catalyst type on gaseous product yields [mole gas/kg C in wastewater] in the detailed form in hydrothermal gasification of alkaloid wastewater in the presence of AK group catalysts.....	107
5-24. COD results and COD removal efficiencies of the SCWG of Alkaloid wastewater in the absence of catalyst (NC) and in the presence of catalyst	108
5-25. TOC analysis results and TOC removal efficiencies of the SCWG of Alkaloid wastewater in the absence of catalyst (NC) and in the presence of catalyst	109
5-26. Surface elemental composition of A2 catalyst.....	118
5-27. Surface elemental composition of A21 catalyst.....	123
5-28 Surface elemental composition of A3 catalyst.....	126
5-29. Surface elemental composition of A31 catalyst.....	129
5-30. Surface elemental composition of A4 catalyst.	132
5-31 Surface elemental composition of A41 catalyst.....	135
5-32. Surface elemental composition of B2 catalyst.....	138

LIST OF TABLES (CONTINUED)

Table	Page
5-33. Surface elemental composition of B21 catalyst.....	141
5-34. Surface elemental composition of B3 catalyst.....	144
5-35. Surface elemental composition of B31 catalyst.....	148
5-36. Surface elemental composition of B4 catalyst.....	151
5-37 Experimental conditions of BET analysis.	164
5-38 Multipoint BET results	164
5-39 Multipoint BET results of catalyst A2.....	165
5-40 Multipoint BET results of catalyst A21	166
5-41 5 61 Multipoint BET results of catalyst B2	167
5-42 Multipoint BET results of catalyst B21	168
5-43. Reaction conditions, and results of HTG of alkaloid wastewater in the absence of catalyst and in the presence of 0.5 g NaOH at various reaction temperatures with 15 mL of wastewater (T:temperature, NO:NaOH, and 3:300°C, 4:400°C, 5:500°C, 6:600°C	172
5-44. Reaction conditions, and results of HTG of alkaloid wastewater in the absence of catalyst and in the presence of 0.5 g KOH at various reaction temperatures with 15 mL of wastewater (T:temperature, KO:KOH and 3:300°C, 4:400°C, 5:500°C, 6:600°C)	172
5-45. Reaction conditions, and results of HTG of alkaloid wastewater in the absence of catalyst and in the presence of 0.5 g Na ₂ CO ₃ at various reaction temperatures with 15 mL of wastewater.....	173

LIST OF TABLES (CONTINUED)

Table	Page
5-46. Reaction conditions, and results of HTG of alkaloid wastewater in the absence of catalyst and in the presence of 0.5 g K_2CO_3 at various reaction temperatures with 15 mL of wastewater	173
5-47. The effect of catalyst type on gaseous product yields [mole gas/kg C in wastewater] in the detailed form in hydrothermal gasification of alkaloid wastewater in the presence of NaOH, KOH, Na_2CO_3 , K_2CO_3 at 300 °C...176	176
5-48. The effect of catalyst type on gaseous product yields [mole gas/kg C in wastewater] in the detailed form in hydrothermal gasification of alkaloid wastewater in the presence of NaOH, KOH, Na_2CO_3 , K_2CO_3 at 400 °C...177	177
5-49. The effect of catalyst type on gaseous product yields [mole gas/kg C in wastewater] in the detailed form in hydrothermal gasification of alkaloid wastewater in the presence of NaOH, KOH, Na_2CO_3 , K_2CO_3 at 500 °C...178	178
5-50. The effect of catalyst type on gaseous product yields [mole gas/kg C in wastewater] in the detailed form in hydrothermal gasification of alkaloid wastewater in the presence of NaOH, KOH, Na_2CO_3 , K_2CO_3 at 600 °C...179	179
5-51. COD analysis results and COD removal efficiencies of the SCWG of Alkaloid wastewater absence of catalyst and in the presence of NaOH (NO), KOH (KO), Na_2CO_3 (NC), K_2CO_3 (KC) catalysts.....	181
5-52. TOC analysis results and TOC removal efficiencies of the SCWG of Alkaloid wastewater absence of catalyst and in the presence of NaOH (NO), KOH (KO), Na_2CO_3 (NC), K_2CO_3 (KC) catalysts.	182

LIST OF TABLES (CONTINUED)

Table	Page
5-53. Reaction conditions, CGE, produced gas amount and TOC values of hydrothermal gasification of alkaloid wastewater with various catalysts at 500 °C.....	184
5-54. COD analysis results and COD removal efficiencies of the SCWG of Alkaloid wastewater wastewater in the presence of Nickel based various catalysts at 500°C.	186
5-55. COD analysis results and COD removal efficiencies of the SCWG of Alkaloid wastewater wastewater in the presence of Nickel based various catalysts at 500°C.	186
5-56. TOC analysis results and TOC removal efficiencies of the SCWG of Alkaloid wastewater in the presence of Nickel based various catalysts at 500°C. ...	187
5-57. Opium Alkaloid Wastewater characteristics	188
5-58. LC/MS-MS analysis results of raw alkaloid wastewater and aqueous product obtained in HTG of wastewater at various reaction temperatures without catalyst.....	189

LIST OF SYMBOLS AND ABBREVIATIONS

<u>Symbols</u>	<u>Explanations</u>
C_i	concentration of the component 'i' in the gas product (vol.%)
κ	weight of solid residue (g)
n_i	number of carbon atoms of the component 'i' in the gas product
m	weight of the biomass in feed (g)
M	molar mass of the carbon (g mol^{-1})
T	Temperature ($^{\circ}\text{C}$)
T_c	Critical Temperature ($^{\circ}\text{C}$)
P	Pressure (bar)
P_c	Critical Pressure (bar)
R	universal gas constant, $8.3143 \text{ J mol}^{-1} \text{ K}^{-1}$
T	Temperature (K)
TOC_{aq}	Total organic carbon content of the aqueous product (g L^{-1})
TOC_{ww}	Total organic carbon content of the feed wastewater
V_{gas}	volume of the gas product under ambient conditions (L)
V_{aq}	volume of the aqueous product under ambient conditions (L)

LIST OF SYMBOLS AND ABBREVIATIONS (CONTINUED)Abbreviations

BET	Brunauer–Emmett–Teller
CGE	Carbon gasification efficiency (%)
CLE	Carbon liquefaction efficiency (%)
COD	Chemical oxygen demand
FID	Flame ionization detector

1. INTRODUCTION

An Opium Alkaloids Plant is located in the city of Afyon, Turkey, producing alkaloids, using the opium poppy capsule, such as: morphine, codeine, thebaine, etc. for pharmaceutical purposes. The statistical data shows that the global demand for alkaloids are as high in 2013 as in the past two decades. The global consumption of morphine as pain reliever has increased fourfold, particularly in high-income countries in recent years. Turkey is one of twelve licensed countries for opium poppy cultivation worldwide and together with Australia, Spain, France, Hungary, and India one of the largest producer of poppy straw rich in morphine. According to the International Narcotics Control Board (INCB) reports (INGB, 2016), these six countries have met about 93 per cent of the global needs of poppy straw rich in morphine (in morphine equivalent) in 2015.

The wastewater generated from the Opium Alkaloids Plant in Afyon contains some alkaloids (codeine, morphine, and thebaine), aniline, phytin, toluol, acetic acid (Aydin et al. 2010), wax type compounds, soluble components of cellulose, lignin, and hemicellulose (Kaçar et al. 2003; Aydin et al. 2010). This high strength wastewater has a dark-brown color originating from materials resistant to biodegradation (Koyuncu 2003) and is discharged into Eber Lake via the Akarçay River around the city of Afyon. The existing treatment plant is a two-stage system formed of biological (aerobic/anaerobic) treatment and chemical precipitation. Since there are some operating problems, the treatment plant does not work properly (Sevimli et al. 2000; Koyuncu 2003) and causes an environmental problem in this region.

The studies reported on the treatment of opium alkaloid wastewater by various treatment methods consist of characterization (Sevimli et al. 1999; Aydin et al. 2010), biological and/or chemical treatment (A.F. Aydin 2002; Aytimur and Atalay 2004; Kunukcu and Wiesmann 2004), long-term anaerobic treatment (Aydin et al. 2010) and simulation of it using the Anaerobic Digestion Model No. 1 (ADM1) (Dereli et al. 2010), pretreatment by wet air oxidation (WAO), (Kaçar et al. 2003), gamma irradiation as pre-treatment (Bural et al. 2010), Fenton oxidation of pretreated opium alkaloid wastewater (A.F. Aydin, M. Altinbas, M.F. Sevimli), anaerobic pretreatment and post treatment with lime and ozone (Sevimli et al.

2000), and membrane technology for advanced treatment (Koyuncu 2003). The treated wastewater should meet the standards outlined in the Turkish Water Pollution Control Regulation (WPCR, 2004) shown in Table 2.5. The COD removal from the wastewater is between 33% and 88% of the initial COD value in these researches as seen in Table 1.1. There are some treatment researches performed with diluted or pretreated forms of this wastewater and have low influent COD concentrations. The removal efficiencies reached >90 % in these studies, but, they cannot be considered for comparison of the treatment methods applied to the original wastewater. The results obtained in the treatment studies of the original wastewater, show that the COD content of the treated effluent is way above the discharge limits specified in the WPCR (2004).

The water gains high diffusivity avoiding mass transfer limitation and strong solvent properties hindering coke formation and poisoning of the catalyst in the critical region. Supercritical water (SCW) provides a homogeneous medium at near-critical and supercritical conditions due to great miscible characteristics with organic and inorganic compounds (Brunner 2014). A superior side of the hydrothermal gasification processes (HTG) is that there is no necessity for the drying the biomass as opposed to classical gasification. The HTG processes are extensively investigated as the conversion of the organic content of biomass to biofuel products (Sina et al. 2012; Onwudili and Williams 2013), oxidation of specific compounds or sludge (Cocero et al. 2000), and the extraction of various waste materials (Kronholm et al. 2003; Tülay Güngören, et al. 2007). Supercritical water gasification (SCWG) and supercritical water oxidation (SCWO) are both being studied as a waste treatment alternative for industrial wastewaters. In the gasification case the main objective is to produce a high-energy content gaseous product using a hydrolysis mechanism while in the oxidation case it is to destroy the organics using oxidation reaction by means of an oxidant agent. The effluent of SCWG is mainly composed of H₂, CH₄, CO₂, as H₂O, CO₂, and the inorganic salts are principally produced in the SCWO process.

Comprehensive researches have been conducted on the HTG of real biomass samples (Yanik et al. 2007; Madenoğlu et al. 2012; Akgül et al. 2014), and model compounds of biomass in the last decades (Yoshida and Matsumura 2001; Güngören Madenoğlu et al. 2013; Castello et al. 2014; Madenoğlu et al. 2015).

Residues of the unused parts of the plants have a moisture content up to 80%, animal wastes, municipal wastes (He et al. 2014), agriculture based industrial wastes (Holliday et al. 1997), and other wastes containing organic carbon such as activated sludge (Afif et al. 2011) formed in the wastewater treatment used in HTG studies in recent years. Industrial wastewaters have started to take place as feedstock in literature used in hydrothermal gasification studies. There are two studies with black liquor that is formed during cellulose production using a sulfate method (Sricharoenchaikul 2009; Cao et al. 2011), olive mill wastewater (Sö and Akgün 2011), wood gasification process wastewater (Di Blasi et al. 2007), coking wastewater (Du et al. 2010) and with various wastewaters (Yan et al. 2007; I. G. Lee 2010; Lee and Ihm 2010; Zhiyong and Xiuyi 2014; Falamarzian et al. 2014), etc. A wide range of wastewaters having different compositions and components in crude forms have been used in the HTG processes. The chemical oxygen demand (COD) removal efficiencies varied from 45 - 99 % depending on the chemical composition of the wastewater and the operated hydrothermal gasification conditions.

Opium capsules are processed with a water-lime solution and morphine is extracted, then a second stage extraction step is conducted with organic solvents and acid. Wastewater is generated during the recovery operation of the organic solvents and alcohol groups as a by-product. The amount of wastewater produced is reported as 27.5 m³/h. In this study, the HTG of opium alkaloid wastewater was carried out in a batch autoclave system with a temperature range of 400 - 600°C with and without a catalyst during a reaction time of 1h. The main objective is to determine the optimum reaction conditions and the appropriate catalyst in gasifying the organic part, which causes environmental pollution, with a high product efficiency. The organic carbon in the wastewater reacts with the supercritical water to produce an H₂ and CH₄ rich gas. The chemical oxygen demand (COD) value of the wastewater is the most important indicator for the success of the study and it should decrease to 95-96 % of the initial content to provide discharge limit requirement. Thus, the toxic and poisonous COD contents of the wastewater is reduced and there is no need to further treat it reducing energy production. This complex wastewater was tried as a feedstock in the HTG studies for the first time and an advanced treatment was proposed by processing it in a supercritical water

medium to prevent this significant environmental problem around Lake Eber. Supercritical water gasification is promising as an effective treatment alternative for this high-strength alkaloid wastewater and in the production of hydrogen and methane with its high organic carbon content characteristics.

Table 1.1 Comparison of COD contents and obtained COD Removal Efficiencies (COD_{RE}) in treatability studies of opium alkaloid wastewater with conventional techniques and by HTG method.

COD of feedstock, ppm	Applied method	COD_{RE}, %	COD of treated wastewater, ppm	Ref
27700	Biological, Chemical and Combination of them	88.0	3324	Aytimur G., et al., 2004
26650	Wet Air Oxidation	26.0	19720	Y. Kacar et al., 2003
Diluted forms 5000-16000	Anaerobic treatment	90 % for 5000 ppm 62 % for 16000 ppm	500 6080	Sevimli M.F. et al., 2000
<u>Effluent of full-scale aerobic treatment plant (COD:2.000)</u>	Membrane technology	>96.0	80	İ Koyuncu, 2003
<u>Effluents of a lab-scale two stage biological treatment system (COD:650)</u>	Fenton's oxidation	90.0	65	Aydın et al., 2002
19000	Anaerobic treatment with gamma rays	about 80%	3800	Özdemir, R. T., 2006
32050 (RAW, as taken from plant)	HTG (600C and 425 bars with K_2CO_3)	95.8	1347	In this study 2017

2. GENERAL INFORMATION

2.1 Industrial Wastewater

Industrial wastewater is generated during the processing of raw materials in the production steps such as washing, heating, separation, transport, purification, or as reaction products. Each industry branch has different production technology, production type and capacity, qualitative and quantitative properties of the wastewater generated show great differences. So, the industries must be handled separately to determine the treatment prevention technologies and introduce the options. (Şengül 1989). Some industrial wastewaters may be discharged into the sewer system if they have no damaging effect on it. The wastewaters which will be discharged to a surface of ground water should be well examined and treated adequately according to the discharge limits and conditions (Abdulrazzak Alturkmani, 2013). In some organized industrial zones there is a central treatment system, and plants pretreat wastewaters before sending to it. In our country as well as in some other countries do not have adequate and healthy drinking and use water. The reclaiming and reusing wastewater is becoming more important as the issue of limited water resources and the ever-increasing water requirements are met (Kavaklı, 1997). The parameters must be analyzed in the wastewaters depends on the type of industry. The parameters generally categorized as physical, chemical and biological (Şengül, 1989) and measuring some of the parameters according to type of the industry are adequate.

- a) Physical parameters: The principal physical parameters of wastewater are color, odor, temperature, turbidity, total solid content, total suspended solid (TSS), precipitable solid matter, conductivity, and radioactivity.
- b) Chemical parameters: The main chemical characteristics measured in wastewater are pH (power of hydrogen), alkalinity, acidity, chemical oxygen demand (COD), total organic carbon content (TOC), toxic matters (phenols, CN⁻), total nitrogen, Total Kjeldahl Nitrogen (TKN), phosphorus, heavy metals (Hg, Cd, Cr, Zn), fats, oils, and grease, free chlorine.

c) Biological parameters: Basic biological characteristics are coliforms, and other organisms (Salmonella, Shigella, Anthrax, Viruses, Algae, Nematodes, and other worms) and examined by biological tests.

In Table 2-1, some chemical substances are given with the industry types in which they are generated from.

Table 2-1. Substances present in industrial effluents (Bond & Straub, 1974)

Substances	Present in Wastewaters from
Acids	Chem. manufacture, mines, textiles manufacture
Alkalies	Cotton and straw kierung, wool scouring
Acetic acid	Acetate rayon, beet root manufacture
Ammonia	Gas and coke and chem. manufacture
Arsenic	Sheep dipping
Cadmium	Plating
Chromium	Plating, chrome tanning, alum anodizing
Citric acid	Soft drinks and citrus fruit processing
Copper	Copper plating, copper pickling
Cyanides	Gas manufacture, plating, metal cleaning
Fats, oils, grease	Wool scouring, laundries, textile industry
Fluorides	Scrubbing of flue gases, glass etching
Formaldehyde	Synthetic resins and penicillin manufacture
Free chlorine	Laundries, paper mills, textile bleaching
Hydrocarbons	Petrochemical and rubber factories
Mercaptans mills	Oil refining, pulp
Nickel	Plating
Nitro compounds	Explosives and chemical works
Organic acids	Distilleries and fermentation plants
Phenols	Gas and coke manufacture., chem. plants
Starch	Food processing, textile industries
Sugars	Dairies, breweries, sweet industry
Sulfides	Textile industry, tanneries, gas manufacture.
Sulfites	Pulp processing, viscose film manufacture.
Tannic acid	Tanning, sawmills
Tartaric acid	Dyeing, wine, leather, chem. manufacture
Zinc	Galvanizing zinc plating, rubber process.

2.1.1 Treatment Methods Applied to Industrial Wastewaters

Industrial wastewaters are treated by various conventional and/or advanced processes depending on the type of the industry and the required safe discharge characteristics, organic or inorganic content, amount of wastewater generated, toxicity, etc. Conventional methods may be classified into three classes: Physical, chemical and biological treatments. The combination of these methods are also widely investigated and used to achieve more efficient treatment.

2.1.1.1 The physical and chemical treatment

Physical treatment processes includes adsorption, sedimentation, membrane processes, solids removal (clarification, precipitation), degasification, flotation and skimming, etc. There are also physico-chemical processes such as chemical precipitation phosphorus removal, activated carbon adsorption, etc. Chemical treatment methods are chlorination, ozonation, wet air oxidation, UV irradiation, neutralization, coagulation-flocculation, ion exchange etc.

Coagulation-flocculation is a chemical treatment method used for elimination of the suspended particles and may improve the efficiency of the next treatment step (such as sedimentation or filtration) or as a post-treatment option. Coagulation is used to neutralise the negative charges of the suspended solids and prevent repelling each other and simplify the agglomeration. Consequently they act as a large body for settling or be filtering. **Adsorption** is the transfer of atoms, ions or molecules from the liquid or gas phase to the surface of a solid, via physical or chemical steps. In Marmara Research Center, TÜBİTAK, treatability studies of the pretreated form of wastewater from opium processing industry were done by adsorption with activated carbon, diatomite and perlite in 1994 (Kınlı 1994), but not considerable results were obtained. They also investigated coagulation of pollutants with $\text{Al}_2\text{SO}_4 \cdot 18\text{H}_2\text{O}$ (alum), FeCl_3 , $\text{Fe}_2(\text{SO}_4)_3$ and $\text{FeSO}_4 \cdot 7\text{H}_2\text{O}$ and best removal efficiencies were achieved with alum, $\text{Fe}_2(\text{SO}_4)_3$ and FeCl_3 . Effluent COD was lowered to 550-600 ppm from initial COD of 1000 ppm by 40-45% efficiency as lowest which is not much effective (Turkish Atomic Energy Authority, 2011).

Membrane processes basically include electrodialysis, ultrafiltration, nanofiltration and reverse osmosis, etc. They are very efficient to produce high quality water removing dissolved inorganics but has some disadvantages such as

high-cost, fouling of the membrane surfaces, low treatment capacities flows, and involved pre-treatment. In the study of Koyuncu (2003), ultrafiltration, nanofiltration and reverse osmosis were investigated and details of this study is given in section 3.3 (Koyuncu 2003).

Wet air oxidation is a chemical treatment technique and is the oxidation of non-biodegradable dissolved or suspended compounds to less bio-resistance ones in water medium. It is proposed as a pretreatment in the study of Kaçar et al. (Kaçar et al. 2003) for opium processing wastewater, and they investigated operating conditions such as temperature, pressure, pH, etc. Experimental finding shows that 26% COD removal was obtained at 150°C and 0.65 MPa with 2.0 h of reaction time. **Catalytic wet air oxidation (CWAO)** is a used for high strength, and non-biodegradable compounds in wastewaters. Noble metals and metal oxides catalyst addition lowers the operating conditions in wet air oxidation that requiring high temperature and pressure and make the process more efficient (Guolin Jing, Mingming Luan 2016). It is an oxidation technique that oxidize organics and inorganics by oxygen or air in the presence of catalyst. Catalytic wet air oxidation (CWAO) was used in the study of Aytimur et al. (Aytimur and Atalay 2004) as chemical treatment and activated sludge technique as biological treatment. In CWAO, the catalyst used was $\text{FeCl}_2 \cdot 4\text{H}_2\text{O}$ (Ridel—de Haén).

In **chemical oxidation** studies done with opium alkaloid wastewater (Turkish Atomic Energy Authority 2011), they used potassium permanganate, hydrogen peroxide and potassium persulfate as oxidant but with coagulation better results were obtained. The COD removals were not enough to meet required standards with chemical oxidation.

Advanced oxidation methods are novel and effective for wastewater treatment and used to removal of pollutants resistant to conventional techniques significantly. As advanced oxidation processes, fenton oxidation, and ozone oxidation were used in the treatment studies of opium processing industry wastewater. Details of the applied advanced oxidation methods for opium processing wastewater were given in Section 3.3.

2.1.1.2 The biological treatment

Biological treatment processes use microorganisms to eliminate organic pollutant by coagulating and equalization. They are separated into two main classes according to oxygen existence in the process; anaerobic and aerobic. Microorganism degrade the biodegradable pollutant material in the absence of oxygen in **anaerobic** processes. This method is applied in opium alkaloid wastewater treatment by some researchers to raw wastewater (Sevimli et al. 1999; Kunukcu and Wiesmann 2004; Aydin et al. 2010). Due to COD content of this wastewater is soluble and biodegradable in a high ratio as reported, biological treatment studies are done in literature. In **Aerobic** digestion, waste compounds are destructed by aerobic microorganisms. Bural et al. applied aerobic biological treatment after an anaerobic pretreatment of wastewater since it has organic substances in a significant amount and aerobic process can not achieve treatment directly, alone. Kunukçu et al. compared aerobic and anaerobic digestion and dissolved oxygen demand are measured to observe the removal efficiencies and they are found that aerobic biological treatment is more efficient with 75.3 % and anaerobic digestion and WAO process have lower degradation activity (39.7 % and 25.7% COD removals, respectively) (Kunukcu and Wiesmann 2004)

Activated sludge is a viable option in biological processes for the treatment of various industrial wastewaters as well opium processing wastewater. This method involves microorganisms (bacteria and protozoa), aeration and a settling steps and recycling to treat domestic or industrial wastewaters. Opium alkaloid wastewater is treated by a 2-stage activated sludge system installed in the plant. But there are some operational problems and design errors so the system could not work anymore due to unrestrained temperature rise in the aeration tank which is mainly caused by the effect of the dirt layer and a long hydraulic retention time (Sevimli et al. 1999). The other biological treatment techniques are trickling filtration, oxidation ponds, lagoons, septic tanks, nitrification, etc (Gahr et al. 1994).

2.2 Opium Alkaloid Manufacturing

Alkaloid definition made by Pelletier is given as “Alkaloid is a cyclic compound containing a nitrogen in a negative oxidation state which is of limited distribution in living organisms.” Alkaloids are produced from various types of plants but most common, opium poppy capsule is used since it has high content and variety of alkaloids. Opium poppy plant (*Papaver somniferum*) is processed to obtain, opium and poppy straw as raw materials. Alkaloids such as morphine, thebaine, codeine and oripavine are extracted from opium and poppy straw basically. Concentrate of poppy straw is a product obtained in the process of extracting alkaloids from poppy straw. (International Narcotics Control Board (INCB), 2014). The most important alkaloids are given in Table 2-2. Alkaloids, like other secondary metabolites, are also involved in defense against herbivores and pathogens in plants. Approximately 12,000 known alkaloids, depending on their biological activity, are used as pharmaceuticals, stimulants, narcotics and poisons (Gürkök et al. 2010).

Poppy has been growing in Anatolia since the Hittites, and even in the Ottoman period was one of the major income sources of the country. Until the establishment of the Republic of Turkey (1923), there was no restriction on growing of opium poppy. However, it was accepted as a narcotic drug with the laws in 1933, and by 1938, the purchase and storage of the product was put under state control by the establishment of TGB (Turkish Grain Board). Poppy agriculture is under the control of the United Nations in Turkey, India, Australia, France, Spain, Hungary, Czech Republic and China. The United Nations has accepted Turkey and India as 'traditional poppy producers'. Fig. 2-1 shows production in main producing countries, in morphine equivalent in 2006-2015 (INCB, 2016).

Table 2-2. The most important alkaloids in the opium poppy (Önmez, 2007)

Name	Formula	Scientist found	Date
Morphine	C ₁₇ H ₁₉ O ₃ N	Serturmer	1816
Narcotine	C ₂₂ H ₂₃ O ₇ N	Robiquet	1817
Codeine	C ₁₈ H ₂₁ O ₃ N	Robiquet	1832
Narseine	C ₂₃ H ₂₇ O ₈ N	Pelletier	1832
Thebaine	C ₁₉ H ₂₁ O ₃ N	Merck	1835
Pseudomorphine	C ₁₇ H ₁₈ O ₃ N	Smiles	1835
Papaverine	C ₂₀ H ₂₁ O ₄ N	Hesse	1848
Cryptopine	C ₂₁ H ₂₅ O ₅ N	Hesse	1864
Roadine	C ₂₁ H ₂₁ O ₆ N	Hesse	1867
Lantopine	C ₂₃ H ₂₅ O ₄ N	Hesse	1870
Mekonidine	C ₂₁ H ₂₃ O ₄ N	Hesse	1870
Codamine	C ₂₀ H ₂₅ O ₄ N	Hesse	1870
Laudanine	C ₂₀ H ₂₅ O ₄ N	Hesse	1870
Laudanosine	C ₂₁ H ₂₇ O ₄ N	Hesse	1871
Hydrocotarnine	C ₁₂ H ₁₅ O ₃ N	Hesse	1871
Oxynarcotine	C ₂₂ H ₂₃ O ₈ N	Becket ve Wright	1876
Protepine	C ₂₀ H ₁₉ O ₅ N	Hesse	1878
Xanthine	C ₂₀ H ₁₉ O ₅ N	Smith	1893
Papaveramine	C ₂₁ H ₂₅ O ₆ N	Hesse	1903
Aporeine	C ₁₈ H ₁₆ O ₂ N	Pavesi	1905
Neopine	C ₁₈ H ₂₁ O ₄ N	Smith	1911
Porfidroxine	C ₁₉ H ₂₃ O ₄ N	Rakshit	1919
Narcotoline	C ₂₁ H ₂₁ O ₇ N	Wrede	1937

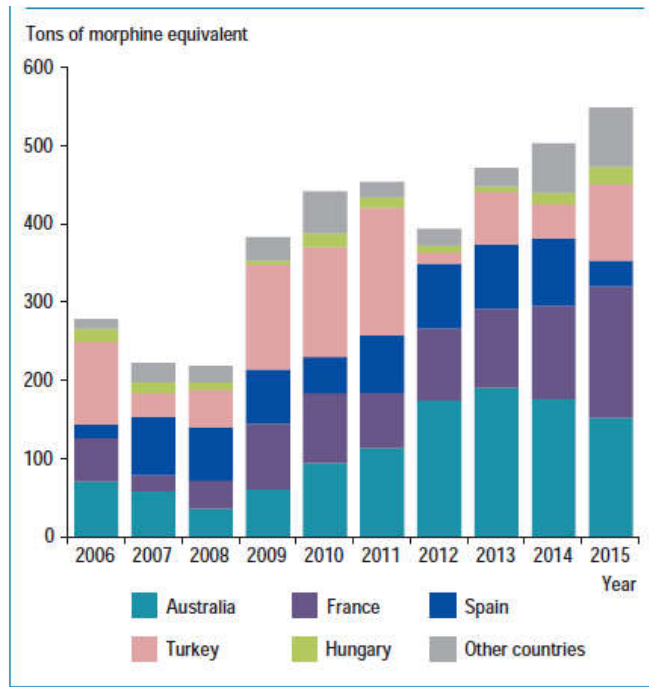


Figure 2-1. Total anhydrous morphine alkaloid contained in all poppy straw varieties: production in main producing countries, in morphine equivalent, 2006-2015 (NGB, 2016).

2.3 Opium Alkaloid Plant in Turkey

In order to evaluate the traditional poppy product and to meet the legal alkaloid requirement of the market, Opium Alkaloids Factory, which was established in 1976 in city of Afyonkarahisar, province of Bolvadin, began trial production in 1981, and started to active manufacturing in 1986. Afyon Alkaloids Plant is the world's largest factory with the technology of the most modern techniques of the time and the unprocessed poppy capsule processing capacity of 20,000 tons / year. Afyon Alkaloids Plant consists of two parts as extraction and derivatives unit.

2.3.1 Extraction Unit

The extraction unit, shown in Fig. 2-2, which is made up of modern equipment, is designed to produce crude morphine (CPS-M). The extraction unit is composed of solid-liquid, liquid liquid and crystallization sections by processing unlanced poppy capsules separated from their seeds. In this unit; crude morphine,

containing 80-93 % anhydrous morphine alkaloid (AMA) is produced by extraction. The percentage of AMA content in the crude morphine can be adjusted according to the requirement of the customer. Depending on the morphine rate of the poppy capsules the extraction unit has an average capacity of 100 tons/year and is at the level of covering 30-35 % of the world trade of licit morphine requirement (TGB, 2013).



Figure 2-2. Extraction unit (TGB, 2013)

2.3.2 Derivatives Unit

The derivatives unit, shown in Fig. 2-3, is based on the raw morphs produced in the extraction unit to synthesize high value semi-synthetic pharmaceutical raw materials (Active Pharmaceutical Ingredients) suitable for pharmacological standards accepted in the world and has a flexible production design and equipment. The type and quantity of the production can be determined according to the customer request (TGB, 2013). The Active Substance Master File which describes the quality of an API and is an essential document for the marketing authorisation of medicinal products, is available for codeine and codeine phosphate which are the most required products. The studies for the Active Substance Master File for other products are continuing. The derivatives unit, designed with a multi-purpose production structure, has the capacity of changing 38% of the morphine produced in the extraction unit to derivatives. The product specification and quantity can be arranged according to customer requirements. All derivatives are produced in conformity with the major pharmacopeias such as British Pharmacopoeia (BP), the European Pharmacopoeia (EP), United States Pharmacopoeia (USP), International Pharmacopoeia (Ph. Int), and current rules of Good Manufacturing Practices.



Figure 2-3. Derivatives Unit (TGB, 2013)

Semi-synthetic products produced;

Codeine
 Codeine Phosphate
 Codeine Hydrochloride
 Codeine sulphate
 Dionine (Ethyl Morphine Hydrochloride)
 Morphine Hydrochloride
 Morphine Sulphate
 Dihydrocodeine Bitartrate
 Dihydrocodeine Thiocyanate

2.4 Production of Alkaloids in Afyonkarahisar Plant

Opium poppy capsules are grinded as first operation, then mixed with lime-water solution and sent to retention step. The mixture is pressed and the pH is adjusted with H_2SO_4 and Na_2CO_3 . After filtration, it is extracted with organic chemicals (acetic acid, toluene, butanol). In crystallization section, morphine is separated by sedimentation and centrifuged. Through the column, the recovery of organics is carried out and the wastewater is generated. Process flow diagram is shown in Fig. 2-4 and the equipments of the treatment plant are given in Fig. 2-5.

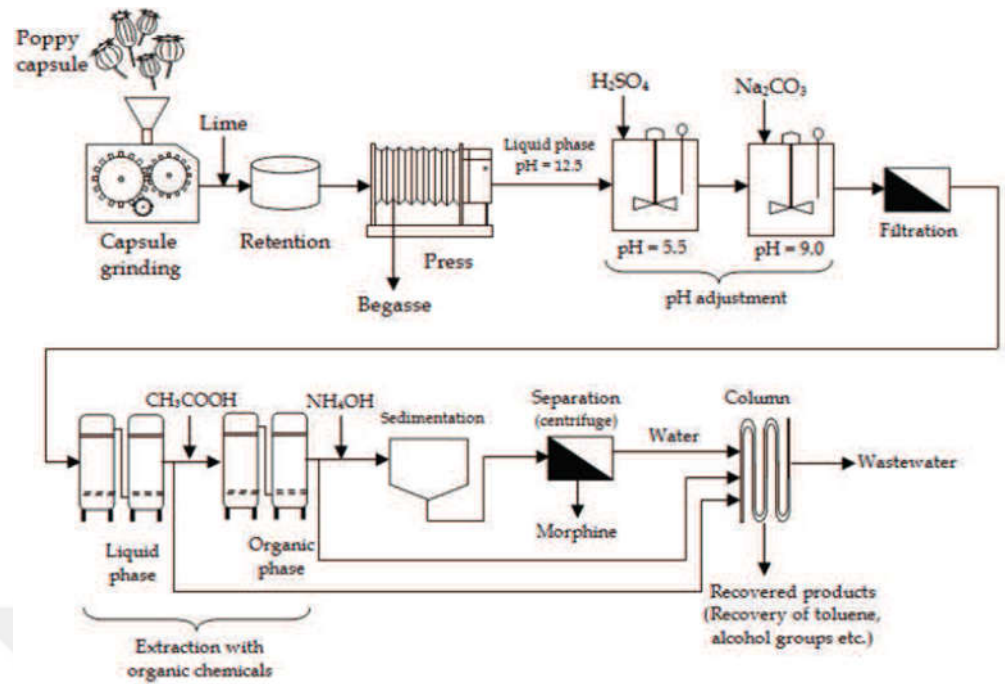


Figure 2-4. Process flow diagram for an opium alkaloid industry (Ersahin, 2011)

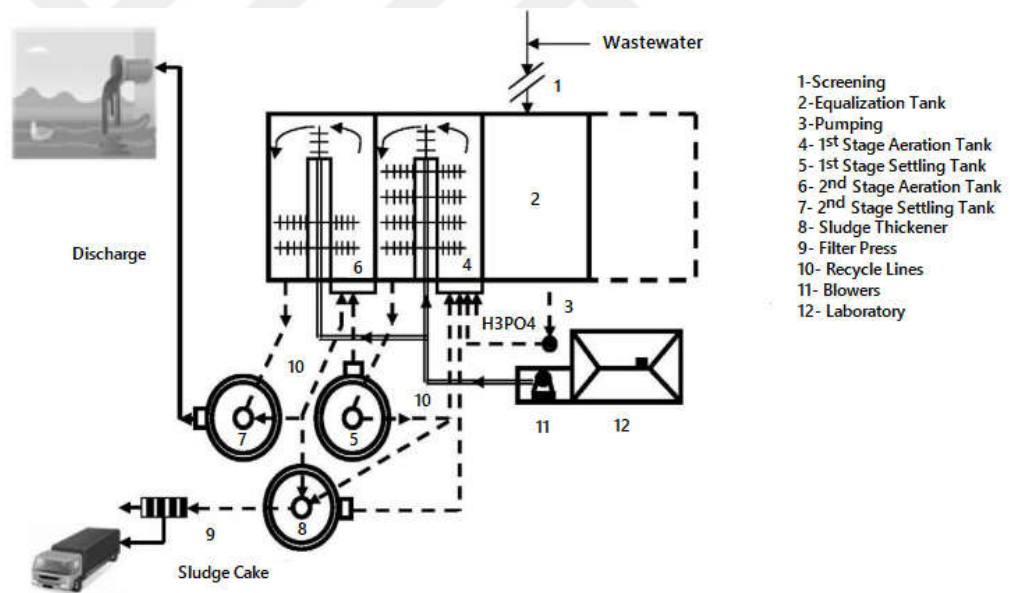


Figure 2-5. Alkaloid treatment plant process equipments (Turkish Atomic Energy Authority, 2011)

2.5 Alkaloid Wastewater

Existing treatment plant is not working because of design error. The treatment plant So, now the new treatment plant is being constructed. It consist of membrane bioreactor (MBR), Microfiltration (MF), Ultrafiltration (UF) and Nanofiltration (NF).

Alkaloid wastewater characteristics and discharge limits:

Opium processing wastewater in Afyon, generates a wastewater that has the specifications given below in Table 2-3 as reported by company authority during an oral interview. The characterization studies were done for this wastewater and a brief data obtained in literature was given in Table 2-4. According to the Water Pollution Control Regulation, published in 2004 in the official newspaper, discharge limits for alkaloid production industry effluent were given in Table 2-5.

Table 2-3. Technical specifications taken from the authorities of the wastewater treatment plant (Afyon Alkaloids Plant, 2017, oral interview).

BOD (Biological Oxygen Demand)	7000-17000 mg/L
COD	25000-45000 mg/ L
Temperature	Summer:35-50°C Winter: 26-40°C
TSS (mg/L)	250-3900 mg/L
pH	4-6,5
Total Kjeldahl Nitrogen (TKN-N)	400-850 mg/L
NH₄-N	54-280 mg/L
TP	6-8 mg/L
Sulphate (SO₄)	7000-14000 mg/L
Volatile fatty acid	7000-15000 mg/L
Total hardness	1000-1200 mg CaCO ₃ /L
Ca hardness	1000 mg CaCO ₃ /L
Conductivity	24.0000-30.000 μS/cm
TDS	26.000-33.000 mg/L
Na	4000-7000 mg/L
K	4000-6000 mg/L
Alkalinity	1500-5000 mg/lt (CaCO ₃)

Table 2-4. Comparison of the wastewater characterization results of the researchers and treatment plant

Parameters	Deshkar, 1982	Kınlı, 1994	Cil. 1993	Sevimli, 1999	Wastewater Treatment Plant	TAEA & METU, 2011	Aydın, 2002	Ozdemir, 2006	Bural, 2008
pH	8.4	4.89	5.1	4.95	5.5	4.96		4.5-5.2	4.5-5.36
TCOD (mg/L)	18,800	23,251	21,200	36,500	31,085	33,000-40,000		22,000-34,780	30,000-43,078
SCOD (mg/L)	-	-	-	32,620	29,180	31,050		-	28,500-40,525
BOD5 (mg/L)	15,000	14,450	14,700	-	-	-		21,250	16,625-23,670
TSS (mg/L)	38	1450	1214	1400	700	1320	565-2295	1120-1700	555-2,193
TKN (mg/L)	1870	230	404	1030	1120	1001.2		1001.2	396-1001
NH ₄ -N (mg/L)	35	62	147	140	168	61.6-172.5	73-141	61.6-172.5	61.6-259
Total P (mg/L)	1.3	29	15	65	-	5.21	-	4-5.21	4-5.21
Na (mg/L)							700-10,445		
K (mg/L)							315-457		
Color (Pt-CO)						4,750	2150-2550	4750	4375-4750
Alkalinity (mg CaCO ₃ /L)	-	1450	5294	-	13	1050	315-4450	144-1050	1050-4200
Conductivity (μS/cm)							18,900-22,800		
Protein, ppm								5330	5330-6630
Carbohydrate, ppm								10,000	10,000

Table 2-5. Discharge limits for opium alkaloid production plants (WPCR, 2004)

Parameter	Unit	Composite Sample (24h)
COD	mg/L	1.500
TKN	mg/L	15
TSS	mg/L	200
pH	-	6-9

2.6 Supercritical Fluids

Three phases of matter is represented with a pressure-temperature phase diagram in Figure 2-6. Pressure-temperature phase diagram of the matter Solid-liquid, liquid-gas and solid-gas phase boundaries are separated with the phase separation lines. There are two-phases together on these lines and in triple point, solid-liquid and gas phases coexist. The liquid-vapor line ends at a point which is called as supercritical point of the matter. This specific temperature and pressure are shown as T_c and P_c , respectively. The properties of the fluids above the thermodynamic critical point varies significantly depending on the process conditions. The gains superior specifications such as low viscosity, high diffusivity, low density, minimal surface tension etc. The process needs can be met by adjustable supercritical fluid (SCF) properties. Dissolving capacity of SCF changes comparing the normal state and can dissolve compounds which are unlike their molecular structure. The common used supercritical fluids are water, carbon dioxide, helium and some refrigerants (Pioro and Mokry 2011).

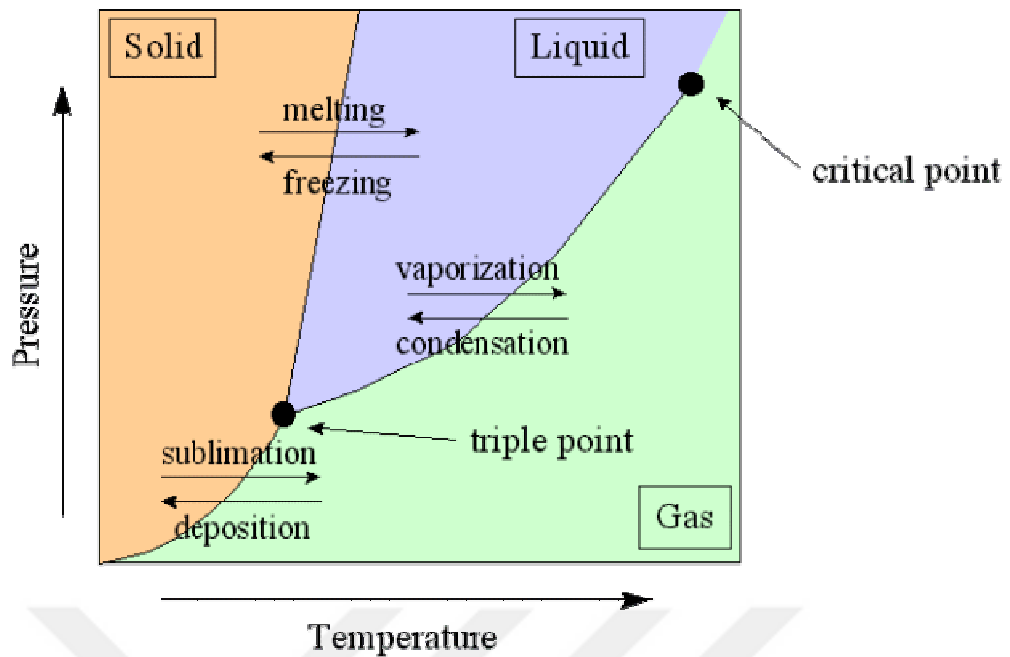


Figure 2-6. Pressure-temperature phase diagram of the matter (Blaber, 1996).

Table 2-6. Critical parameters of selected fluids (Piro and Duffey, 2007)

Fluid	P_{cr} , MPa	T_{cr} , °C	ρ_{cr} , kg/m ³
Carbon dioxide (CO ₂)	7.3773	30.978	467.6
Freon-12	4.1361	111.97	565.0
Freon-13 a	4.0593	101.06	511.9
Water (H ₂ O)	22.064	373.95	322.29

2.6.1 Applications of Supercritical Fluids

The principal applications of supercritical fluids may be categorized as (Brunner 2010; Vazquez da Silva 2010; Knez et al. 2014).

2.6.1.1 Supercritical Fluid Extraction and Fractionation:

The classical solvent extraction requires the complete removal of solvent from the extracted solid and organic solvents must be purified to use again. In SCF extraction, the usage of organic solvent is eliminated and the separation of solvent from the extracted material is done by depressurization (Knez et al. 2014). This method provides selective extraction and fractionation of the desired compounds.

Supercritical (SC) CO₂ is used extensively in commercial applications such as decaffeination of coffee, denicotination of cigarette, extraction of the essential oils from plants and seeds, as a refining and fractionating operation for vegetable oils, production of sesame oil, extraction of spices for food, fragrances for cosmetic, and, antioxidant, nutraceuticals for pharmaceutical industries.

2.6.1.2 Supercritical Fluid Chromatography (SCFC)

This technique is tried for thermo-labile compounds as first (Vazquez da Silva 2010) by using supercritical chlorofluoromethanes. SCFC presents many advantages due to superior characteristics of SCFs, diffusion of solutes in SCF is very high than liquids and it provides very rapid separation. The main difference between SCFC and conventional GC and HPLC method, using SCF as mobile phase. It also reduces the waste originating from the use of organic solvent.

2.6.1.3 Hydrothermal Processing In Energy Applications

SC water and SC CO₂ is extensively studied in the power-plant steam generators and alternative for commercially used refrigerants, respectively (Pioro and Mokry 2011). Supercritical Rankine cycles were investigated for the recovery of heat and lower the cost of electricity (Larsen et al. 2013). SCW provides a media for fast hydrolysis of biomass with the advantage of no need for drying and convert it to hydrogen and methane rich gaseous product at supercritical water conditions. Comparing to conventional gasification, it decreases tar and coke formation, it is possible to carry out without catalyst at high temperatures (Wen et al. 2009). In biodiesel and bio-oil and valuable chemical production SCF are also widely studied (Wen et al. 2009; Tan and Lee 2011). SCW transesterification (SCTE) technique eliminates the limitations in conventional transesterification of oils and produces higher quality biodiesel comparing to using SC methanol generally.

2.6.1.4 Polymer Processing

SCFs are widely used in micro/nano particle production, composite polymer manufacturing, and impregnation or as solvent, anti-solvent, foaming agent, plactizers, etc. Technologies supported by supercritical fluids, especially CO₂, is

used in pharmaceutical, fine chemicals, dyeing, paint, food and polymer industries (Özcan et al. 1998; Hakuta et al. 2003; Girotra et al. 2013; Long et al. 2014; Esfandiari 2015). In dyeing operation in textile industry, SCF dyeing provides many advantages in economic and environmental point of view: it eliminates water/organic solvent use, decrease costs and SCFs can be recycled (Liao and Chang 2012). In polymer processing, conventional methods requires high temperatures, and organic solvent use and is not suitable for heat-sensitive materials. SC CO₂ is used in various applications in polymer and fine particle production such as (Brunner 2010; Knez et al. 2014):

- ✓ Rapid expansion of the supercritical solution (RESS):
- ✓ Supercritical antisolvent precipitation (SAS):
- ✓ Particles from gas saturated solutions (PGSS):
- ✓ Fluid-assisted micro-encapsulation (FAME)
- ✓ Impregnation: Concentrated powder formulation (CPF):
- ✓ PCA (precipitation by compressed antisolvent),
- ✓ SEDS (solution enhanced dispersion by supercritical fluid),
- ✓ ASES (aerosol solvent extraction system),
- ✓ SAA (supercritical assisted atomization)

2.6.1.5 Supercritical Cleaning and Drying

In conventional dry cleaning, organic solvents especially perchloroethylene is used and its residues on the clothes and it is categorized in the carcinogen risk chemicals. SC CO₂ is recently used as drying operations in in textile and food industry (Brown and Submitted). Since SCF technology removes the surface tensions on the interfaces while applying on a solid medium, it effectiveness is greater than at lower temperatures. In the perspective of environment, it extinguishes the organic waste in conventional dry cleaning and it has no residue on textile materials.

2.7 Supercritical Water (SCW)

Water above its critical temperature and pressure ($T_c=373.95^\circ\text{C}$ and $P_c = 22.064 \text{ MPa}$) becomes supercritical where the liquid and gas phases are miscible and indistinguishable (Shanableh 1996). The critical conditions of water is relatively high comparing to other fluids as shown in Table 2-6 due to its strong hydrogen bond structure. The physical properties of supercritical water greatly different comparing to ambient water as give inTable 2-7. Properties of water in various conditions . Water is an efficient solvent and reaction medium for various compounds under supercritical conditions.

Table 2-7. Properties of water in various conditions (Kramer and Vogel, 2000; Kruse and Dinjus, 2007).

	Normal water	Subcritical water		Supercritical water	
Temperature ($^\circ\text{C}$)	25	250	350	400	400
Pressure (MPa)	0.1	5	25	25	50
Density, ρ (g cm^{-3})	1	0.8	0.6	0.17	0.58
Dielectric constant, ϵ (F m^{-1})	78.5	27.1	14.07	5.9	10.5
Ionic product, pK_w	14	11.2	12	19.4	11.9
Heat capacity, C_p ($\text{KJ Kg}^{-1} \text{ K}^{-1}$)	4.22	4.86	10.1	13	6.8
Dynamic viscosity, η (mPa s)	0.89	0.11	0.064	0.03	0.07

2.7.1 Density

Density of water decreases with increasing temperature and pressure from ambient to critical conditions: $d=1 \text{ g/cm}^3$ at 25°C and 0.1 MPa to $d=0.17 \text{ g/cm}^3$ at 400°C and 25 MPa substantially. Around the critical point, the density of water sharply decrease as shown in Figure 2-7. Variation of density of water with temperature and pressure with increasing temperature at the stated pressure levels. Hydrolysis reactions are favored with high water density so operating at subcritical conditions is recommended (He et al. 2014). Ambient water hydrogen bond lattice

weaken resulting in lower densities at near-critical temperature. The increase in pressure results in increase in density of water as seen in the lines of various pressures.

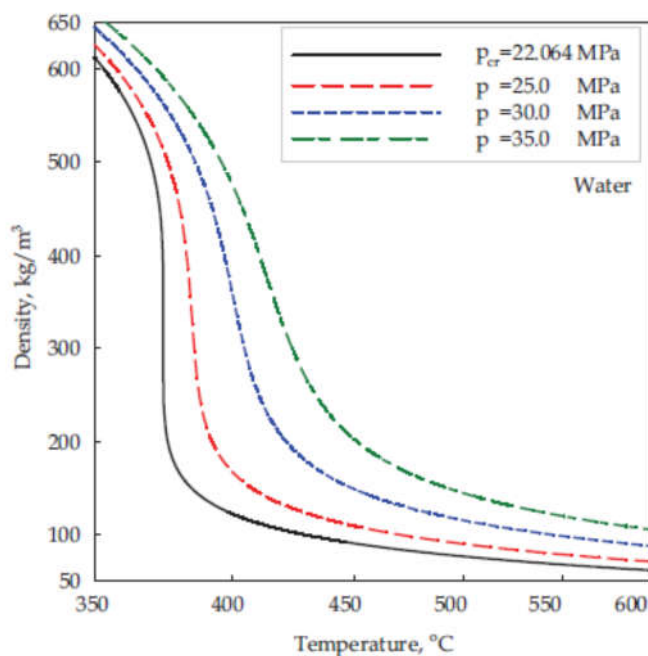


Figure 2-7. Variation of density of water with temperature and pressure (Piroo and Duffey, 2007).

2.7.2 Dielectric constant, ϵ (Relative permittivity)

Dielectric constant of a fluid is related to polarity and dissolution capacity of the solvent. Water at normal conditions has a higher dielectric constant ($\epsilon=80$) than the SCW ($\epsilon=5$) at critical point (He, 2014) due to diminishing intermolecular interactions based on hydrogen bonding and decreasing dipoles of molecules (García Jarana et al. 2008). Dependence of dielectric constant of water on temperature and pressure is given in Fig. 2-8. The higher dielectric constant of ambient water makes it a good solvent for polar substances. SCW with its lower dielectric constant like common non-polar solvents ($\epsilon_{\text{ethanol}}=28$ and $\epsilon_{\text{benzene}}=2.3$ at 25°C (Iwamura et al. 2016) gains ability to solve non-polar organics. While the hydrocarbon solubility is enhanced under supercritical conditions, the inorganics solvation capability of SCW decreases as shown in Figure 2.9.

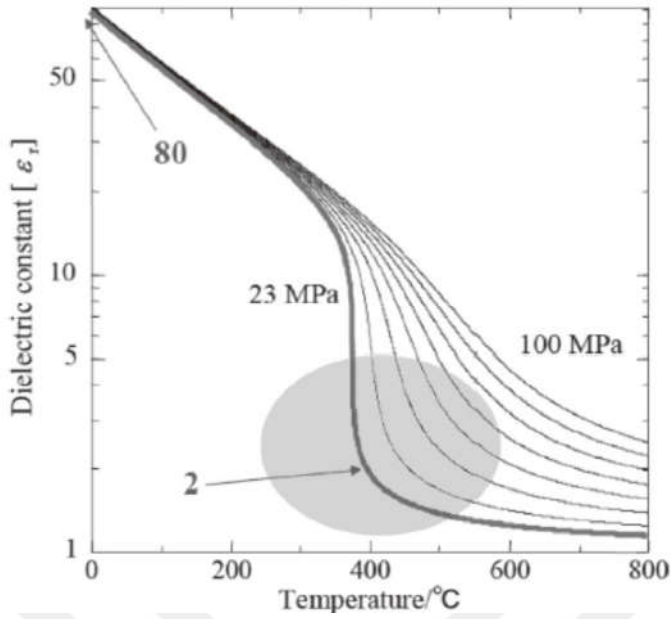


Figure 2-8. Dependence of dielectric constant of water on temperature and pressure (Iwamura et al., 2016)

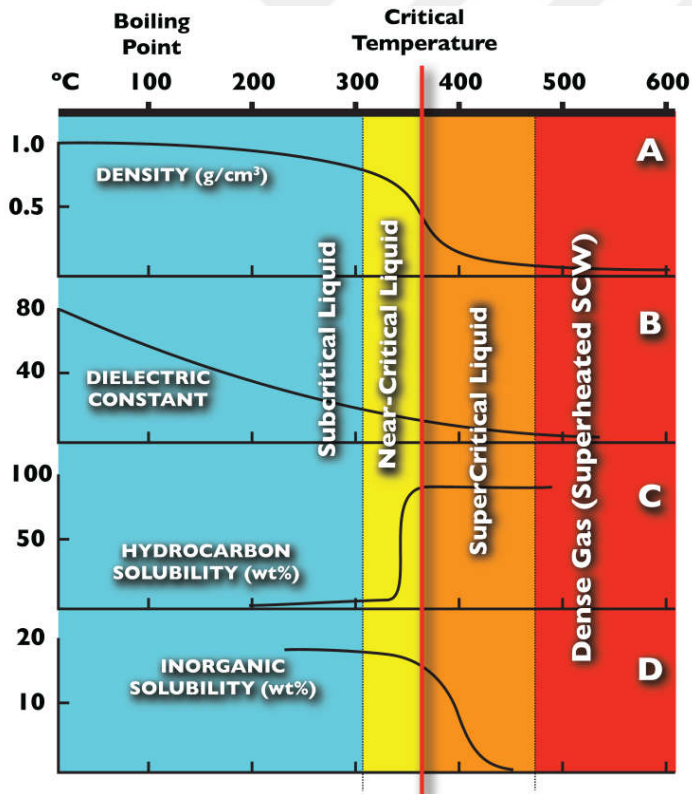
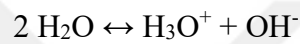


Figure 2-9. Variation of properties of water (He et al., 2014)

2.7.3 Ion Product Constant of Water, K_w

K_w is obtained the production of the ion concentrations of water. Up to critical point, the ion product of water it reaches a maximum and above critical point it starts to decrease ($K_w=10^{-14}$ at ambient conditions and $K_w=10^{-23}$ at supercritical point conditions) as shown in Figure 2-10. Ion product constant of water at various temperatures and pressures is given in Table 2-8. The pH values of water varied at different temperatures as: pH= 5.6 is at 25°C, and pH=8 at critical point (Garcia Jarana et al. 2008). Ionization reaction of water into its ions is an endothermic reversible reaction and forms hydronium $[H_3O^+]$ and hydroxyl $[OH^-]$ ions.



$$K_w = [H_3O^+] \cdot [OH^-]$$

The reactions in near and supercritical water medium may be controlled by adjusting the operating temperature and pressure. Since the ion product constant is highly dependent on conditions, the concentrations of the ions decrease at supercritical water conditions. The ionic product formation favored at sub and near critical region as stated above while radical formation is lower compared to relatively high temperatures and pressures. Reaction in SCW conditions is mainly carried out by radical mechanism due to low ionic product of water above supercritical point.

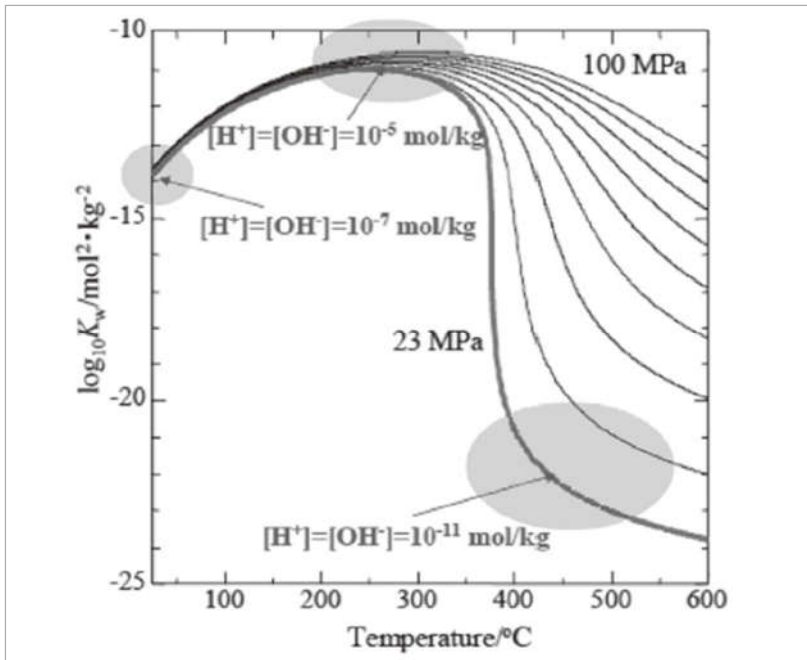


Figure 2-10 Dependence of ion product constant of water (K_w) on temperature and pressure (Iwamura et al., 2016).

Table 2-8. Ion product constant of water at various conditions (Xu, 2014).

K_w	Temperature, °C	Pressure, MPa
10^{-14}	25	0.1
10^{-11}	320	25
$10^{-19.4}$	400	25
$10^{-20.9}$	420	25
10^{-22}	500-600	25

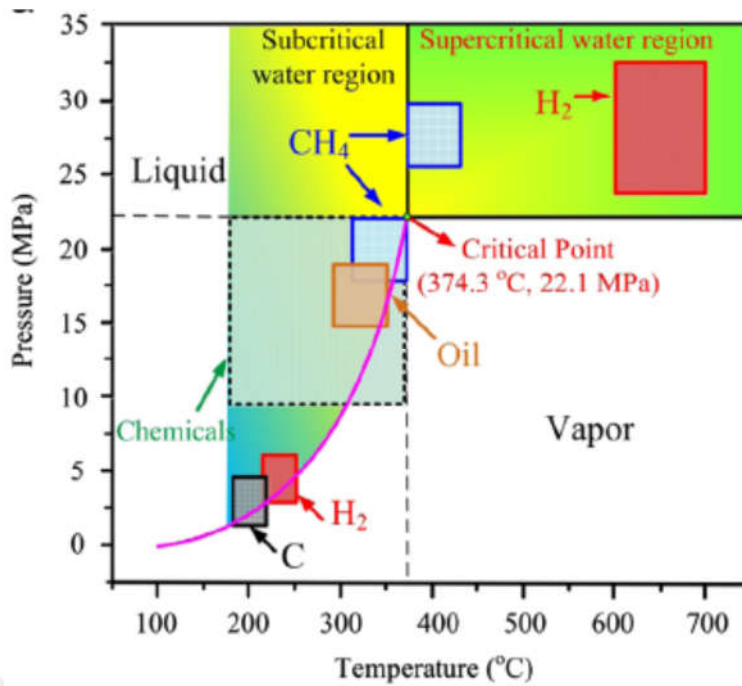


Figure 2-11 Properties of Water in Subcritical, Near-Critical, and Supercritical Conditions, Adapted from (Zhang et al., 2010).

2.7.4 Dynamic Viscosity (μ) and Diffusivity (D)

Water molecule becomes highly compressible at supercritical conditions and the little changes in pressure result in significant variations in physical and transport properties and solvation characteristics (Kalinichev, 1993). The spaces between the water molecules are larger under supercritical conditions thus hydrogen bonds weaken due to temperature rise and this situation causes lower water densities. Temperatures above T_c of water affect the molecular motion velocity, and as a result, the viscosity of water is lower in the supercritical region as shown in Fig. 2-13. For example, at a pressure of 22 MPa, $\mu = 70$ Pa.s (at 350°C) and $\mu = 27$ Pa.s (at 400°C). The viscosity varies with pressure and higher pressures lead to an increment in dynamic viscosity levels. The diffusivity of water increases with temperature and pressure decrease. Variation of diffusivity of water by temperature and pressure is given in Fig. 2-12. Lower viscosity and higher diffusivity values provide a rapid and high yield reaction medium, lowering the mass transfer limitations.

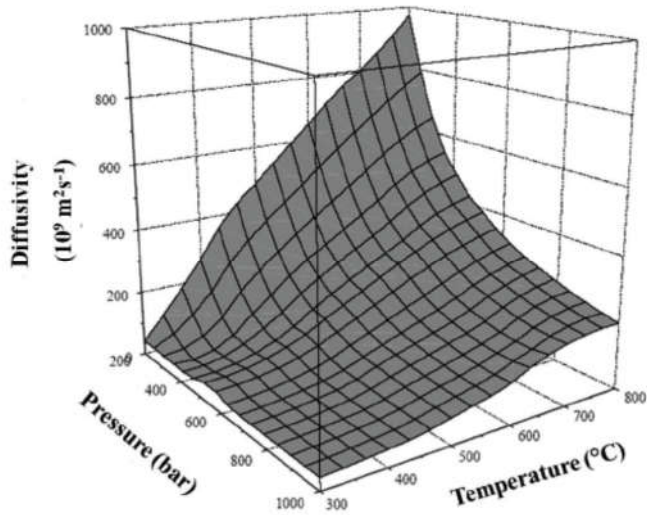


Figure 2-12 Variation of diffusivity of water on temperature and pressure (Madenoglu, 2011)

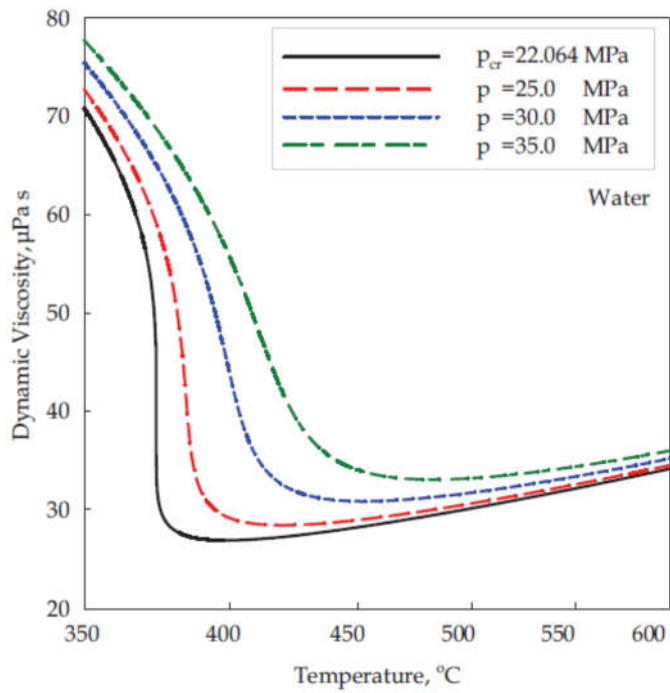


Figure 2-13 Variation of dynamic viscosity of water on temperature and pressure (Piro and Duffey, 2007).

2.8 SCW in Chemical Reactions

SCW is used in many application as a reaction medium or a component of the reaction such as reactant, hydrogen donor, and a catalyst. The variation in the properties of water above critical point give a chance to tune the properties as optimum for many processes. The changing concentrations of ionic products provide selectivity in ionic and radical reactions as mentioned in work of Kruse and Dinjus (Bu et al. 2002). Hydrolysis, hydration, oxidative reactions and hydrogen participation are the main classes of the reactions that SCW takes place.

2.8.1 Water as Reactant, Product and Catalyst

SCW may participate to the chemical reactions such as hydrolysis, decarboxylation, Claisen rearrangement, pinacol rearrangement, dehydration/hydration, and cyclization reaction, etc in the absence of catalyst (Iwamura et al. 2016). Hydrolysis is a bond cleavage reaction of organic molecules with the effect of acid/base formed in the reaction of water and salt. Hydrolysis of various biomass model compounds, polymers, resin, cellulose, ethers, esters, amides, amines, nitroalkanes, and alkyl halides in high temperature water (above 200°C) is widely investigated (Akiya and Savage 2002). The hydrolysis degree is changed depending on the molecule type, while hydrocarbons are resistant to hydrolysis. Biomass constituents' hydrolysis to smaller molecules in supercritical water provides higher yields of reactions comparing to hydrolysis in normal condition.

Some thermally unstable reactants that includes hetero-atoms behave different in the presence of water and not only pyrolysis, also hydrolysis reactions are carried out in high temperature water medium. As the water density increase, the hydrolysis is promoted. Hydrolysis and pyrolysis proceeds as competing pathways and at elevated temperatures, pyrolysis is more dominant. Hydrolysis products such as carboxylic acids and ammonia behave as acid/base catalyst and enhances the reaction kinetics. Autocatalysis for diphenyl ether hydrolysis was investigated as the acid autocatalyst in high temperature (Penninger et al. 1999).

Hydration of cyano groups in nitriles (Akiya and Savage 2002), olefins (Akizuki et al. 2014) and other organic compounds were investigated by some researchers.

Ogunsola (Ogunsola, 2000) proposed that hydrogen atoms join to the reactions of isoquinoline and quinoline of pyrolysis in water medium at supercritical conditions. In a study of Kruse and Ebert, D₂O was used instead of H₂O as reaction medium for pyrolysis of tert.-butylbenzene to understand the role of SCW in an experiment. They determined varying amount of deuterium in the products by mass spectrometry and conclude that water acts a part within the radical chain mechanism (Kruse and Ebert 1996). Park et al. found supporting results and proposed a mechanism for gasification of organic compounds over RuO₂ catalyst and showed that the hydrogen in gaseous product come from water molecules. They studied with D₂O instead of water and saw the products are only CD₄ and D₂ and the reaction mechanism is given below, in Fig. 2-14.

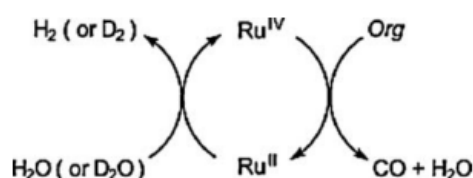


Figure 2-14 Reaction mechanism of organic compounds over RuO₂ catalyst (Park and Tomiyasu 2003)

Water serves as hydrogen donor at high temperatures and increases the hydrogen amount produced affectively (Kruse and Dinjus, 2007).

The water gas shift reaction (WGS) is another important reaction that carries out in supercritical water medium, it converts CO molecules to CO₂ and produces H₂ via the reaction of CO + H₂O ↔ CO₂ + H₂. Hydrogen production from aqueous biomass solution by hydrothermal gasification is possible by means of WGS reaction (Guo et al. 2010b).

Due to quite reactive structure of supercritical water, to proceed the hydrothermal gasification without catalyst is possible and it is supported by some researches (Susanti et al., 2012; Gutiérrez Ortiz et al., 2013; Susanti et al., 2014; Iwamura et al., 2016). Increasing ion product of water at supercritical water conditions results high H₃O⁺ and OH⁻ concentrations and behave as an acid/base catalyst in the reactions. The Cannizzaro reaction is a base-catalyzed reaction and occurs with a strong base at normal conditions, it proceeds at high temperature water medium without catalyst. Methanol and formic acid has been produced by Cannizzaro reaction from formaldehyde (Tsujino et al., 1999) in HTW in the absence of added catalysts. Similarly acetaldehyde (Nagai et al. 2003) that forms

ethanol and acetic acid via Cannizzaro-type disproportionation reaction without any added catalyst in supercritical water.

Xu et al. (1997) demonstrated ethanol, 1-propanol, 2-propanol, glycol, glycerol, and xylose dehydration in the presence of acid catalyst while tert-butyl alcohol dehydrates in supercritical water without any added catalyst (Xu et al. 1997). Penninger and Kersten (1999) dealt with hydrolysis of diphenylether in SCW conditions and found that reaction proceeds through ionic intermediates and protons behave as acid catalyst (Penninger et al. 1999). Although some organics hydrolyze at standard conditions by means of acid catalyst, supercritical conditions may eliminate need for catalyst in some cases. Dehydration of cyclohexene proceeds with the catalyst effect of ionic product of water (H_3O^+) at hot water medium (Kuhlmann et al. 1994).

2.8.2 Supercritical Water Oxidation (SCWO) Reactions

The bonds between carbon atoms of the organic compounds are broken and decomposition with the aid of oxidation with oxidative agents (air, oxygen, hydrogen peroxide, etc.) in supercritical water is carried out in SCWO processes. The products are formed mostly CO_2 and H_2O . The oxidative treatment of organic waste-containing materials in SCW is a more developed form of wet air oxidation (Dietrich et al. 1985; Mishra et al. 1995) that is applied in relatively low temperatures and pressures (320°C and 20 MPa). In this technique, the time of the reaction is longer and the complete destruction can not be achieved and it requires bigger reactor volumes, higher costs to obtain high destruction rates. Controlled incineration of the waste streams generate toxic and harmful products such as dioxins and NO_x , and complete combustion can not be succeeded. SCWO has some superiorities considering these disadvantages of alternatives. Only some minutes are enough for complete conversion and typical conditions are $500\text{--}700^\circ\text{C}$ and 24–50 MPa for this advance technique (Kritzer 2004).

Very diverse materials such as wastes from paper and chemical industry, sewage sludges, wastes includes, dyes, oils, refinery which consists organics at high amounts are studied in this field (Cocero et al. 2000; Shin et al. 2009; Klingler and Vogel 2010).

2.8.3 Supercritical Water Gasification (SCWG) Reactions

Gasification of various feedstocks (biomass, model compounds of biomass, industrial organic wastes, wastewaters, byproducts of bioenergy applications, etc.) at the supercritical condition of water, 22.1 MPa and 374°C, is called as supercritical water gasification (SCWG) and/or hydrothermal gasification (HTG). It is one of the biomass thermochemical conversion technique with classical gasification and pyrolysis which requires less than 10wt.% of water content. The main advantage of this technique is to provide opportunity to utilize green and wet biomass and waste as feedstock. A simplified scheme of conversion of biomass to products in SCW is given in Fig. 2-15 (Reddy et al. 2014) to clarify the reaction steps.

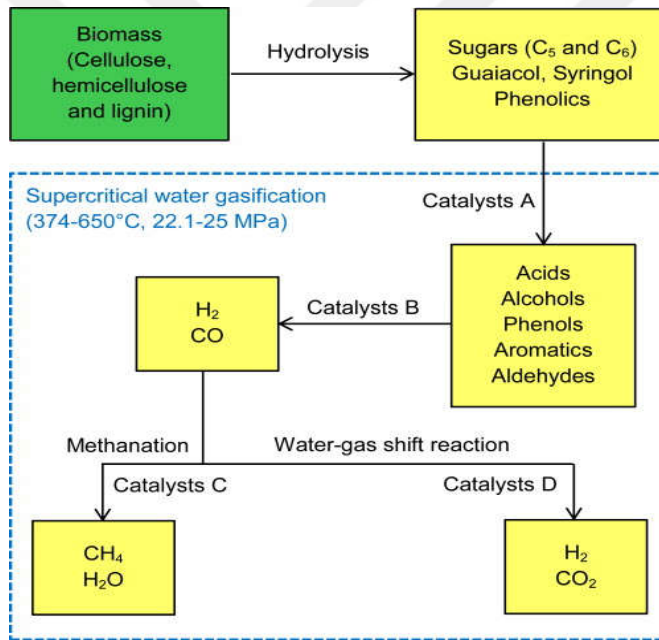


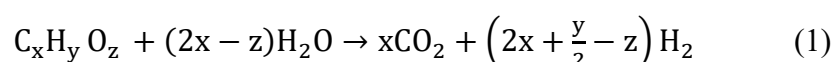
Figure 2-15. Typical reaction routes in supercritical water gasification of biomass (Reddy et al. 2014). Catalysts A (e.g., Ni, Ru, Rh, Pt, Pd, Ni/Al₂O₃, Ni/C, Ru/Al₂O₃, Ru/C and Ru/TiO₂); Catalysts B (e.g., Ni, Ru, Pt and activated carbon); Catalysts C (e.g., Ni, Rh, Ru, Pt and activated carbon) and Catalysts D (e.g., Ni, Ru, NaOH, KOH, K₂CO₃ and Trona).

3. LITERATURE REVIEW

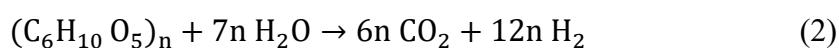
3.1 Hydrothermal Gasification Studies

Utilization of biomass by various conversion techniques for the purpose of energy, fuel, heat, etc are researched with interest. Combustion, pyrolysis, torrefaction, conventional gasification, fermentation, hydrolysis, and supercritical water gasification (SCWG) are the main technologies studied for long years. Supercritical water gasification studies were started by Amin and Modell's investigations in Massachusetts Institute in 1970's. Amin realized that organics degraded to hydrogen and methane in water medium forming significant amount of char and tar. Modell performed gasification experiments in supercritical water and observed that char and tar almost disappeared (Modell et al., 1978).

Type and the ratio of main constituents of biomass resources vary depending on the type of biomass substantially. Gasification characteristics of cellulose, lignin, hemicellulose and extractives are different in supercritical medium. The other contents may affect the reaction mechanisms and yield of H₂ and CH₄ with basic parameters such as temperature, pressure, catalyst type, feedstock concentration, etc. Distribution of organic compounds (alcohols, acids, aldehydes, ketons, phenols and furfurals) in aqueous product differ depending on biomass type. If the molecule formula of organic content in plant structure represented as C_xH_yO_z, theoretical SCWG reaction to form maximum hydrogen can be written as below:

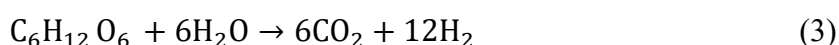


For cellulose:



For the monomers of cellulose, hemicellulose, and SCWG reaction:

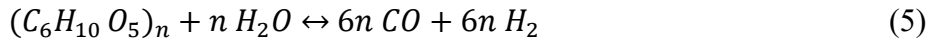
(Glucose/Fructose degradation):



Gasification of biomass or other organic wastes start about 250°C in hot-pressurized water. The gaseous product is rich in hydrogen above 600°C and

nearly complete gasification, while the gas product is rich in methane below 600°C. CO is formed at a very low yields in hydrothermal gasification comparing to conventional gasification and reforming processes (Yan et al. 2006; Lu et al. 2007; Kruse 2008). C₂-C₄ hydrocarbons are also produced at very low percentages in gaseous product mixture in HTG.

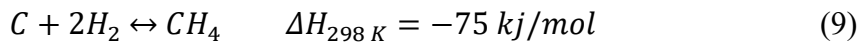
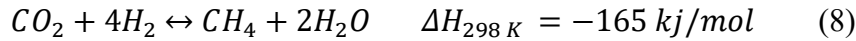
Cellulose may degrade to CO via reaction (5) parallel to reaction (2) since it does not completely convert to H₂ and CO₂. So, reaction below may occur:



CO yields decreases as the temperature reaches and exceeds critical temperature and the formed CO is reacted with water molecule to produce CO₂ and H₂ via water-gas shift reaction (6) and/or reacts with H₂ to produce CH₄ via methanation reaction of CO (7):



Methane may be formed by methanation reaction of CO₂ (8) or carbon methanation reaction (9):



A large number of biomass reactions occur in SCWG simultaneously. A gaseous product containing H₂ or CH₄ in a high ratio is dependent on the reaction temperature, and pressure as well as the composition of the biomass and catalyst type.

3.2 Hydrothermal Gasification (HTG) of Various Wastewaters

An important part of the HTG researches in literature is intended to increase the feedstock types which may be introduced to the gasification. Remaining residues of the unused roots, stems, branches, and leaves parts of all kinds of plants which have a moisture content up to 80%, animal wastes, municipal wastes, agriculture based industrial wastes and other wastes containing organic carbon such as activated sludge that is formed in the wastewater treatment, used in SCWG studies

in recent years. Also, some industrial wastewaters hydrothermal gasification studies began to take place in literature. There are two studies with black liquor that is formed during cellulose production by sulfate method, one study with olive mill wastewater and another one with wood gasification process wastewaters. Additionally amino acid production wastewaters, coking plant wastewaters, from hydrothermal liquefaction, food industries, etc. are investigated by hydrothermal gasification method (Cao, 2011; Breinl 2015; Jarana, 2008; Kıpçak 2017). Additionally wastewater from a pharmaceutical industry (Falamarzian et al., 2014), from a plant producing acrylonitrile (Shin et al., 2009) and three different industrial waste streams (distillery, oil refinery and petrochemical complex) were gasified in supercritical water medium (Seif et al., 2016).

In the first study related to hydrothermal gasification of black liquor, feed material has a moisture content of 81.4%. Approximately 40% of the solid part is composed of organics such as NaOH and Na₂S as majors. Quartz capillary column with a length of 15 cm and an inner diameter of 1mm was used. A conversion of 84.8% was achieved at the reaction temperature of 650°C (Cao, 2011). In the second study with black liquor, a tubular reactor (Hastelloy C-276) has a length of 10.85 mm and an inner diameter of 1.24 mm was used. The wastewater with a COD of 95g/L was treated at a COD removal efficiency of 88.6% at 600°C (Cao et al, 2011).

Supercritical water gasification of olive mill wastewater was carried out in a tubular reactor has an inner diameter of 4.35 mm and a length of 280 cm. Continuous operation was performed at 25 MPa and 550°C with a feedstock containing 24 g/L COD and 6138 mg/L TOC values. A gas composition was obtained as: 9.2% H₂, 34.8% CH₄, 4.0% C₂H₆ and 49.3% CO₂. At the end of reaction, TOC was reduced to 1570.3 (Kıpçak et al., 2011).

In another research, wood gasification process wastewater was used as feed material and studied at the temperature range of 450-550°C and a pressure of 25 MPa. The studies were carried out in a continuously operating reactor system with inner diameter of 8.27 mm and length of 712 mm and the retention time was varied from 46 to 114 seconds. The content of the original wastewater is found as similar

with low temperature pyrolysis liquid product. Approximately 30 types of organic compounds were determined such as acetic acid, propionic acid, furfural derivatives, and derivatives of phenol, hydroquinone and vanillin. TOC content of this wastewater was 6.5-31 g / L and 30% to 70% of the TOC content can be gasified by reacting in hydrothermal gasification. Chemicals in the wastewater and the aqueous effluent of the reaction were determined by GC. Changes of these chemicals in the range of 450-550°C were also determined. It has been observed that these substances were unable to react completely (Blasi et al., 2007).

Hydrothermal gasification of amino acid manufacturing process wastewater was performed in a tubular reactor made of Hastelloy C-276 steel. The reactor length was 293 mm and inner diameter was 6.22 mm, the reaction conditions were 600-700°C and 28 MPa. SCWG of this wastewater was carried out in the presence of activated carbon-Nickel catalyst and COD decreased by 90% of the initial value. In the obtained gas, 59.2% H₂, 30.3% CO₂ and 9.9% CH₄ were determined (Lee et al, 2010).

A food industry wastewater has more than 85% moisture content and a COD value of 100 000 mg O₂ / L was hydrothermally gasified and a COD reduction of 99% was achieved with activated carbon-Ni catalyst. In a study conducted with the production of wine distillation wastewater using KOH as catalyst and O₂ as an oxidant in a 2.5 m long tubular reactor. The initial COD value of 27 g/L was reduced in the range of 45% to 18% depending on the conditions (Lee et al., 2010).

From these results, it is seen that the conversion of the organics in the wastewater to the gaseous products by hydrothermal gasification are distinct. The reason of this is the difference in chemical composition of wastewater depending on the type of the industrial sector. So, all wastewaters must be examined separately.

3.3 Treatment Studies of Opium Alkaloid Wastewater

There are a lot of study on the treatment of this wastewater by various methods like chemical, biological (aerobic and anaerobic medium) and wet air oxidation (Sevimli et al. 2000; Aydın 2002; Kaçar et al. 2003; Bural et al. 2010; Aydın et al. 2010). In these researches it is reported that the COD removal of the wastewater is nearly between 33-80% ratios of the initial COD value. According to these ratios, the treated wastewater COD values are above 3000 mg O₂/L and requires very long periods. And this is more than twice of the discharge limit.

Aydın et al. (2010) studied with a wastewater sample from opium alkaloid industry effluents has a COD of 5500-16200 mg/L. In this long-term anaerobic treatability studies, a lab-scale anaerobic up-flow sludge blanket reactor (UASBR) was operated for 825 days. Best COD removal was achieved in 98 days in the period of L6 with an influent COD of 16200 mg/L and the effluent COD was 3080. Results indicated that this method can be applied as a pretreatment to full-scale aerobic activated sludge process (Aydın et al. 2010).

Sevimli et al. (1999) investigated characterization and treatment of opium alkaloid wastewater (Sevimli et al. 1999) by evaluating the existing treatment plant performance and proposing the design improvements for upgrading and treatment technique alternatives. Anaerobic treatment, ozone oxidation and lime treatment were suggested as supplementary units or replacing the existing one. Ozone oxidation studies were done in a semi-batch bubble reactor as a post treatment option of aerobically treated wastewater. Color and COD removals were 87% and 30%, respectively in an ozonation period of 30 min. Anaerobic treatments were done in a anaerobic up-flow sludge blanket reactor (UASBR) and 70% of COD was removed and a 5770 m³/day biogas recovery was expected.

A wet air oxidation study was performed by Y.Kaçar et al. (2003) with alkaloid wastewater has a COD content of 26.65 g/L and 3.95g/L BOD₅. Wet air oxidation experiments were carried out in a 0.75 L of glass reaction vessel. This study is suggested as a pretreatment operation. At 150°C and 6 bar conditions with an air flow rate of $1.57 \times 10^{-5} \text{ m}^3 \text{ s}^{-1}$, 26% COD removal was reached at the end of

the reaction time of 2 h. This method requires the biological treatment as continuation of it, alone not enough (Kaçar et al., 2003).

In a study of Aytimur and Atalay, alkaloid wastewater has a COD of 27.700 mg/L and a BOD of 3950 mg/L was used. Biological treatment, chemical treatment (catalytic wet air oxidation) and the combination experiments of them were performed. The best results obtained as 88% of COD removal by biological treatment but it is required 6 days of residence time and 4.5 L/min of air flow. Catalyst, $\text{FeCl}_2 \cdot 4\text{H}_2\text{O}$ (Ridel—de Haén), was added according to the desired loading value. In chemical oxidation, 35% of COD removal could be achieved at highest. This method was applied at 160°C and 1 g/L of catalyst loading. The results of the combinations were not promising (Aytimur and Atalay, 2004).

In the work of Aydın and Sarıkaya (2002), a two-step biological treated wastewater, with an up-flow anaerobic sludge bed reactor and an aerobic sequencing batch reactor, has a COD of 700 mg/L was used. This wastewater had biologically non-degradable pollutants. Fenton oxidation was investigated as an advanced oxidation alternative for this pretreated water. A 90% of COD removal and 95% of decolorization were obtained. Optimum oxidation condition was found at pH=4 and the ratio of $\text{H}_2\text{O}_2/\text{FeSO}_4$: 200 mg/L / 600 mg/L (Aydın et al., 2002).

In the study of Koyuncu (2003), UF, NF and reverse osmosis (RO) experiments were done with the effluent of opium processing wastewater treatment plant with a COD content of 1900-2000 mg/L and 950 mg/L were used. Different type of membranes were tried and their performances in COD, color and conductivity removal were tested. Membrane processes were suggested as appropriate for advanced treatment of this wastewater. Complete color removal and high COD and conductivity removals were accomplished with all types of NF and RO membranes (Koyuncu, 2003).

Özdemir used diluted forms of Afyon alkaloids wastewater with COD contents of 2400, 6000 and 9600 mg/L. The highest anaerobic treatment efficiency of 77% was achieved in BM included (biochemical methane) reactor with the inlet COD content of 9600 mg/L. To investigate the effect of gamma rays, alkaloid wastewater

with inlet COD contents of 14 and 25 g/L, and two irradiation doses of 40 and 140 kGy were used. Irradiation had no effect on wastewater with inlet COD of 14 g/L. However, wastewater treatment speed in the reactors containing wastewater with an inlet COD of 25 g/L and received 140 kGy or 40 kGy doses irradiation has been higher than the original reactor containing wastewater after a certain time (Özdemir 2006).

All of the studies show that enough level of treatment of this wastewater from Afyon Alkaloids Plant was hard because of its complex structure and high resistant to treatment. Possibly for this reason, by disregarding the polluting of the environment, discharge limit value in 1995 is excessively reduced in 2004 regulation.

There was no research reported in literature on the utilization of this wastewater, from Afyon Alkaloids Plant which is a specific industry, for energy production. Hydrogen and methane which are used as clean energy sources will be produced from the wastewaters by supercritical water gasification as the first time.

4. MATERIAL AND METHOD

4.1 Feedstock

The feedstock used in this study is opium alkaloid plant wastewater from Afyon Alkaloids Plant – Turkey. The influent wastewater used in the experiments had a COD content of 32,050-35,000 mg O₂/L and a TOC content of 11,500 mg/L from an analysis performed in our laboratory. The wastewater samples were used without filtering, and were only mixed before being fed into the reactor for homogenous sampling and reproducibility.

4.1.1 Characterization of wastewater

Alkaloid wastewater characterization tests were done and the specifications of the samples taken in the different time period varied so the results were given as two section according to dates of supplied. Tests were done in Ege University Chemical Engineering Department research laboratories mostly, some of them are made in other departments in the faculty. Tests and measurements can be listed:

- ✓ COD
- ✓ TOC
- ✓ pH
- ✓ Total Dissolved Solids, (TDS)
- ✓ Conductivity
- ✓ Protein
- ✓ Carbohydrate
- ✓ NH₄-N
- ✓ TKN
- ✓ Color
- ✓ Turbidity
- ✓ Salinity
- ✓ Resistance
- ✓ Ions concentrations (Na⁺, K⁺, Ca⁺, Mg⁺)

Additionally raw wastewater and the aqueous product of gasification studies in the absence of catalyst at 400, 500 and 600°C were analysed in LC-MS-MS instrument to detect the possible compounds. Before analysis samples are prepared as followed:

- ✓ Extraction with ethyl acetate three times,
- ✓ Drying with N₂ gas
- ✓ Dissolving in methanol
- ✓ Filtration

To determine the amount of monosaccharides (Glucose, Mannose, Galactose, Xylose, Rhamnose, Arabinose, etc.) vs and the total carbohydrate content of the wastewater sample, analysis were done by HPLC-Refractive Index (RI) Detector and in both column HPX 87H, 300 mmx 7,5 mm and Nucleogel SugarPb, 300 mm x 7,8 mm. Guard columns were used for protection of the columns and extension of the life span of them. Before analysis in HPLC, isolation was done and the procedure was given in 4.1.1.1 below.

4.1.1.1 Isolation of hemicellulose (Hydrolysis) procedure

Raw wastewater sample was dewatered and the residue content was isolated to analyze the carbohydrate content and the composition in HPLC-RI. The steps for hydrolysis of **hemicellulose** in residue was given below:

1. 0.5 g of sample is obtained from dewatering in hot plate.
2. 4.5 mL of H₂SO₄ (%72) is added
3. Stirred for 4h
4. It is waited in desiccator during 1 night
5. Extract by addition of 150 mL of water
6. Filtration at room temperature (glass filter)
7. Precipitation of filtrate until pH=7 by Ba(OH)₂.8H₂O
8. Filtration with blue grade filter paper
9. Complete volume of 250 mL
10. Analyze in HPLC-RI within 3 days

Table 4-1. HPLC Operating Conditions for Biorad Aminex HPX-87H column

Column	Biorad Aminex HPX-87H (300 mm x 7,8 mm.)
Mobile Phase	0.05 % H ₃ PO ₄ (pH:2.25)
Flowrate	0,6 mL/min
Dedector	RI
Column Temperature	40°C
Dedector Temperature	30°C
P_{max}	93 bar
Injection Volume	20 µL

Biorad and Nucleogel sugar Pb columns operating conditions in HPLC are given in Table 4-1 and 4-2.

Table 4-2. HPLC Operating Conditions for Nucleogel sugar Pb column

Column	Macherey Nagel Nucleogel Sugar Pb, (300 mmx7.8 mm)
Mobile Phase	100 % ultra pure water
Flowrate	0.4 mL/min
Dedector	RI
Column Temperature	80°C
Dedector Temperature	50°C
P_{max}	40 bar
Injection Volume	20 µL

Carbohydrate analysis in the raw wastewater and the monomers of the cellulose was done by HPLC-RI. LC/MS-MS is used to determine detection of compounds in raw wastewater and aqueous products. Operating conditions of it is given in Table 4-3 and a picture of the instrument is given in Fig. 4-1.

Table 4-3. Technical features and operating conditions of LC/MS-MS.

LC (Prominence) parameters		
Column	Shimpack ODS 75*4.6 mm 5 μ m	
Mobile Phase	A: 10 mM Ammonium formate (aq) B: Methanol	
Pump Flowrate	0.4 mL/min	
Detector	MSMS (LCMS-8030)	
Column oven temperature	40°C	
Gradient program of mobile phase	Time (min)	Concentration of B (%)
	0	5
	10	95
	15	95
	15.01	5
	20	5
MSMS Parameters		
Nebulizer gas flowrate	3 L/min	
DL Temperature	250°C	
Heating block temperature	400°C	
Drying gas flowrate:	15 L/min	



Figure 4-1. LC/MS-MS instrument

4.2 Experimental set-up

Autoclave is made of stainless steel for the corrosion resistance and has an inner volume of 100 cm³. It contains temperature control units, furnace, autoclave agitation system, gas collection and measurement units with high pressure valves,

manometer, gas discharging pipes, etc. Schematic of set-up and picture of reactor are given in Fig 4-2 and 4-3.

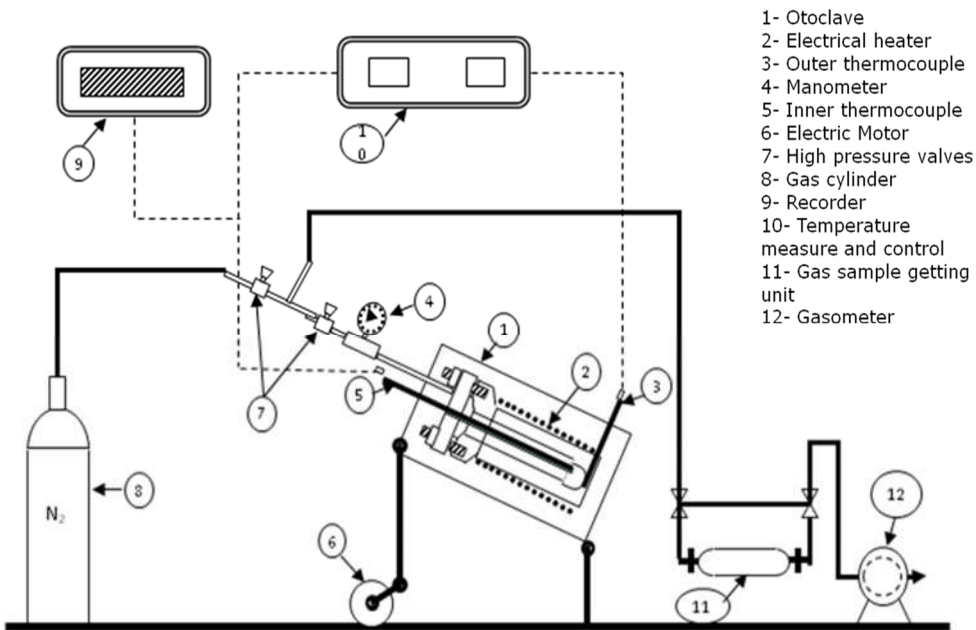


Figure 4-2. Batch SCWG system

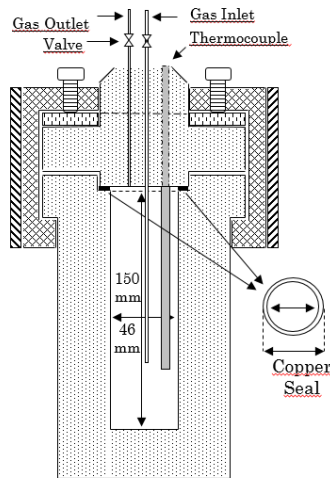


Figure 4-3. Batch autoclave reactor photograph and schematic representation

4.3 Catalyts

The catalyst used in can be categorized into three groups. Alkali catalysts (NaOH, KOH, K_2CO_3 , Na_2CO_3), Nickel based catalysts, (Raney Nickel 4200, Raney Nickel 2800, Activated Nickel, Nickel- Silica/Alumina), Original and Activated Red Mud catalysts (A and B group consist activated form of red mud without nickel and with 10 %, 20 % and 30 % nickel). Red mud is a by-product emerging at alumina production. It was supplied by Alumina Plant in Seydişehir/Turkey, as a sludge and it was filtered and dried at 110°C. Original red mud contains Fe_2O_3 (37.7%), Al_2O_3 (17.3%), SiO_2 (17.1%), Na_2O (7.1%), CaO (4.5%), and TiO_2 (4.8%).

4.3.1 Catalyst preparation procedure from red mud:

600 mL of red-mud mixtures (~30 % solid content) are put into the two separate 2L of beakers (A and B) and are heated while mixing (90-95°C). 35-37 % of HCl ($d=1.18 \text{ g/cm}^3$) was added into the beakers up to pH ~ 4-6 slowly and finally 50 mL of HCl was added then mixtures are heated at 90-95°C during ~1 h. A schematic representation of the preparation of all types of red mud with activation procedure is given in Fig. 4-4.

A) Precipitation by NH_3 (25 %, $d=0.91 \text{ g/cm}^3$): NH_3 was added into the mixture until pH~8 slowly by mixing at high temperature. It is heated at 90-95°C during ~30-60 min then filtered through the filter paper by means of water trompe at high temperature and washed until it does not react with Cl with hot pure water (*). It is dried at 105-110°C for 1 night, grinded, weighed and sieved and labelled as “A”.

A-1) 30 g (A) is taken, and calcined during 2 h at 500°C. It is cooled down and remaining balance (92.2 %) weighed. The catalytic experiments are done.

A-2) 50 g (A) is taken, remaining balance (%) in (A-1) is considered and (50x92.2%) is calculated. A 25.3 g of aqueous concentrated solution of $Ni(NO_3)_2 \cdot 6H_2O$ (10% Ni) is impregnated. It is dried at 105-110°C for a night,

cooled and weighed. It is calcined during 2h at 500°C, cooled down, grinded, and sieved. The surface area is measured and the catalytic experiments are done.

A-2-1) 25 g (A-2) is taken, reduced by NaBH₄ in the aqueous medium is done, filtered and washed with hot pure water. It is dried for 1 night at 105-110°C, weighed, sieved and the surface area of it is measured and the catalytic experiments are done (pH must be <8).

A-3) 50 g (A) is taken, remaining balance (%) in (A-1) is considered and (50x92.2%) is calculated. 56.9 g of aqueous concentrated solution of Ni(NO₃)₂.6H₂O (20% Ni) is impregnated. It is dried at 105-110°C for 1 night, cooled and weighed. It is calcined during 2h at 500°C, cooled down, grinded and sieved. The catalytic experiments are done.

A-3-1) 25 g (A-3) is taken, and reduced by NaBH₄ in the aqueous medium is done, filtered and washed with hot pure water. It is dried for a night at 105-110 °C, weighed, sieved and the catalytic experiments are done (pH must be <8).

A-4) 50 g (A) is taken, remaining balance (%) in (A-1) is considered and (50x92.2%) is calculated. 97.7 g of aqueous concentrated solution of Ni(NO₃)₂.6H₂O (30% Ni) is impregnated. It is dried at 105-110°C for a night, cooled and weighed. It is calcined during 2h at 500°C, cooled down, grinded, and sieved. The catalytic experiments are done.

A-4-1) 25 g (A-4) is taken, reduced by NaBH₄ in the aqueous medium is done, filtered and washed with hot pure water. It is dried for 1 night at 105-110°C, weighed, sieved. The catalytic experiments are done (pH must be <8).

B) Precipitation by K₂CO₃ solution (25 %) : K₂CO₃ solution is added into the mixture until pH~8 slowly by mixing at high temperature. Foam is formed since CO₂ produced, so the mixture may run over. To prevent this, solution should be added slowly and mixed with glass rod. Addition of K₂CO₃ is ended while pH ~8, mixing is continued and waited at a temperature about 90-95°C for 30-60 min. Then

filtered through the filter paper by means of water tromp at high temperature and washed until it does not react with Cl with hot pure water (*). It is labelled as “B”.

B-1) 30 g (B) is taken, and calcined during 2 h at 500°C. It is cooled down, remaining balance (94.5 %) weighed, and the catalytic experiments are done.

B-2) 50 g (B) is taken, remaining balance (%) in (B-1) is considered and (50x94.5%) is calculated. 25.96 g of aqueous concentrated solution of Ni(NO₃)₂.6H₂O (10% Ni) is impregnated. It is dried at 105-110°C for a night, cooled and weighed. It is calcined during 2h at 500°C, cooled down, grinded and sieved. The surface area is measured and the catalytic experiments are done.

B-2-1) 25 g (B-2) is taken, reduced by NaBH₄ in the aqueous medium is done, filtered and washed with hot pure water. It is dried for a night at 105-110°C, weighed, sieved and the surface area of it is measured. The catalytic experiments are done (pH must be <8).

B-3) 50 g (B) is taken, remaining balance (%) in (B-1) is considered and (50x94.5%) is calculated. 58.41 g of aqueous concentrated solution of Ni(NO₃)₂.6H₂O (20% Ni) is impregnated. It is dried at 105-110°C for 1 night, cooled and weighed. It is calcined during 2 h at 500°C, cooled down, grinded, sieved. The catalytic experiments are done.

B-3-1) 25 g (B-3) is taken, reduced by NaBH₄ in the aqueous medium is done, filtered and washed with hot pure water. It is dried for 1 night at 105-110°C, weighed, sieved and the catalytic experiments are done (pH must be <8).

B-4) 50 g (B) is taken, remaining balance (%) in (B-1) is considered and (50x94.5%) is calculated. 100.15 g of aqueous concentrated solution of Ni(NO₃)₂.6H₂O (30% Ni) is impregnated. It is dried at 105-110°C for a night, cooled and weighed. It is calcined during 2 h at 500°C, cooled down, grinded, and sieved. The catalytic experiments are done.

B-4-1) 25 g (B-4) is taken, reduced by NaBH_4 in the aqueous medium is done, filtered and washed with hot pure water. It is dried for 1 night at $105\text{-}110^\circ\text{C}$, weighed, sieved and the catalytic experiments are done (pH must be <8).

* Cl^- reaction control: 3-4 drops are taken from filtration. 1-2 drops dropped from the mixture of 20 mL 0.1 M AgNO_3 + 5mL concentrated 65% HNO_3 . If there is a white precipitate-turbidity, it means Cl^- presents.

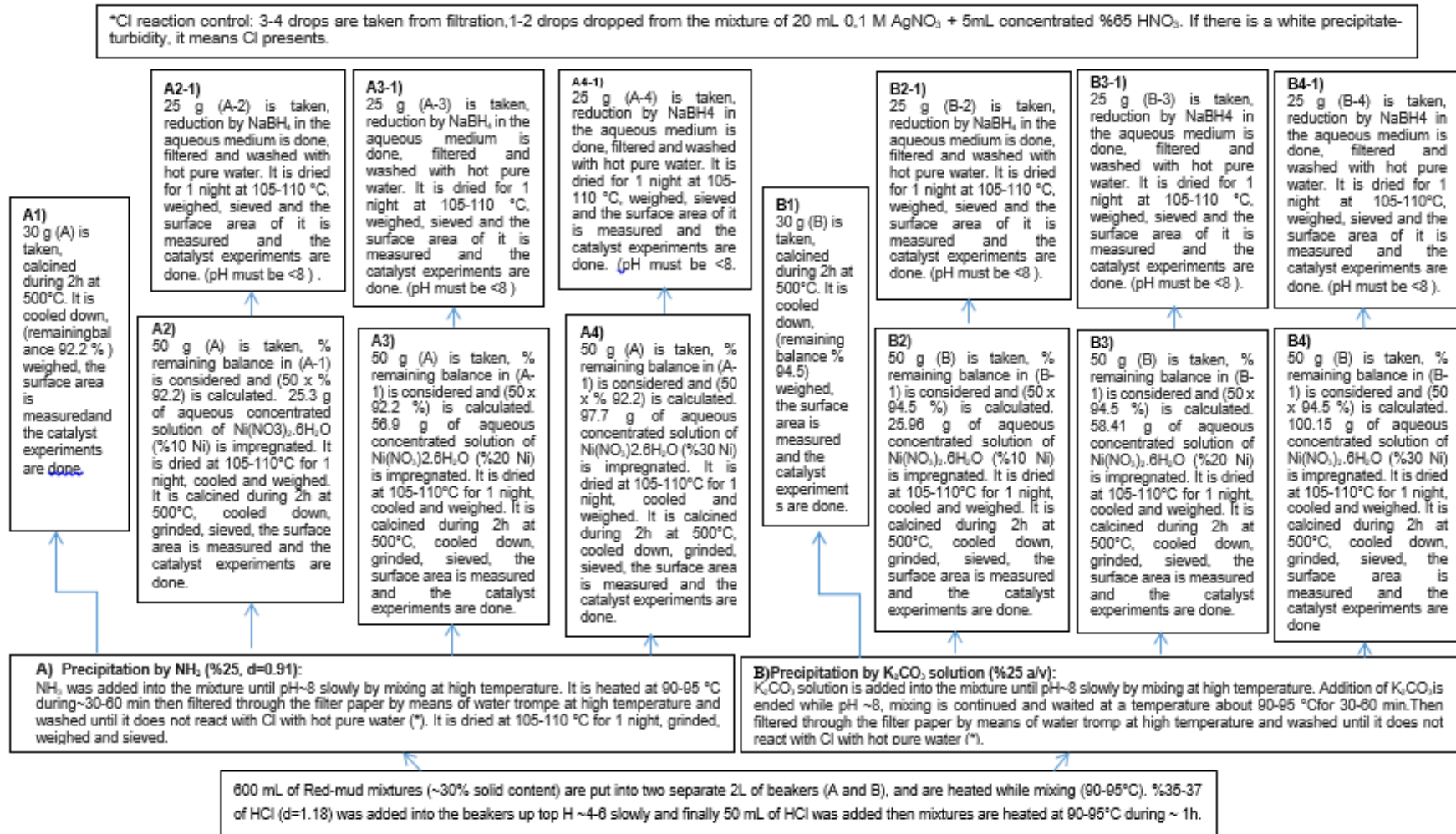


Figure 4-4. Schematic representation of red mud activation procedure

4.4 Experimental Procedure

Hydrothermal gasification experiments are carried out in batch autoclave reactor system as shown in Fig. 4-5 and the analysis equipments for the products are given in Table 4-4. For the batch autoclave reactor system, experimental procedure may be explained briefly: As a first step, the feedstock solution is fed to the reactor and the cover of the reactor is closed in a very tight way to avoid gas leakages under high pressure. The air was displaced with an inert gas stream (nitrogen) and the valves are closed. The operating temperatures are selected as 300°C (sub critical), 400°C (near critical), 500°C and 600°C (supercritical). The reactor system was heated to the desired temperature at 5 K min⁻¹ and held at this temperature for 1 h and it was cooled to ambient temperature. The amount of gaseous product was measured with the help of gasometer, filled with CO₂. The gas sample is taken using specially designed gas-sampling syringes for gas chromatography (GC) analysis. The composition of gaseous products was determined by GC instrument. The products remaining in the reactor were washed with water and then it was filtered to separate solid residue. At the end of this filtration, liquid and solid parts analyzed by HPLC, Colorimeter and TOC equipments in the laboratory.



Figure 4-5. Batch autoclave reactors while the experiments are being performed.

4.5 Analysis equipments

Table 4-4. Equipments used in the analysis of alkaloid wastewater and hydrothermal gasification studies

Products	Compounds	Equipment
Gaseous	CO, CO ₂ , H ₂ , CH ₄ ve C ₂ -C ₄ hydrocarbons	GC (HP 7890A)
Aqueous	Alcohols and sugars	HPLC (Agilent 1200 Series)
	Total Organic Carbon in in aqueous product and raw feedstock	TOC (Shimadzu TOC-VCPH)
	Possible compounds (136 chemicals)	LC/MS-MS (Shimadzu LC-MS 8030)
Solid residue	Total Organic Carbon	TOC-SSM (Solid Sample Module, SSM-5000A)

4.5.1 Gaseous Product Analysis

The composition of the gaseous products (H₂, CO₂, CO, CH₄, C₂H₆, C₂H₄, C₃H₈, and C₄H₁₀) were determined with gas chromatography (Agilent Technologies HP 7890A, USA) with a standard deviation of $\pm 2\%$. C₂H₆, C₂H₄, C₃H₈, and C₄H₁₀ are referred to as C₂ - C₄ hydrocarbons in the following sections for simplicity. It is equipped with serially arranged 7 columns (Hayesep Q 80/100 mesh (0.5 m long \times 2 mm i.d.), a Hayesep Q 80/100 mesh (1.8 m long \times 2 mm i.d.), a Molsieve 5A 60/80 mesh (2.4 m long \times 2 mm i.d.), a Hayesep Q 80/100 mesh (0.9 m long \times 2 mm i.d.), a Molsieve 5A 60/80 mesh (2.4 m long \times 2 mm i.d.), a DB-1 (pre-column), and an HP-Plot Al₂O₃ S (25 m long \times 0.32 mm i.d.). The 3 detectors were serially connected with a special adapter (2 thermal conductivity detectors (TCD) and a flame ionization detector (FID)). Calibration was accomplished with a standard gas mixture from the HatGaz Company in Kocaeli, Turkey. The oven temperature program was: 60°C isothermal for 1 min, 20°C min⁻¹ to 80°C, and 30°C min⁻¹ to 120°C isothermal for 2.66 min. The carrier gas used was Helium. Technical details are given in Table 4-5 and the picture of GC is given in Fig. 4-6 in our laboratory.



Figure 4-6. Gas Chromatography (AGILENT, GC 7890A) Gas Chromatography (AGILENT, GC 7890A)

Table 4-5. Technical features and operating conditions of HP GC 7890A gas chromatography.

Columns	Column 1 Hayesep Q 80/100 mesh (0.5m long x 2mm i.d.) Column 2 Hayesep Q 80/100 mesh (1.8m long x 2mm i.d.) Column 3 Molsieve 5A 60/80 mesh (2.4m long x 2mm i.d.) Column 4 Hayesep Q 80/100 mesh (0.9m long x 2mm i.d.) Column 5 Molsieve 5A 60/80 mesh (2.4m long x 2mm i.d.) Column 6 DB-1 (pre-column) Column 7 HP-Plot Al ₂ O ₃ S (25m long x 0.32mm i.d.)
Oven	60°C isothermal for 1 min.
Temperature	20°C/min. to 80°C
Program	30°C/min. to 120°C isothermal for 2.66 min.
Mobile phase	Helium
Operating mode	Split (Ratio= 80:1, Flowrate= 60 mL/min)
Injection Temperature	250°C
Detector	Front signal – FID- 250°C
Temperature	Back signal – TCD- 250°C Auxiliary signal – TCD- 250°C

4.5.2 Liquid Product Analysis

Amounts of total carbon (TC) and inorganic carbon (IC) in liquid phase were analyzed by TOC analyzer, shown in Fig. 4-7, to calculate the conversion at the end of the reaction. The amounts of chemical oxygen demand were measured

with the COD analysis equipment, shown in Fig. 4-8, of Merck Company (Thermo-reactor and spectrophotometer) and Merck COD test kits in the range of 500-10.000 mg/L and 10-150 mg/L.

The amounts of sugar monomers present in the aqueous solutions were analyzed by High Performance Liquid Chromatography (HPLC-RI). The raw wastewater and the aqueous product of the hydrothermal gasification, of the alkaloid wastewater without a catalyst, were analyzed using Liquid Chromatography with mass spectroscopy, MSMS (LC/MS-MS) to determine the compounds degraded in the gasification studies. The samples are prepared for LC/MS-MS using some steps as defined in a previous study (Bural, 2008).



Figure 4-7. Total Organic Carbon Analyzer (SHIMADZU TOC-VCPH, JAPAN)



Figure 4-8. COD analysis equipments (thermo-reactor and spectrophotometer).

4.6 Experimental Studies Completed

Experimental studies during the thesis periods are summarized in Tables 4-6 to 4-10.

Table 4-6. Non-catalytic and catalyst amount optimization with K_2CO_3 (3:300°C, 4:400°C, 5:500°C, 6:600°C, K: K_2CO_3 , K1:0.125g of K_2CO_3 , K2:0.250g of K_2CO_3 , K3:0.375g of K_2CO_3 , K4:0.500g of K_2CO_3 , K5:0.625g of K_2CO_3):

Catalyst amount, g	Reaction temperature, °C			
	300	400	500	600
-	AF-T3	AF-T4	AF-T5	AF-T6
0.125	AF-T3K1	AF-T4K1	AF-T5K1	AF-T6K1
0.250	AF-T3K2	AF-T4K2	AF-T5K2	AF-T6K2
0.375	AF-T3K3	AF-T4K3	AF-T5K3	AF-T6K3
0.500	AF-T3K4	AF-T4K4	AF-T5K4	AF-T6K4
0.625	AF-T3K5	AF-T4K5	AF-T5K5	AF-T6K5

Table 4-7. Pressure effect experiments (P1:200 bar, P2:275 bar, P3:350 bar, P4:425 bar)

No catalyst, 500°C			
200 bar (10 mL)	275 bar (12.5 mL)	350 bar (15 mL)	425 bar (20 mL)
AF-T5-P1	AF-T5-P2	AF-T5-P3	AF-T5-P4
No catalyst, 600°C			
200 bar (8 mL)	275 bar (10 mL)	350 bar (12.5 mL)	425 bar (15 mL)
AF-T6-P1	AF-T6-P2	AF-T6-P3	AF-T6-P4
In the presence of K₂CO₃, 500°C			
200 bar (10 mL+ 0.333g K ₂ CO ₃)	275 bar (12.5 mL+ 0.416g K ₂ CO ₃)	350 bar (15 mL + 0.500 g K ₂ CO ₃)	425 bar (20 mL+ 0.666g K ₂ CO ₃)
AF-T5K-P1	AF-T5K-P2	AF-T5K-P3	AF-T5K-P4
In the presence of K₂CO₃, 600°C			
200 bar (8 mL+ 0.266 g K ₂ CO ₃)	275 bar (10 mL+ 0.333 g K ₂ CO ₃)	350 bar (12.5 mL+ 0.416 g K ₂ CO ₃)	425 bar (15 mL+ 0.500 gK ₂ CO ₃)
AF-T6K-P1	AF-T6K-P2	AF-T6K-P3	AF-T6K-P4

Table 4-8. Activated red mud catalyst experiments

A (Precipitation with NH₃)	A1 (Calcination at 500°C)	
	A2 (10% Ni)	A2-1 (reduction of A2 by NaBH ₄)
	A3 (20% Ni)	A3-1 (reduction of A3 by NaBH ₄)
	A4 (30% Ni)	A4-1 (reduction of A4 by NaBH ₄)
B (Precipitation with K₂CO₃)	B1 (Calcination at 500°C)	
	B2 (10% Ni)	B2-1 (reduction of B2 by NaBH ₄)
	B3 (20% Ni)	B3-1 (reduction of B3 by NaBH ₄)
	B4 (30% Ni)	B4-1 (reduction of B4 by NaBH ₄)

Precipitation of red mud with K_2CO_3 and NH_3 was investigated as two different catalyst group. The main purpose was to eliminate Na_2O , CaO , and other soluble compound in acid and increase the percentage of other compounds to enhance the effectiveness of the catalyst. It was expected that the gaps in catalyst surface would be different because of the molecular structure and sizes of K_2CO_3 and NH_3 are distinct. The effectiveness of activated red mud which are precipitated by NH_3 would be higher due to bigger size of molecule. The BET analysis results in section 5.3.1.5 shows catalysts in “A group” has larger surface area and verified this expectation.

Table 4-9. Activated red mud catalyst (A group) with K_2CO_3 experiments (K: K_2CO_3 addition)

AK (Precipitation with NH_3)	A1 (Calcination at 500 °C)	
	A2-K (10% Ni)	A21-K (reduction of A2 by $NaBH_4$)
	A3-K (20% Ni)	A31-K (reduction of A3 by $NaBH_4$)
	A4-K (30% Ni)	A41-K (reduction of A4 by $NaBH_4$)

Table 4-10. Experiments with alkali and Nickel-based catalysts

		Reaction temperature (°C)	Catalyst amount/ volume of wastewater
Alkali catalysts	NaOH	500	0.5 g/15 mL
	KOH	500	0.5 g/15 mL
	K_2CO_3	500	0.5 g/15 mL
	Na_2CO_3	500	0.5 g/15 mL
Nickel-based catalyst	Raney Nickel 4200	500	0.5 g/15 mL
	Raney Nickel 2800	500	0.5 g/15 mL
	Activated Nickel	500	0.5 g/15 mL
	Nickel- Silica/Alumina	500	0.5 g/15 mL

5. RESULTS AND DISCUSSION

Carbon gasification efficiency (g C in gaseous/g C in biomass), carbon liquefaction efficiency (g C in aqueous/g C in biomass) and residue (g C in residue/g C in biomass) were expressed by using following formulas;

$$\text{Carbon gasification efficiency (CGE, \%)} = \frac{\sum_i n_i C_i \frac{PV_{gas}}{RT} M}{V_{feed} TOC_{ww}} \times 100$$

$$\text{Carbon liquefaction efficiency (CLE, \%)} = \frac{TOC_{aq} V_{aq}}{V_{feed} TOC_{ww}} \times 100$$

$$\text{Residue efficiency (RE, \%)} = \frac{TOC_R \kappa}{V_{feed} TOC_{ww}} \times 100$$

5.1. Influence of Temperature and Catalyst amount on Gasification of Opium Alkaloid Wastewater

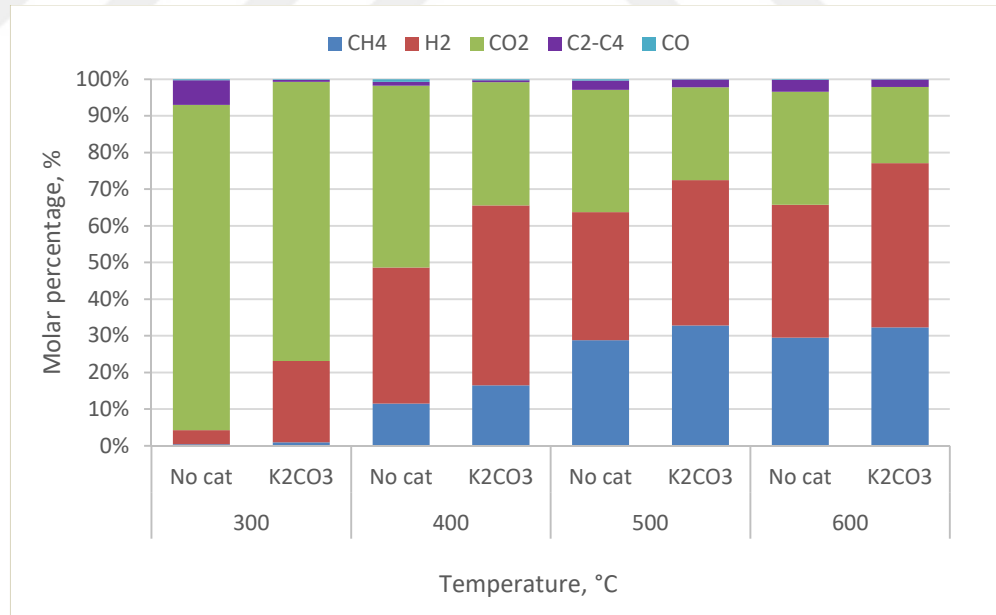


Figure 5-1. Temperature and catalyst effects (0.5 g of K₂CO₃) on the gaseous product composition in hydrothermal gasification of alkaloid wastewater.

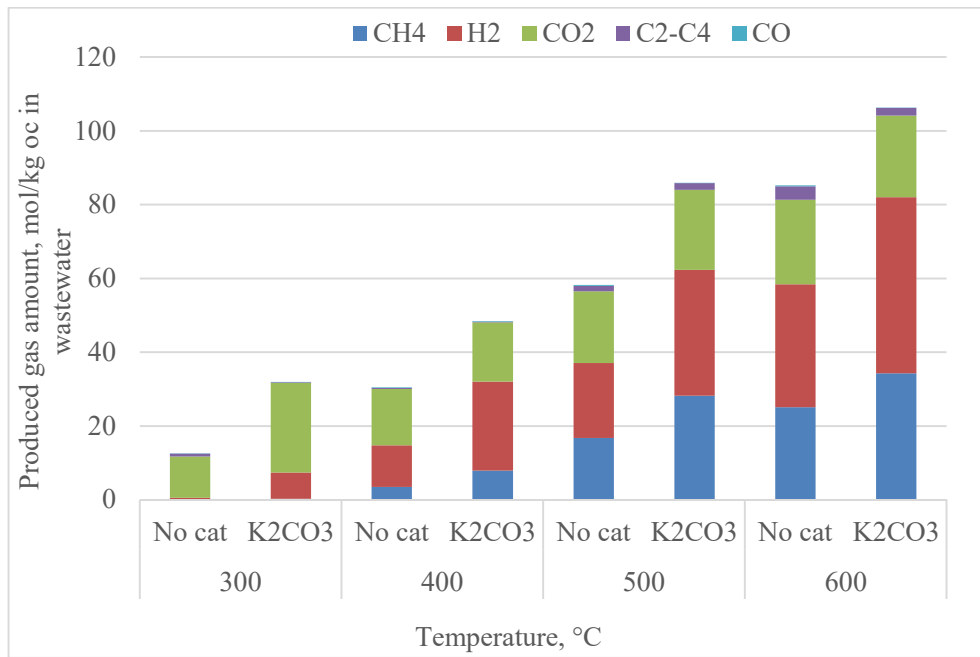


Figure 5-2. Temperature and catalyst effects (0.5 g of K₂CO₃) on the gaseous product yields (mol/kg organic carbon in wastewater) composition in hydrothermal gasification of alkaloid wastewater.

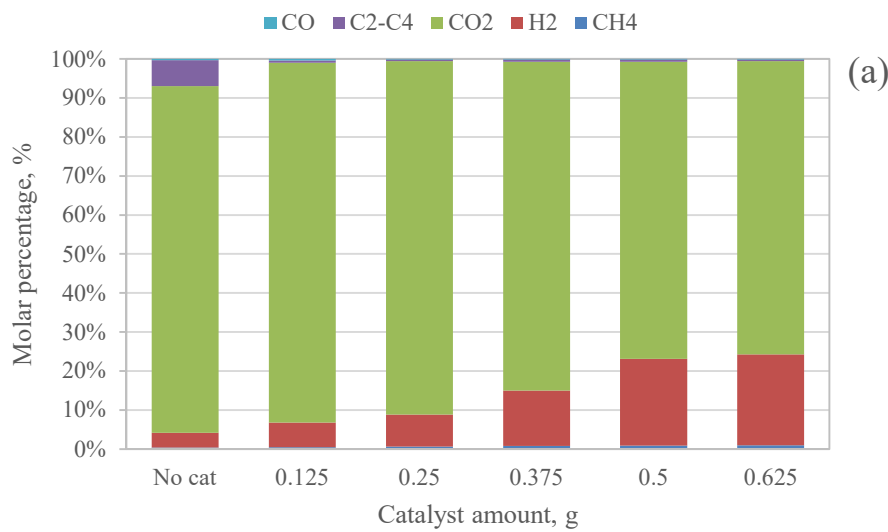


Figure 5-3. The effects of the catalyst amount on the gaseous product composition in hydrothermal gasification of alkaloid wastewater at various reaction temperatures (a) 300°C, (b) 400°C, (c) 500°C, and (d) 600°C).

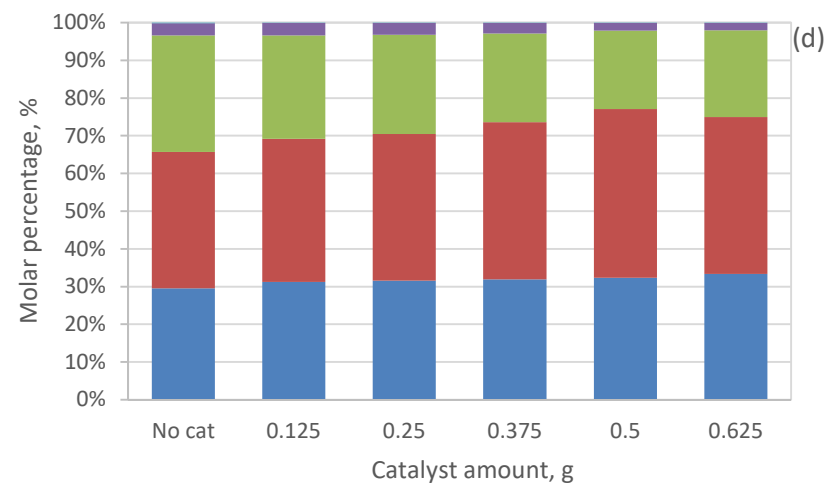
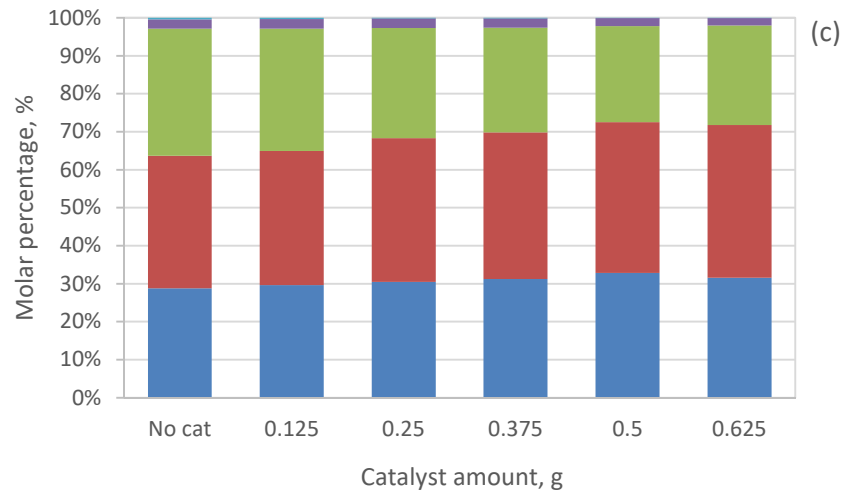
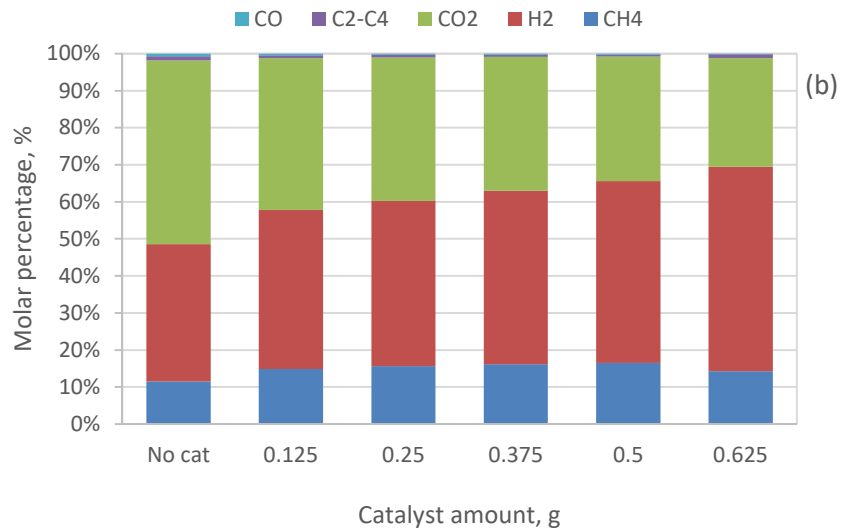


Figure 5.3. The effects of the catalyst amount on the gaseous product composition in hydrothermal gasification of alkaloid wastewater at various reaction temperatures (a) 300°C, (b) 400°C, (c) 500°C, and (d) 600°C (continued).

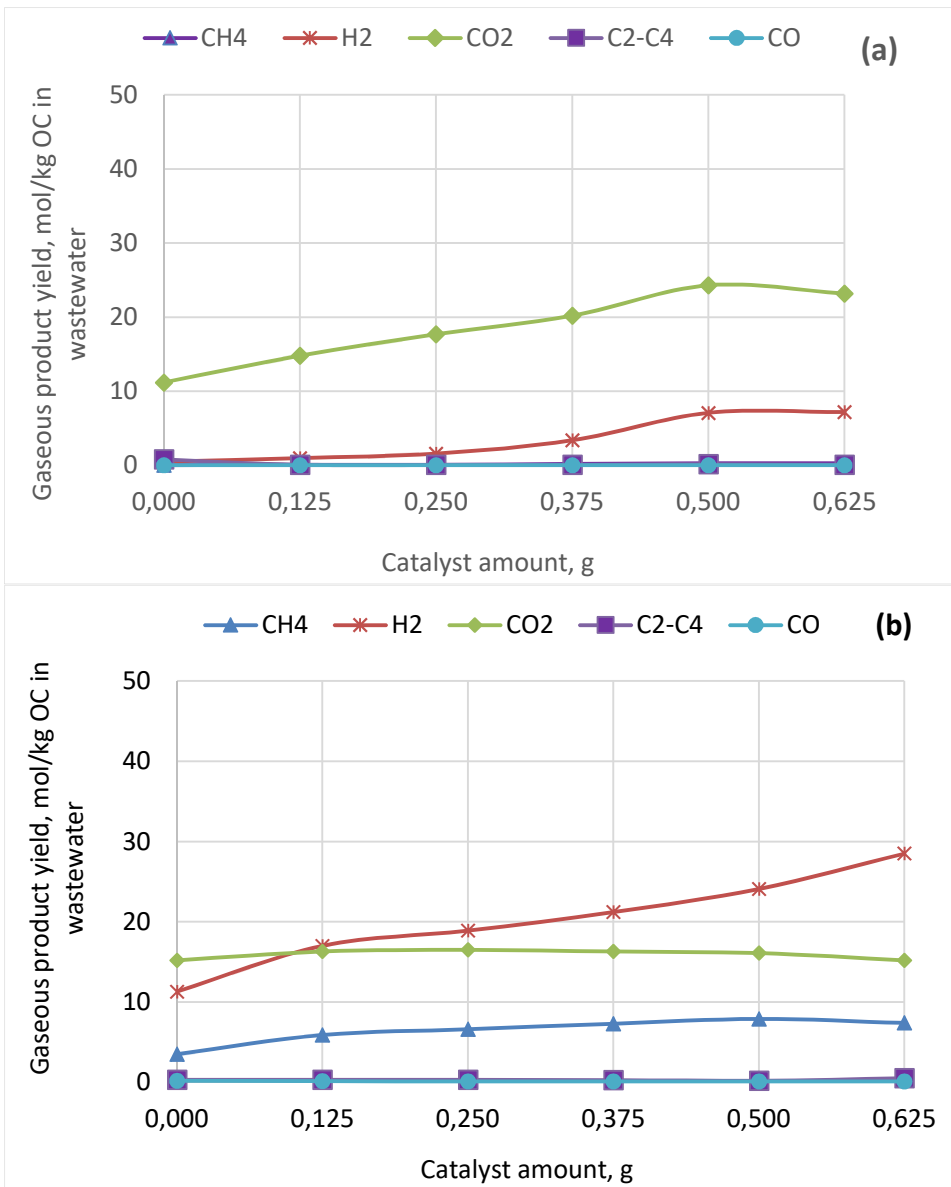


Figure 5-4. The effects of the catalyst amount on the gaseous product yields in hydrothermal gasification of alkaloid wastewater at various reaction temperatures (a) 300°C, and (b) 400°C.

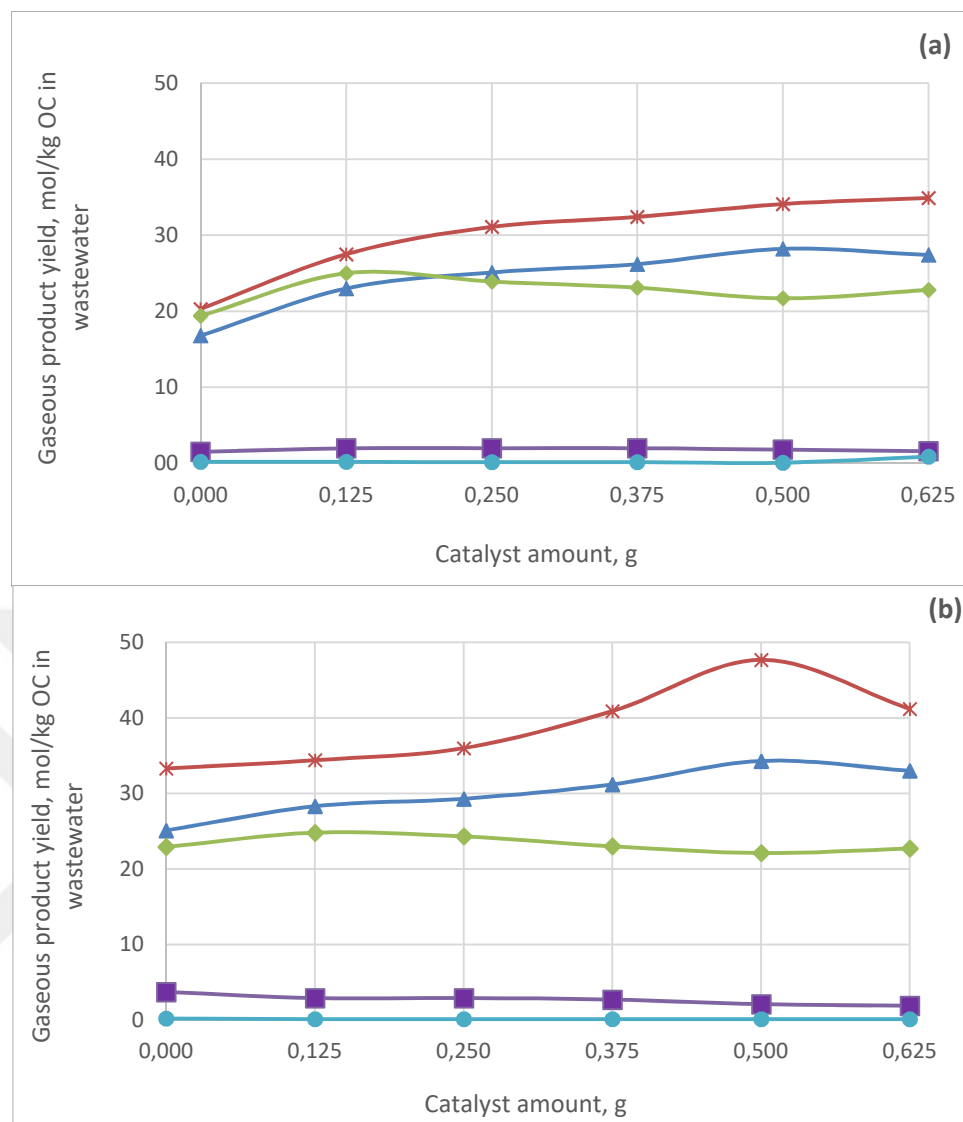


Figure 5-5. The effects of the catalyst amount on the gaseous product yields in hydrothermal gasification of alkaloid wastewater at various reaction temperatures (a) 500°C, and (b) 600°C.

Table 5-1. Reaction conditions and experimental results in the presence of various amounts of K_2CO_3 and at 300°C & 400°C.

<i>Exp Code</i>	<i>T, °C</i>	<i>P, bar</i>	<i>Catalyst</i>	<i>Catalyst Amount</i>	<i>Gaseous Product Yield, mol gas/kg C in ww</i>	<i>CGE, %</i>	<i>TOC_{RE}, %</i>	<i>COD_{RE}, %</i>
AF-T3	300	80	-	-	12.59	14.5	26.0	9.3
AF-T4	400	240	-	-	30.5	23.7	41.0	37.1
AF-T3-K1	300	115	K_2CO_3	0.125	16.0	17.7	33.2	8.81
AF-T3-K2	300	90	K_2CO_3	0.250	19.5	21.6	35.9	17.4
AF-T3-K3	300	90	K_2CO_3	0.375	23.9	23.9	41.2	18.2
AF-T3-K4	300	110	K_2CO_3	0.500	31.9	29.8	49.2	19.5
AF-T3-K5	300	120	K_2CO_3	0.625	30.9	29.0	49.3	19.1
AF-T4-K1	400	255	K_2CO_3	0.125	39.7	27.8	47.4	40.8
AF-T4-K2	400	260	K_2CO_3	0.250	42.4	28.8	49.8	45.9
AF-T4-K3	400	240	K_2CO_3	0.375	45.2	29.4	55.2	43.7
AF-T4-K4	400	235	K_2CO_3	0.500	48.4	29.9	58.3	47.3
AF-T4-K5	400	230	K_2CO_3	0.625	51.7	28.7	57.0	51.4

Table 5-2. Reaction conditions and experimental results in the presence of various amounts of K_2CO_3 and at 500°C & 600°C.

<i>Exp Code</i>	<i>T, °C</i>	<i>P, bar</i>	<i>Catalyst</i>	<i>Catalyst Amount</i>	<i>Gaseous Product Yield, mol gas/kg C in ww</i>	<i>CGE, %</i>	<i>TOC_{RE}, %</i>	<i>COD_{RE}, %</i>
AF-T5	500	365	-	-	58.2	47.9	74.5	75.8
AF-T6	600	440	-	-	85.2	68.5	85.6	88.7
AF-T5-K1	500	360	K_2CO_3	0.125	77.7	64.0	84.9	87.3
AF-T5-K2	500	355	K_2CO_3	0.250	82.3	65.2	87.1	88.0
AF-T5-K3	500	350	K_2CO_3	0.375	83.9	65.4	88.3	85.2
AF-T5-K4	500	355	K_2CO_3	0.500	85.9	65.6	89.3	88.9
AF-T5-K5	500	322	K_2CO_3	0.625	87.6	65.3	92.0	89.4
AF-T6-K1	600	425	K_2CO_3	0.125	90.5	72.8	90.7	91.8
AF-T6-K2	600	445	K_2CO_3	0.250	92.6	73.0	91.6	91.6
AF-T6-K3	600	450	K_2CO_3	0.375	97.9	73.6	92.2	92.2
AF-T6-K4	600	455	K_2CO_3	0.500	106.3	74.0	92.8	92.8
AF-T6-K5	600	442	K_2CO_3	0.625	98.9	72.8	96.6	95.1

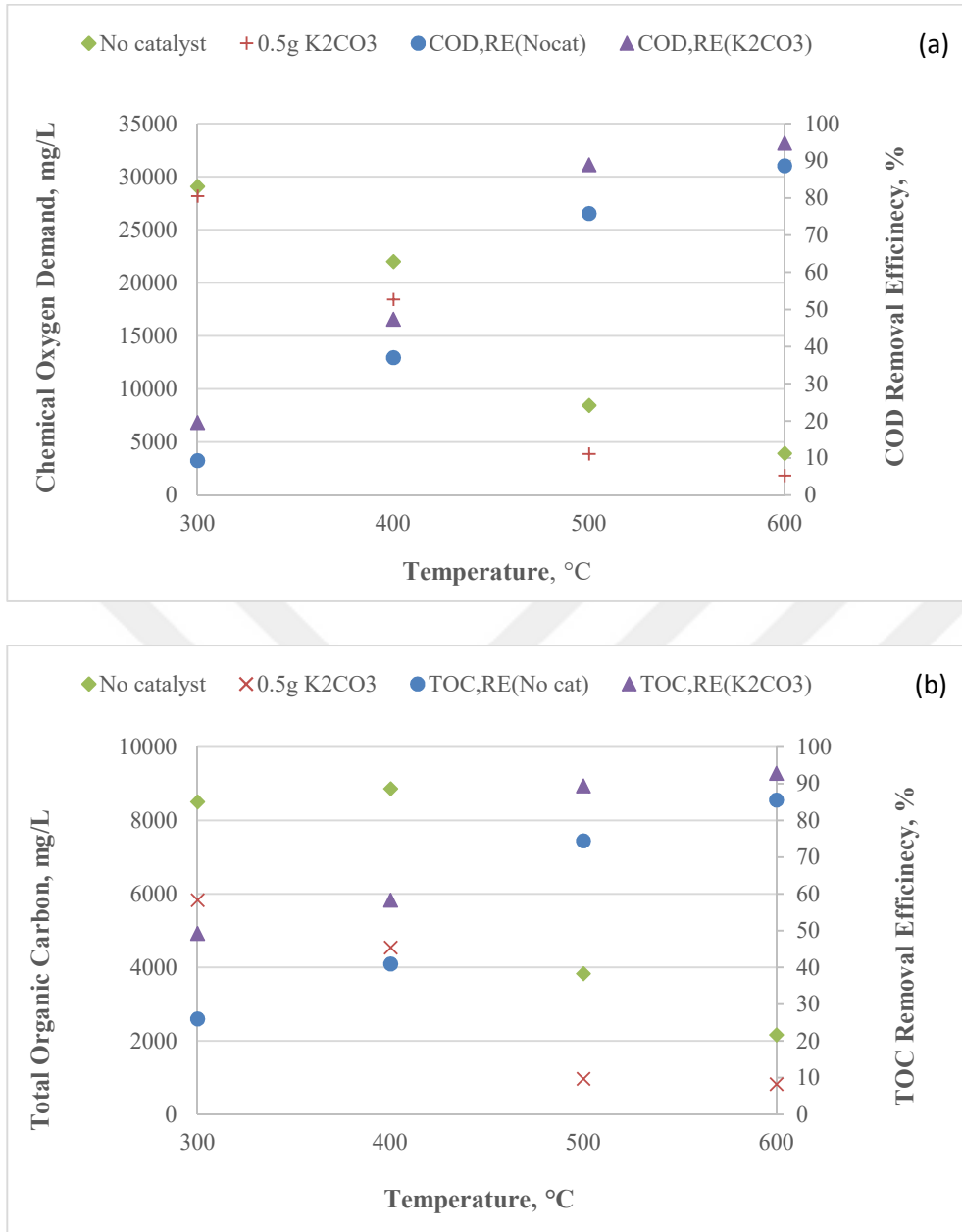


Figure 5-6. The effects of temperature and catalyst (0.5g K₂CO₃) on TOC values and TOC removal efficiencies (a) and COD values and COD removal efficiencies (b) in hydrothermal gasification of alkaloid wastewater at various reaction temperatures 300°C, 400°C, 500°C, and 600°C.

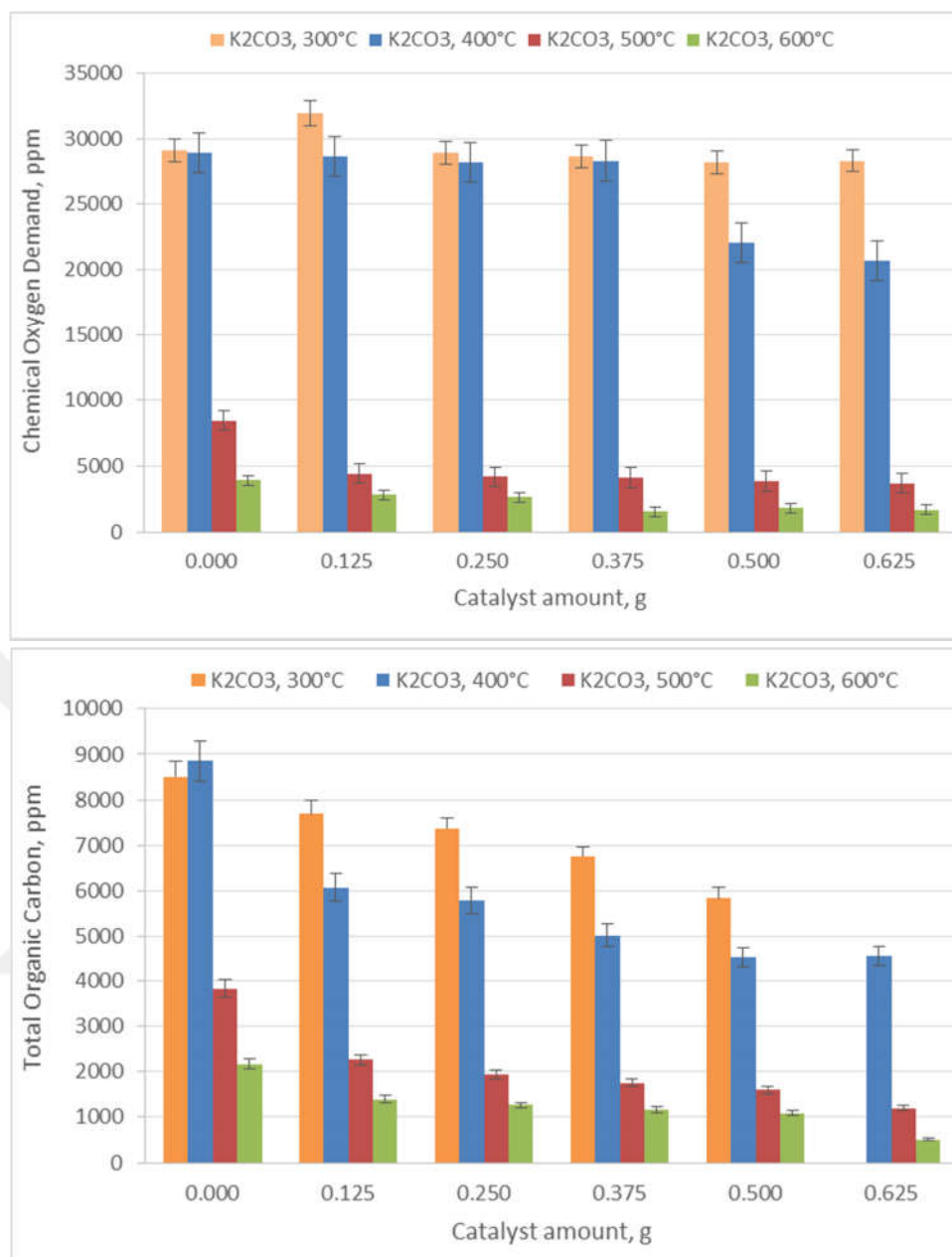


Figure 5-7. The effects of various amount of catalyst on TOC and COD values in hydrothermal gasification of alkaloid wastewater at various reaction temperatures 300°C, 400°C, 500°C, and 600°C.

5.1.1 Carbon Gasification Efficiencies (CGE, %), and Amount of Produced gas (mol gas/kg C in wastewater)

The CGE values and the produced gas amounts are shown in Table 5-1 and Table 5-2 at 300°C, 400°C, 500°C, and 600°C in the absence and presence of different amounts of catalysts. The raw alkaloid wastewater fed to the reactor in this study has a TOC content of 11,500 ppm. The gas amounts and gasification

efficiencies obtained at the end of the hydrothermal gasification were calculated based on the organic carbon in the wastewater. The dominant parameter of the gasification of carbon in the alkaloid wastewater is temperature as observed, which is similar in the HTG of a biomass (Lu et al. 2011; Madenoğlu et al. 2015). As the reaction temperature increase from 300 to 600°C, the CGE and the total number of gaseous products increased from 14.5 to 74% and 12.59 to 85.2 mol/kg C, respectively without catalyst. The catalyst addition promotes CGE and produced gas amounts generally. Increasing the amount of catalyst to 0.5 g of K_2CO_3 enhanced the CGE by 3-14% at 300°C, 4-6% at 400°C, 17% at 500°C, and 5.5% at 600°C approximately. The literature findings supports that CGE is promoted by alkali catalyst addition. In the work of Schmieder et al., they observed complete gasification by addition of KOH or K_2CO_3 (Schmieder and Abeln, 2000). Chakinala studied with glycerol at 600°C and 250 bar with a 5s of residence time and found that K_2CO_3 enhanced the glycerol gasification efficiency up to a maximum of 84% (Chakinala et al., 2010). CGE values standard deviations are ranges between 1.6-4.8%.

The produced gas amounts reached the maximum with the addition of K_2CO_3 at 31.9, 51.7, 87.6, and 106.3 mol/kg C at 300°C, 400, 500, and 600°C. Increasing the amount of K_2CO_3 does not affect the CGE substantially and the total gas amount is increased slightly at above reaction temperature of 400°C. The most favorable amount of catalyst was found as 0.500 g of K_2CO_3 , since no increase was observed with 0.625 g of K_2CO_3 compared with 0.500 g at 600°C. The reason should be that the equilibrium was provided at the specified reaction temperature with catalyst and so the increase in amount of catalyst did not make an enhancement. In the work of D'Jesús et al. (D'Jesús, and Boukis, 2006) varying concentrations from 0 to 500 mg/L of potassium (in the form of $KHCO_3$) were used as a catalyst. They observed that gasification yield increased from 82% to 92% by increasing the catalyst amount. The higher potassium concentrations, above 500 ppm, do not promote a higher gasification yield. A similar trend was observed in terms of existence of most favorable amount of catalyst even the level of the concentration of potassium is different in this study. Addition of more K_2CO_3 did

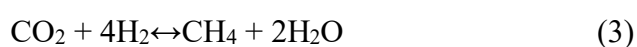
not make an increment on H₂ and CO₂ yields in the study of Sinag et al. (2012), either (Sinag and, Kruse, 2012).

The sum of the desired gaseous yields (CH₄ and H₂) increased with increasing temperature from 14.8 to 54.94 mol/kg C without a catalyst in the temperature range of 400-600°C while there is only 5.5 mol H₂/kg C and almost never CH₄ at 300°C. The ratio of the sum of the desired gaseous product in the total gas product increased from 48.5 to 65.7 % because of the effects of the temperature increments. 74% of total organic carbon was converted to gaseous product at 600°C and at 0.500 g of catalyst as highest, and remaining was converted to aqueous product and taken as residue (tar) from the reactor.

5.1.2 The Composition and Yields of the Gaseous Product

The composition and yields of the gaseous product without a catalyst and with various amounts of K₂CO₃ are given in Figs. 5-3 to 5-5. For comparison, the results obtained in the HTG of the alkaloid wastewater without a catalyst are given with the results of the determined the most appropriate catalyst amount (0.5 g) in Fig. 5-1 and 5.2. The catalysts used in SCWG studies may be categorized as alkali, metal, metal oxide and carbon-based. The purpose of catalyst addition is to promote gasification, to economize the process providing to study at lower temperatures for similar product yields (Guo et al. 2010a). Alkali catalyst such as NaOH, KOH, Na₂CO₃, K₂CO₃ and Ca(OH)₂ catalyze the water gas shift reaction (reaction 4 given below), and produce more H₂ and CO₂ lowering CO yields (Kruse et al. 2000; Watanabe et al. 2003; Ali Sinag, Kruse and Schwarzkopf 2003; Ali Sinag, Andrea Kruse 2004; Yanik et al. 2008). Sinag et al. studied gasification of glucose in the presence of 0.5 wt. % K₂CO₃ and observed significant decrease in CO yield and higher H₂, CO₂, and CH₄ yields per mole of glucose. Akgül et al. (2012) investigated the effects of NaHCO₃ and the KHCO₃ on water-gas shift reaction at 10 and 23 MPa and 230–300°C and found that water-gas shift reaction is remarkably promoted at high salt concentrations but they did not obtain gas using only salt (Akgül and Kruse 2012).

The gasification behavior of alkaloid wastewater in supercritical water has not been examined in literature before. This wastewater is a plant derived waste containing carbohydrates and proteins in the amounts of 10,000 mg/L and 5,000 - 6,000 mg/L of protein (Bural, 2008), besides unrecovered alkaloids such as morphine, codeine, thebaine, and aniline, toluol, and vax-like compounds (Aydın 2002; Kaçar et al. 2003). The reactions proposed for biomass degradation can be given for this wastewater because of its plant originated structure.



The organic content of the wastewater is degraded to produce gaseous products such as CH₄, H₂, CO₂, and CO. Gaseous product distribution is highly affected by temperature and catalyst as seen in Figs 5-1 and 5-3. The yields of each gases are given in Figs 5-2 and 5-4 at various reaction temperatures and the addition of 0.5 g of K₂CO₃. The use of K₂CO₃ and an increase in temperature strongly promoted these reactions and the yields of CH₄, and H₂ were elevated to 34.3 and 47.7 mol/kg C, respectively. The yields of CH₄ increased from 3.5 to 25.1 mol/kg C with varying the temperature from 400 to 600°C without a catalyst. In the case of an added 0.5g of K₂CO₃, the yields of methane are increased at 400 and 500°C (125% and 68%, respectively) with a higher ratio than 600°C (37%). Comparison of the catalytic run at 500°C in the presence of 0.5g of K₂CO₃ and a non-catalytic run at 600°C, can be concluded that the use of a catalyst provides for a study at lower reaction temperature to obtain similar CH₄ and H₂ yields. The hydrogen yields are enhanced with the K₂CO₃ at the ratios of 113, 68, and 43% by increasing the temperature from 400°C to 600°C and from near 0 to 7.1 mol/kg C at 300°C.

Hydrogen is basically formed from the degradation of carbohydrate content of alkaloid wastewater and water gas-shift reaction as mentioned in literature (Lee et al. 2002; Ali Sinag et al., 2003; Guo et al. 2012). The formate salt can be shown as the source of this increase. Hence the CO is consumed in the formation reaction

of HCOO^-K^+ , the CO levels are observed very low in all catalytic runs while producing CO_2 and H_2 . Some portion of produced CO_2 may be solved in supercritical water medium and react to form methane via reaction (3). The reason of the decrease in CO_2 yields may be the result of methanation reaction and higher methane yields supports this explanation.

CO_2 yields are the third highest yields obtained in the gaseous product mixture. As it is emphasized in the work of Kıpçak et al. (2011), water in supercritical conditions dissociates to H^+ and OH^- ions and react with organic carbon and carbon containing compounds in wastewater to form CO and CO_2 . The water gas shift reaction (4) also contributes to the CO_2 yields while the yields of CO decreases. In our study, alkaloid wastewater has an alkalinity and potassium content varying at the ranges of 1500-5000 mg/L, and 4000-6000 mg/L, respectively according to the gathered information from factory authorities. This high potassium content of wastewater may also leads to decrease in percentage of CO_2 while the yields of CO_2 (mol/kg OC) are not affected significantly using a catalyst while increasing or elevating the reaction temperature slightly. This finding is similar to that of the Sinag et al. study with straw in the presence of K_2CO_3 . They explained the lower CO_2 ratios with catalyst by high K content (15wt.%) of straw (Schmieder et al., 2000; Ali Sinag et al., 2003).

The $\text{C}_2\text{-C}_4$ yields are very low and increase with temperature slightly while CO yields are lower than 1.0 mol/kg C at all studied temperatures. The amount of catalyst added cause some variations in gaseous product distributions at all studied temperatures while at 300°C and 400°C, this effect is seen markedly. Molar percentages of CO_2 obtained with 0.125 g of catalyst is reduced from 41% to 28% with 0.625 g of catalyst as the percentage of H_2 yields increase from 42 to 55% at 400°C. Hydrogen formation is accelerated with the addition of an alkali catalyst and wastewater acts as an H atom donor in supercritical conditions making a great affect in the yields of H_2 (Kruse and Dinjus 2007). The mole percent of H_2 is increased with an increase in the amount of catalyst generally. The molar fraction of CH_4 in the gaseous product mixture is not affected with a change in the catalyst amount directly. The variations in the yield of product gases are shown in Fig. 4

showing the effect of temperature and catalyst amounts. A 0.5 g of K_2CO_3 can be evaluated as the most favorable amount for the H_2 and CH_4 yields, since the total yields reach the maximum at this amount for 500 and 600°C reaction temperatures. The CO and $C_2 - C_4$ yields are slightly decreased with the increasing amount of K_2CO_3 with promoted degradation and methanation reactions. The literature findings verified that as the alkali catalyst amount/concentration rise the yields/percentage of the CH_4 and H_2 increases (Yan et al. 2007). The composition of CH_4 and H_2 are enhanced with the higher KOH concentrations at the ratios of about 5% and 3.7%, respectively. The composition of the gaseous were determined with gas chromatography with a standard deviation of $\pm 2\%$. Standard deviations for the gaseous product compositions varied within 1.8-3.9% for all cases according to the repetitions done for each case. Alkali catalysts enhanced gasification while the effect of the catalyst on gaseous product yields depend on the biomass contents (Yanik et al. 2008). Muangrat et al. (2010) investigated various alkali catalysts and ordered the effectiveness in H_2 production as: $NaOH > KOH > Ca(OH)_2 > K_2CO_3 > Na_2CO_3 > NaHCO_3$ (Muangrat et al. 2010).

5.1.3 Variation of TOC and COD Values and Removal Efficiencies

Alkaloid wastewater used in this study has a COD of 35,000 ppm and a TOC of 15,000 mg/L. Treated alkaloid wastewater should have a COD below 1,500 ppm for a safe discharge as indicated in the WPCR, 2004 that is shown in Table 1. An approximate COD removal efficiency of 95.7% is needed to provide this limit for the water with a specified COD content. As reported in literature so far, the best COD removal rate is 88% by biological treatment of raw wastewater with an initial chemical oxygen demand of 27.7 g/L (Aytimur and Atalay 2004) with a treatment period of 6 days. There are very few effective treatment studies on this wastewater and some of them were already accomplished with pre-treated or diluted alkaloid wastewater and/or proposed as an advanced or pretreatment method. There is no suggested alternative method to reduce the COD of the original raw wastewater coming from the plant to the levels of 1,500 mg/L with a unique step in a short time and effectively. Table 5-1 and Table 5-2 shows that the best COD removal efficiency ratios obtained in our work is nearly 95 % at 600°C and within the catalyst amount range of 0.375 - 0.625 g of K_2CO_3 with a reaction time of only 1h.

These results are promising, considering the required COD removal efficiency of 95.7%, in the treatment of this wastewater by HTG. The operating cost should be decreased by integrating the energy generated with the produced hydrogen and methane. The elevated temperature reduced the COD and TOC values significantly. While the temperature increased from 300 to 600°C, the COD and TOC removal ratios also increased from 19 to 95% and 49 to 96%, respectively. COD and TOC content of the aqueous product and the removal efficiencies obtained within the studied range of temperature and catalyst amount was presented in Figs 5-6 and 5-7. It shows us that, the values of TOC and COD removal are close in 500°C and 600°C ($\text{COD}_{\text{RE}}=88.9\%$, and $\text{TOC}_{\text{RE}}=89.3\%$ at 500°C, $\text{COD}_{\text{RE}}=94.7\%$ and $\text{TOC}_{\text{RE}}=92.8\%$). In terms of process economy, 500°C should be selected. The most effective parameter in the COD and TOC destruction using SCWG is the reaction temperature as confirmed in many researchers found in literature (Yan et al. 2007; Lee 2010; Söğüt and Akgün 2011; Breinl 2015). Lee et al. (2010) found COD removal efficiencies above 99% at very high reaction temperature of 700°C, with Ni-Y/activated charcoal in the hydrothermal gasification of wastewater from food waste treatment processes. The increase in catalyst amount makes a slight increase in removal efficiencies. At all temperatures studied, varying increments between 4-10% in TOC and COD removals were observed. Standard deviations for TOC and COD results were given with error bars on Figure 5-7. The experiments were done at least 3 times to obtain repeatable results during whole thesis study. The deviation of the TOC of aqueous product varied between 3-10%, lower at high concentrations and higher at low concentrations because of dilution.

5.2 Influence of Pressure on Gasification of Opium Alkaloid Wastewater

Table 5-3. Reaction conditions, CGE, produced gas amount and TOC values of hydrothermal gasification of alkaloid wastewater in the absence of catalyst and at various reaction pressures.

	Reaction Temp. (°C)	Reaction Pressure (bar)	Set Pressure (bar)	CGE (%)	CLE (%)	TOC (mg/L)	Produced gas amount [mmol/L ww.]
AF-T5-P1	500	198	200	57.7	24.0	2766	875
AF-T5-P2	500	270	275	55.9	24.9	2866	819
AF-T5-P3	500	345	350	55.5	25.6	2943	767
AF-T5-P4	500	420	425	55.1	28.6	3296	750
AF-T6-P1	600	209	200	70.8	11.9	1367	1125
AF-T6-P2	600	270	275	70.3	12.2	1406	1083
AF-T6-P3	600	372	350	69.4	12.8	1466	1014
AF-T6-P4	600	430	425	68.7	14.4	1665	961

(CGE: Carbon Gasification Efficiency (%); CLE: Carbon Liquefaction Efficiency (%))

Table 5-4. Reaction conditions, CGE, produced gas amount and TOC values of hydrothermal gasification of alkaloid wastewater with K₂CO₃ catalyst and at various reaction pressures.

	Reaction Temp. (°C)	Reaction Pressure (bar)	CGE (%)	CLE (%)	TOC (mg/L)	Produced gas amount [mmol/L ww.]
AF-T5K-P1	500	198	78.0	7.0	799	1347
AF-T5K-P2	500	270	77.0	7.5	866	1292
AF-T5K-P3	500	345	74.9	8.4	966	1208
AF-T5K-P4	500	420	73.1	10.1	1165	1111
AF-T6K-P1	600	197	87.5	5.7	652	1608
AF-T6K-P2	600	270	87.2	6.0	686	1583
AF-T6K-P3	600	355	86.8	6.6	759	1555
AF-T6K-P4	600	425	85.8	7.1	826	1528

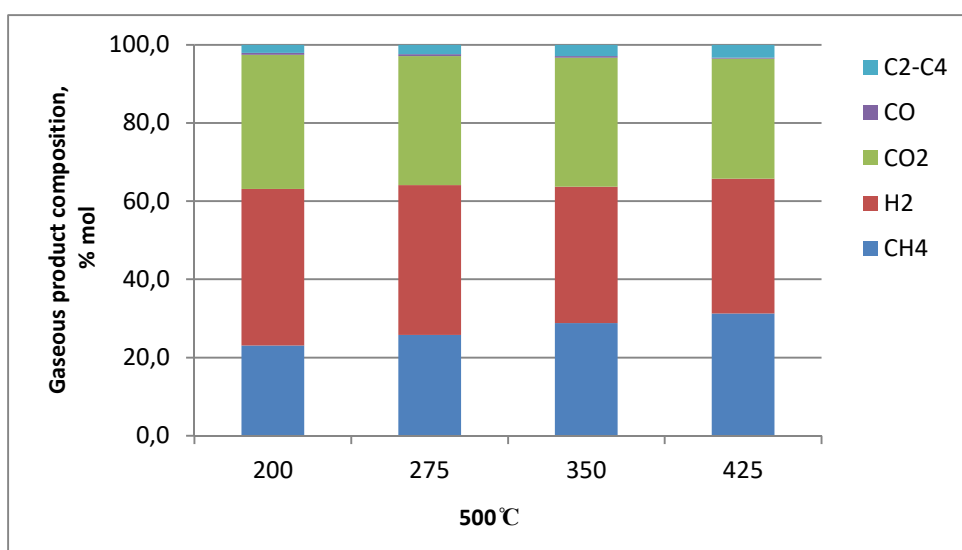


Figure 5-8. Effect of various operating pressures on gaseous product distribution in hydrothermal gasification of alkaloid wastewater at 500°C without catalyst.

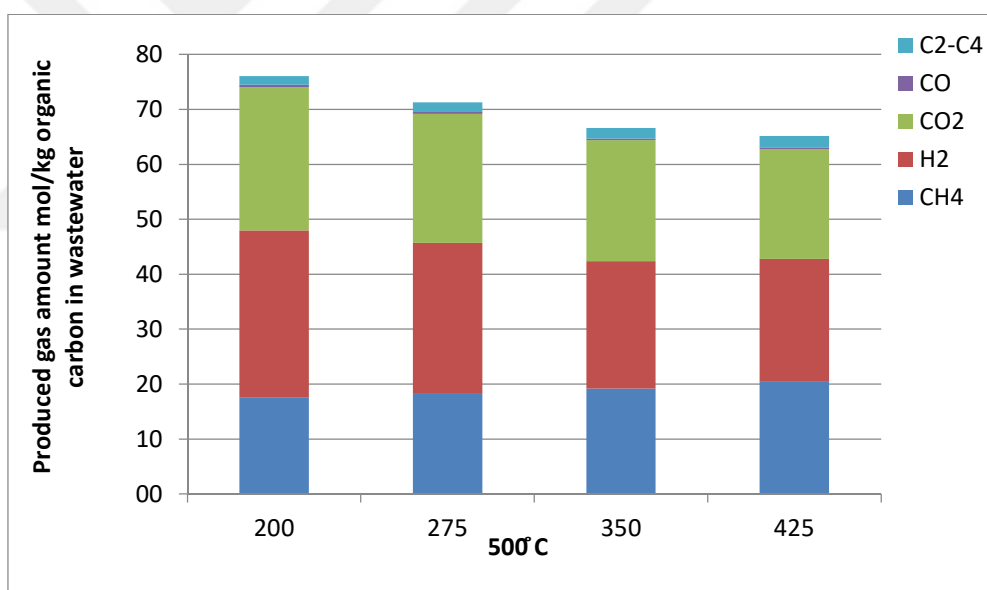


Figure 5-9. Effect of various operating pressures on gaseous product yields [mol/kg organic carbon in wastewater] in hydrothermal gasification of alkaloid wastewater at 500°C without catalyst.

Table 5-5. The effect of various operating pressures on gaseous product yields [mol/kg organic carbon in wastewater] in hydrothermal gasification of alkaloid wastewater at 500°C without catalyst.

mol/kg C in ww.	AF-T5-P1	AF-T5-P2	AF-T5-P3	AF-T5-P4
CH₄	17.6	18.4	19.2	20.4
H₂	30.4	27.3	23.2	22.4
CO₂	26.1	23.5	22.0	20.0
C₂-C₄	0.38	0.36	0.3	0.19
CO	1.6	1.7	1.9	2.2
Total	76.1	71.3	66.6	65.2

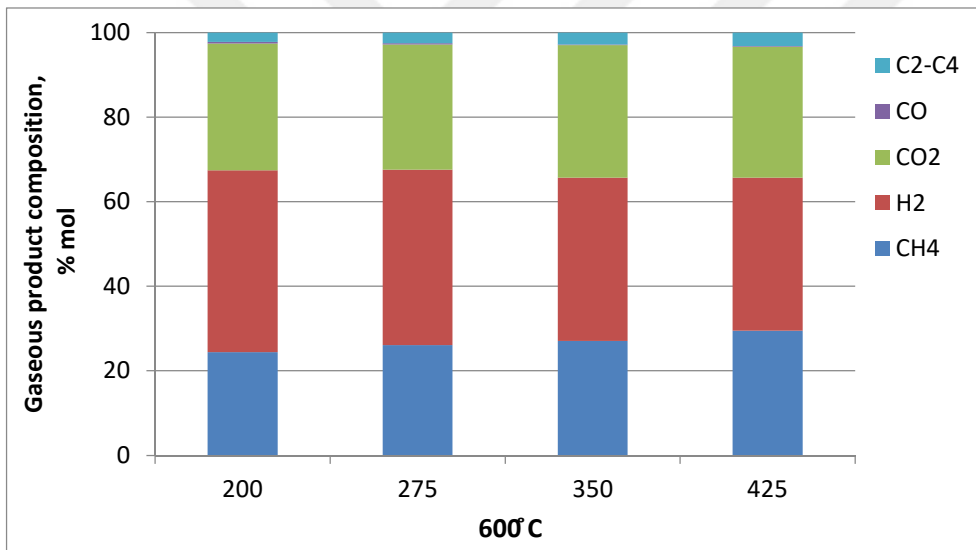


Figure 5-10. Effect of various catalysts on gaseous product distribution in hydrothermal gasification of alkaloid wastewater at 600°C without catalyst.

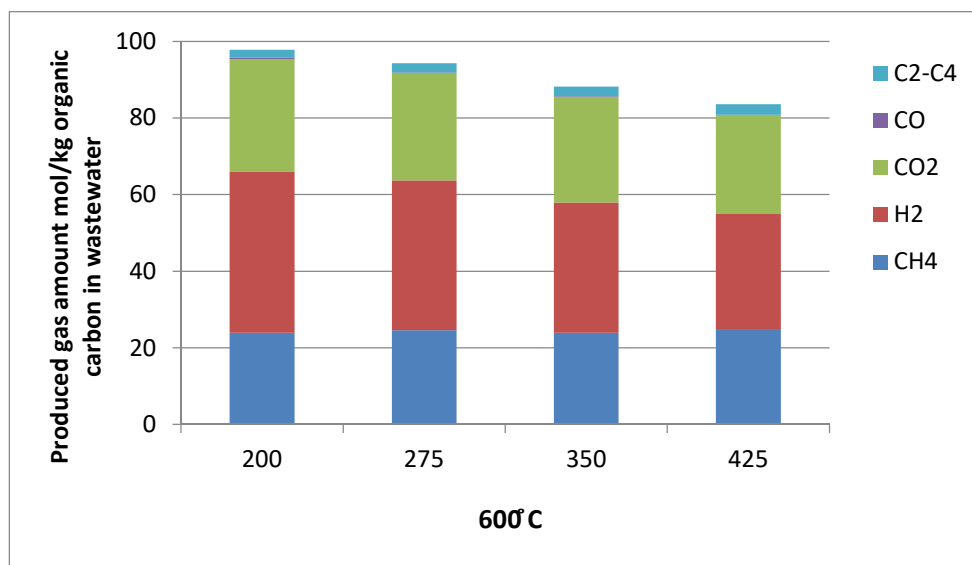


Figure 5-11. Effect of various catalysts on gaseous product yields in [mol/kg organic carbon in wastewater] in hydrothermal gasification of alkaloid wastewater at 600°C without catalyst.

Table 5-6. The effect of various operating pressures on gaseous product yields [mol/kg organic carbon in wastewater] in hydrothermal gasification of alkaloid wastewater at 600°C without catalyst

mol/kg C in ww.	AF-T6-P1	AF-T6-P2	AF-T6-P3	AF-T6-P4
CH ₄	23.9	24.6	23.9	24.7
H ₂	42.1	39.1	34	30.2
CO ₂	29.3	27.9	27.6	25.8
C ₂ -C ₄	0.4	0.28	0.18	0.16
CO	2.1	2.4	2.5	2.7
Total	97.8	94.28	88.18	83.56

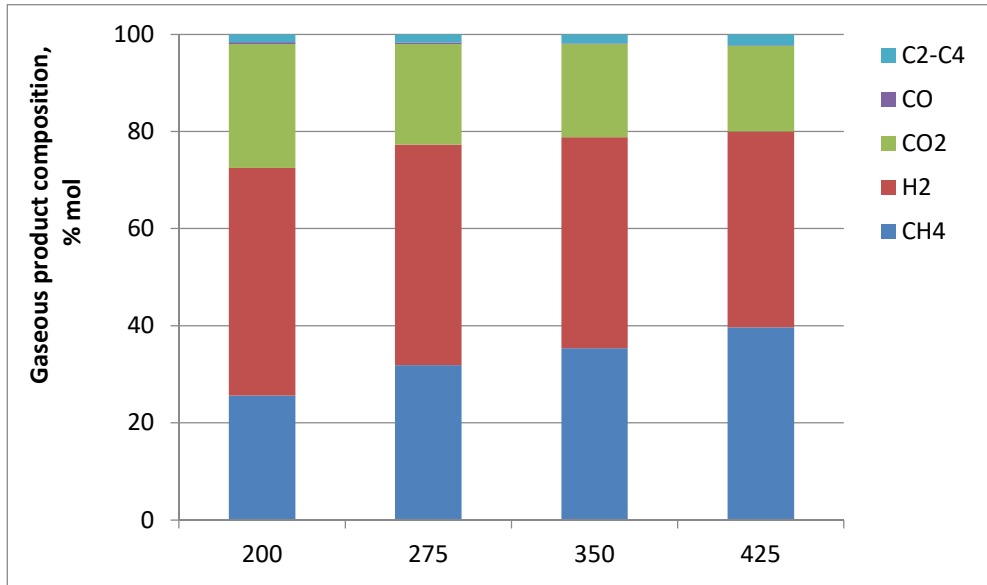


Figure 5-12. Effect of various operating pressures on gaseous product distribution in hydrothermal gasification of alkaloid wastewater at 500°C with K_2CO_3 catalyst.

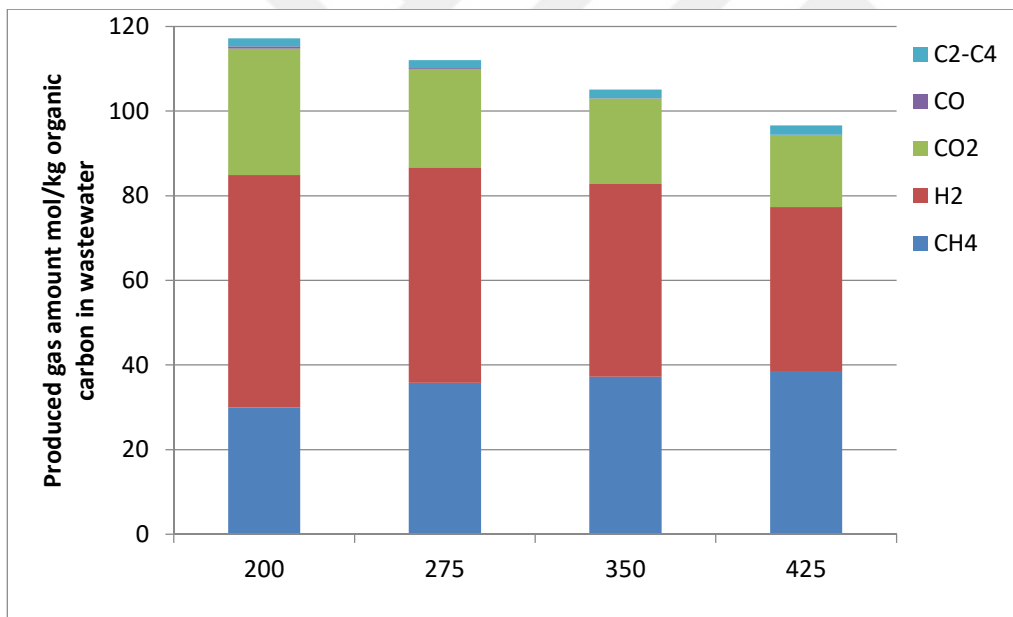


Figure 5-13. Effect of various operating pressures on gaseous product yields in [mol/kg organic carbon in wastewater] in hydrothermal gasification of alkaloid wastewater at 500°C with K_2CO_3 catalyst.

Table 5-7 The effect of various operating pressures on gaseous product yields [mol/kg organic carbon in wastewater] in hydrothermal gasification of alkaloid wastewater at 600°C without catalyst.

Mol/kg C in ww	AF-T5K-P1	AF-T5K-P2	AF-T5K-P3	AF-T5K-P4
CH₄	30.0	35.8	37.2	38.4
H₂	54.9	50.9	45.6	38.9
CO₂	29.9	23.2	20.2	17
C₂-C₄	0.5	0.3	0.1	0.1
CO	1.9	1.9	2	2.2
Total	117.2	112.1	105.1	96.6

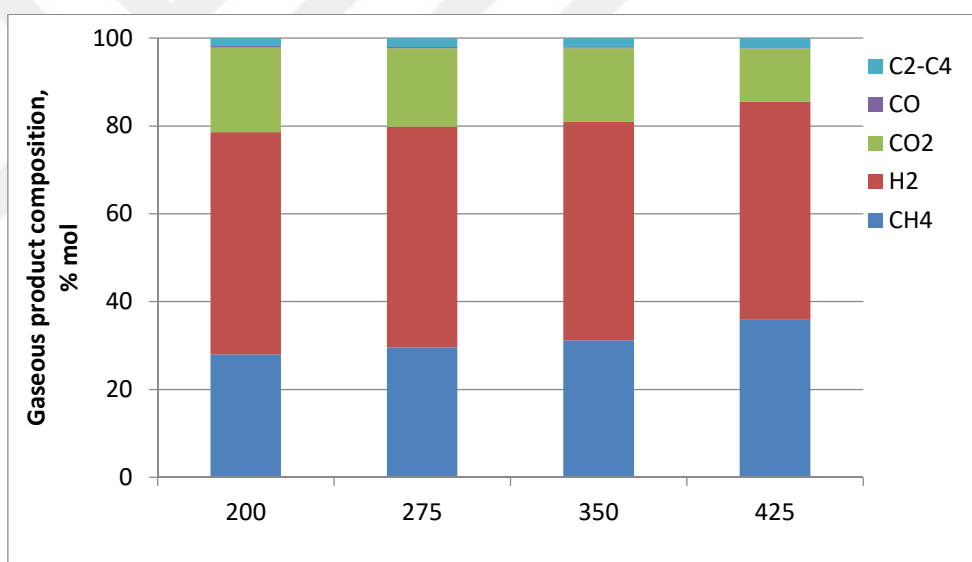


Figure 5-14. Effect of various operating pressures on gaseous product distribution in hydrothermal gasification of alkaloid wastewater at 600°C with K₂CO₃ catalyst.

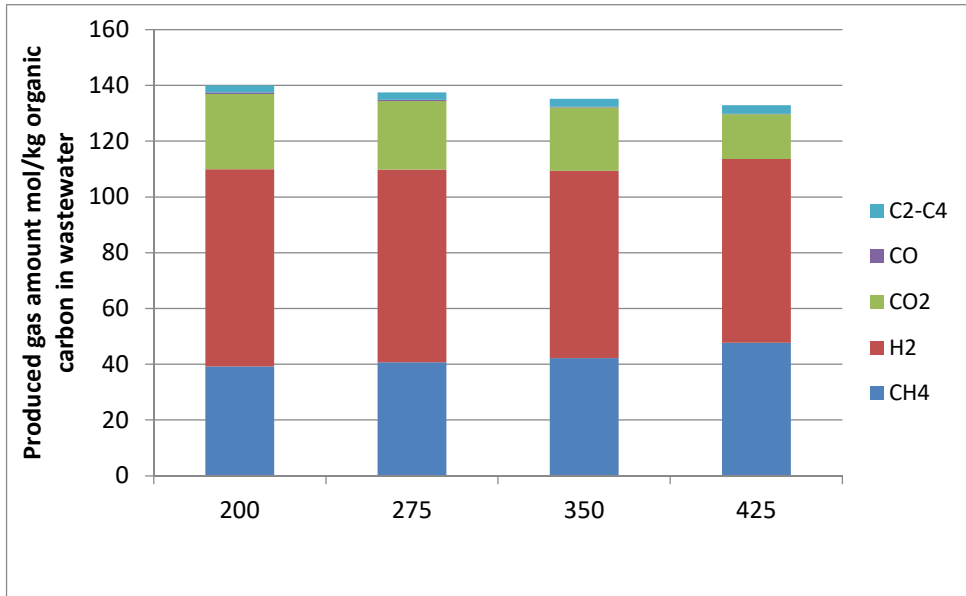


Figure 5-15. Effect of various operating pressures on gaseous product yields [mol/kg organic carbon in wastewater] in hydrothermal gasification of alkaloid wastewater at 600°C with K₂CO₃ catalyst.

Table 5-8. Effect of various operating pressures on gaseous product yields [mol/kg organic carbon in wastewater] in hydrothermal gasification of alkaloid wastewater at 600°C with K₂CO₃ catalyst

Mol/kg C in ww	AF-T6K-P1	AF-T6K-P2	AF-T6K-P3	AF-T6K-P4
CH₄	36.0	33.5	32.3	24.4
H₂	46.3	40.3	52.3	38.3
CO₂	20.0	18.8	21.1	27.6
C₂-C₄	0.4	0.38	0.4	0.37
CO	2.2	3.0	2.6	2.6
Total	36.0	33.5	32.3	24.4

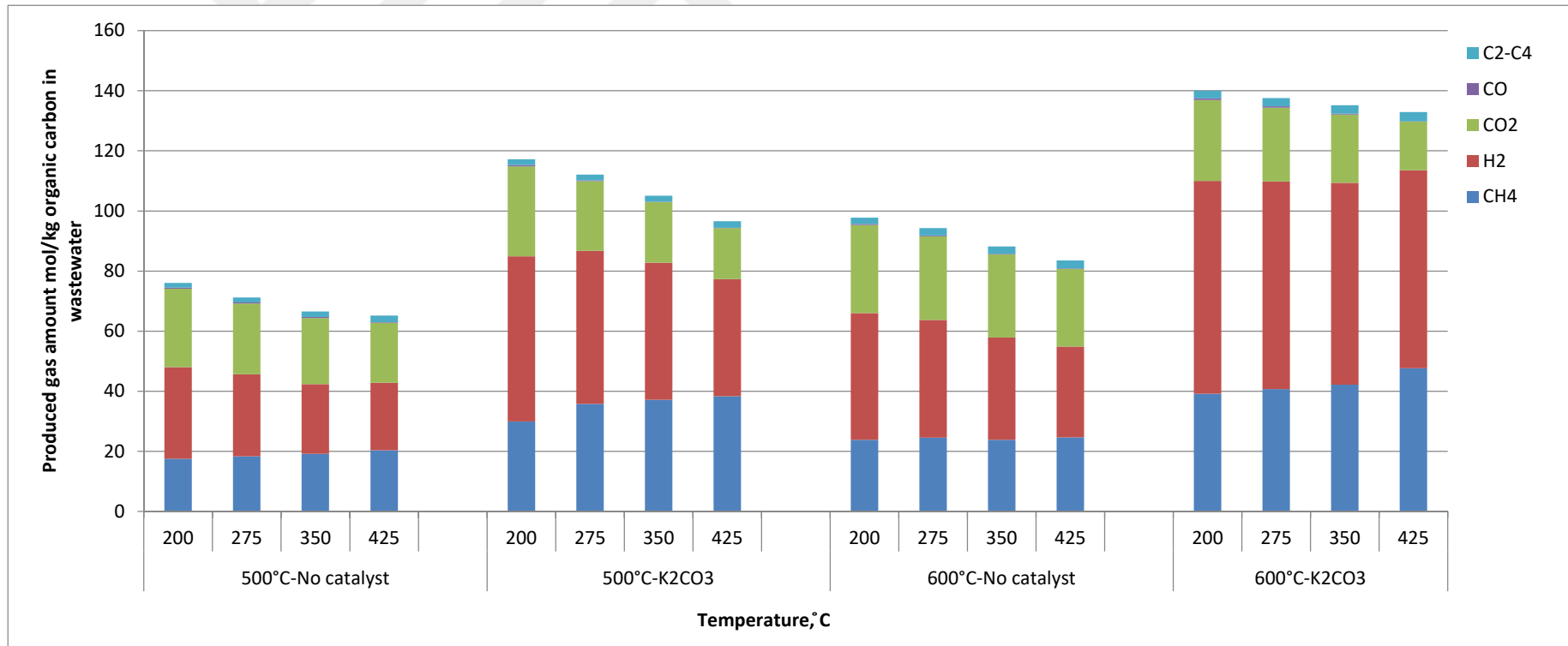


Figure 5-16. Comparison of the gaseous product yields [mole/kg organic carbon] in hydrothermal gasification of alkaloid wastewater at various operating pressures and with and without catalyst.

Table 5-9. COD analysis results and COD removal efficiencies of the SCWG of Alkaloid wastewater absence of catalyst and in the presence of K_2CO_3 (KC) catalysts at various pressure and temperatures.

Experiment Code	Conditions Pressure [bar] and Temperature [°C]	Volume of wastewater [mL], and catalyst amount [g]	COD Reactor Effluent [mg/L]	COD Removal Efficiency [%]
Raw wastewater		-	32050	-
AF-T5-P1	200 bar & 500°C	10 mL/No catalyst	9000	71.9
AF-T5-P2	275 bar & 500°C	12.5mL/No catalyst	7400	76.7
AF-T5-P3	350 bar & 500°C	15mL/No catalyst	6370	80.1
AF-T5-P4	425 bar & 500°C	20mL/No catalyst	5400	83.1
AF-T6-P1	200 bar & 600°C	8mL/No catalyst	4875	84.8
AF-T6-P2	275 bar & 600°C	10mL/No catalyst	3100	90.3
AF-T6-P3	350 bar & 600°C	12.5mL/No catalyst	3490	89.1
AF-T6-P4	425 bar & 600°C	15mL/No catalyst	3950	87.7
AF-T5K-P1	200 bar & 500°C	10 mL/0.333g	5225	83.7
AF-T5K-P2	275 bar & 500°C	12.5mL/0.416g	5960	81.4
AF-T5K-P3	350 bar & 500°C	15mL/0.560g	3650	88.6
AF-T5K-P4	425 bar & 500°C	20mL/0.666g	3425	89.3
AF-T6K-P1	200 bar & 600°C	8mL/0.266g	4190	86.9
AF-T6K-P2	275 bar & 600°C	10mL/0.333g	2600	91.9
AF-T6K-P3	350 bar & 600°C	12.5mL/0.416g	2240	93.0
AF-T6K-P4	425 bar & 600°C	15mL/0.500g	1330	95.8

Table 5-10. TOC analysis results and TOC removal efficiencies of the SCWG of Alkaloid wastewater absence of catalyst and in the presence of K_2CO_3 (KC) catalysts at various pressure and temperatures.

Experiment Code	Conditions Pressure [bar] and Temperature [°C]	Volume of wastewater [mL], and catalyst amount [g]	TOC Reactor Effluent, [ppm]	TOC Removal Efficiency, [%]
Raw wastewater		-	11500	
AF-T5-P1	200 bar & 500°C	10 mL/No catalyst	2770	76
AF-T5-P2	275 bar & 500°C	12.5mL/No catalyst	2865	75
AF-T5-P3	350 bar & 500°C	15mL/No catalyst	2945	74
AF-T5-P4	425 bar & 500°C	20mL/No catalyst	3295	71
AF-T6-P1	200 bar & 600°C	8mL/No catalyst	1370	88
AF-T6-P2	275 bar & 600°C	10mL/No catalyst	1405	88
AF-T6-P3	350 bar & 600°C	12.5mL/No catalyst	1465	87
AF-T6-P4	425 bar & 600°C	15mL/No catalyst	1665	86
AF-T5K-P1	200 bar & 500°C	10 mL/0.333g	800	93
AF-T5K-P2	275 bar & 500°C	12.5mL/0.416g	865	93
AF-T5K-P3	350 bar & 500°C	15mL/0.560g	965	92
AF-T5K-P4	425 bar & 500°C	20mL/0.666g	1165	90
AF-T6K-P1	200 bar & 600°C	8mL/0.266g	650	94
AF-T6K-P2	275 bar & 600°C	10mL/0.333g	685	94
AF-T6K-P3	350 bar & 600°C	12.5mL/0.416g	760	93
AF-T6K-P4	425 bar & 600°C	15mL/0.500g	825	93

5.2.1 CGE (%), CLE (%) and Amount of Produced Gas in the Absence and Presence of K_2CO_3

The effect of reaction temperature and pressure on CGE, CLE, gaseous product distribution and yields, TOC, COD content of aqueous product is investigated and given in Figs 5-8 to 5-16, and Tables 5-3 to 5-10 in this section. The studied conditions are the pressure range of 200-425 bar, reaction temperatures of 500°C and 600°C for both catalytic (K_2CO_3) and non-catalytic experiments. A comparison graph including all runs is given in Fig 5-16. The volume of wastewater and the catalyst amounts were determined to maintain the objected reaction pressures. Pre-experiments were done to provide pressures with a maximum deviation of ± 0.5 M Pa and the determined values were given in section 4.6 and Table 4-7.

Carbon gasification efficiency is slightly decreased by a ratio within 2-3% as increasing pressure while the carbon liquefaction efficiency is increased (3-4%) at 500°C and non-catalytic runs. Similarly, at 600°C pressure enhance liquefaction efficiency and reduced gasification efficiency very slightly. In catalytic-pressure effect experiments, trends are similar as in non-catalytic experiments, that pressure effect at 500°C is little more apparent than at 600°C. Temperature increment from 500 to 600°C and catalyst addition promoted gasification and the highest CGE value is reached as 87.5% at 600°C and 200 bars with K_2CO_3 . The catalyst use improved CGE from 57.7 to 78% at 500 °C, and at 600°C, 70.8 to 87.5% while it decreased CLE values from 24% to 7% at 500°C and from 11.9 to 5.7% at 600°C at 200 bars. At the other operated pressures, similar variations are observed. The effect of temperature is seen stronger than pressure from the point of gasification. Madenoğlu et al. (2013) studied with glucose to determine the best conditions to obtain high valuable gaseous and aqueous products yields and minimum residue. They concluded that CGE increases at high temperatures and low pressures while the temperature is more effective than the effect of pressure on the gaseous product composition. It is explained by dielectric constant of water is significantly lower at high temperatures as it is a little higher at high pressures (Madenoglu et al. 2013).

In the formation of gaseous and aqueous product, the ionic and radical mechanisms are responsible due to change of density and ionic product. At elevated temperature, decrease in density cause less ionic product and the radical mechanism is enhanced (Dinjus and Kruse 2004). The total produced gas amount is promoted as the temperature goes up from 500 to 600°C from 875 to 1125 mmol/liter while it decreased as the pressure goes up from 200 to 425 bar slightly, 750 mmol/liter at 500°C, 961 mmol/liter at 600°C. The increasing pressure reduced the amount of the produced gas and CGE (by 4-5%) while it promoted CLE at slightly at 500 and 600°C in a previous work of us done with real biomass samples of wood residues (Cengiz et al. 2016). The highest CGE and produced gas was obtained in the HTG of pine tree sawdust at 80.9% and 1238.0 g gas/kg biomass, at 600°C and 20.0 MPa in the presence of K_2CO_3 .

Based on literature, K_2CO_3 is one of the most effective catalysts in supercritical water gasification studies. The catalyst enhanced the total gaseous product yield significantly at the ratios of 54% at 500°C and 43% at 600°C. The pressure increase caused a small reduction in the total produced gas amount for catalytic runs also. Chakinala et al. (2010) studied glycerol and microalgae gasification in batch (quartz capillaries) and continuous flow reactors and investigated (Chakinala et al. 2010). They reported that the addition of K_2CO_3 promoted the glycerol gasification efficiency and results higher hydrogen yields catalyzing the water-gas shift reaction.

5.2.2 Gaseous product distribution and yields

The gaseous product obtained is mainly composed of H_2 , CO_2 , CH_4 , and a little CO , and C_2-C_4 in HTG of opium alkaloid wastewater at all studied conditions. The molar percentages and the yields of the gaseous product (mole/kg C in wastewater) for all cases are given in Figs 5-8 to 5-15 and Tables 5-5 to 5-8. The molar percentage of CH_4 is changed from 23.1 to 31.3% at 500°C and from 24.4 to 29.5% at 600°C in the absence of catalyst as the pressure increases within 200-425 bar range. H_2 molar percentage is varied from 40.0 to 34.4 % at 500°C and 43 to 36.2% at 600°C in non-catalytic runs. It shows us, the pressure enhanced

methanation reactions while decreasing H₂ formation. Ionic product, K_w affects the reaction mechanism in supercritical water medium and it increases with the increasing pressure or the decreasing temperature. At high K_w values (higher than 10⁻¹⁴), ionic mechanism (hydrolysis) is dominated due to increase of pressure while increasing temperature promotes the pyrolysis (free-radical) reaction. H₂ yield decreases with increasing pressure, but using catalyst increases the H₂ yield from 30.4 to 50.9 mol/kg C in wastewater at 500°C and 200 bars and at 600°C, yield of H₂ increases similarly. The trend is as expected due to supercritical water properties variation as mentioned above.

There is limited number of study on the effect of pressure in hydrothermal gasification of biomass/wastewater. The effect of pressure may be changed according to the studied temperature and the levels of pressure. Since the density variation of free radical and ionic reactions are opposite, the free radical reaction rate decrease with pressure while that of the ionic reactions are promoted with pressure because of higher ionic products at higher densities as shown in Figure 5-17 (Basu and Mettanant 2009).

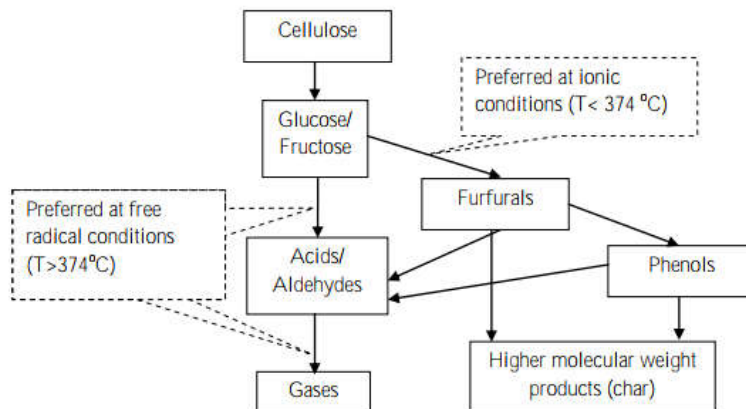


Figure 5-17. Reaction mechanisms depending on the conditions (Basu and Mettanant 2009).

Demirbas (2004) investigated hydrogen production from fruit shell within 650-750 K and 23-48 MPa, and found that increase in pressure and temperature cause higher hydrogen yields (Demirbas 2004). In contrast, Hao et al. found that hydrogen is slightly higher as the pressure decrease in 0.1 M of glucose gasification (Hao et al. 2003). We found that the pressure has a negative effect on hydrogen yields in the gasification of wood residues within the studied conditions which are

same with this experimental part. The highest yields of hydrogen obtained in the presence of K_2CO_3 at $600^\circ C$ was 27.0 mol/kg for pine tree sawdust and 24.7 mol/kg for fir tree sawdust at the lowest reaction pressures of 20.5 MPa and 20.3 MPa, respectively. Madenoglu et al. (Madenoglu et al. 2013) stated that the hydrogen and carbon dioxide yields decrease with increasing pressure at constant temperature while methane yield increase. Lu et al. investigated the effect of process parameters (temperature, pressure, and residence time and feedstock concentration) by using orthogonal experimental design method within 3 levels for each parameter. They found that the increasing pressure, H_2 yield, CH_4 yield and CGE have a tendency to increase, and then decreases.

The catalyst addition promoted formation of both CH_4 and H_2 and the sum of the molar percentage of H_2 and CH_4 from 65.8 to % 80.0 % at 425 bar & $500^\circ C$ and from 65.7 to 85.5% at 425 bar & $600^\circ C$. At the same time, CH_4 yield slightly increases by increasing pressure at $500^\circ C$ using catalyst and without catalyst. CH_4 yield remains almost constant without catalyst as the temperature rises while in catalytic runs it decrease. For maximum H_2 yield, $500^\circ C$, 200 bar and K_2CO_3 addition should be selected and to maximize CH_4 , $600^\circ C$, 425 bar and non-catalytic run should be selected.

Carbon dioxide yields are lowered by the increase of pressure and increased from 500 to $600^\circ C$ slightly. K_2CO_3 addition has also reduced the CO_2 yield at $600^\circ C$ while the effect of catalyst at $500^\circ C$ is not clear, since at 20.0 MPa, it is higher than catalytic run but at 42.5 MPa, it is seen as decreased. CO and C_2-C_4 hydrocarbons yields are very low comparing to H_2 , CH_4 and CO_2 . The yields of CO are slightly increased by increasing pressure and catalyst addition while the yields of C_2-C_4 hydrocarbons are decreased at high pressures. Temperature is not much effective on C_2-C_4 hydrocarbons yields, slightly decrease with increasing temperature in non-catalytic runs and slightly increase in catalytic runs.

Some valuable researches have been done to evaluate the importance of the parameter in supercritical water gasification (Lu et al. 2006; Madenoglu et al. 2013; Reddy et al. 2014; Kang et al. 2016). Lu et al. (2006) ordered parameters which effect the gaseous product formation especially hydrogen yields as temperature > pressure > feedstock concentration > residence time. Kang (2016) has investigated

different parameters and reported that the order of importance for hydrogen production is: temperature > catalyst loading > catalyst type > biomass type.

5.2.3. Variation of TOC and COD Removal Efficiencies

TOC (11500 mg/L) and COD (32050 mg/L) content of wastewater lowered by hydrothermal gasification technique successfully in both non-catalytic and catalytic runs at 500 and 600°C and are shown in Tables 25 & 26. COD removals varied between 71.9-95.8% in this experimental part of the thesis. COD content in the aqueous product decreases with increasing temperature and pressure but temperature is more effective in COD removal. COD decreased from 9000 to 4875 mg/L with 100°C temperature increment at 200 bars while, COD lowered to 5400 mg/L as pressure increases from 20.0 to 42.5 MPa. Catalyst use has a substantial effect since COD is reduced from 9000 to 5225 mg/L at 500°C but this effect is less at 600°C. In the point of process economy, K₂CO₃ addition provides COD removals at 500°C as high as in 600°C non-catalytic runs and to prefer catalyst addition instead of temperature increase will be reasonable. COD content removal achieved at 95.8% as maximum at 600°C and 42.5 MPa in the presence of K₂CO₃.

TOC content of the aqueous product destructed with a ratio between 71-94% in the studied range of temperature, pressure in non-catalytic and catalytic runs. TOC removal increased at elevated temperatures and lower pressures. The most significant parameter is catalyst addition at 500°C while catalyst promoted TOC removal at 600°C, too. Temperature is also effective and TOC content is lowered from 2770 to 1370 mg/L as the temperature increases from 500 to 600°C and improved removal by a ratio of %12 at 200 bars. At higher pressures, same tendency was observed. The highest TOC removals were reached at 600°C and in the presence of K₂CO₃, pressure effect is not seen clearly in this case but lowest pressure, 20.0 MPa, may be given as the best condition within studied pressure range.

5.3 Influence of Catalysts on Gasification of Opium Alkaloid Wastewater

5.3.1 Influence of Red Mud Catalysts on Gasification of Opium Alkaloid Wastewater

5.3.1.1 Experimental results of A group catalysts

Hydrothermal gasification studies were done with the catalysts in A group, which includes A1, A2, A3, A4, A21, A31, and A41 with 0.5 g of catalyst and 20 mL of wastewater at 500°C in this part.

- ✓ **A1** (Precipitation of red mud with NH_3 + Calcination)
- ✓ **A2** (Precipitation of red mud with NH_3 + 10% Ni impregnation + Calcination)
- ✓ **A3** (Precipitation of red mud with NH_3 + 20% Ni impregnation + Calcination)
- ✓ **A4** (Precipitation of red mud with NH_3 + 30% Ni impregnation + Calcination)
- ✓ **A21** (Reduction of A2 by NaBH_4 : Precipitation of red mud with NH_3 + 10% Ni impregnation + Reduction by NaBH_4)
- ✓ **A31** (Reduction of A3 by NaBH_4 : Precipitation of red mud with NH_3 + 20% Ni impregnation + Reduction by NaBH_4)
- ✓ **A41** (Reduction of A4 by NaBH_4 : Precipitation of red mud with NH_3 + 30% Ni impregnation + Reduction by NaBH_4).

Table 5-11. Reaction conditions, CGE, produced gas amount and TOC values of hydrothermal gasification of alkaloid wastewater at 500°C with the effect of catalyst type in the presence of A-group catalysts.

	Reaction Temperature (°C)	Reaction Pressure (bar)	CGE (%)	TOC (mg/L)	Produced gas amount (mmol/L ww.)
No catalyst	500	365	55.5	2843	766
Original Red Mud	500	405	57.6	2125	773
A1	500	410	62.7	2000	896
A2	500	420	65.3	1250	948
A3	500	410	69.4	1065	1000
A4	500	405	67.1	1201	970
A21	500	425	68.3	1595	1135
A31	500	440	71.3	1685	1010
A41	500	420	70.5	1975	990

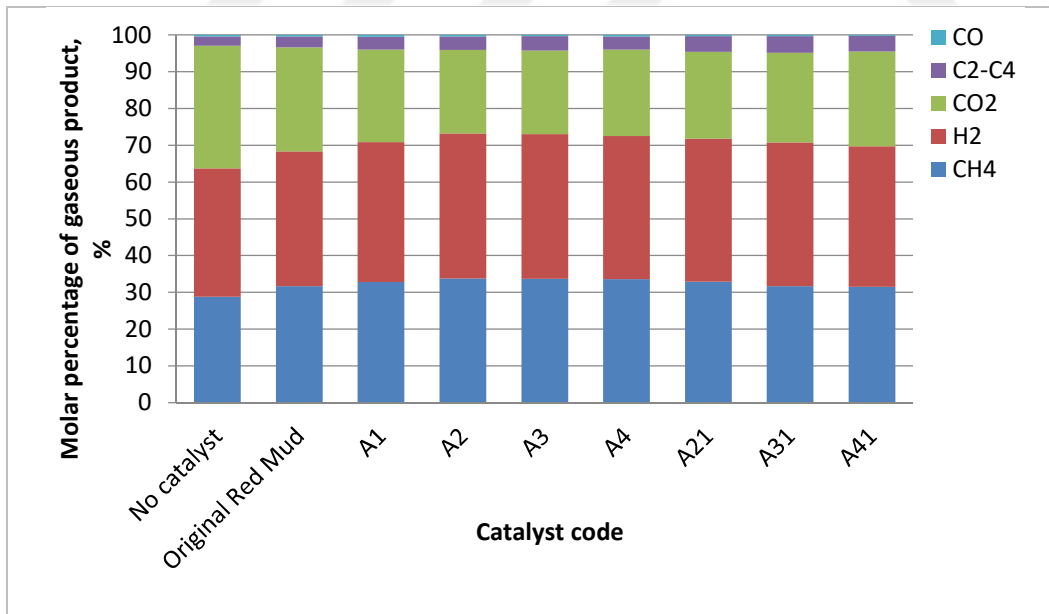


Figure 5-18. Gaseous product distribution in hydrothermal gasification of alkaloid wastewater in the presence of A-group catalysts.

Table 5-13. The effect of catalyst type on gaseous product yields [mole gas/kg C in wastewater] in the detailed form in hydrothermal gasification of alkaloid wastewater in the presence of A-group catalysts.

mol/kg C in ww	No catalyst	Original RM	A1	A2	A3	A4	A21	A31	A41
CH₄	16.8	22.1	25.6	27.8	29.3	28.3	27.7	27.8	27.1
H₂	20.3	23.8	29.7	32.5	34.1	32.8	32.8	34.3	32.8
CO₂	19.4	18.9	19.5	18.7	19.8	19.8	19.9	21.4	22.2
C₂-C₄	0.2	3.1	2.7	3.0	3.4	3.0	3.6	3.9	3.7
CO	1.5	0.3	0.4	0.3	0.3	0.3	0.3	0.3	0.2
Total	58.2	68.2	77.9	82.3	86.9	84.2	84.3	87.7	86.0

Table 5-14. COD results and COD removal efficiencies of the SCWG of Alkaloid wastewater in the absence of catalyst (NC) and in the presence of Red Mud (RM) and A-group catalysts.

Experiment Code	Catalyst	COD of Reactor Effluent [mg/L]	COD Removal Efficiency [%]
Raw wastewater	-	32050	-
AF-T5 average	-	8470	73.6
AF-RM	Original Red Mud	7610	76.3
AF-A1	Precipitation of red mud with NH ₃ + Calcination	5630	82.4
AF-A2	Precipitation of red mud with NH ₃ + 10% Ni impregnation + Calcination	5325	83.4
AF-A3	Precipitation of red mud with NH ₃ + 20% Ni impregnation + Calcination	5025	84.3
AF-A4	Precipitation of red mud with NH ₃ + 30% Ni impregnation + Calcination	5100	84.1
AF-A21	<i>Reduction of A2 by NaBH₄</i> (Precipitation of red mud with NH ₃ + 10% Ni impregnation + Reduction by NaBH ₄)	6550	79.6
AF-A31	<i>Reduction of A3 by NaBH₄</i> (Precipitation of red mud with NH ₃ + 20% Ni impregnation + Reduction by NaBH ₄)	6475	79.8
AF-A41	<i>Reduction of A4 by NaBH₄</i> (Precipitation of red mud with NH ₃ + 30% Ni impregnation + Reduction by NaBH ₄)	5625	82.4

Table 5-15. TOC analysis results and TOC removal efficiencies of the SCWG of Alkaloid wastewater absence of catalyst (NC) and in the presence of Red Mud (RM) and A-group catalysts.

Experiment Code	Catalyst	TOC Reactor Effluent [mg/L]	TOC Removal Efficiency [%]
Raw wastewater	-	11500	-
AF-T5	-	2843	75.3
AF-RM	Original Red Mud	2125	81.5
AF-A1	Precipitation of red mud with NH ₃ + Calcination	2000	82.6
AF-A2	Precipitation of red mud with NH ₃ + 10% Ni impregnation + Calcination	1250	89.1
AF-A3	Precipitation of red mud with NH ₃ + 20% Ni impregnation + Calcination	1065	90.7
AF-A4	Precipitation of red mud with NH ₃ + 30% Ni impregnation + Calcination	1201	89.6
AF-A21	Reduction of A2 by NaBH ₄ (Precipitation of red mud with NH ₃ + 10% Ni impregnation + Reduction by NaBH ₄)	1595	86.1
AF-A31	Reduction of A3 by NaBH ₄ (Precipitation of red mud with NH ₃ + 20% Ni impregnation + Reduction by NaBH ₄)	1685	85.3
AF-A41	Reduction of A4 by NaBH ₄ (Precipitation of red mud with NH ₃ + 30% Ni impregnation + Reduction by NaBH ₄)	1975	82.8

Opium alkaloid wastewater was gasified in supercritical water conditions at, 500°C, and a pressure range of 40.5- 44.0 MPa in the presence of “A Group” catalysts. The experiments were also carried out without catalyst and with original red mud (ORM) catalyst to understand the effect of activation of the catalyst better, in the absence of catalyst, pressure is reached to 36.5 MPa and with ORM, 40.5 MPa is recorded as reaction pressure. This group includes activated forms of red mud with NH₃ and nickel impregnated forms in varying ratios (10%, 20% and 30%). The effect of A group catalysts on carbon gasification efficiencies, gaseous product distribution and yields of hydrogen, methane, carbon dioxide, C₂-C₄ hydrocarbons, carbon monoxide were given in Table 5-11 to 5-15 and Figures 5-18 and 5-19. For accuracy, each run was repeated five times. The effect of red mud derivatives on the product efficiencies, gaseous product yields, and COD and TOC removal efficiencies were examined.

➤ **CGE (%) of wastewater and total amount of produced gas per unit volume**

Carbon gasification efficiencies and the amount of total gas product in the unit of *mmol gas/L* wastewater is represented in Table 5-11 for the studied conditions. The catalyst addition increases CGE and produced gas amounts significantly except original red mud. Kıpçak et al. (2017) used Ni/Al₂O₃ and Ru/Al₂O₃ catalysts in gasification of olive mill wastewater within 400-600°C of reaction temperatures. They also concluded that catalyst enhanced the gasification and the yields of methane and hydrogen (Kıpçak and Akgün 2017). GCE is promoted from 55.5 % in the absence of catalyst up to 70.5 and 71.3 % with the catalyst A31 and A41 as maximum. The most effective forms of red mud in terms of carbon gasification into valuable gaseous products are found as 20 % and 30 % of Nickel-impregnated ones.

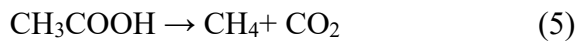
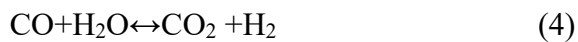
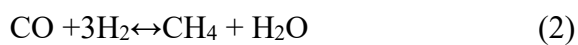
The investigation of the effect of red mud in HTG studies is very rare. Yanik et al. (2008) used red mud in the gasification of various type of waste (sunflower stalk, corncob, and vegetable-tanned leather waste) as a catalyst. They found that red mud increases gasification of corn-cob significantly and was proposed as a promising natural catalyst (Yanik et al. 2008). The corncob was gasified in supercritical water at 500°C and 357 bar in the presence of red mud in this study

and it was seen that the gas amount increased from 340.0 to 426 g gas/kg biomass. Since red mud is a by-product from aluminum production, utilizing it as a catalyst is both valuable and economical.

The produced gas amount promoted by activation of red mud since all the activated forms increased gas amount at varying ratios of 17-48%. Nickel impregnation enhanced gasification while the effect of reduction by NaBH₄ is not so effective between A3 & A31, A4 & A41 which includes 20 and 30% of Nickel, respectively. At lower nickel impregnation ratio (10%), reduction has a positive effect in the total produced gas amount as seen from the difference between A2 and A21.

➤ **The composition and yields of the gaseous product**

The molar percentage and the yields of the gaseous product without a catalyst and with red mud catalysts are given in Figs 5.1 and 5.2. The decomposition characteristics of this specific wastewater in HTG has not been studied before in literature. Its content was investigated in few researches (Aydin et al., 2010, Bural, 2008, and Kaçar et al., 2003). The alkaloid industry is a biomass-based plant and the wastewater contains 10,000 mg/L of carbohydrate and 5,000 - 6,000 mg/L of protein as expected. Additionally, it has acetic acid and sulphuric acid from extraction and has pH adjustment steps during production. The reactions for glucose and acetic acid are given below representing the biomass degradation:



The organic content arising from the carbohydrate and organic acid content in the alkaloid wastewater was decomposed to produce gaseous products, such as CH₄, H₂, CO₂, and CO as stated via reactions (1-5). Additionally, low amounts of C₂ - C₄ hydrocarbons were generated at the end of HTG process. In non-catalytic and catalytic cases at 500°C, the main gases in the product gas mixture is H₂, CO₂,

and CH₄ in hydothermal gasification of this wastewater in the. The percentage of H₂ increased from 34.9 % to 38.1-39.4 % and percentage of CH₄ is also increased from 28.8 % to 31.5-33.8 % at varying ratios with A group catalyst. Conversely, the molar percentage of CO₂ decreased from 33.0 % to between 22.7-25.8 % with the addition of A group catalysts of red mud. The nickel impregnation effect in the gaseous product distribution is not clear since the yield of gases should be evaluated to determine.

The yields of each gas are given in Fig.2 and the total of the gaseous product yields for each run are given in Table 3. Comparing the yields in the non-catalytic run to the catalytic runs, it is seen that the yields of H₂ and CH₄ dramatically increased. In a study of De Blasio et al. they gasified black liquor in stainless steel and INCONEL 625 at supercritical conditions to estimate catalytic effect INCONEL 625 alloy which contains nickel as the main element. They found that nickel content promotes hydrogen production as in this study while significant influence on carbon gasification efficiency was not observed (De Blasio et al. 2016).

The original red mud increased the CH₄ amount (mmol/L wastewater) by 32% while enhancing the H₂ formation by 17%. The catalytic effect of original red mud originated from the iron and aluminum containing structure of it. Activated red mud catalysts also show good catalytic activity in hydrogen production and the yields of hydrogen reached 34.1 and 34.3 as the highest with A3 and A31 catalyst while the yield of H₂ was only 20.3 mol/kg C in wastewater. The other activated red mud derivatives result very similar hydrogen yields. The methane yields are extremely enhanced by changing ratios of 52-74 % with activated red muds in group A. The yields of CO₂ were slightly increased with A31 and A41 catalyst while almost unchanged with others in A group and original red mud. The yields of C₂ - C₄ in gaseous product accelerated from 0.2 to 3.9 mol/kg C in wastewater by both original and activated red mud derivatives in this group. The very low CO level, 1.5, also declines further in the product gas around to 0.2-0.3 mol/kg C in wastewater. These results show us original red mud is effective in terms of hydrogen and methane formation in hydothermal gasification of opium processing wastewater and the activation and nickel impregnation increased the catalytic effect of it due to higher CH₄ and H₂ yields in activated forms of it. The changing impregnation ratio of

nickel did not make a significant effect. In the case of the promotion of the H₂ and CH₄ production, the order of effectiveness in the catalytic performance of the catalysts may be given as: Original Red Mud < Activated Red Mud without nickel (A1) < A2, A21, A4, A1 < A3, A31.

In the study of Yanik et al., 2008, red mud is defined as iron based catalysts and mentioned that it has catalytic activity in hydrogen production with the studied feedstocks in the operated conditions. Together with the supercritical water acting as a catalyst, iron oxide active sites enhanced the water gas shift reaction towards CO₂ and H₂ from CO as stated similarly in the study of Uddin et al. (2008). The yields of CO decreased with the usage of a catalyst from 17.25 to 3-4 mmol/L levels. Nickel is widely used in biomass gasification as a catalyst (Azadi et al., 2012, Buffoni et al., 2009, and Minowa et al., 1998), and it is reported that nickel promotes hydrogen yields because of its selectivity for H₂. The activation process for red mud also promotes the effectiveness of it in the case of hydrogen and methane formation.

➤ **COD and TOC content of the aqueous product and removal efficiencies**

The original alkaloid wastewater has a COD of 32,050 ppm and a TOC of 11,500 ppm used in this study. The COD and TOC contents of the aqueous product at the end of HTG experiments were given in Table 5-14 and

Table 5-15. The results show that COD was lowered to the levels of 5100-6550 ppm by supercritical water gasification technique in an hour of operation with “A group” of activated red mud. This is a successful result hence it provides COD removal of approximately 84% while TOC removal was achieved by 91 % as maximum in the presence of A3 in this experimental section. The catalyst use improved COD and TOC removal by 10 and 15%, respectively at 500°C. Kazemi et al. investigated hydrothermal treatment of distillery wastewater in a batch tubular reactor at temperatures of 250–400°C, reaction time of 30–120 min, initial COD concentration of 9600–26,200 mg L⁻¹ at constant pressure of 25.0 MPa in the presence and absence of various homogeneous and heterogeneous catalysts (Kazemi et al. 2015). They concluded that COD removal is mainly dominated by

temperature increase while homogeneous and heterogeneous catalysts substantially affected COD and color removal efficiencies. The optimum conditions were obtained at 400°C, 30 min with CuO and MnO₂ (~75%) and 400 °C, 120 min with (80.9%).

The amount of nickel impregnated did not make a sensible change in COD and TOC removal efficiencies while the reduction with NaBH₄ made a slightly negative effect. Higher COD removals needed in the case of discharge limits, so the reaction temperature or impregnated Nickel ratio may be increased.

5.3.1.2 Experimental results of B group catalyst

- ✓ **B1** (Precipitation of red mud with K₂CO₃ + Calcination)
- ✓ **B2** (Precipitation of red mud with K₂CO₃ + 10% Ni impregnation + Calcination)
- ✓ **B3** (Precipitation of red mud with K₂CO₃ + 20% Ni impregnation + Calcination)
- ✓ **B4** (Precipitation of red mud with K₂CO₃ + 30% Ni impregnation + Calcination)
- ✓ **B21** (Reduction of B2 by NaBH₄ : Precipitation of red mud with K₂CO₃ + 10% Ni impregnation + Reduction by NaBH₄)
- ✓ **B31** (Reduction of B3 by NaBH₄ : Precipitation of red mud with K₂CO₃ + 20% Ni impregnation + Reduction by NaBH₄)
- ✓ **B41** (Reduction of B4 by NaBH₄: Precipitation of red mud with K₂CO₃ + 30% Ni impregnation + Reduction by NaBH₄).

Table 5-16. Reaction conditions, CGE, produced gas amount and TOC values of hydrothermal gasification of alkaloid wastewater at 500°C with the effect of catalyst type in the presence of B-group catalysts.

	Reaction Temperature (°C)	Reaction Pressure (bar)	CGE (%)	TOC (mg/L)	Produced gas amount [mmol/L ww.]
No catalyst	500	365	55.5	2843	766
Original Red Mud	500	405	57.6	2125	773
B1	500	430	62.3	1675	896
B2	500	425	62.9	1325	948
B3	500	435	64.2	1200	1000
B4	500	430	64.5	1504	970
B21	500	420	68.6	1675	979
B31	500	440	72.6	1500	1010
B41	500	425	70.8	1760	990

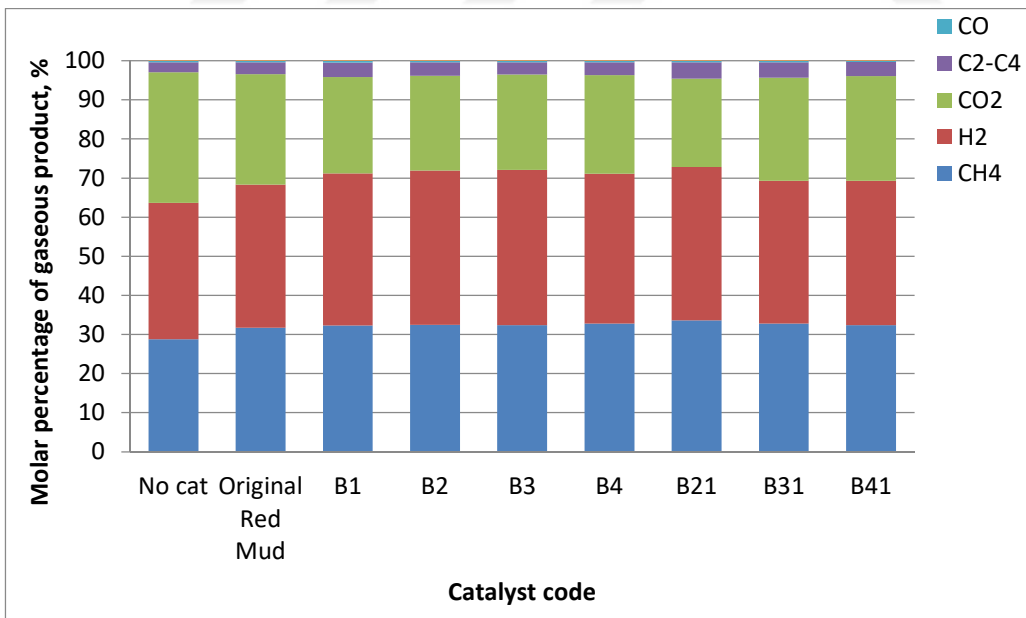


Figure 5-20. The effect of catalyst type on gaseous product distribution in hydrothermal gasification of alkaloid wastewater in the presence of B-group catalysts.

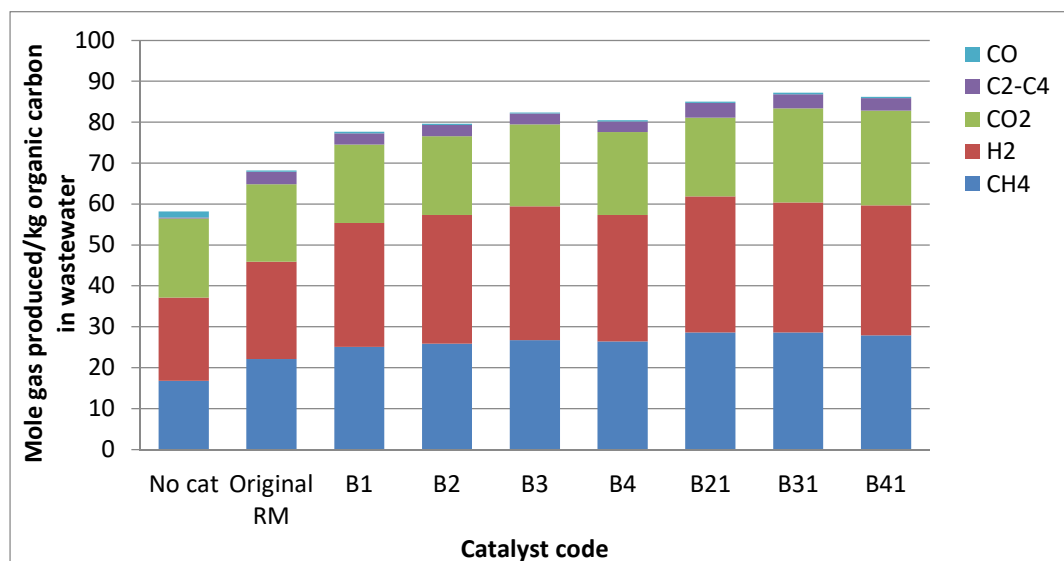


Figure 5-21. The effect of catalyst type on gaseous product yields in hydrothermal gasification of alkaloid wastewater in the presence of B-group catalysts.

Table 5-17. The effect of catalyst type on gaseous product distribution in the detailed form in hydrothermal gasification of alkaloid wastewater in the presence of B-group catalysts.

Molar percentage (%)	No catalysyt	Original RM	B1	B2	B3	B4	B21	B31	B41
CH ₄	28.8	31.7	32.3	32.5	32.4	32.8	33.6	32.8	32.4
H ₂	34.9	36.6	38.9	39.4	39.7	38.3	39.2	36.5	36.9
CO ₂	33.0	28.3	24.6	24.3	24.4	25.2	22.6	26.4	26.8
C ₂ -C ₄	0.4	0.4	0.5	0.4	0.4	0.4	0.4	0.4	0.3
CO	2.9	3.0	3.7	3.4	3.1	3.3	4.2	3.9	3.6
Total	100	100	32.3	32.5	32.4	32.8	33.6	32.8	32.4

Table 5-18. The effect of catalyst type on gaseous product yields [mole gas/kg C in wastewater] in the detailed form in hydrothermal gasification of alkaloid wastewater in the presence of B-group catalysts.

mol/kg C in ww	No catalysyt	Original RM	B1	B2	B3	B4	B21	B31	B41
CH₄	16.8	22.1	25.1	25.9	26.7	26.4	28.6	28.6	27.9
H₂	20.3	23.8	30.3	31.4	32.7	30.9	33.3	31.8	31.8
CO₂	19.4	18.9	19.1	19.3	20.1	20.3	19.2	23.0	23.1
C₂-C₄	0.2	3.1	2.8	2.7	2.6	2.6	3.6	3.4	3.1
CO	1.5	0.3	0.4	0.3	0.3	0.3	0.3	0.4	0.3
Total	58.2	68.2	77.7	79.6	82.4	80.5	85.0	87.2	86.2

B group catalysts which includes B1, B2, B3, B4, B21, B31, and B41 with 0.5 g of catalyst and 20 mL of wastewater were used in this experimental part in the hydrothermal gasification of opium processing wastewater. The reaction pressure was 500°C and a pressure range of 42.5-44.0 MPa was obtained. The results of non-catalytic and with original red mud (ORM) catalyst were compared to catalytic runs to determine the effect of activation of the B group catalyst. This group includes activated forms of red mud with K₂CO₃ and nickel impregnated forms in varying ratios (%10, %20 and %30). The effect of B group catalysts on carbon gasification efficiencies, gaseous product distribution and yields of hydrogen, methane, carbon dioxide, C₂-C₄ hydrocarbons, carbon monoxide were given in Table 5-16 - 5-20 and Figs 5-20 and 5-21. For accuracy, each run was repeated five times. The effect of red mud derivatives on the product efficiencies, gaseous product yields, and COD and TOC removal efficiencies were examined.

➤ **CGE (%) of wastewater and total amount of produced gas per unit volume**

Carbon gasification efficiencies and the amount of total gas product in the unit of *mmol gas/L* wastewater is represented in Table 5-16. B group catalysts promoted carbon gasification efficiencies by changing ratios of 7-17% with the effect of activation and reduction by NaBH₄. Original red mud make not a considerable effect on gasification but reduced TOC value of the aqueous product by 25%. The highest gasification ratios were obtained with reduced form of activated red mud in this group. Reduction process resulted a better catalytic activity of red mud as it is seen from the results: CGE with B2, B3 and B4 catalysts were 62.9, 64.2 and 64.5% while with reduced forms of them B21, B31, B41, CGE values were increased up to 68.6, 72.6, 70.8%, respectively. Nickel impregnation was slightly increased gasification, while the amount of impregnated nickel did not a significant effect. The produced gas amounts were ascended with addition of catalysts in B group. The highest gaseous product amounts were reached with B3 and B31 (1000 and 1010 mmol/L wastewater) while the others give similar catalytic activity in terms of produced gas quantities. Gaseous product amounts enhanced by varying ratios of 17-32% within B group.

➤ **The composition and yields of the gaseous product**

The main gaseous compounds in the product gas mixture are CH₄, H₂ and CO₂ as expected, and little amount of CO and C₂-C₄ compounds were produced. The molar percentage of methane and hydrogen increased while carbon dioxide decreased. Carbon monoxide and C₂-C₄ hydrocarbons molar ratios were not changed much. The molar percentage of CH₄ rised from 28.8 to 33.6% with B21 as maximum while the other catalyst make similar effect. The molar percentage of H₂ rised from 34.9 to 39.7% with B3 as highest while with the other catalyst has a changing molar ratio of H₂ between 36.5-39.4%. The molar percentage of CO₂ decreased from 33% to the levels of 22.6-28.8%. The effect of catalyst type can be seen in CO₂ ratios more than H₂, while hardly seen in CH₄.

The yields of CH₄, H₂ and C₂-C₄ compounds were improved by addition of catalyst while CO₂ did not change remarkable except B31 and B41 and the yields of CO decreased. B group catalyst enhanced methane and hydrogen formation greatly, from 16.8 to 28.6 mol CH₄/kg C in wastewater with B31 and from 20.3 to 33.3 mol H₂/kg C in wastewater with B21 as the best in the studied range. The yields of methane with reduced form of red mud is a bit higher than others but for hydrogen a generalization can not be made. In terms of total gaseous product yields, it can be concluded that B21, B31 and B41 have slightly higher than non-reduced states of them. The amount of nickel did not make a significant effect.

➤ **COD and TOC content of the aqueous product and removal efficiencies**

The COD and TOC contents of the aqueous product at the end of HTG experiments were given in Table 5-19 and Table 5-20. Chemical oxygen demand and total organic carbon in the raw wastewater is reduced by catalyst use in this experimental part from. COD of the wastewater, 32050 mg/L, lowered to 4940-6240 mg/L levels by a removal range of 81-85 % approximately. This is a good result for only 1h of treatment operation and applied without need for pretreatment even filtration. Discharge limit in terms of COD is 1500 mg/L for this special industrial wastewater, to maintain this value, temperature should be increased. TOC content of raw wastewater, 11500 mg/L, decreased around to 1200-1760 mg/L by removal efficiencies of 85-90%. The effect of catalys type within the activated state of red mud in B group can not be seen clearly since the effectiveness are alike.

Table 5-19. COD results and COD removal efficiencies of the SCWG of Alkaloid wastewater in the absence of catalyst (NC) and in the presence of B group catalyst

Experiment Code	Catalyst	COD of Reactor Effluent [mg/L]	COD Removal Efficiency [%]
Raw wastewater	-	32050	-
AF-T5 average	-	8470	73.6
AF-RM-R1	Original Red Mud	7610	76.3
AF-B1-R1	Precipitation of red mud with K_2CO_3 + Calcination	5800	81.9
AF-B2-R1	Precipitation of red mud with K_2CO_3 + 10% Ni impregnation + Calcination	4940	84.6
AF-B3-R1	Precipitation of red mud with K_2CO_3 + 20% Ni impregnation + Calcination	5860	81.7
AF-B4-R1	Precipitation of red mud with K_2CO_3 + 30% Ni impregnation + Calcination	6240	80.5
AF-B21-R1	<i>Reduction of B2 by $NaBH_4$</i> (Precipitation of red mud with K_2CO_3 + 10% Ni impregnation + Reduction by $NaBH_4$)	5950	81.4
AF-B31-R1	<i>Reduction of B3 by $NaBH_4$</i> (Precipitation of red mud with K_2CO_3 + 20% Ni impregnation + Reduction by $NaBH_4$)	6050	81.1
AF-B41-R1	<i>Reduction of B4 by $NaBH_4$</i> (Precipitation of red mud with K_2CO_3 + 30% Ni impregnation + Reduction by $NaBH_4$)	5230	83.7

Table 5-20. TOC analysis results and TOC removal efficiencies of the SCWG of Alkaloid wastewater in the presence of B group catalyst.

Experiment Code	Catalyst	TOC Reactor Effluent [mg/L]	TOC Removal Efficiency [%]
Raw wastewater	-	11500	-
AF-T5 average	-	2843	75.3
AF-RM	Original Red Mud	2125	81.5
AF-B1	Precipitation of red mud with K_2CO_3 + Calcination	1675	85.4
AF-B2	Precipitation of red mud with K_2CO_3 + 10% Ni impregnation + Calcination	1325	88.5
AF-B3	Precipitation of red mud with K_2CO_3 + 20% Ni impregnation + Calcination	1200	89.6
AF-B4	mud with K_2CO_3 + 30% Ni impregnation + Calcination	1500	86.9
AF-B21	<i>Reduction of A2 by $NaBH_4$</i> (Precipitation of red mud with K_2CO_3 + 10% Ni impregnation + Reduction by $NaBH_4$)	1675	85.4
AF-B31	<i>Reduction of A3 by $NaBH_4$</i> (Precipitation of red mud with K_2CO_3 + 20% Ni impregnation + Reduction by $NaBH_4$)	1500	87.0
AF-B41	<i>Reduction of A4 by $NaBH_4$</i> (Precipitation of red mud with K_2CO_3 + 30% Ni impregnation + Reduction by $NaBH_4$)	1760	84.7

5.3.1.3 Experimental Results of AK (A Group + 0.5 g of K₂CO₃) Group Catalyst

Table 5-21. Reaction conditions, CGE, produced gas amount and TOC values of hydrothermal gasification of alkaloid wastewater at 500°C with the effect of catalyst type in the presence of B-group catalysts.

	Reaction Temperature (°C)	Reaction Pressure (bar)	CGE	TOC (mg/L)	Produced gas amount (mmol/L ww.)
No catalyst	500	365	55.5	2843	766
Original Red Mud	500	405	57.6	2125	773
AK1	500	435	74.0	950	1095
AK2	500	425	76.2	1514	1114
AK3	500	405	76.4	1550	1108
AK4	500	440	76.8	1540	1104
A21K	500	422	76.9	1610	1135
A31K	500	415	73.6	1660	1112
A41K	500	410	74.1	1815	1100
K₂CO₃	500	365	66.2	1200	1003

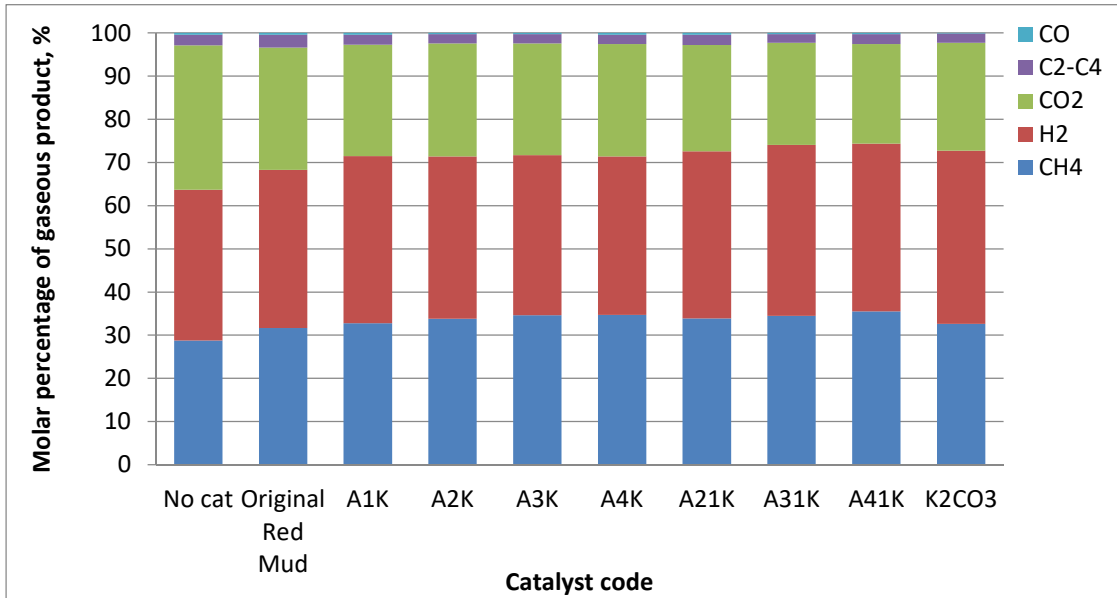


Figure 5-22. Effect of catalyst type of gaseous product distribution in hydrothermal gasification of alkaloid wastewater at 500°C in the presence of AK-group catalysts.

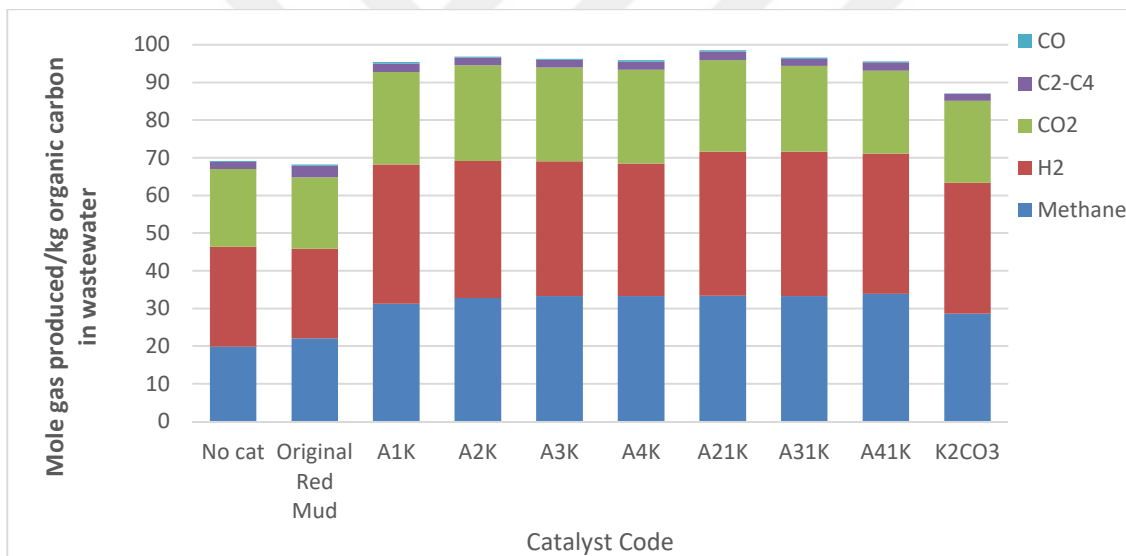


Figure 5-23. The effect of catalyst type on gaseous product yields in hydrothermal gasification of alkaloid wastewater in the presence of AK-group catalysts.

Table 5-22. The effect of catalyst type on gaseous product distribution in the detailed form in hydrothermal gasification of alkaloid wastewater in the presence of AK group catalysts

Molar percentage (%)	No catalyst	Ori. RM	A1K	A21K	A3K	A4K	A21K	A31K	A41K
CH ₄	28.8	31.7	32.8	33.8	34.6	34.7	33.9	34.5	35.5
H ₂	34.9	36.6	38.7	37.6	37.1	36.7	38.7	39.6	38.9
CO ₂	33.0	28.3	25.8	26.2	25.9	26	24.6	23.6	23
C ₂ -C ₄	0.4	0.4	0.4	0.3	0.3	0.4	0.4	0.3	0.3
CO	2.9	3.0	2.3	2.1	2.1	2.2	2.4	2	2.3
Total	100	100	100	100	100	100	100	100	100

Table 5-23. The effect of catalyst type on gaseous product yields [mole gas/kg C in wastewater] in the detailed form in hydrothermal gasification of alkaloid wastewater in the presence of AK group catalysts.

mol/kg C in ww	No catalyst	Original RM	A1K	A21K	A3K	A4K	A21K	A31K	A41K
CH ₄	16.8	22.1	31.3	32	33.3	33.3	33.4	33.3	33.9
H ₂	20.3	23.8	36.9	36.4	35.8	35.2	38.2	38.3	37.2
CO ₂	19.4	18.9	24.6	25.4	24.9	24.9	24.3	22.8	22
C ₂ -C ₄	0.2	3.1	0.4	0.3	0.3	0.4	0.4	0.3	0.3
CO	1.5	0.3	2.2	2.0	2.0	2.1	2.3	1.9	2.2
Total	58.2	68.2	95.4	96.1	96.3	95.9	98.6	96.6	95.6

Table 5-24. COD results and COD removal efficiencies of the SCWG of Alkaloid wastewater in the absence of catalyst (NC) and in the presence of catalyst

Experiment Code	Catalyst	COD of Reactor Effluent [mg/L]	COD Removal Efficiency [%]
Raw wastewater	-	32050	-
AF-T5	-	8470	73.6
AF-RM	Original Red Mud	7610	76.3
A1K	A1 + 0.5 g K ₂ CO ₃	6150	80.8
A2K	A2 + 0.5 g K ₂ CO ₃	6390	80.1
A3K	A3 + 0.5 g K ₂ CO ₃	7210	77.5
A4K	A4 + 0.5 g K ₂ CO ₃	6325	80.3
A21K	A21 + 0.5 g K ₂ CO ₃	6800	78.8
A31K	A31 + 0.5 g K ₂ CO ₃	5400	83.2
A41K	A41 + 0.5 g K ₂ CO ₃	6875	78.5
AF-T5K	K ₂ CO ₃	5125	84.0

Table 5-25. TOC analysis results and TOC removal efficiencies of the SCWG of Alkaloid wastewater in the absence of catalyst (NC) and in the presence of catalyst

Experiment Code	Catalyst	TOC of Reactor Effluent [mg/L]	TOC Removal Efficiency [%]
Raw wastewater	-	11500	-
AF-T5	-	2843	75.3
AF-RM	Original Red Mud	2125	81.5
A1K	A1 + 0.5 g K ₂ CO ₃	950	91.7
A2K	A2 + 0.5 g K ₂ CO ₃	1515	86.8
A3K	A3 + 0.5 g K ₂ CO ₃	1550	86.5
A4K	A4 + 0.5 g K ₂ CO ₃	1540	86.6
A21K	A21 + 0.5 g K ₂ CO ₃	1610	86.0
A31K	A31 + 0.5 g K ₂ CO ₃	1660	85.6
A41K	A41 + 0.5 g K ₂ CO ₃	1815	84.2
AF-T5K average	K ₂ CO ₃	1200	89.6

AK group catalysts are A1K, A2K, A3K, A4K, A21K, A31K, and A41K which are combined with 0.5 g of A group catalyst and 0.5 g of K₂CO₃ to strengthen the effect of A group catalysts. The procedure for the preparation of A group of activated red mud catalysts was given in Fig. 4.4 and AK group was obtained with the addition of K₂CO₃. 20 mL of wastewater and 1.0 g of catalyst were used in the hydrothermal gasification of alkaloid manufacturing wastewater. The reaction pressure was 500°C and a pressure range of 40.5- 44.0 MPa was obtained. The results of non-catalytic and with original red mud (ORM) catalyst and K₂CO₃ alone were given for comparison. The effect of AK group catalysts on carbon gasification efficiencies, gaseous product distribution and yields of product gases were given in

Table 5-21 -Table 5-25 and Figs 5-22 and 5-23. For accuracy, each run was repeated five times. The effect of red mud derivatives on the product efficiencies, gaseous product yields, and COD and TOC removal efficiencies were examined.

➤ **CGE (%) of wastewater and total amount of produced gas per unit volume**

Carbon gasification efficiencies and the amount of total gas product in the unit of *mmol gas/L* wastewater is represented in Table 5-21 AK group catalysts promoted carbon gasification efficiencies from 55.5% up to around 77 % as highest which is significantly higher than obtained CGE values with K_2CO_3 (66%) alone and CGE with A group catalysts (68%) alone. The effect of catalyst combinations is clearly seen on the total produced gas amount and gaseous product yields. The amount of the gaseous product has promoted by a ratio varying in 43-48% with AK catalysts. The amount of product gas did not change by the catalyst type remarkably.

➤ **The composition and yields of the gaseous product**

The gaseous product distribution was given in Table 22 and Figure 5-22. The ratio of methane and hydrogen moles in the product gas is higher but the ratio of carbon dioxide is lower in the presence of catalyst. Carbon monoxide and C_2 - C_4 hydrocarbons has an almost same molar percentage in non-catalytic and catalytic cases. The molar percentage of CH_4 increased to 35.5% (with A41K) as maximum which is 28.8% in the absence of catalyst. The effectiveness in methane formation is very similar in this group while the ratio of nickel impregnation has slightly promoted methane amounts. The molar percentage of H_2 has also enhanced from 34.9 to 39.6% by catalyst use and A31K as the most effective catalyst while the other shows almost indistinguishable catalytic activities. Reduced state of the catalysts slightly increased hydrogen percentages. The molar ratio of CO_2 decreased from 33% to the percentages of 23-26%. The effect of reduction can be seen since slightly lower CO_2 ratios were obtained with A21K, A31K and A41K catalysts.

The amount of produced gaseous (in unit of mol/kg C in wastewater) were increased by addition of AK group of catalyst. The increment in yields of CH_4 , and

H₂ are virtually high while in yields of CO₂ is less and rise in yields of C₂-C₄ compounds and CO very low. AK group catalyst promoted hydrogen production greatly above 38, from 20.3 mol H₂/kg C in wastewater for non-catalytic case while it was nearly 33-34 mol H₂/kg C in wastewater with A and B group. This result shows that addition of K₂CO₃ to A group catalyst give higher yields in case of hydrogen. The methane yields were 16.8 in non-catalytic case and 28-29 mol CH₄/kg C in wastewater with A and B group catalyst. AK accelerated methane formation and the amount of produced nearly doubled, up to the levels of 34-35 mol CH₄/kg C. In terms of methane production, AK group is also the best group in activated red mud catalysts. CO₂ yields are generally increased while reduced catalysts give slightly lower CO₂ than other. The other gaseous did not vary with the effect of catalyst use and type considerably. Total gaseous product yields were reached to 97-98 mol/kg C which is 70% higher than in non-catalytic run.

➤ **COD and TOC content of the aqueous product and removal efficiencies**

COD and TOC in the raw wastewater is lowered by AK group catalyst in this experimental part at the end of HTG studies and the results were given in Table 5-24 and Table 5-25. COD of the wastewater, that is 32050 mg/L, lowered to 8470 mg/L without catalyst by HTG process at 500°C and to 7610 mg/L with original red mud while 5125 mg/L was found in the presence of K₂CO₃. The best COD removal was achieved as 5400 mg/L with A31K (20% Nickel impregnated and reduced form) while the others varied in 6150-7210 mg/L. The addition of K₂CO₃ to A group enhanced gasification while did not a positive effect of COD removal. COD_{RE} values were changed obtained between 78-83% as 80-84% with A and 81-85 % with B. As it is seen, the COD removals were not affected by type of the activation process and K₂CO₃ addition to red mud, much. TOC content of raw wastewater, 11500 mg/L, decreased by removal efficiencies of 75 % without catalyst, 81.5% with original red mud and 90% in the presence of K₂CO₃. A1K is the most effective catalyst in TOC removal with 92% and the others have removal efficiencies within the range of 84-87%.

5.3.1.4 Comparison of the Catalyst Groups

In the case of CGE, TOC removal efficiencies, COD removal efficiencies, H₂ and CH₄ yields with the effect of nickel impregnation, K₂CO₃ addition and reduction by NABH₄ were presented in this section and given in Figs 5-25 to 5-34.

❖ Effect of Red Mud, Activated Red Mud and Nickel Impregnation on CGE, CH₄ and H₂ yields.

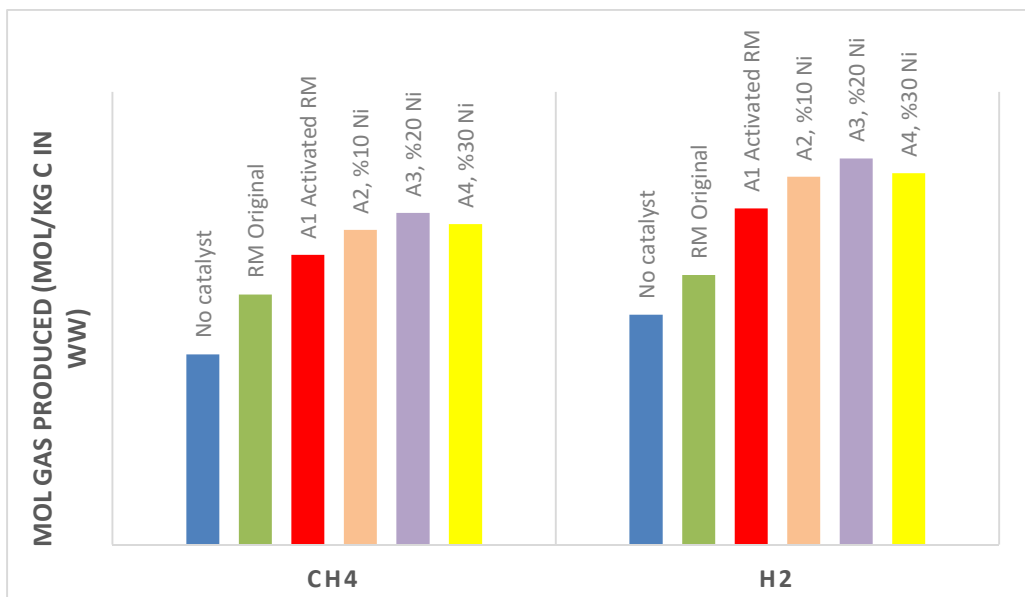


Figure 5-24. Effect of Nickel impregnation in non-reduced A group catalysts on yields of CH₄ and H₂.

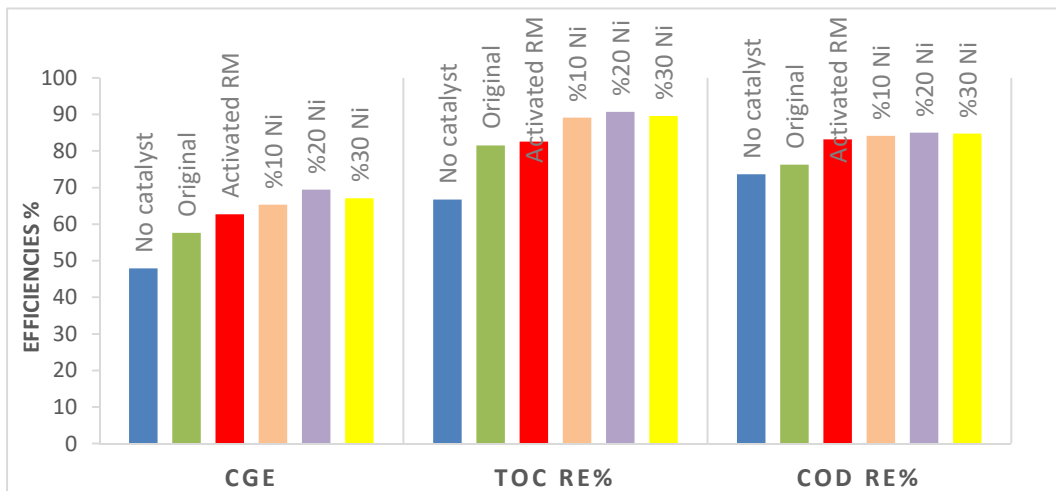


Figure 5-25. Effect of Nickel impregnation in non-reduced A group catalysts on CGE, TOC RE and COD RE.

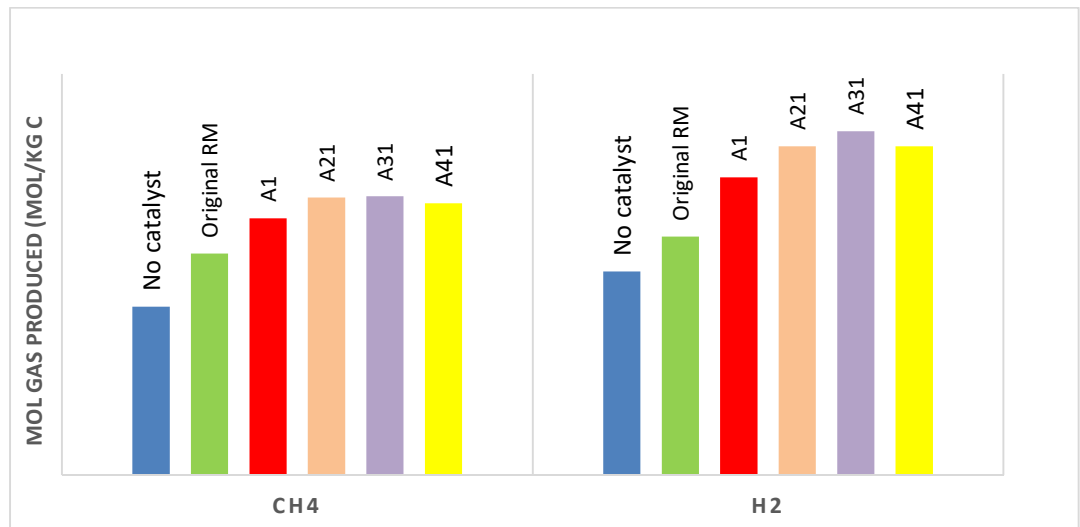


Figure 5-26. Effect of Nickel impregnation in reduced A group catalysts on CGE and yields of CH₄ and H₂.

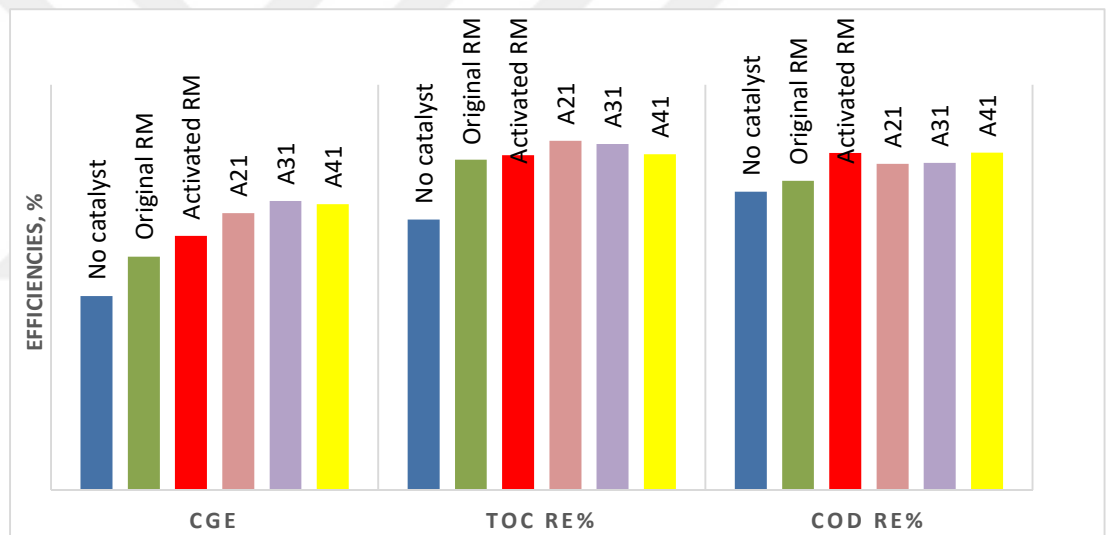


Figure 5-27. Effect of Nickel impregnation in reduced A group catalysts on CGE, TOC_{RE} and COD_{RE}.

❖ **Effect of Reduction and Nickel Impregnation**

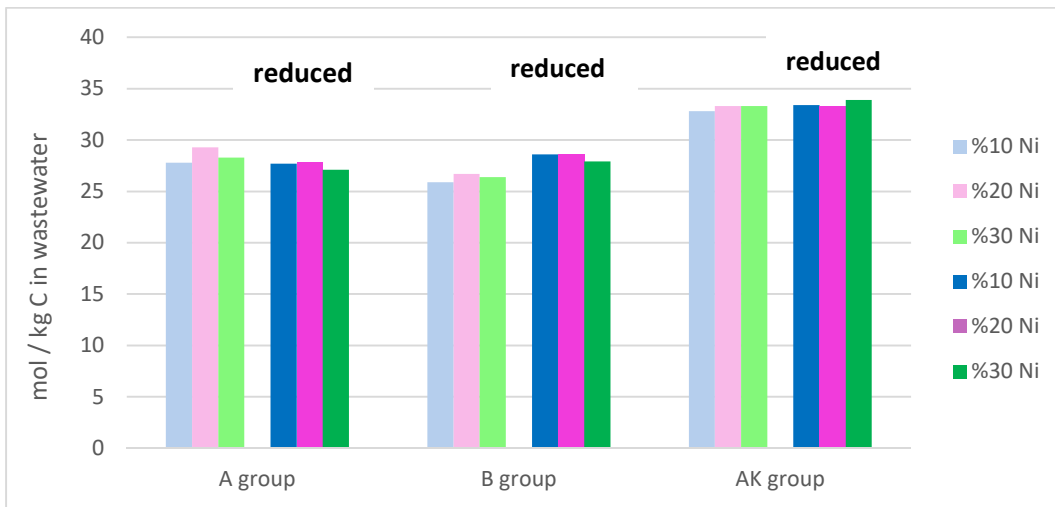


Figure 5-28. Effect of reduction and Nickel impregnation in all catalysts on CH₄ yields.

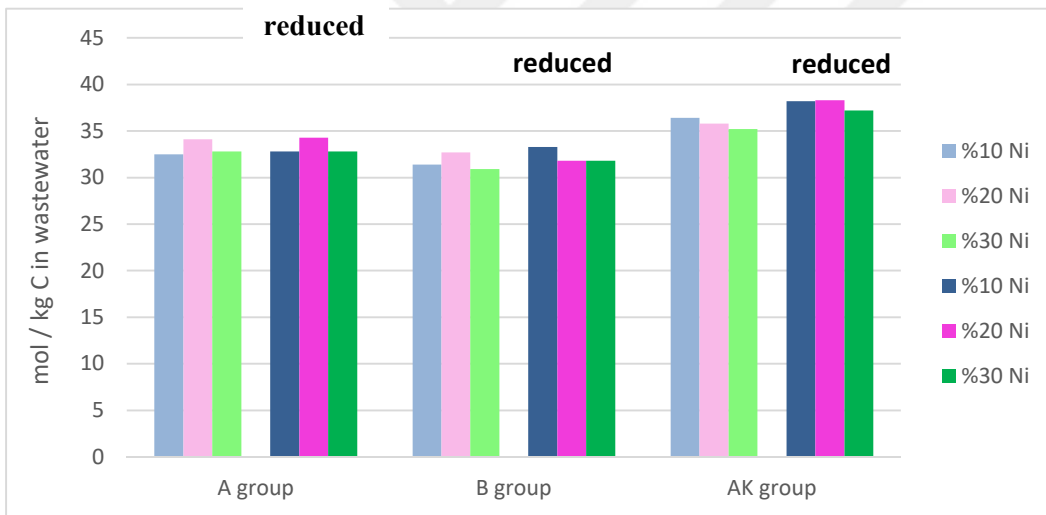


Figure 5-29. Effect of reduction and Nickel impregnation in all catalysts on H₂ yields.

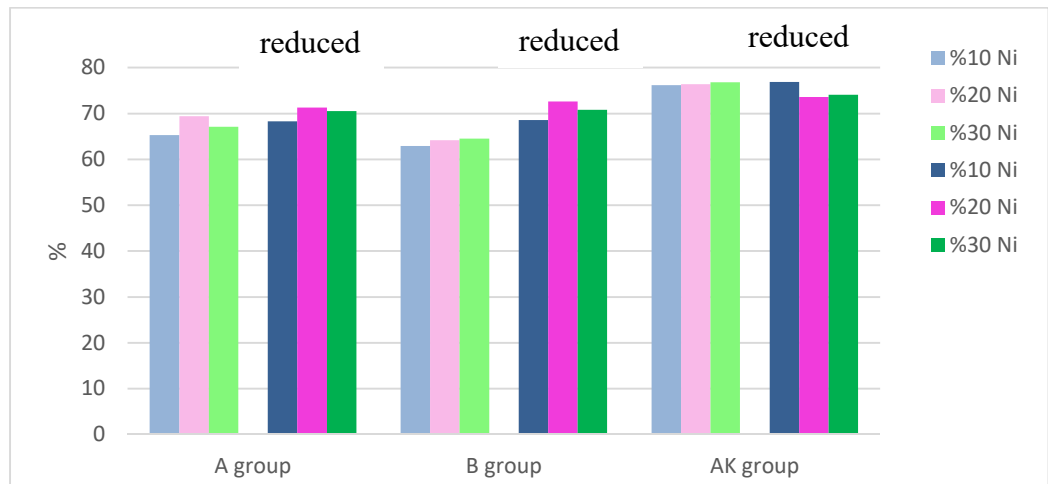


Figure 5-30. Effect of reduction and Nickel impregnation in all catalysts on CGE

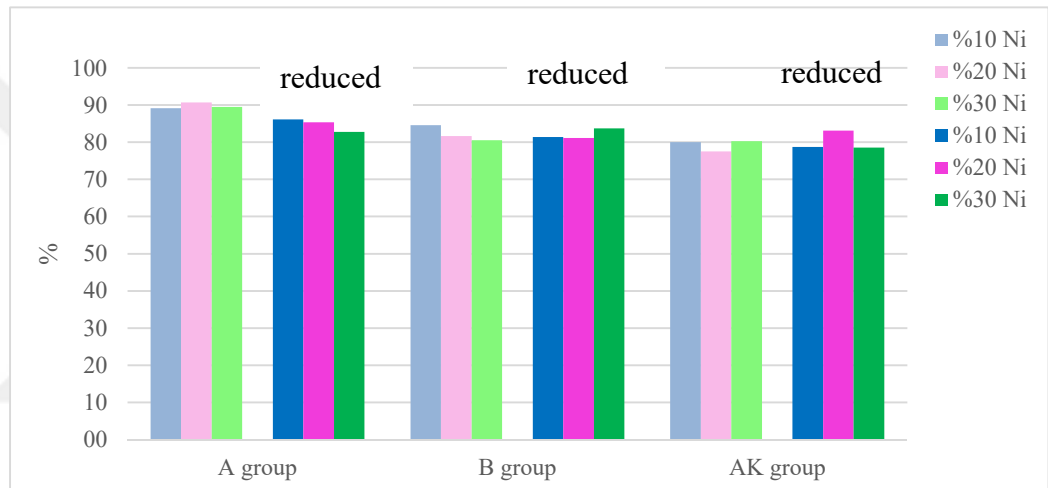


Figure 5-31. Effect of reduction and Nickel impregnation in all catalysts on COD Removal Efficiency.

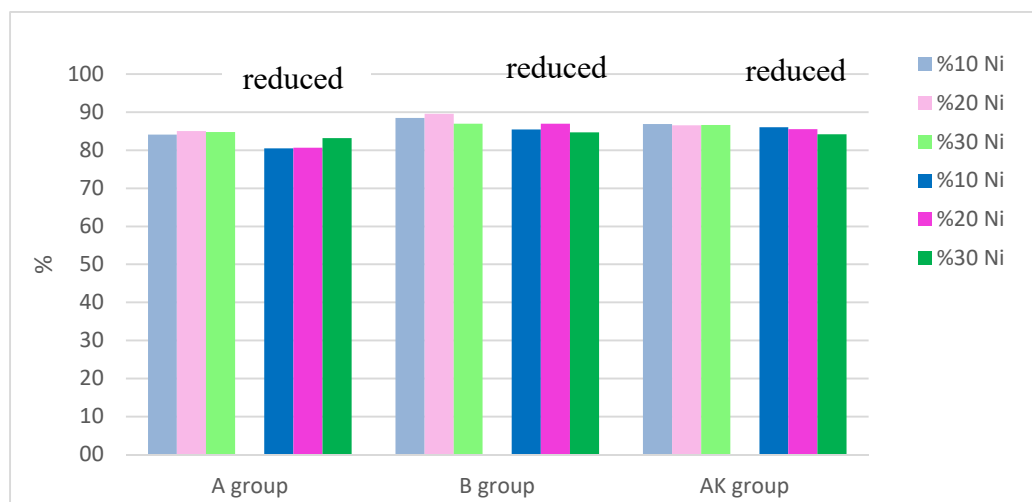


Figure 5-32. Effect of reduction and Nickel impregnation in all catalysts on TOC Removal Efficiency.

❖ Effect of K₂CO₃ addition to A group catalyst



Figure 5-33. Effect of K₂CO₃ addition and Nickel impregnation in A group catalysts on CGE.

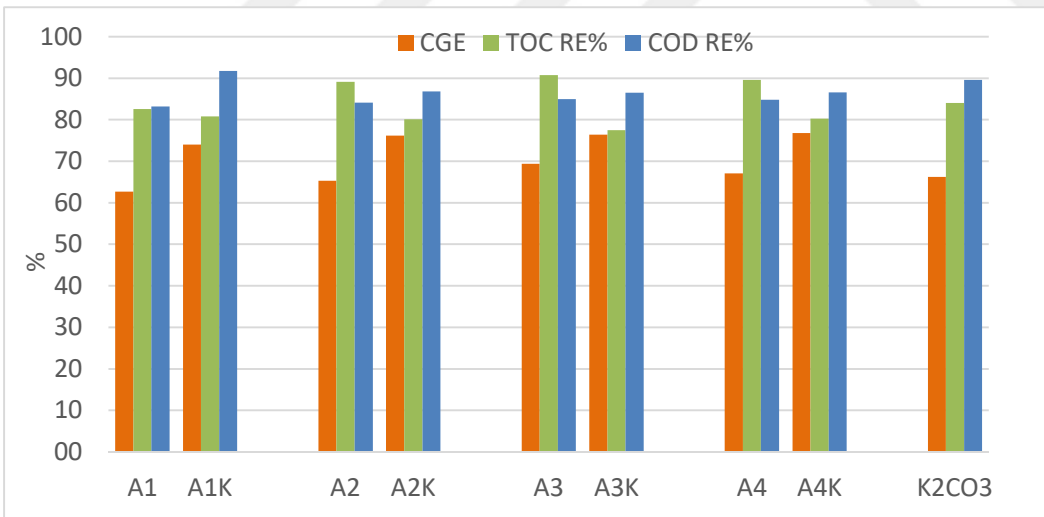


Figure 5-34. Effect of K₂CO₃ addition and Nickel impregnation in A group catalysts on COD_{RE} and TOC_{RE}.

The effect of red mud catalyst type on carbon gasification efficiencies. Gaseous product distribution and yields. TOC and COD removal efficiencies are given in this report.

In the first part of the experimental study the reactions were carried at 500 °C in the presence of 0.5 g of A-group catalysts are shown in Figs 1-2 and Tables 4-5. The most effective catalysts on CGE. A31 (20% Nickel impregnated and reduction by NaBH₄), A41 (30% Nickel impregnated and reduction by NaBH₄), and A3 (precipitation with NH₃, 20% Nickel impregnated) which have CGE of 71.3, 70.5 and 69.4 respectively. In the case of CH₄ and H₂ yields (mol/kg C in wastewater), all catalyst in A group improved yields of these gases. Similarly, the highest yields were reached with A3 and A31 catalysts in whole group. The Nickel impregnation give best result at 20% of Nickel in the studied range. In the case of COD removal, Nickel makes a little improvement comparing with the A1 which has no Nickel impregnation. But reduction with NaBH₄ cause a negative effect on COD removal efficiencies. Non-reduced catalysts in A group have higher removal in COD.

The effect of using different catalyst types on the gas product distribution and gaseous product yields was investigated and shown in Figs 3-4 and Table 5-8 in B group of catalyst. Hydrogen yields are higher with B2, B3 (10% and 20% Nickel impregnated), B21 (10% Nickel impregnated and reduction by NaBH₄) catalysts than the non-catalytic case and with other catalysts in this group. Methane yields were increased in the reduced ones in group more. The most effective catalysts in methane improvement are B21 and B31. COD (Chemical Oxygen Demand) and TOC (Total Organic Carbon) analysis and removal efficiency calculations were done for each study and are shown in Table 7-8. COD of Alkaloid wastewater was analyzed as 32050 mg/L. The results shows removal efficiency is increased with the addition of catalyst. The highest COD removal efficiencies were obtained with B2 and B41. TOC of Alkaloid wastewater was analyzed as 11500 mg/L. TOC removal efficiency was increased with the addition of catalyst effectively. The highest TOC removal efficiency ratios obtained with B2, B3 and B31.

In the last part. K_2CO_3 addition improved CGE at a ratio between percent8-10. Also it makes significant increment on the gaseous product yields. It reduce the TOC removal efficiencies while increase COD removal efficiencies slightly.

5.3.1.5 Analysis Results Of Selected Activated Red Mud Catalysts In SEM, XRD And BET Analysis Equipments

Four red mud activated catalysts (A2, A21, A3, A31, A4, B2, B21, B3, B31, B4) were selected and analyzed for characterization studies and compared to each other.

SEM-EDS ANALYSIS AND MAPPING of A2 (Precipitation with NH_3 + %10 Ni impregnation + Calcination)

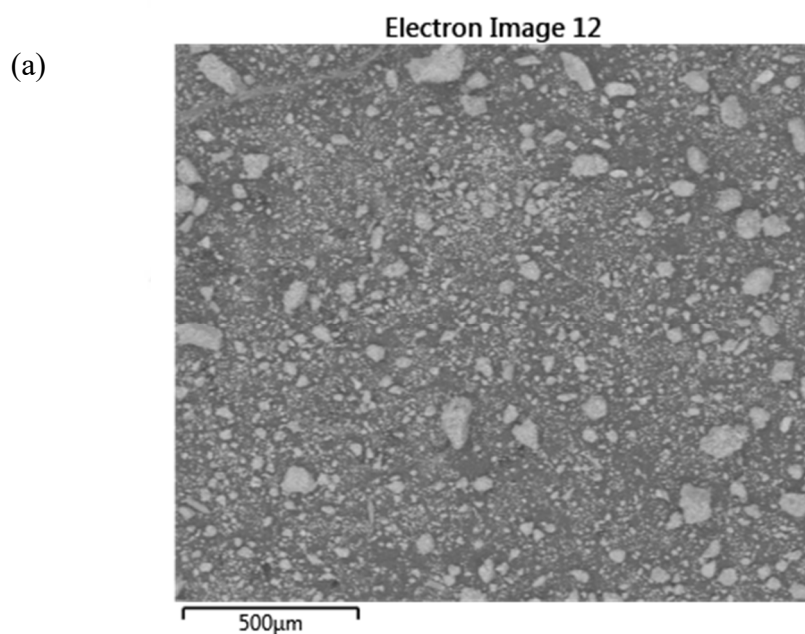


Figure 5-35. General electron image (a) and spectrum (b) of A2 catalyst

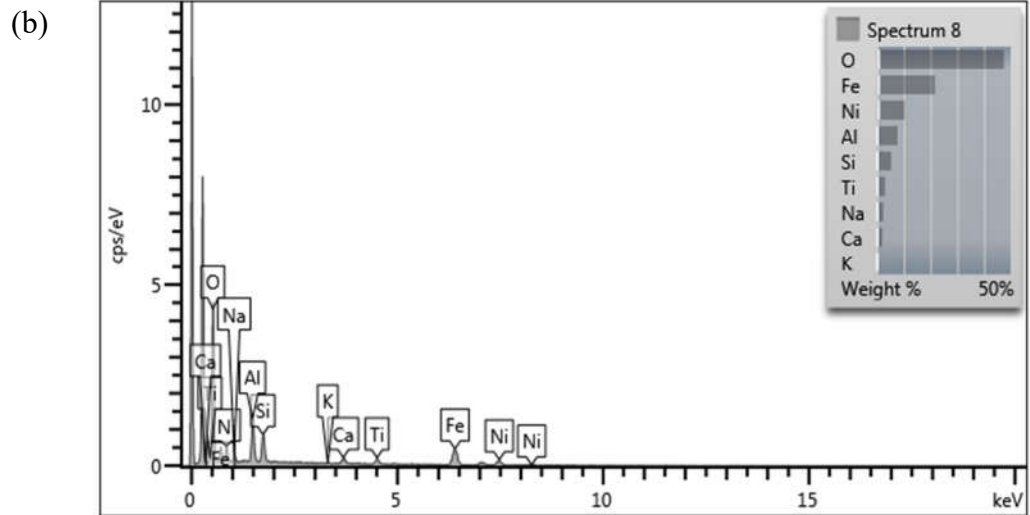


Figure 5-35. General electron image (a) and spectrum (b) of A2 catalyst (continued)

Table 5-26. Surface elemental composition of A2 catalyst

Element	Wt%	Atomic %
O	47.43	70.22
Na	2.35	2.42
Al	7.65	6.72
Si	5.29	4.46
K	0.26	0.16
Ca	1.96	1.16
Ti	2.99	1.48
Fe	21.70	9.20
Ni	10.36	4.18
Total:	100.00	100.00

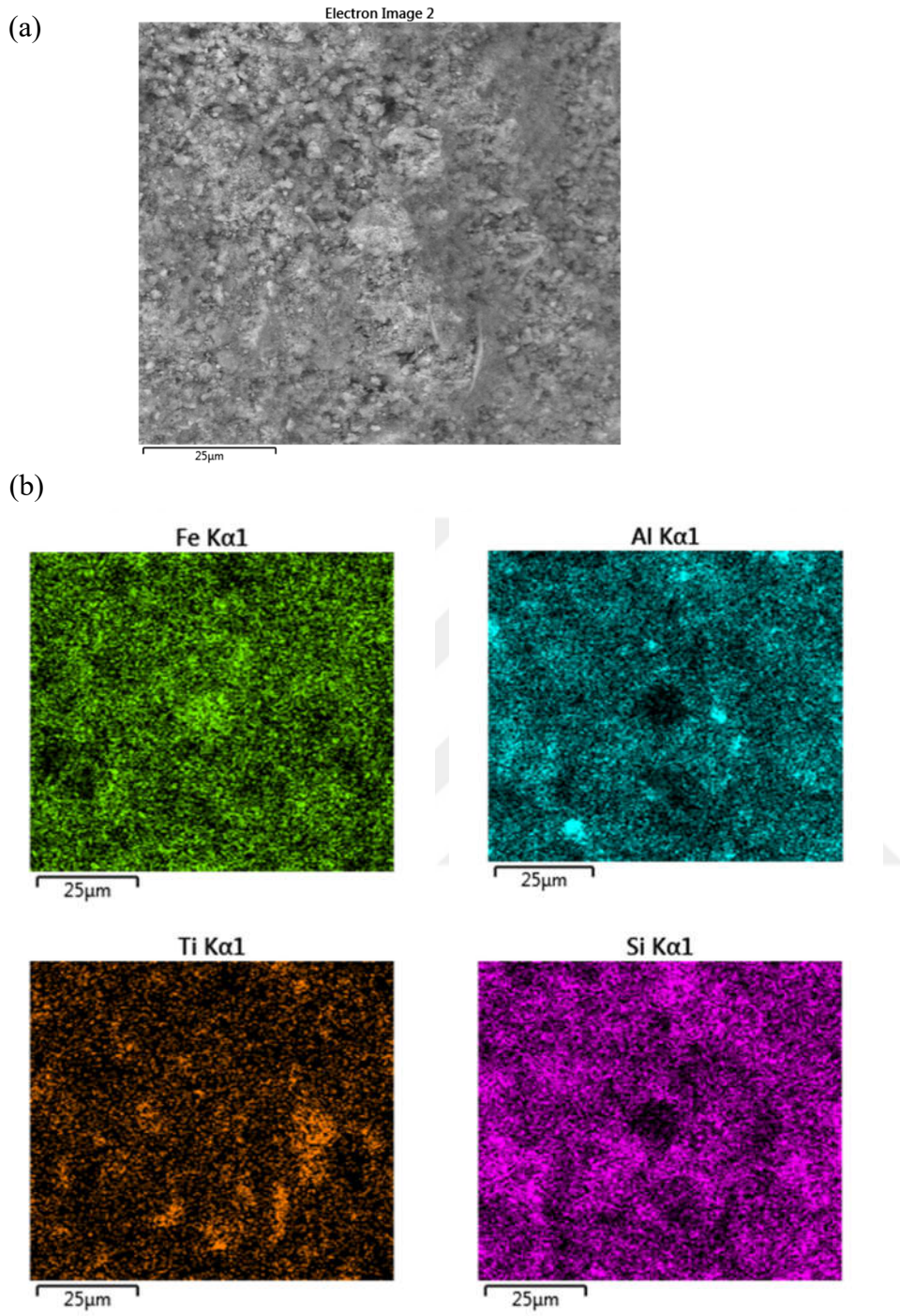


Figure 5-36. Electron image (a) and elemental mapping (b) (continued)

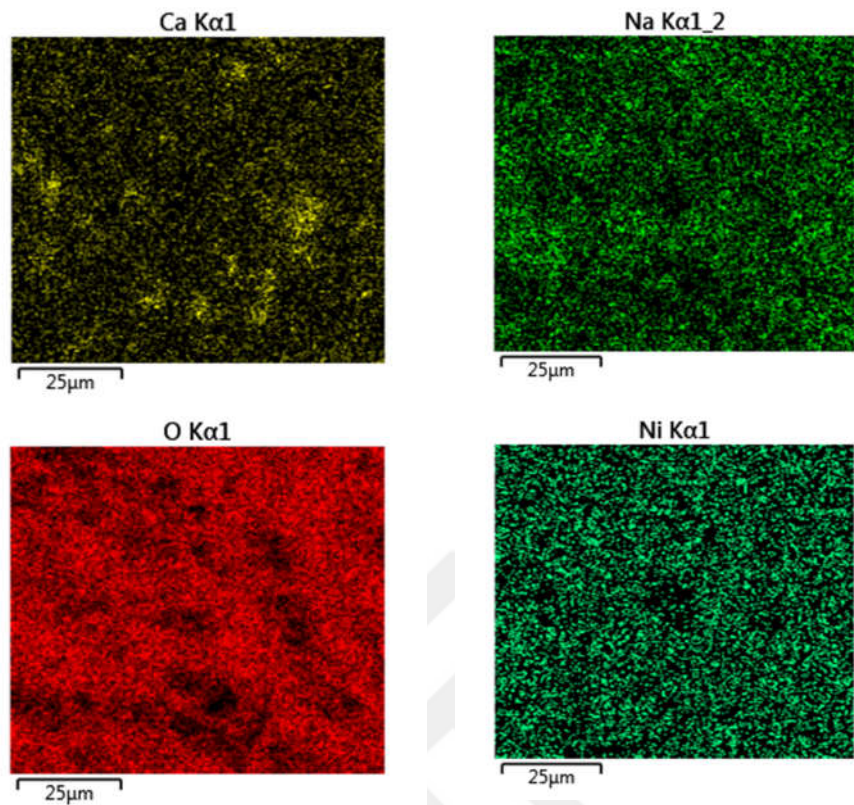


Figure 5-36. Electron image (a) and elemental mapping (b) (continued)

❖ **SEM-EDS ANALYSIS AND MAPPING of A21 (Reduction of A2 by NaBH₄)**

A21 catalyst is prepared by precipitation with NH₃ of red mud, %10 Ni impregnation and lastly reduction by NaBH₄.

(a)

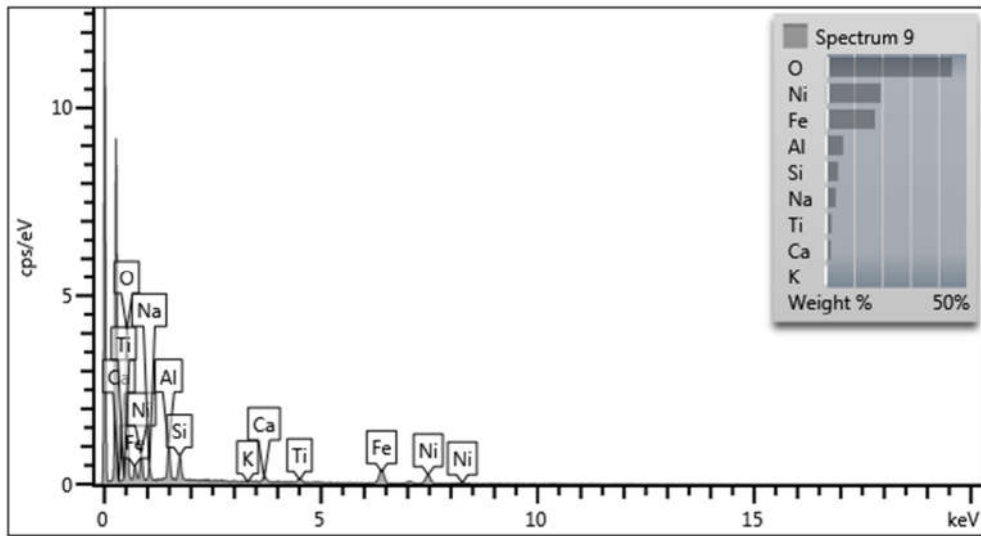
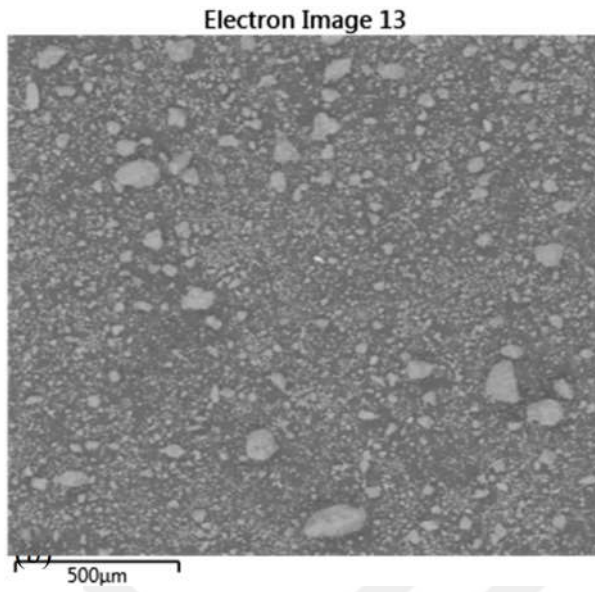


Figure 5-37. General electron image (a) and spectrum (b) of A21 catalyst

Table 5-27. Surface elemental composition of A21 catalyst

Element	Wt%	Atomic %
O	44.88	68.70
Na	3.59	3.82
Al	6.24	5.67
Si	4.44	3.87
Ca	1.73	1.06
Ti	2.05	1.05
Fe	17.50	7.67
Ni	19.57	8.16
Total:	100.00	100.00

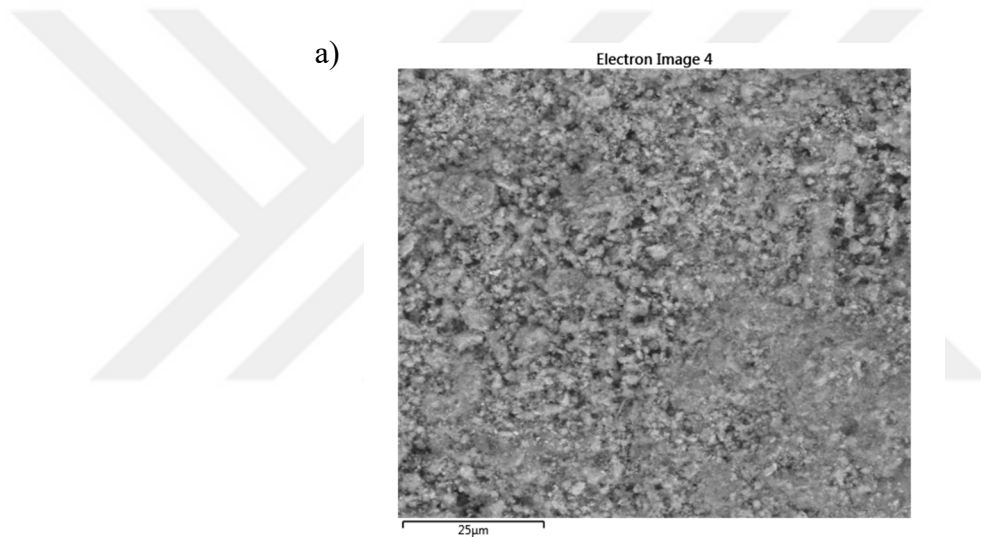


Figure 5-38. Electron image (a) and elemental mapping (b) of A21 catalyst

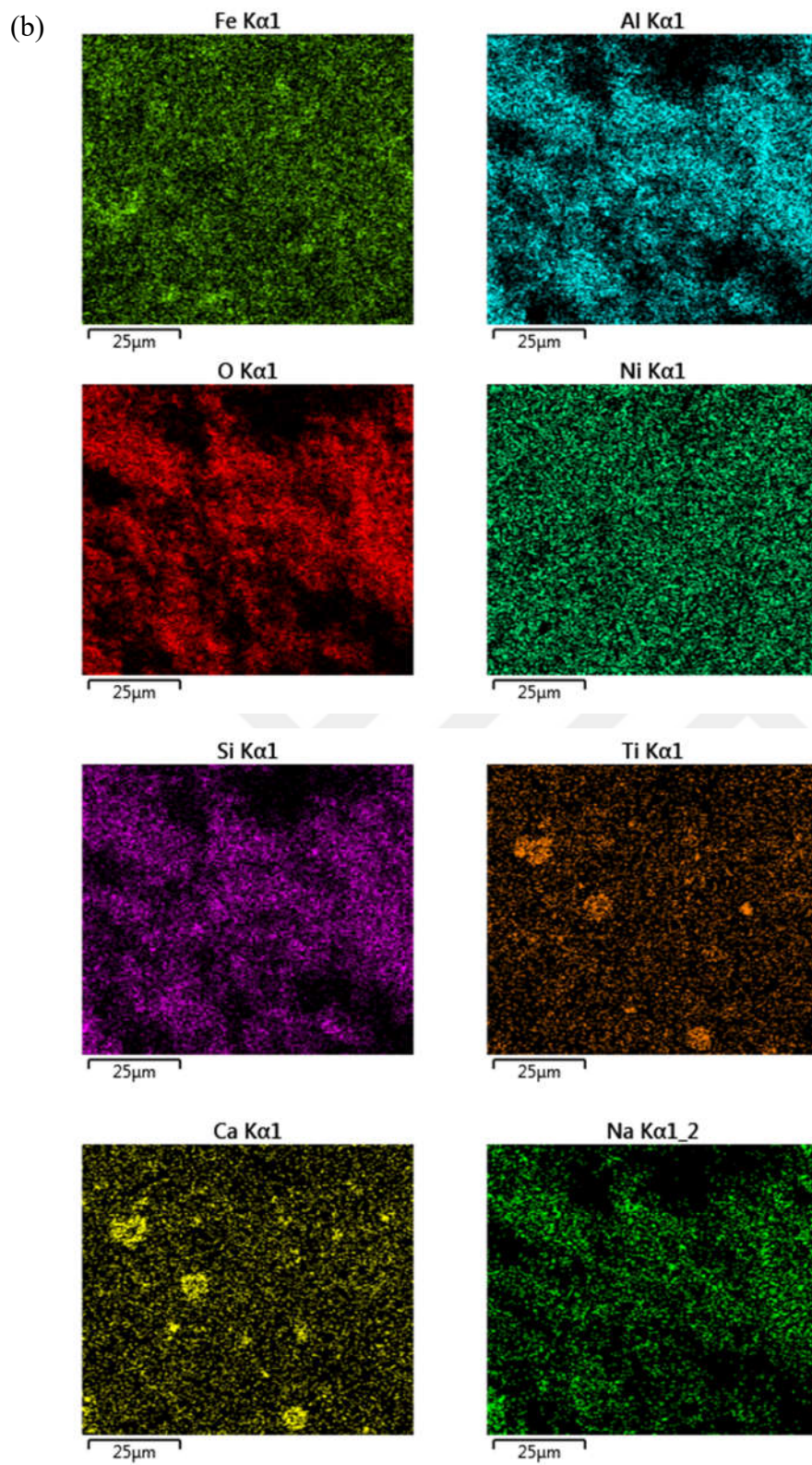
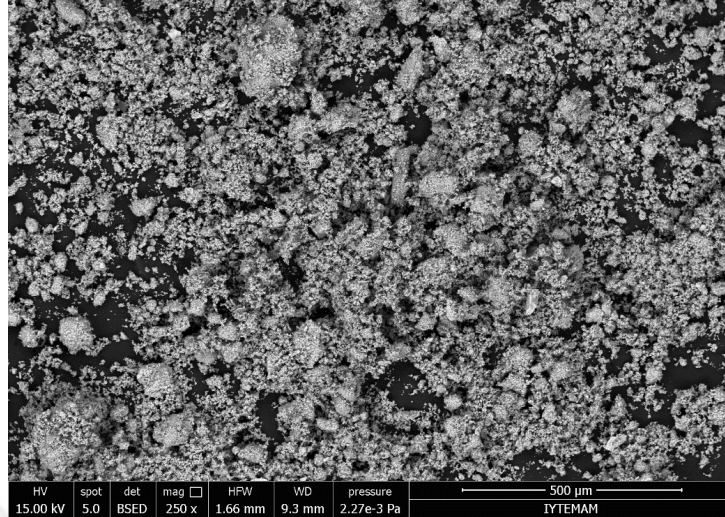


Figure 5-38. Electron image (a) and elemental mapping (b) of A21 catalyst (continued)

❖ **SEM-EDS ANALYSIS AND MAPPING of A3 (Precipitation with NH_3 + %20 Ni impregnation + Calcination)**

(a)



(b)

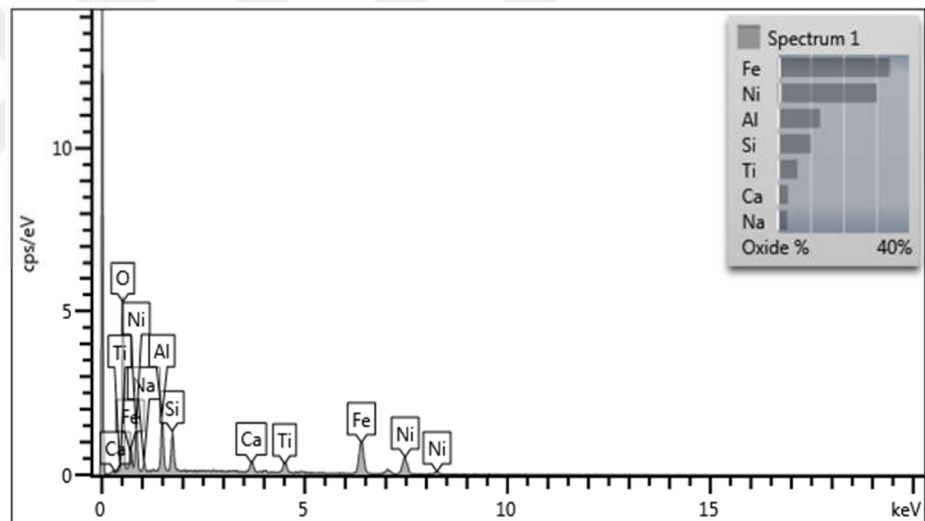
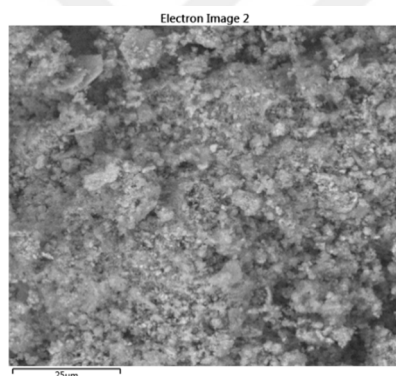


Figure 5-39. General electron image (a) and spectrum (b) of A3 catalyst.

Table 5-28. Surface elemental composition of A3 catalyst

Element	Wt%	Atomic %
O	29.80	54.79
Na	2.23	2.86
Al	6.88	7.50
Si	4.78	5.01
Ca	2.33	1.71
Ti	3.66	2.25
Fe	26.54	13.98
Ni	23.77	11.91
Total:	100.00	100.00

a)



b)

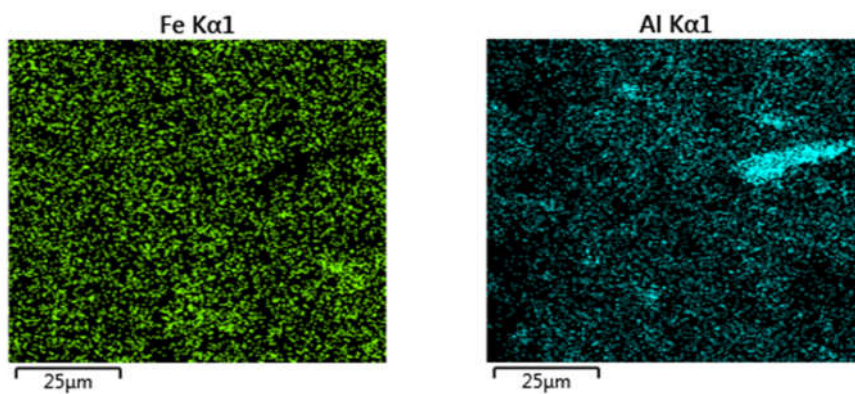


Figure 5-40. Electron image (a) and elemental mapping (b) of A3 catalyst

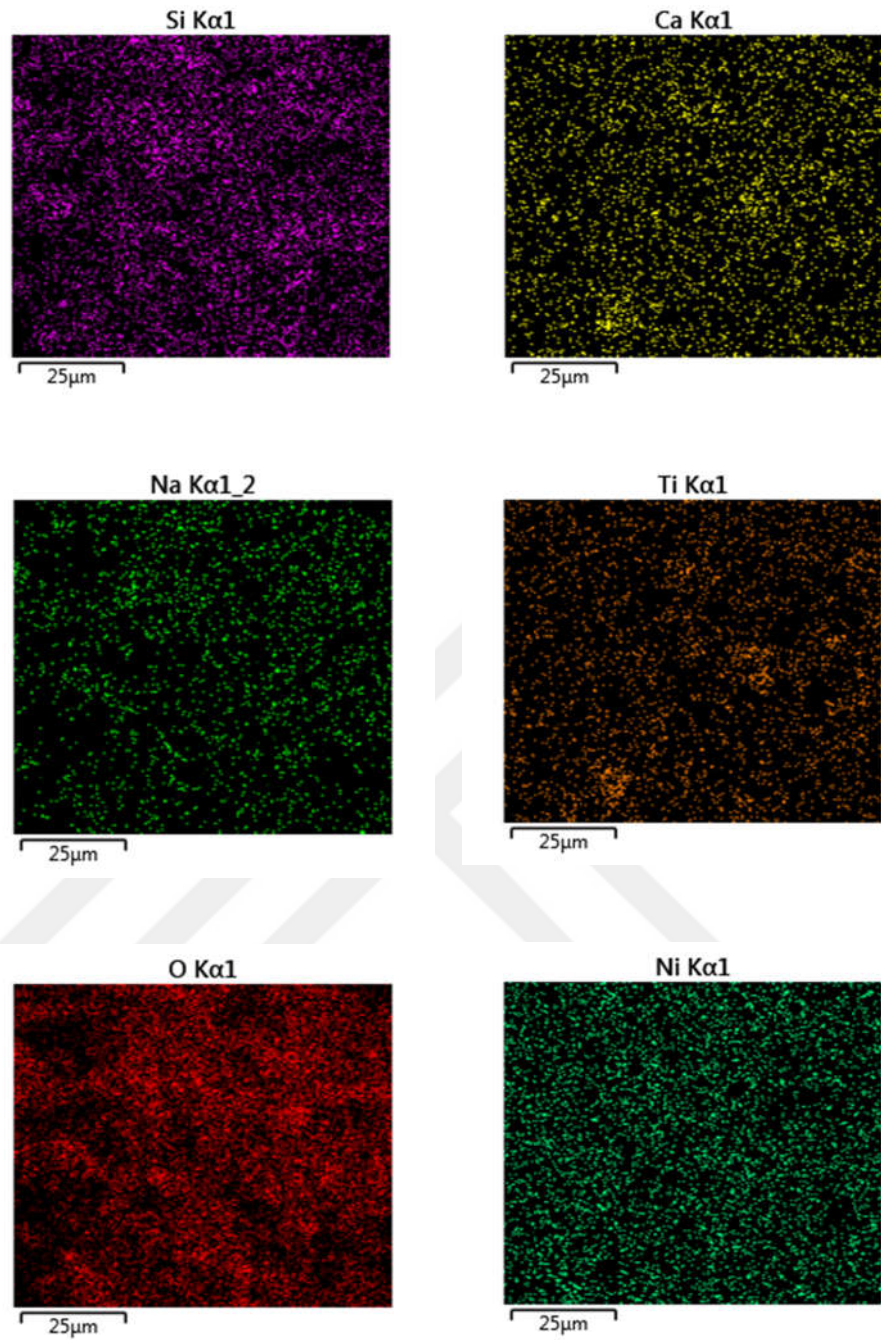
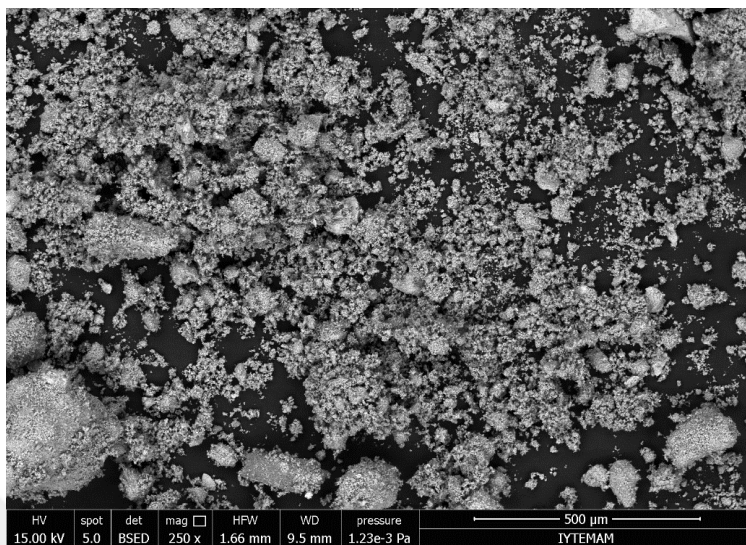


Figure 5-40. Electron image (a) and elemental mapping (b) of A3 catalyst (continued)

❖ **SEM-EDS ANALYSIS AND MAPPING of A31 (Precipitation with NH_3 + %20 Ni impregnation + reduction by NaBH_4 + Calcination)**

a)



b)

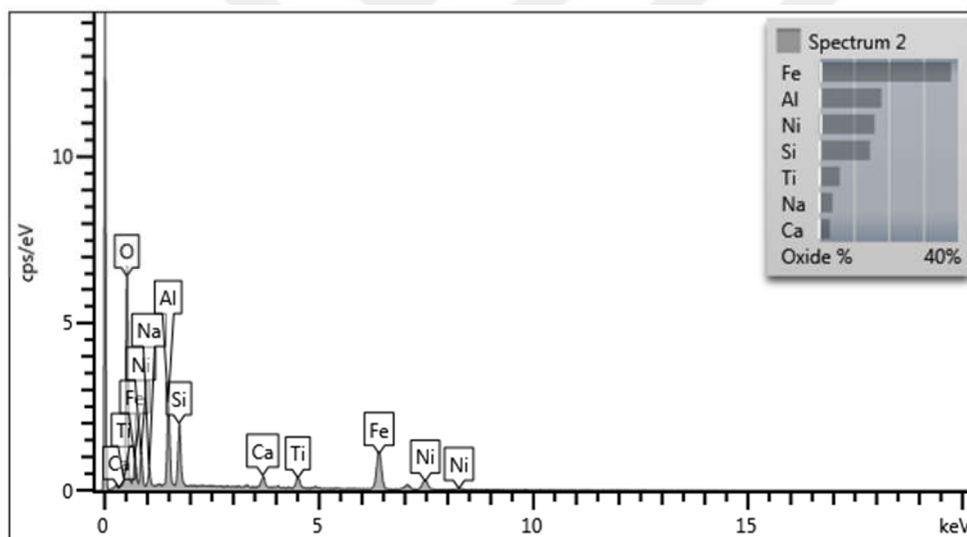
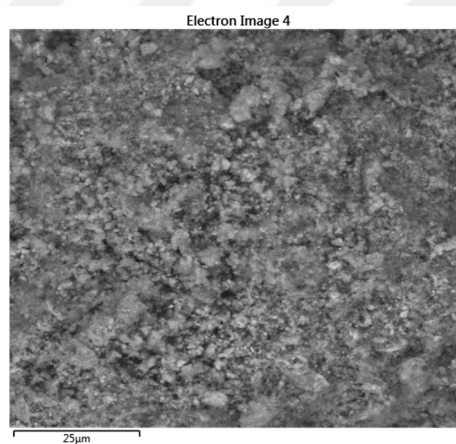


Figure 5-41. General electron image (a) and spectrum (b) of A31 catalys

Table 5-29. Surface elemental composition of A31 catalyst

Element	Wt%	Atomic %
O	32.58	55.94
Na	2.97	3.55
Al	9.54	9.72
Si	6.88	6.73
Ca	2.29	1.57
Ti	3.60	2.07
Fe	29.53	14.53
Ni	12.60	5.89
Total:	100.00	100.00

a)



b)

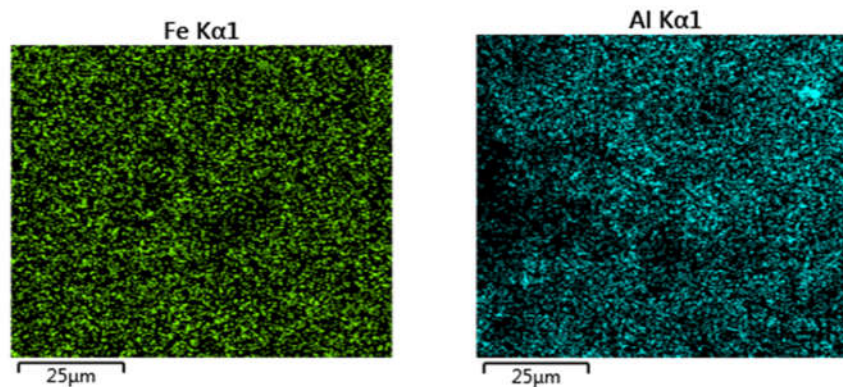


Figure 5-42. Electron image (a) and elemental mapping (b) of A31 catalyst.

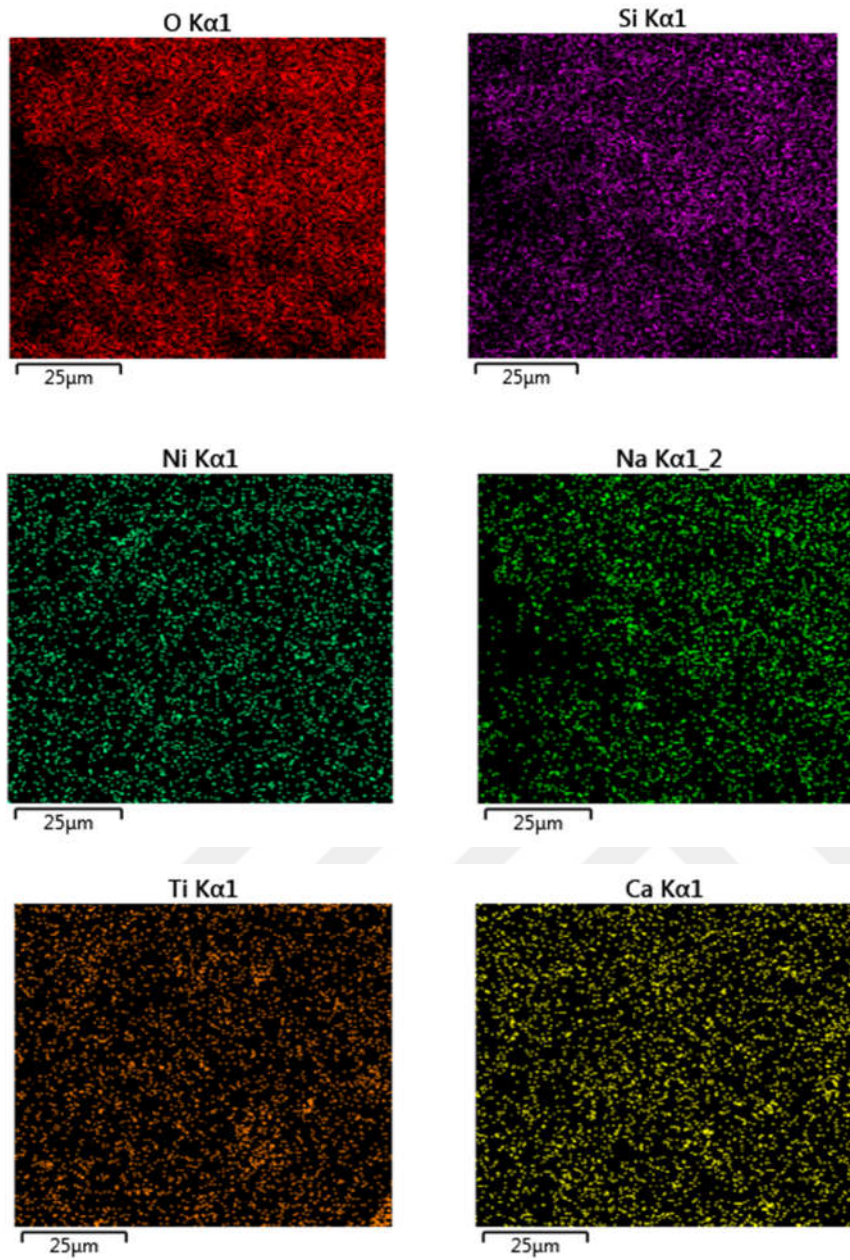


Figure 5-42. Electron image (a) and elemental mapping (b) of A31 catalyst (continued).

❖ SEM-EDS ANALYSIS AND MAPPING of A4 (Precipitation with NH_3 + %30 Ni impregnation + Calcination)

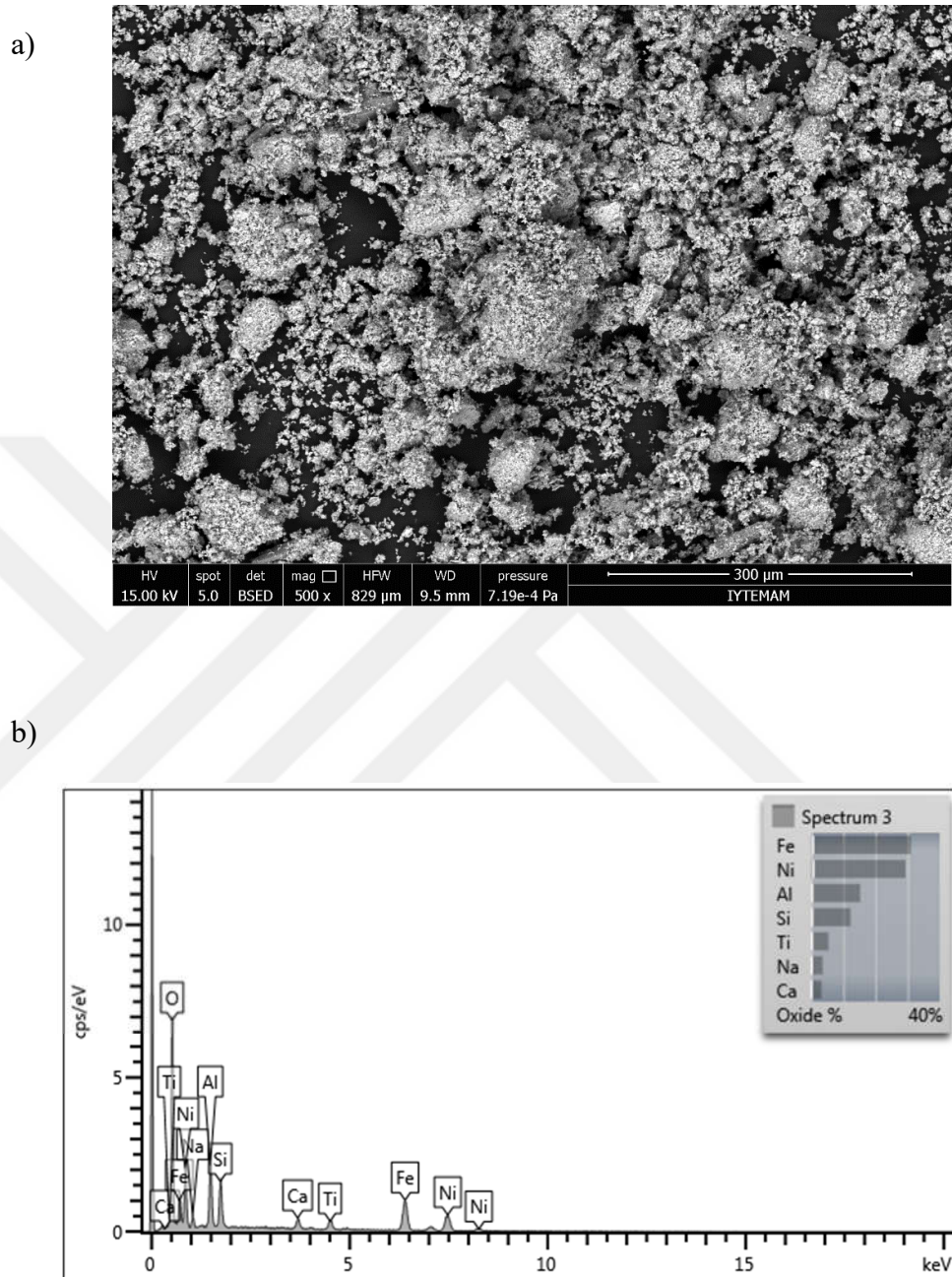


Figure 5-43. General electron image (a) and spectrum (b) of A4 catalysts.

Table 5-30. Surface elemental composition of A4 catalyst.

Element	Wt%	Atomic %
O	30.89	55.20
Na	2.65	3.30
Al	8.05	8.53
Si	5.75	5.85
Ca	2.30	1.64
Ti	3.25	1.94
Fe	24.09	12.33
Ni	23.02	11.21
Total:	100.00	100.00

a)

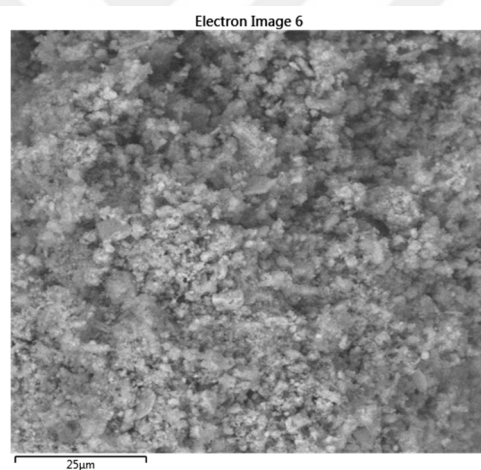


Figure 5-44. Electron image (a) and elemental mapping (b) of A4 catalyst

b)

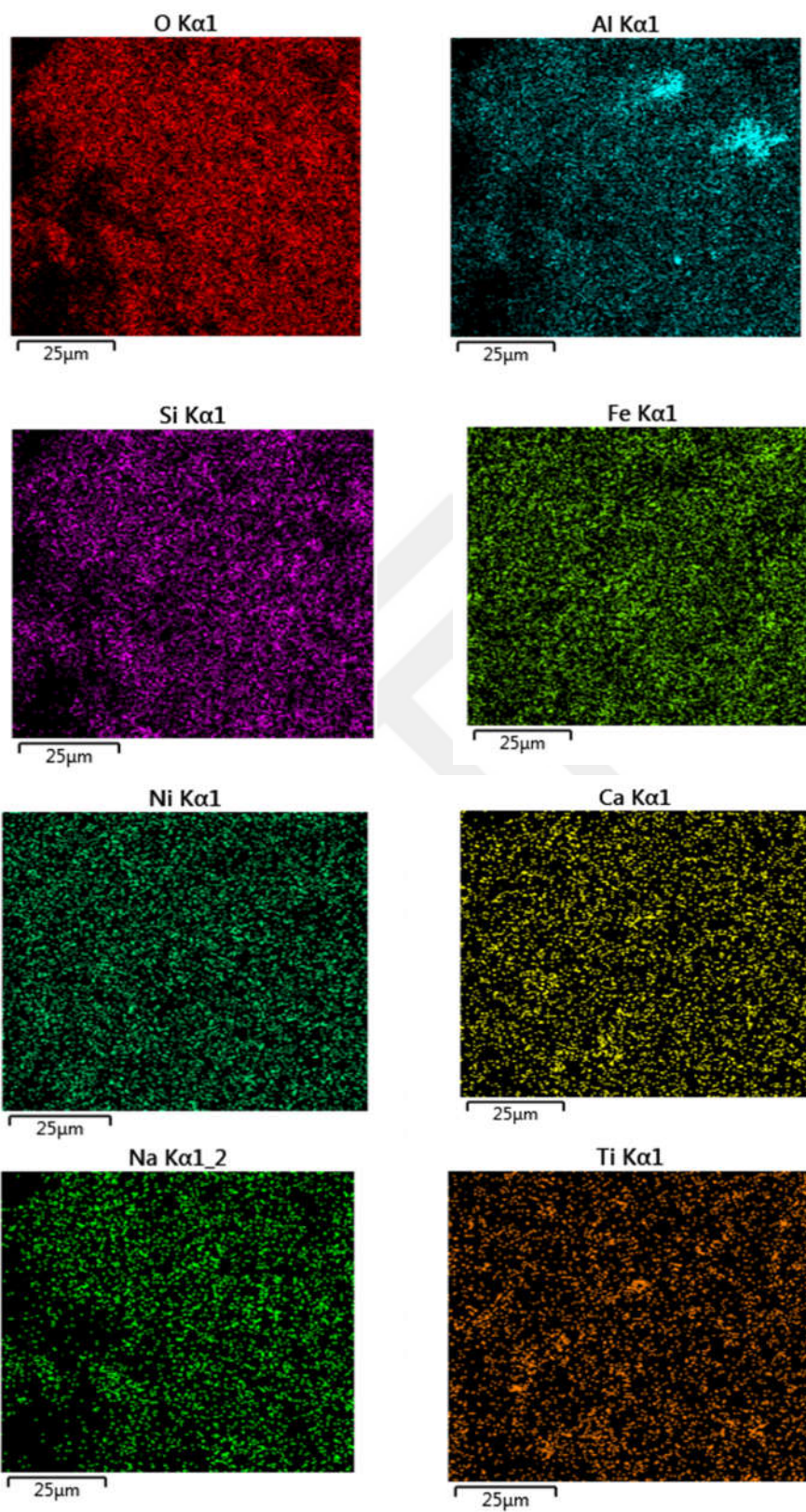
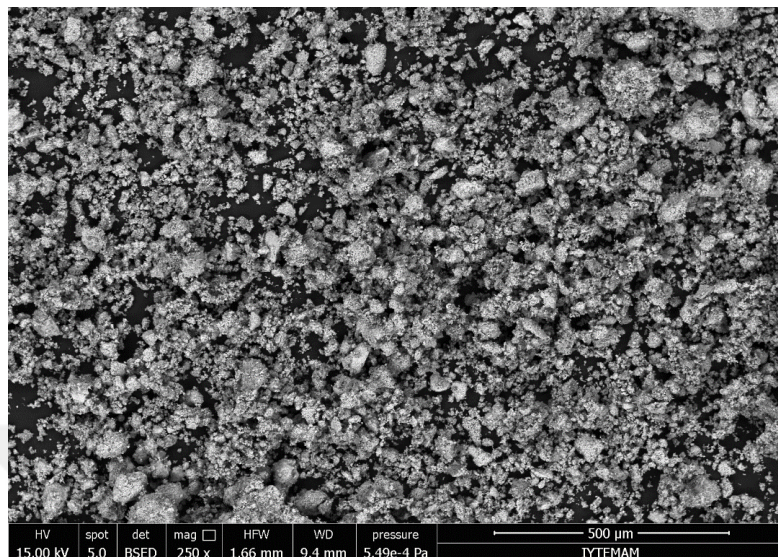


Figure 5-44. Electron image (a) and elemental mapping (b) of A4 catalyst (continued).

❖ SEM-EDS ANALYSIS AND MAPPING of A41 (Precipitation with NH_3 + %30 Ni impregnation + reduction by NaBH_4 + Calcination)

a)



b)

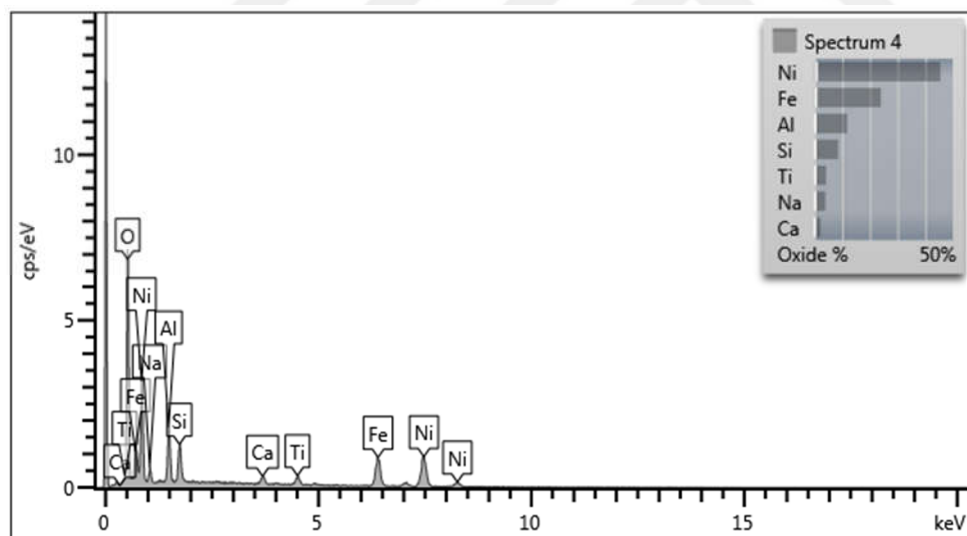


Figure 5-45. General electron image (a) and spectrum (b) of A41 catalysts.

Table 5-31. Surface elemental composition of A41 catalyst

Element	Wt%	Atomic %
O	28.47	53.73
Na	2.90	3.81
Al	6.25	6.99
Si	4.00	4.30
Ca	1.53	1.15
Ti	2.48	1.56
Fe	18.61	10.06
Ni	35.77	18.40
Total:	100.00	100.00

a)

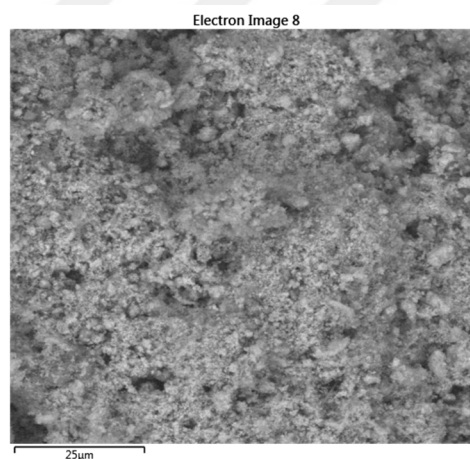


Figure 5-46. Electron image (a) and elemental mapping (b) of A41 catalyst.

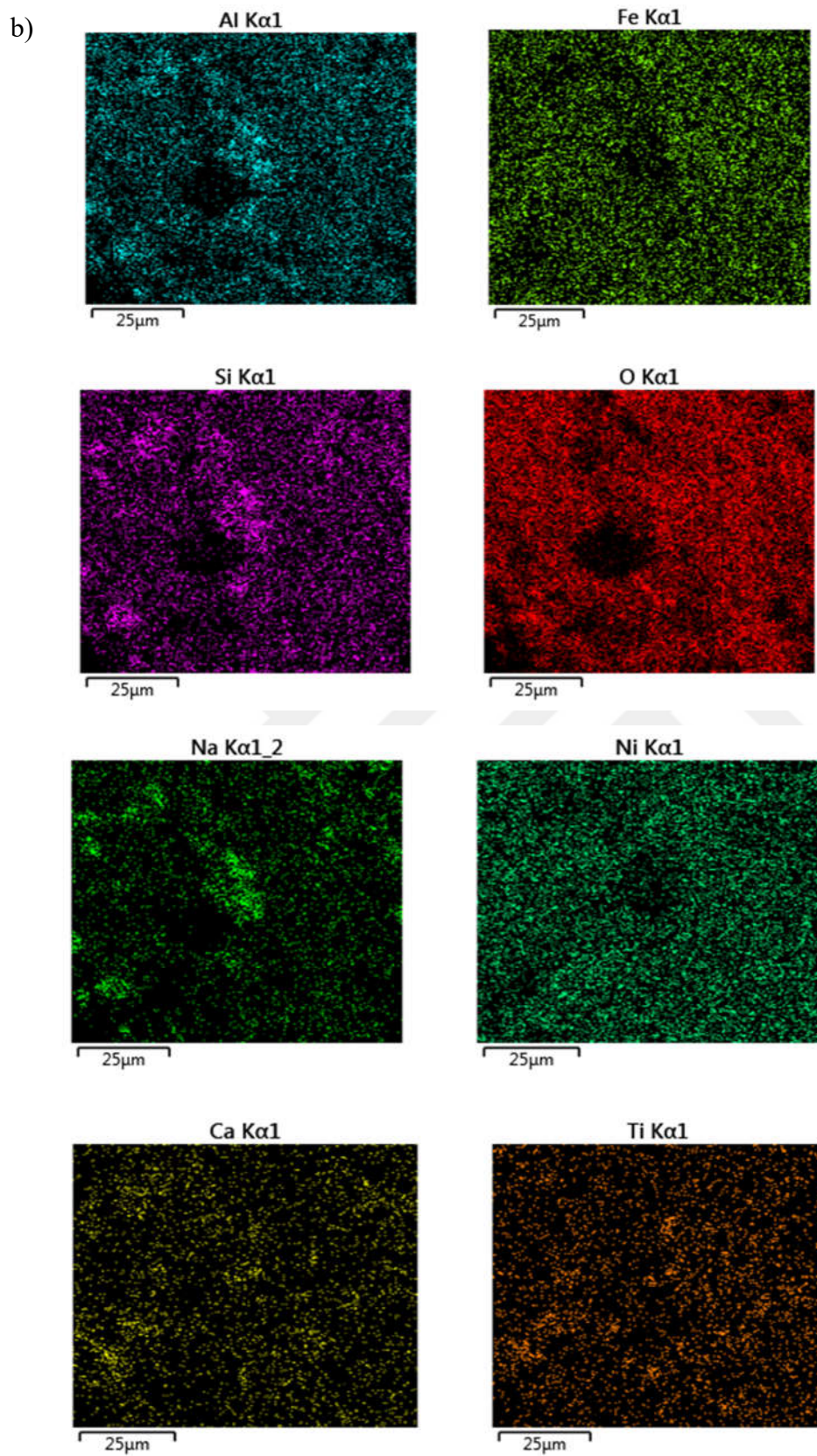


Figure 5-46. Electron image (a) and elemental mapping (b) of A41 catalyst (continued).

SEM-EDS ANALYSIS AND MAPPING of B2 (Precipitation of red mud with K_2CO_3 + %10 Ni impregnation + Calcination)

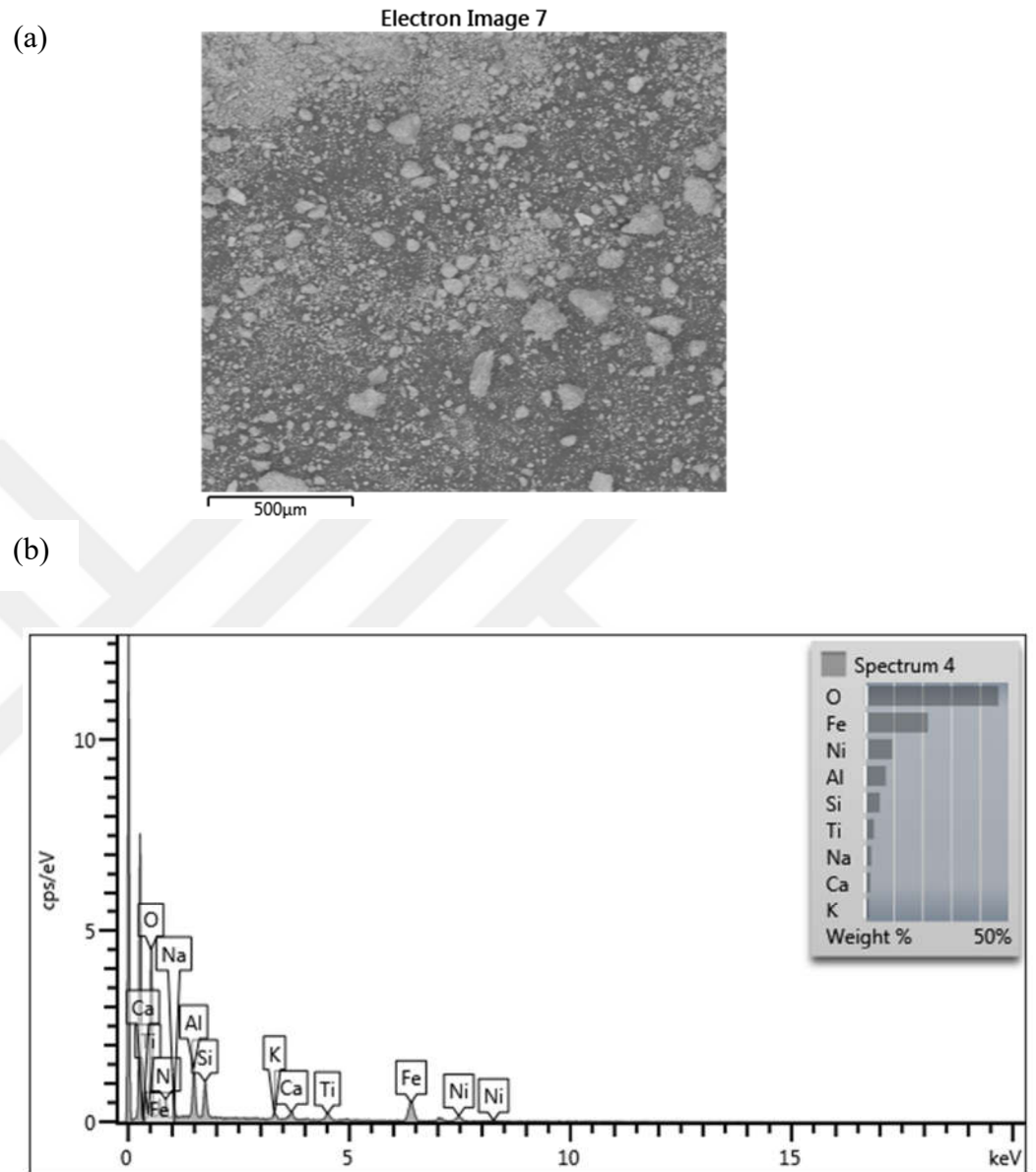


Figure 5-47. General electron image (a) and spectrum (b) of B2 catalyst

Table 5-32. Surface elemental composition of B2 catalyst

Element	Wt%	Atomic %
O	46.59	69.50
Na	2.33	2.42
Al	7.41	6.55
Si	5.28	4.49
K	1.42	0.87
Ca	2.05	1.22
Ti	3.24	1.61
Fe	22.00	9.40
Ni	9.67	3.93
Total:	100.00	100.00

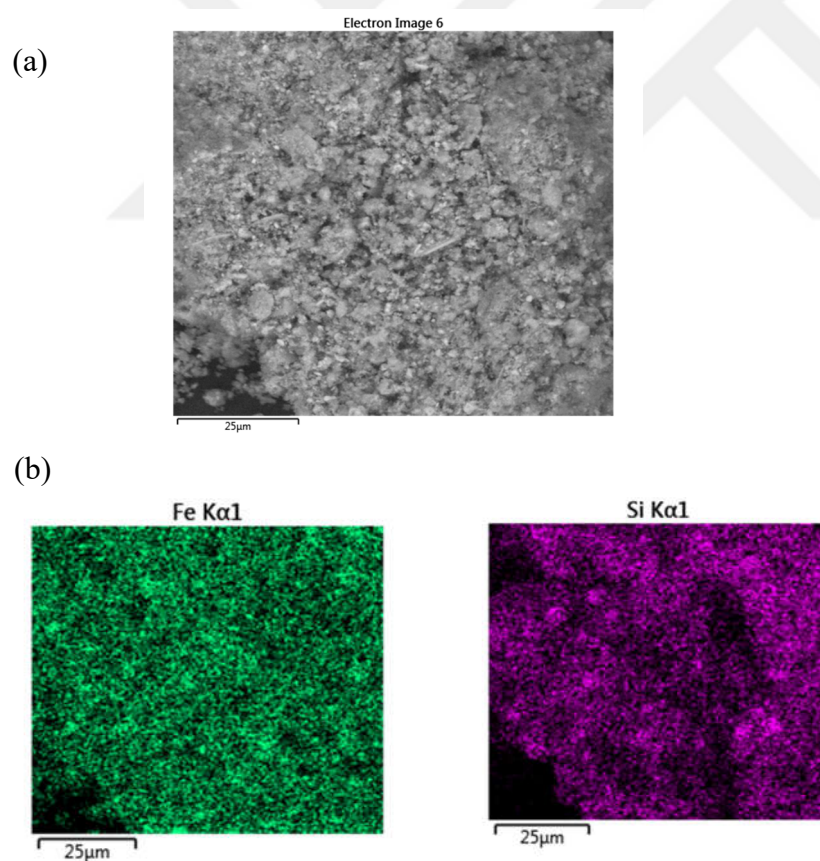


Figure 5-48 Electron image (a) and elemental mapping (b) of B2 catalyst

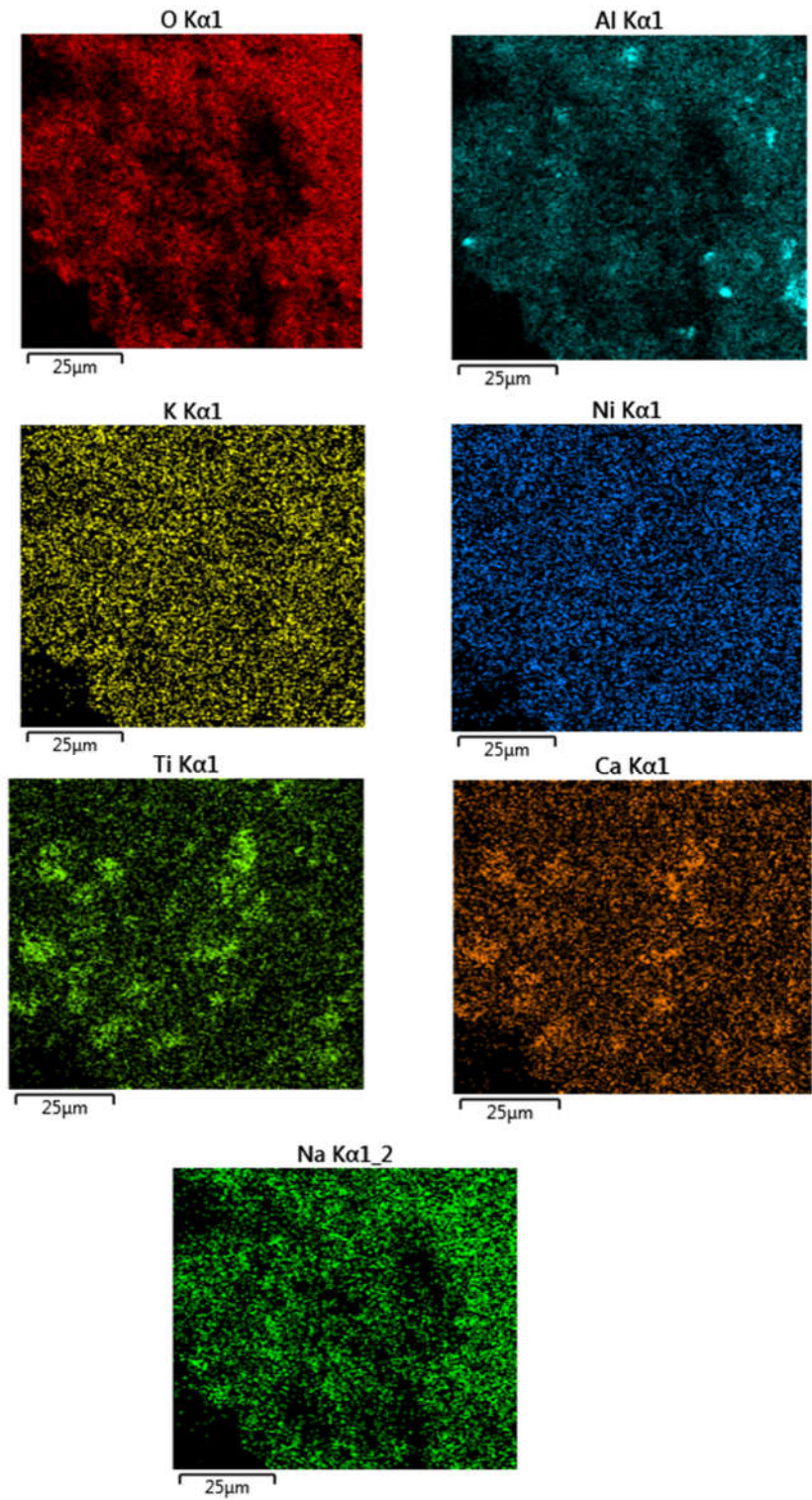
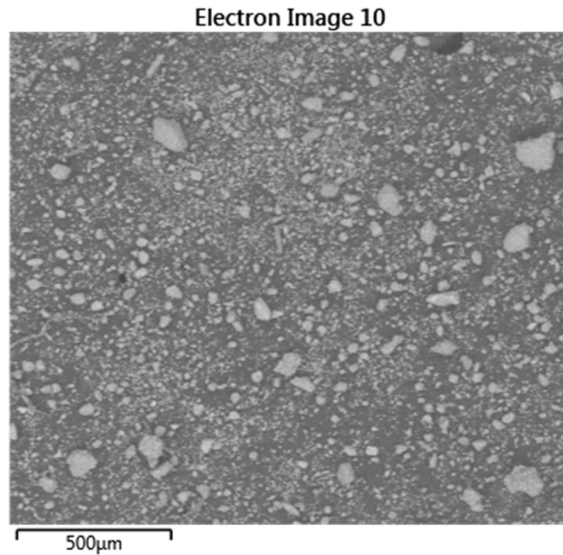


Figure 5-48. Electron image (a) and elemental mapping (b) of B2 catalyst (continued).

❖ SEM-EDS ANALYSIS AND MAPPING of B21 (Reduction of B2 by NaBH_4) B21

Catalyst is prepared by precipitation with K_2CO_3 of red mud, 10% Ni impregnation and lastly reduction by NaBH_4

(a)



(b)

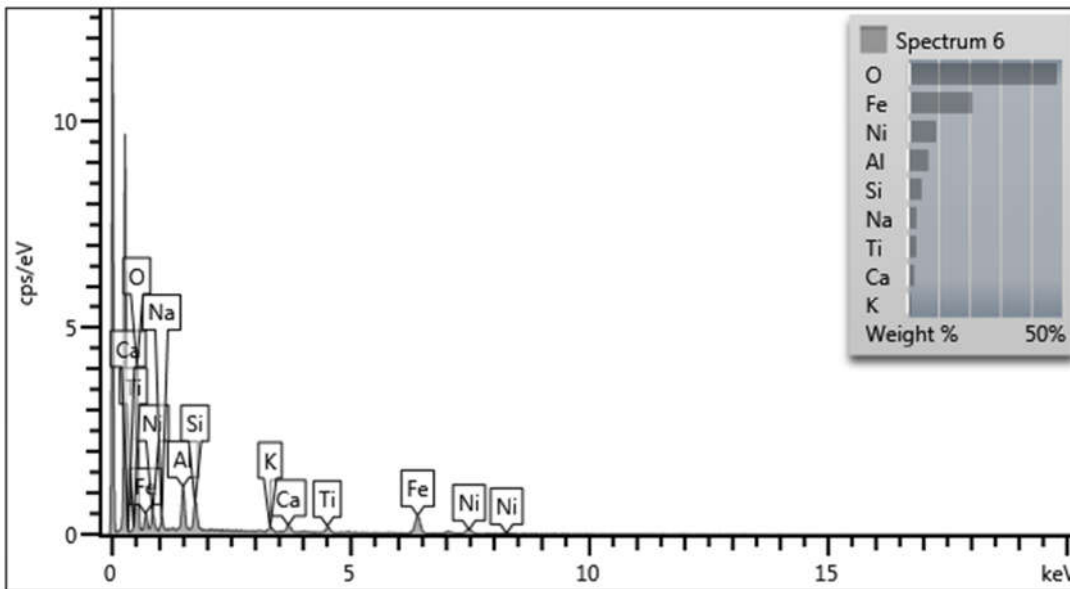


Figure 5-49. General electron image (a) and spectrum (b) of B21 catalyst

Table 5-33. Surface elemental composition of B21 catalyst

Element	Wt %	Atomic %
O	48.34	70.83
Na	3.02	3.07
Al	6.91	6.00
Si	4.71	3.93
K	1.27	0.76
Ca	2.31	1.35
Ti	2.99	1.47
Fe	21.08	8.85
Ni	9.38	3.75
Total:	100.00	100.00

(a)

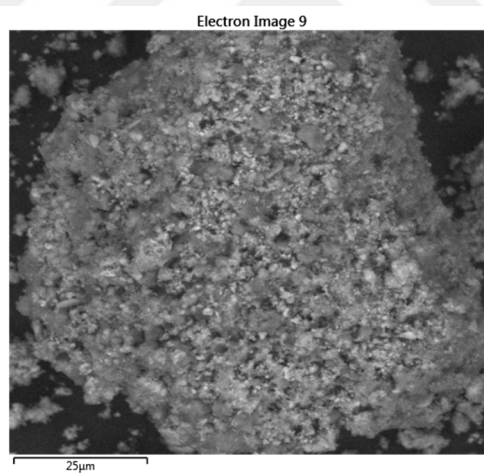


Figure 5-50. Electron image (a) and elemental mapping (b) of B21 catalyst.

(b)

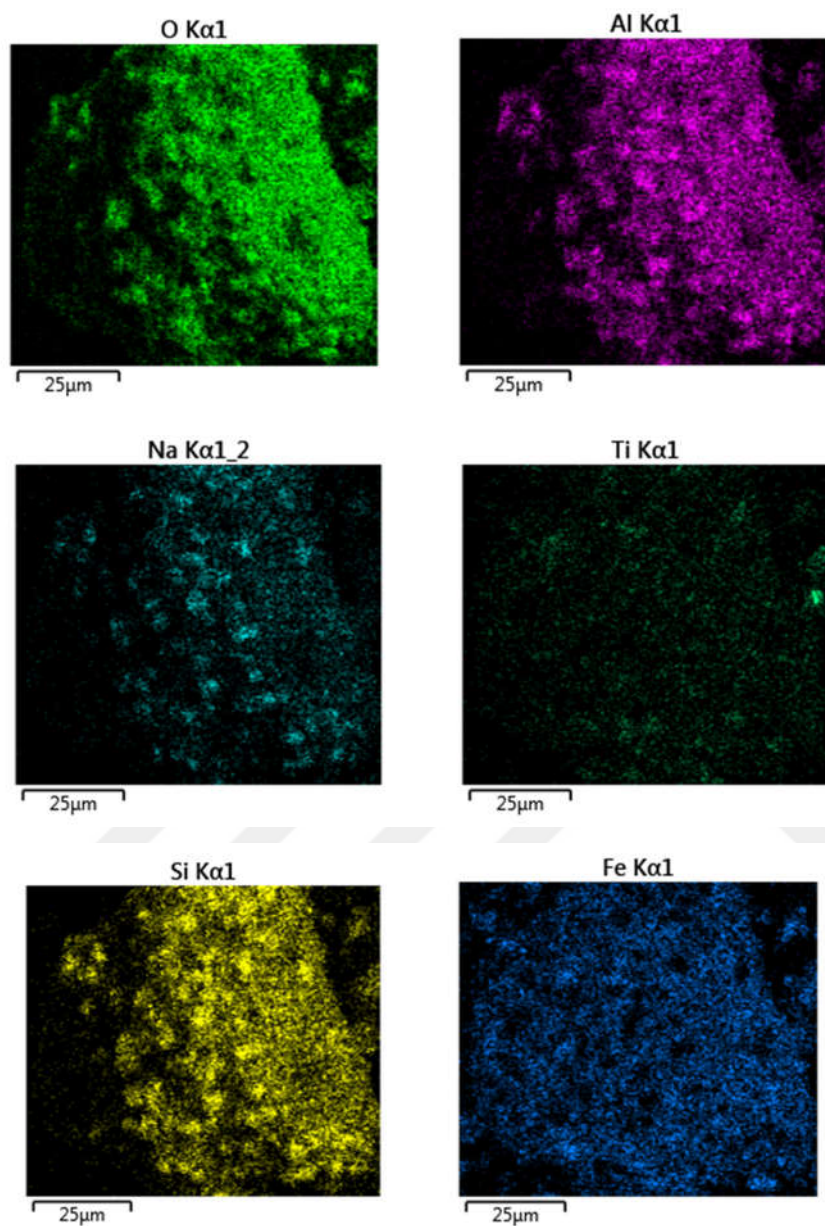


Figure 5-50. Electron image (a) and elemental mapping (b) of B21 catalyst (continued)

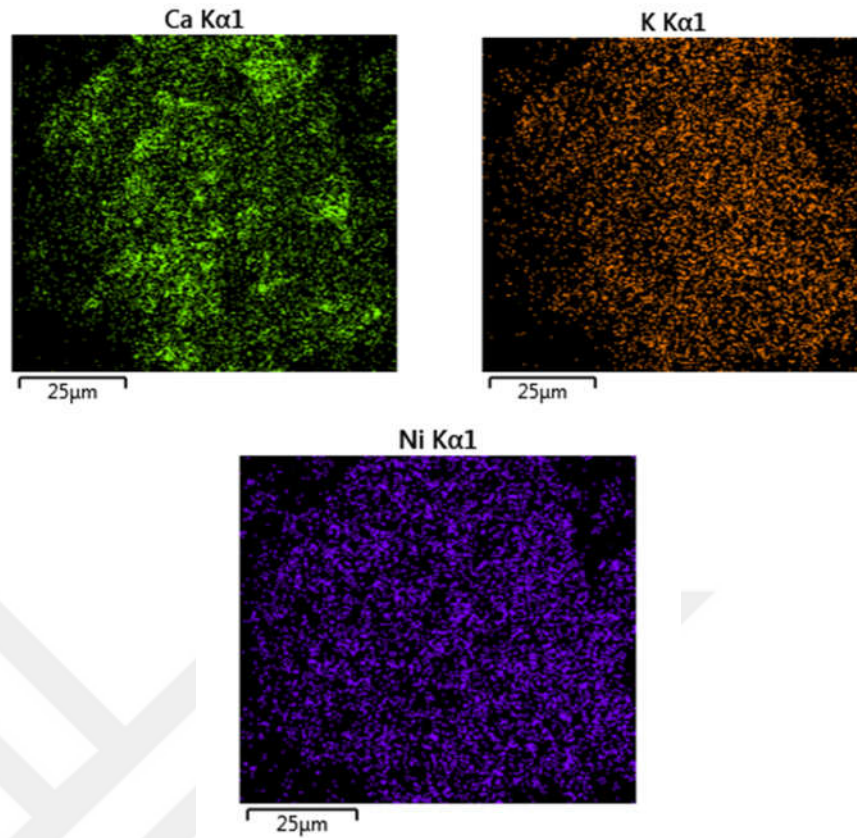


Figure 5-50. Electron image (a) and elemental mapping (b) of B21 catalyst (continued).

❖ **SEM-EDS ANALYSIS AND MAPPING of B3 (Precipitation with K_2CO_3 + 20% Ni impregnation + Calcination)**

a)

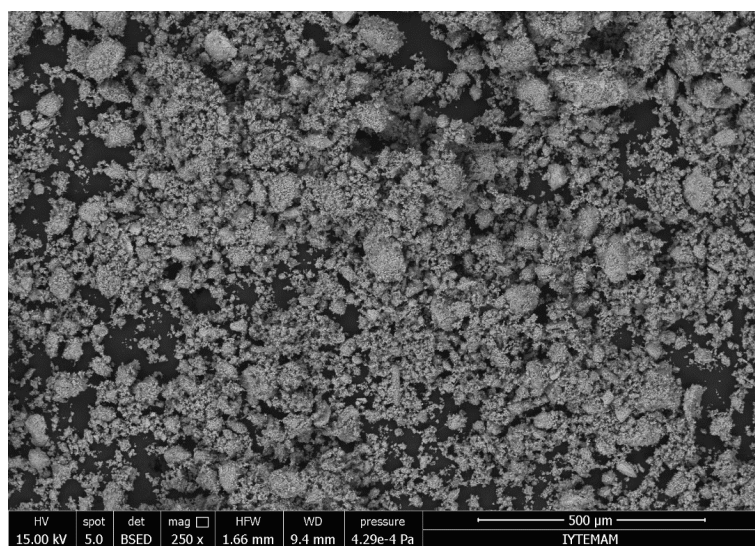


Figure 5-51 General electron image (a) and spectrum (b) of B3 catalysts.

b)

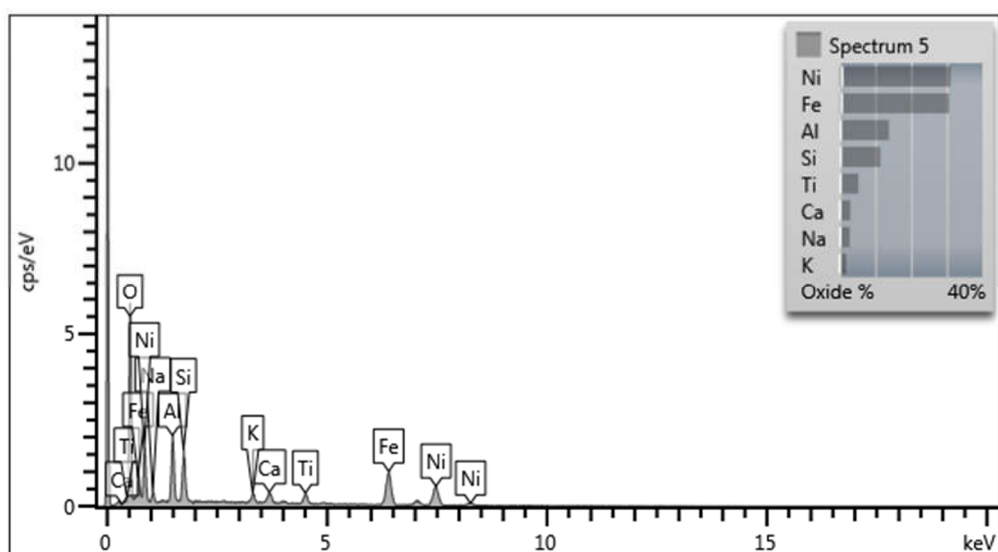
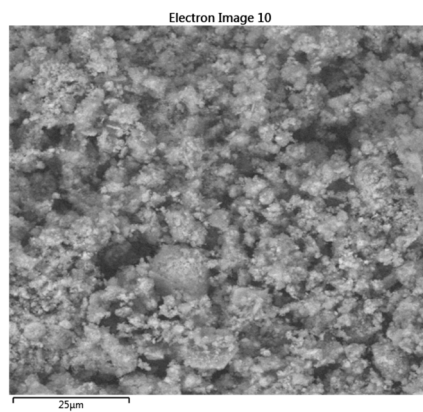


Figure 5-51. General electron image (a) and spectrum (b) of B3 catalysts (continued).

Table 5-34. Surface elemental composition of B3 catalyst.

Element	Wt%	Atomic %
O	30.09	54.74
Na	2.11	2.67
Al	7.32	7.89
Si	5.34	5.53
K	1.55	1.16
Ca	2.15	1.56
Ti	3.15	1.91
Fe	23.89	12.45
Ni	24.40	12.09
Total:	100.0	100.0

a)



b)

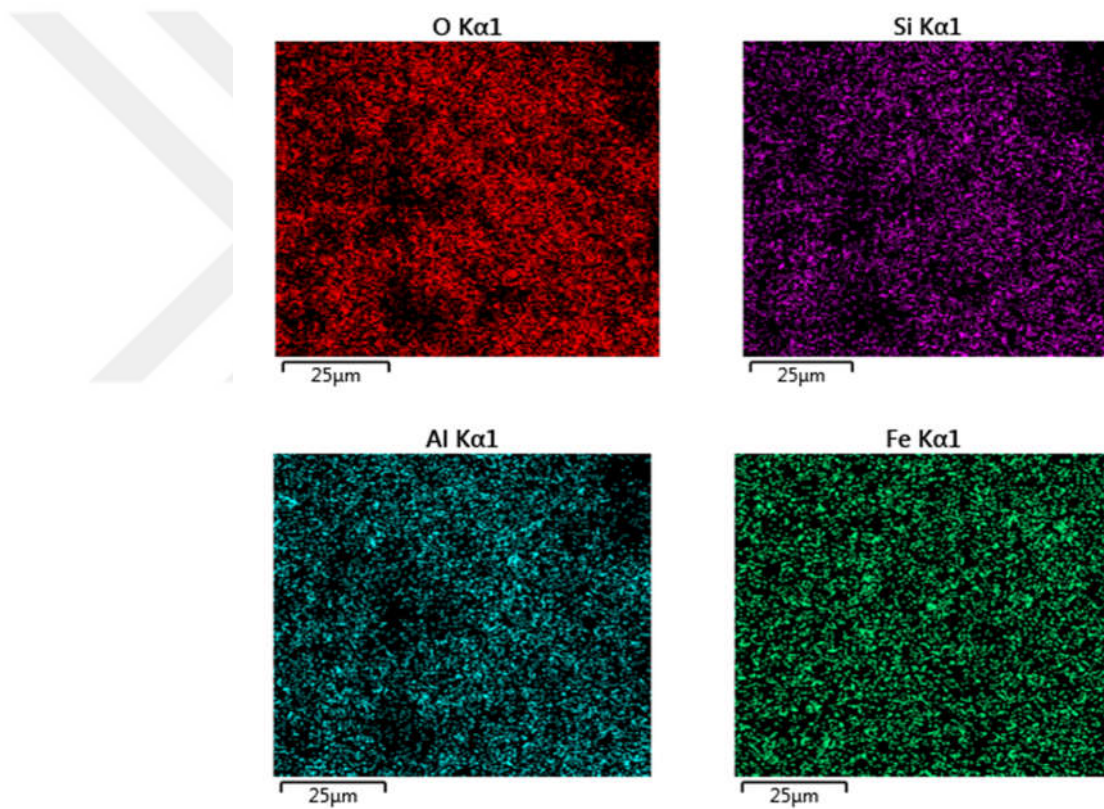


Figure 5-52. Electron image (a) and elemental mapping (b) of B3 catalyst.

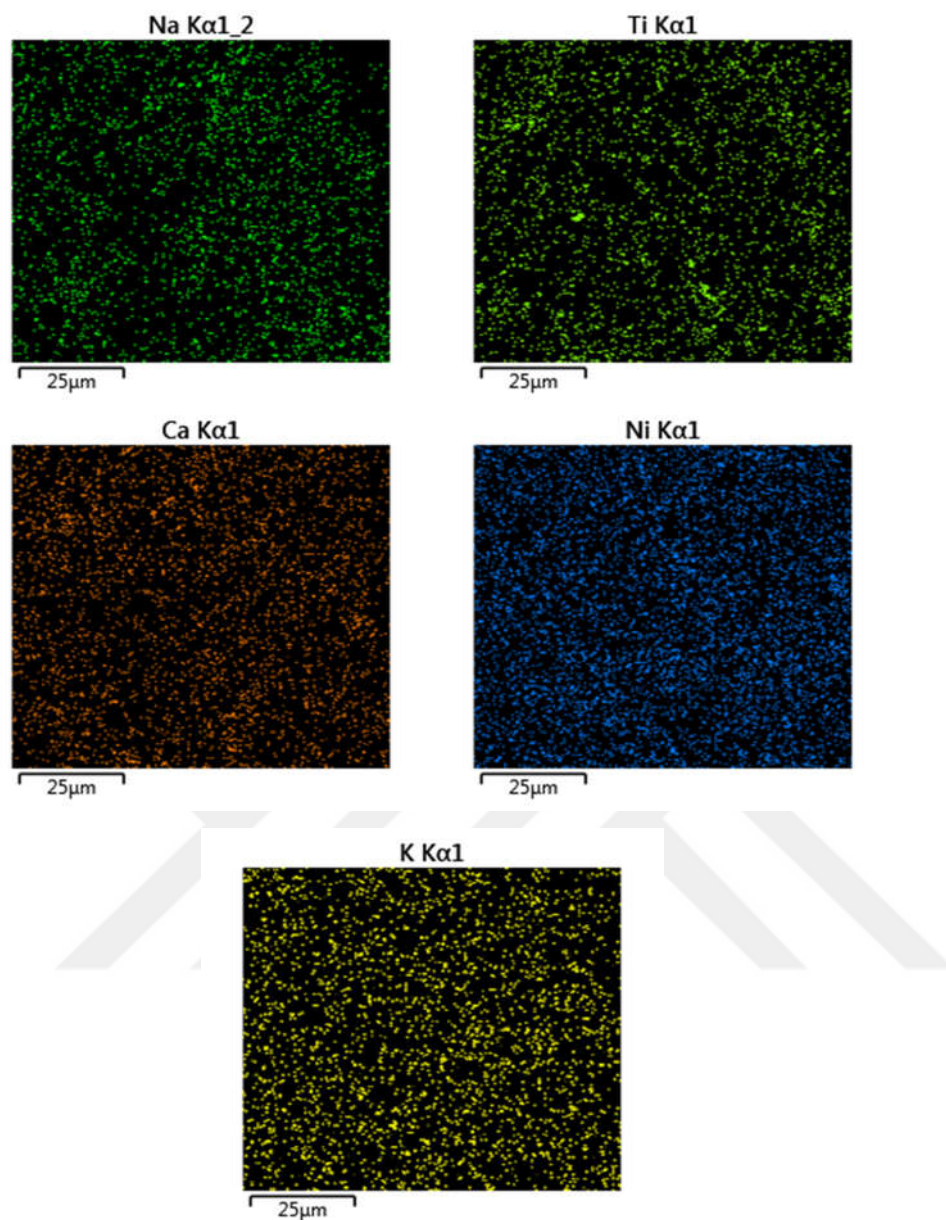
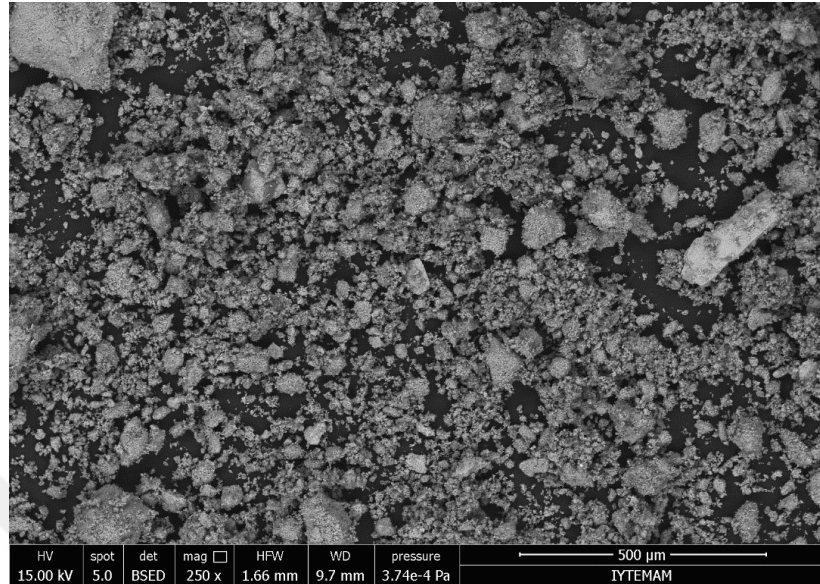


Figure 5-52. Electron image (a) and elemental mapping (b) of B3 catalyst (continued).

❖ SEM-EDS ANALYSIS AND MAPPING of B31 (Precipitation with K_2CO_3 + %20 Ni impregnation + Reduction by $NaBH_4$ + Cacination)

a)



b)

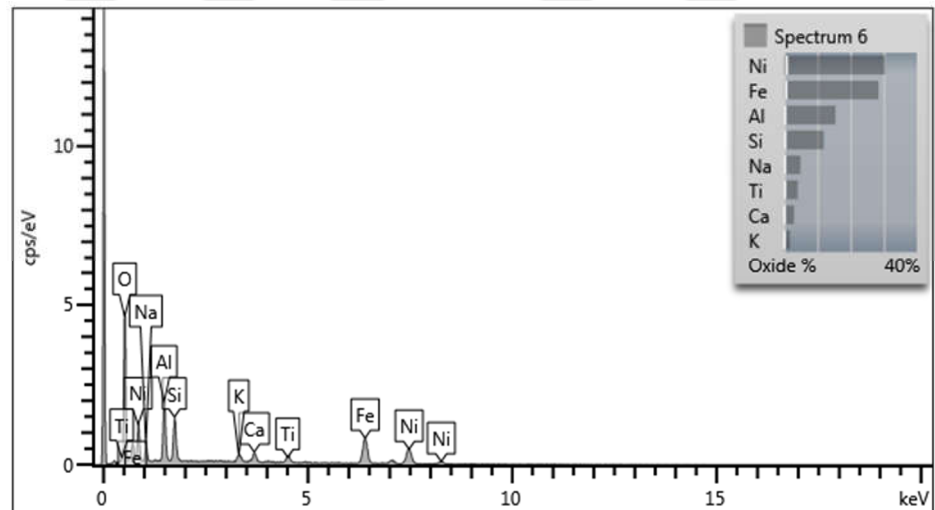


Figure 5-53. General electron image (a) and spectrum (b) of B31 catalysts.

Table 5-35. Surface elemental composition of B31 catalyst.

Element	Wt%	Atomic %
O	30.56	54.33
Na	3.66	4.52
Al	8.18	8.63
Si	5.59	5.67
K	1.44	1.05
Ca	2.14	1.52
Ti	2.48	1.47
Fe	22.05	11.23
Ni	23.89	11.58
Total:	100.00	100.00

a)

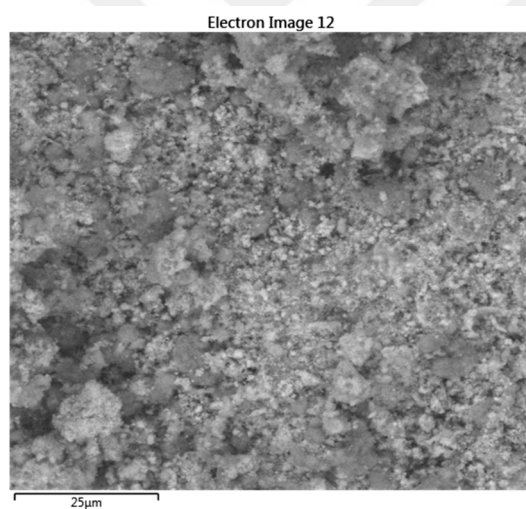


Figure 5-54. Electron image (a) and elemental mapping (b) of B31 catalyst.

b)

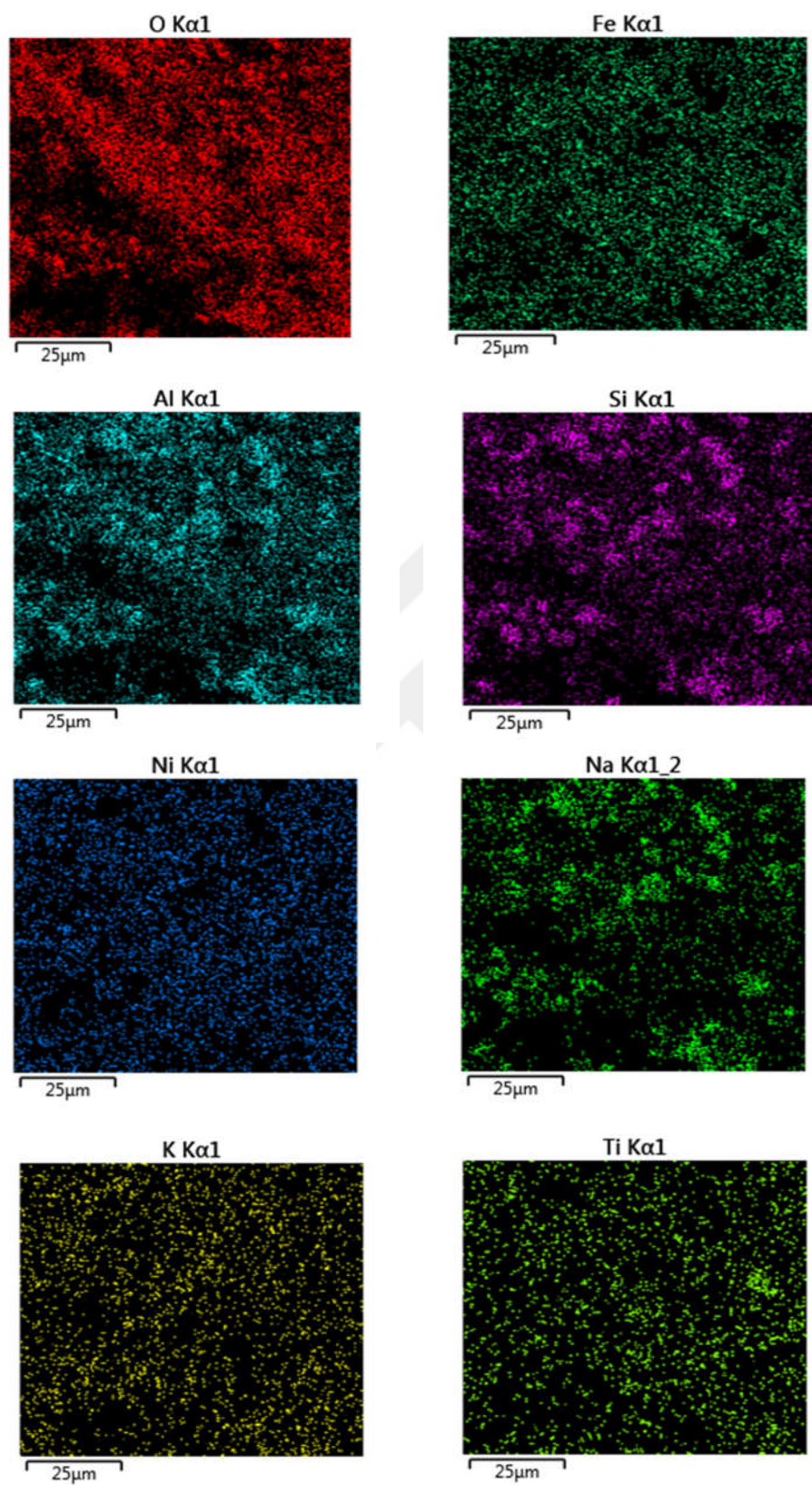


Figure 5-54. Electron image (a) and elemental mapping (b) of B31 catalyst (continued).

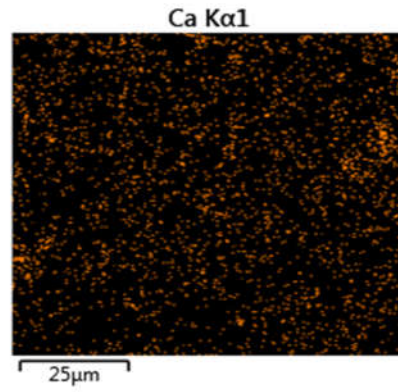


Figure 5-54. Electron image (a) and elemental mapping (b) of B31 catalyst (continued).

❖ ***SEM-EDS ANALYSIS AND MAPPING of B4 (Precipitation with K_2CO_3 + % 30 Ni impregnation + Calcination)***

a)

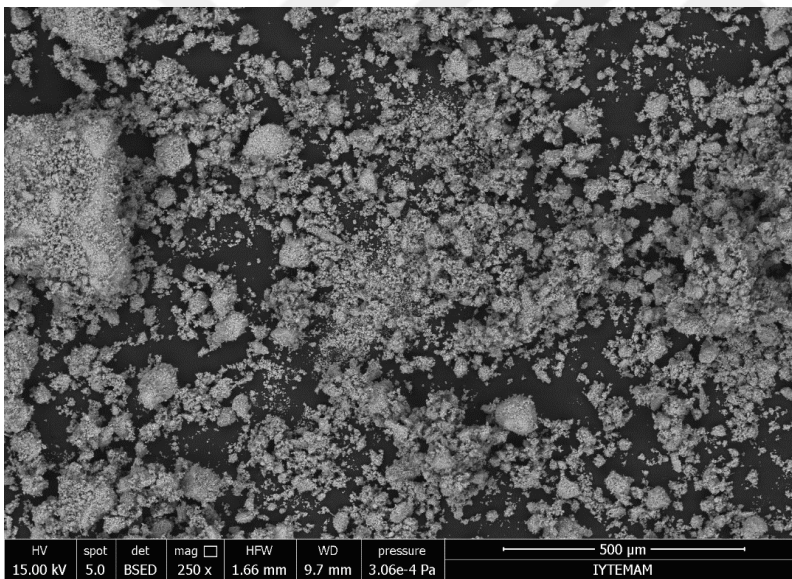


Figure 5-55. General electron image (a) and spectrum (b) of B4 catalysts.

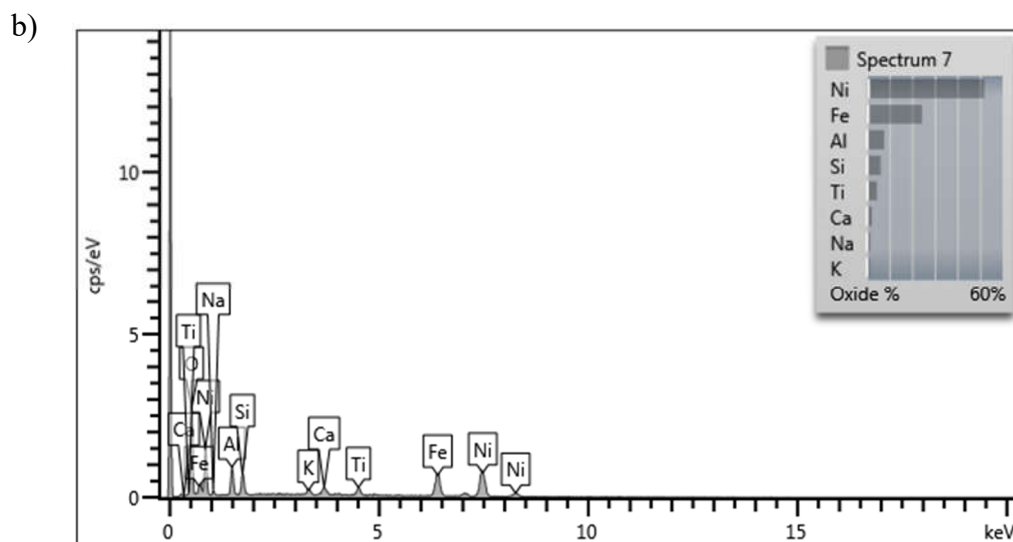
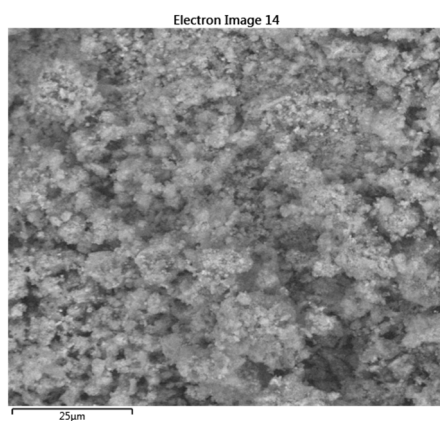


Figure 5-55. General electron image (a) and spectrum (b) of B4 catalysts (continued).

Table 5-36. Surface elemental composition of B4 catalyst.

Element	Wt%	Atomic %
O	26.58	53.12
Na	1.15	1.60
Al	4.08	4.84
Si	2.89	3.29
K	1.14	0.93
Ca	1.64	1.31
Ti	2.72	1.81
Fe	19.00	10.88
Ni	40.80	22.22
Total:	100.00	100.00

a)



b)

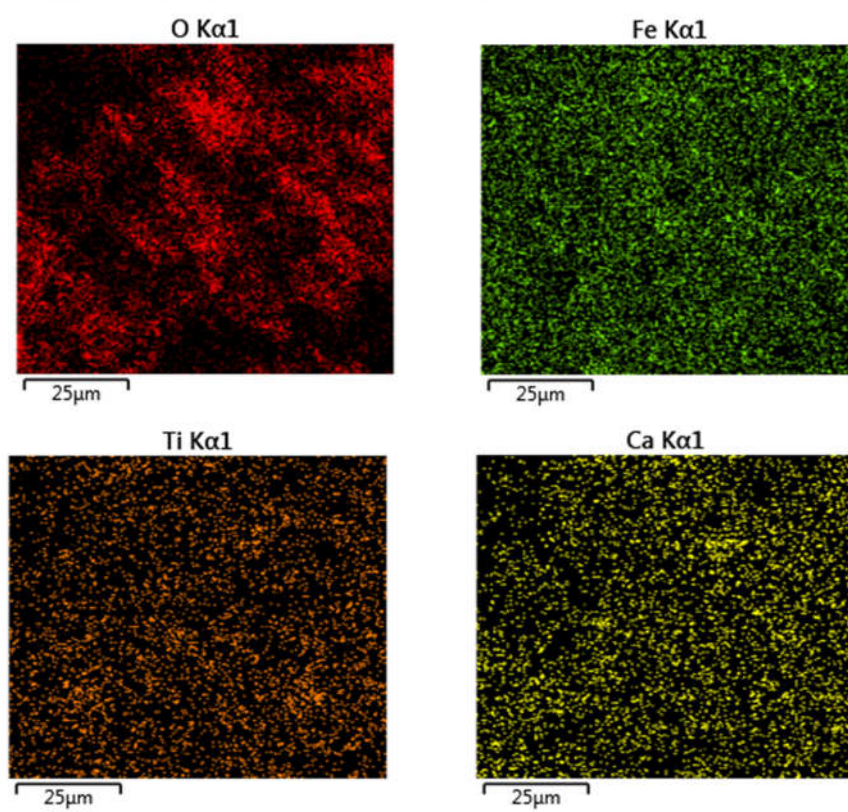


Figure 5-56. Electron image (a) and elemental mapping (b) of B4 catalyst.

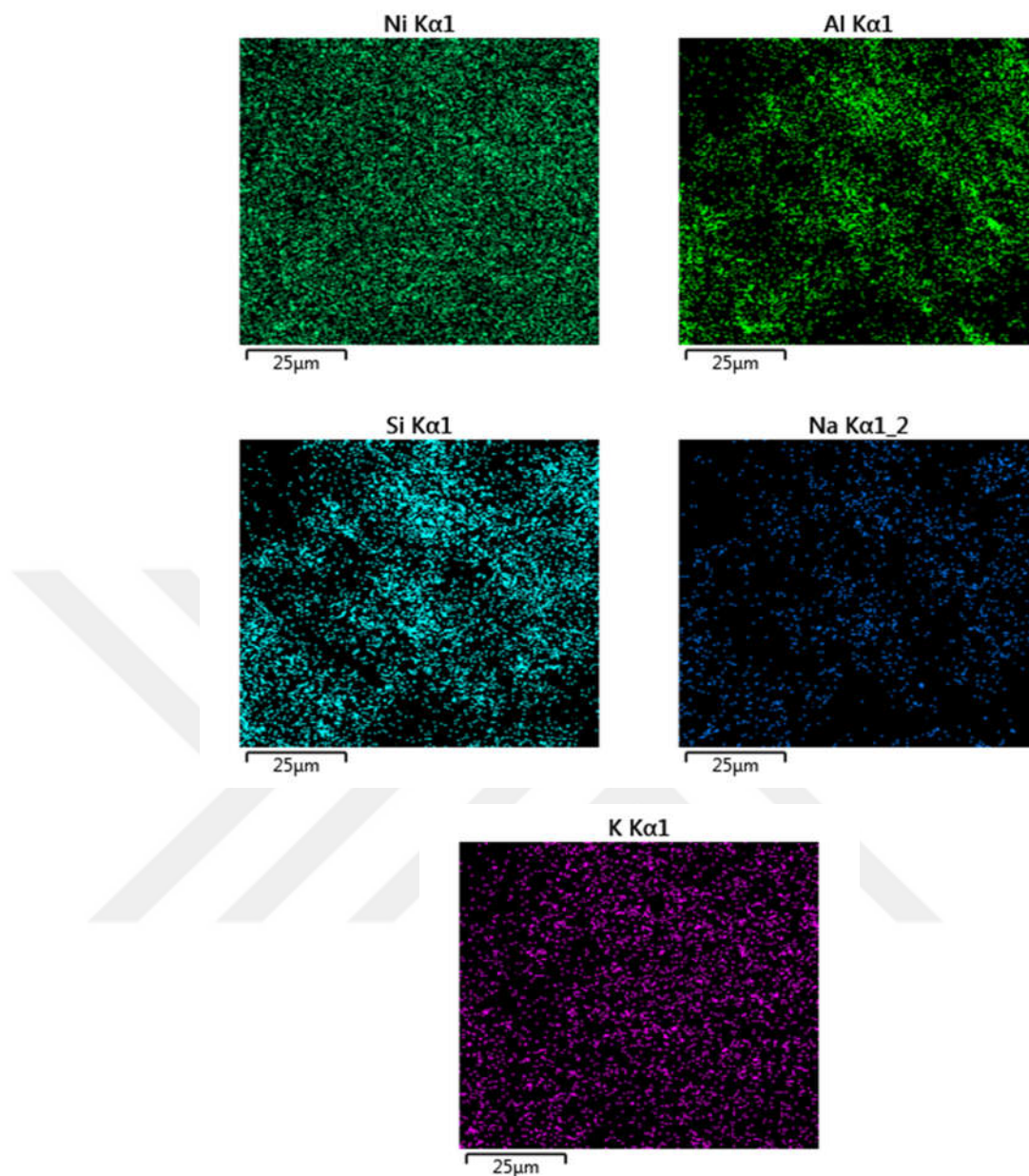


Figure 5-56. Electron image (a) and elemental mapping (b) of B4 catalyst (continued).

❖ Evaluation of SEM-EDS analysis results

The SEM-EDS analysis results shows us the elemental weight percentages of each catalyst approximately. Activated red mud catalysts contains silica, aluminum, iron, calcium, sodium, titanium, in forms of Fe_2O_3 , Al_2O_3 , SiO_2 , Na_2O , CaO and TiO_2 and as minor potassium, etc. Also, this catalysts includes varying ratios of nickel since they are prepared by impregnation of $\text{Ni}(\text{NO}_3)_2 \cdot 6\text{H}_2\text{O}$ and calcination. According to these results given in Tables 5-26 to 5-36, oxygen has the highest weight percentage followed by iron, aluminum and silica with the levels of 17-20%,

6-7%, and silica 4-5%, respectively. General Electron images, spectrums and elemental mappings are given in Figs 5-35 to 5-56 for A2, A21, A3, A31 A4, B2, B21, B3, B31, and B4 catalysts. The impregnation of nickel is aimed at 10wt % in A2 and B2 catalyst and is consistent with the SEM-EDS results. Also SEM photograph of elemental mapping shows that the nickel is distributed homogenously given in elemental mapping of SEM photographs gives us some informations on distribution of the phases and elements in each catalyst surface. In mapping figures, there is a dominant particle containing iron and oxygen and little amount of titanium. Some parts have some elements together and may be determined as structures of goethite ($\text{Fe}_{(1-x)}\text{Al}_x\text{OOH}$), calcium aluminum hydrate ($x.\text{CaO}.y\text{Al}_2\text{O}_3.z\text{H}_2\text{O}$), kaolinite ($\text{Al}_2\text{O}_3.2\text{SiO}_2.2\text{H}_2\text{O}$), CaTiO_3 , etc. A2 and B2 catalysts are reduced NaBH_4 and so the oxygen expected to decrease and so the balanced weight percentages would be increased. The results shows that nickel percentage increased percentages of oxygen, and iron decreased while nickel increases from 9-10% levels up to approximately 20%. The SEM-EDS analysis results show us the elemental weight percentages of each catalyst approximately. Activated red mud catalysts contains silica, aluminum, iron, calcium, sodium, titanium, nickel according to mapping analysis results. They includes nickel since they are prepared by impregnation of $\text{Ni}(\text{NO}_3)_2.6\text{H}_2\text{O}$ and calcination. According to these results given in Tables 5-26 to 36, oxygen has the highest weight percentage followed by iron, nickel, aluminum, and silica. The impregnation of nickel is aimed at 20 wt% in A3 and B3 catalyst and is consistent with the SEM-EDS results as 23%. SEM photograph of elemental mapping shows that the nickel is distributed homogenously which are given in "Nickel" picture of mapping. They also give us some information on the distribution of the phases and elements in each catalyst surface. A4 and B4 should contain 30% of nickel, but A4 includes 23.02% while B4 includes 40.8% Nickel according to EDS results. A3, A4, and B3 are reduced by NaBH_4 and A31, A41, and B31 are obtained. NiO should be reduced to Ni form and the oxide percentage decrease but EDS results are not consistent with the expected.

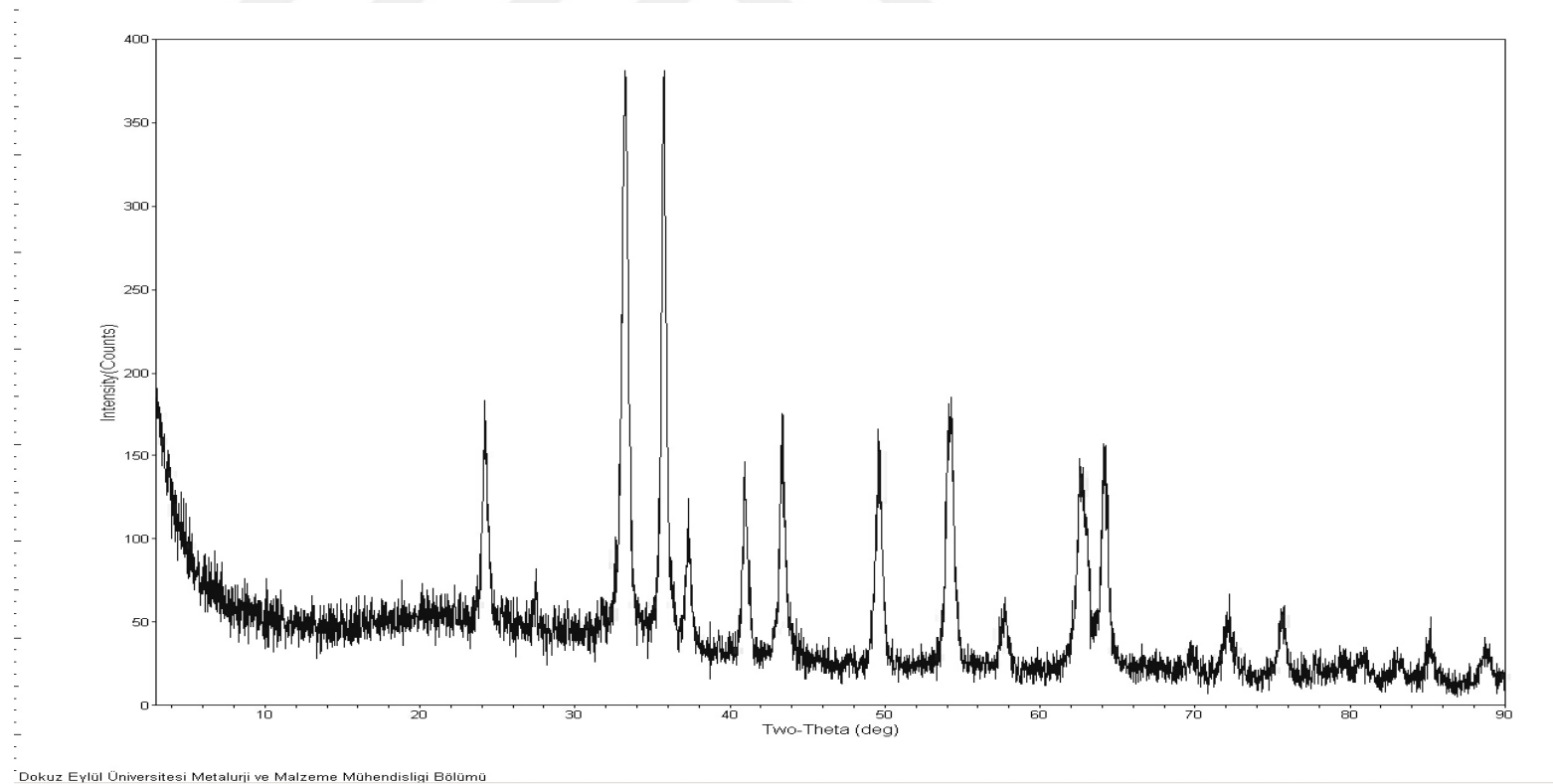
XRD RESULTS for A2, A21, B2, and B21 catalysts

Figure 5-57 XRD analysis of A2 catalyst

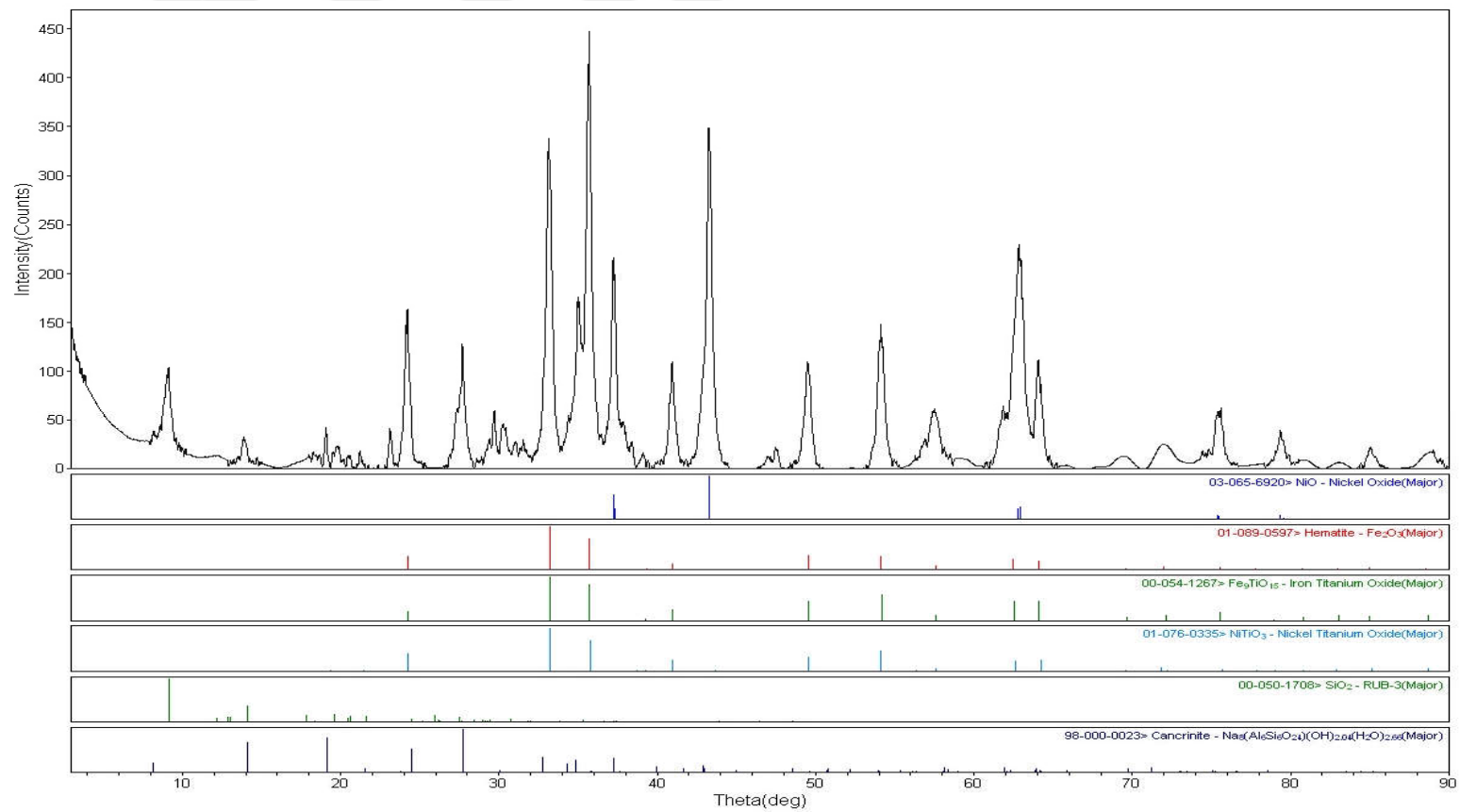
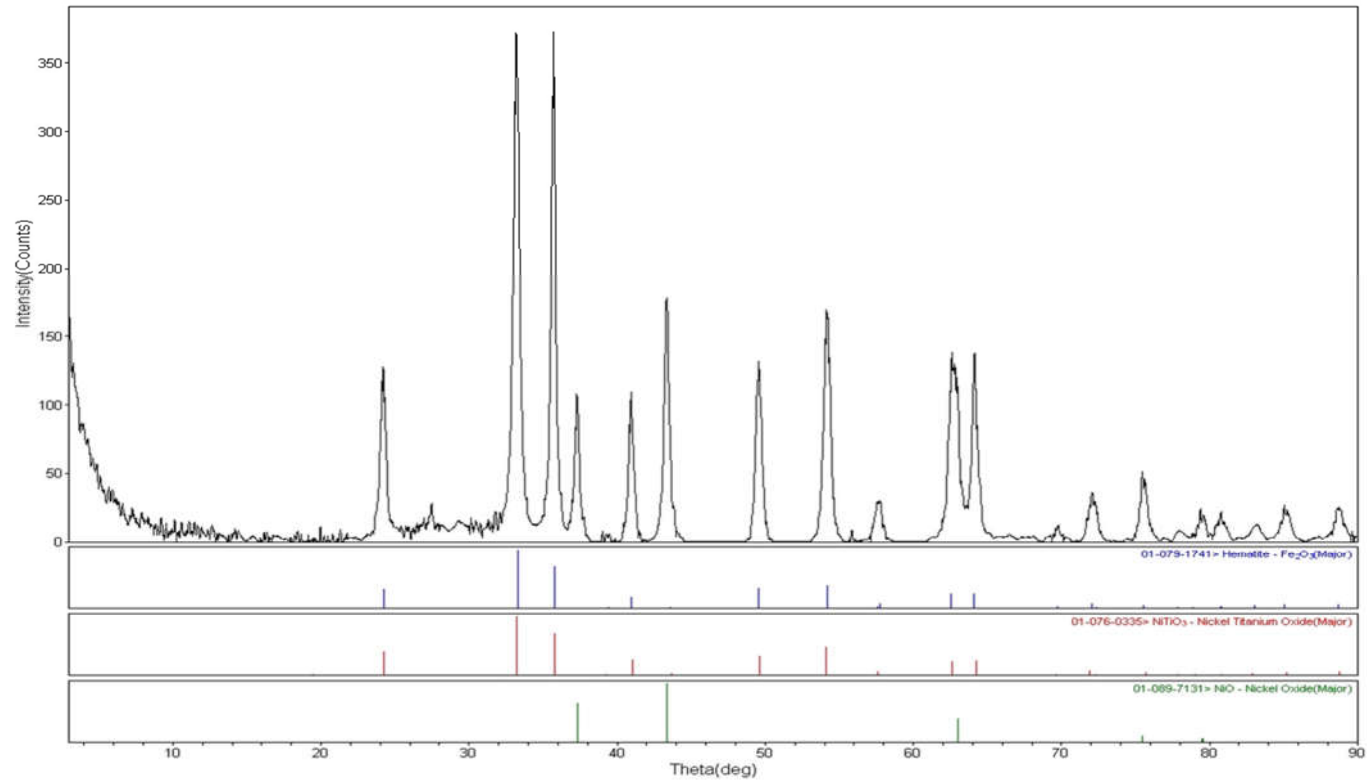
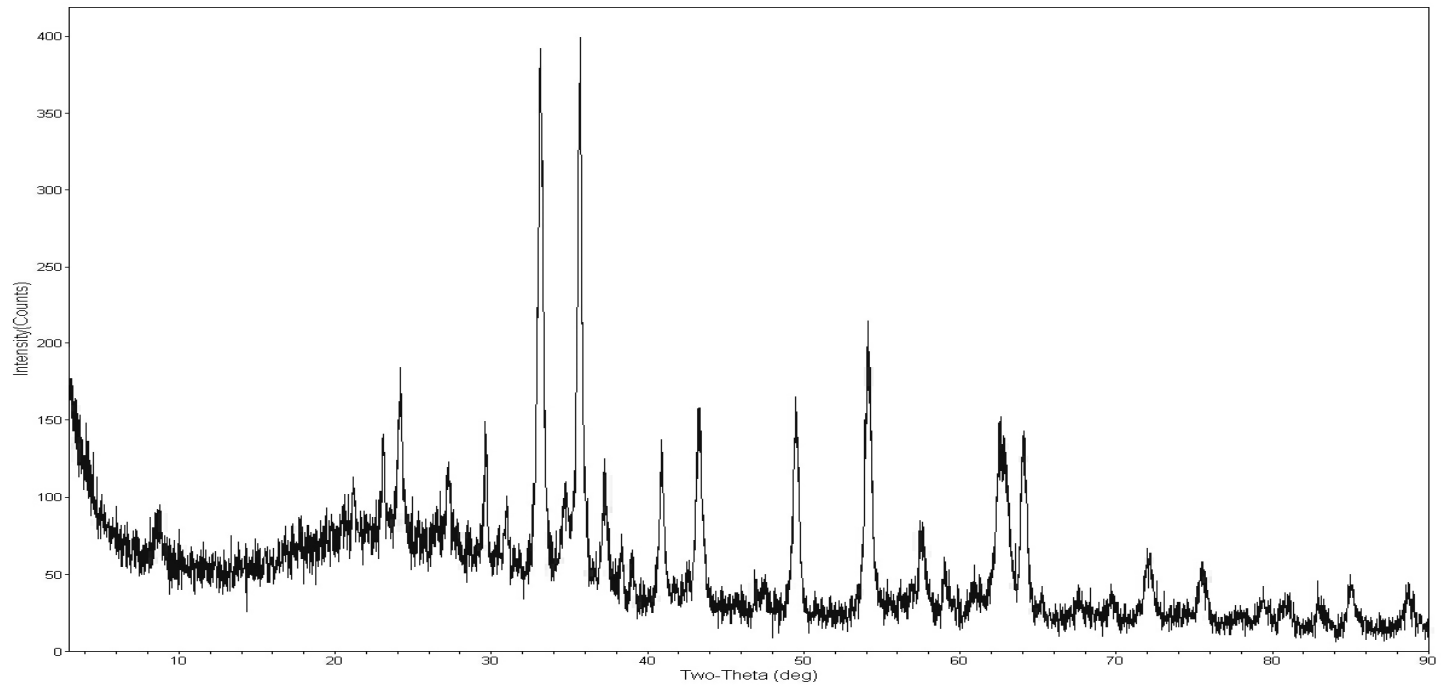


Figure 5-58. A21. XRD, phase analysis results



Dokuz Eylül Üniversitesi Metalurji ve Malzeme Mühendisliği Bölümü

Figure 5-59. B2. XRD, phase analysis results



Dokuz Eylül Üniversitesi Metalurji ve Malzeme Mühendisliği Bölümü

Figure 5-60. XRD analysis of B21 catalyst

❖ Evaluation of XRD and pattern analysis results

The XRD analysis were given in Figs 5-57 to 5-60. Four type of the activated red mud catalysts were selected for analysis to evaluate similar structures of the others also. These are A2, A21, B2, and B21. Since there are many phases in red mud, the nickel and nickel oxide determination from these literature data is difficult and needed pattern analysis. XRD with pattern analysis were done for only A21 and B2 catalysts because of additional cost. Some literature findings were also given here for comparison in The Figs 5-61 and 5-62 shows the red mud, nickel and nickel oxide XRD patterns. In Fig. 5-61, there is SiO_2 , Fe_2O_3 , CaCO_3 , $\text{FeO}(\text{OH})$, $\text{Al}(\text{OH})_3$, Muscovite, $\text{Na}_5\text{Al}_3\text{CSi}_3\text{O}_{15}$ phases were determine in dry red mud by XRD analysis in a research (Ribeiro et al. 2012). In another work, the structural and phase compositions of red mud was examine by means of various analysis techniques: PSA, XRD, FESEM, EDX, BET and FT-IR (Nath and Sahoo 2014). They reported that there are some variataions in literature about red mud characterization. the main components. As seen in Fig. 5-62, Nath et al. found the main phases as Hematite (Fe_2O_3), Gibbsite ($\text{Al}(\text{OH})_3$), Rulite (TiO_2), Calcite (CaCO_3), Sodium aluminum silicate ($\text{Na}(\text{AlSiO}_4)$), Dicalcium silicate (Ca_2SiO_4), and Quartz (SiO_2). Based on literature on red mud and X-ray patterns of activated red mud it can be deduced that the phases are changed after activation process. In B2 catalyst (precipitated by K_2CO_3 and 10% Nickel impregnated, not reduced state), there are Hematite, Nickel Titanium Oxide and Nickel Oxide are deterimed as major components. In A21 (precipitated by NH_3 and 10% Nickel impregnated, reduced state), there are Hematite, Nickel Titanium Oxide and Nickel Oxide and also SiO_2 , Iron Titanium Oxide, Cancrinite $\text{Na}_6\text{Ca}_2[(\text{CO}_3)_2\text{Al}_6\text{Si}_6\text{O}_{24}]\cdot 2\text{H}_2\text{O}$ were found.

In a study done with Nickel and Nickel oxide, XRD results were given as in Fig. 64 (Park et al. 2005). They found that nickel nanoparticle with a size of 5 nm have a face-centered cubic structure. The width of the peaks are found very large and it shows that they have structures nearly amorphous. Fig. 5-63 demonstrates NiO compounds were formed after exposure of Nickel nanoparticles to air. Two theta degree (43.30° as indexed as peak (200) in crystal planes of the bulk NiO) is

found as similar in another work (El-Kemary, 2013) done with nanoparticles as seen in Fig. 5-63 which is consistent with our X-ray results ($2\theta= 43.38$ and 43.29).

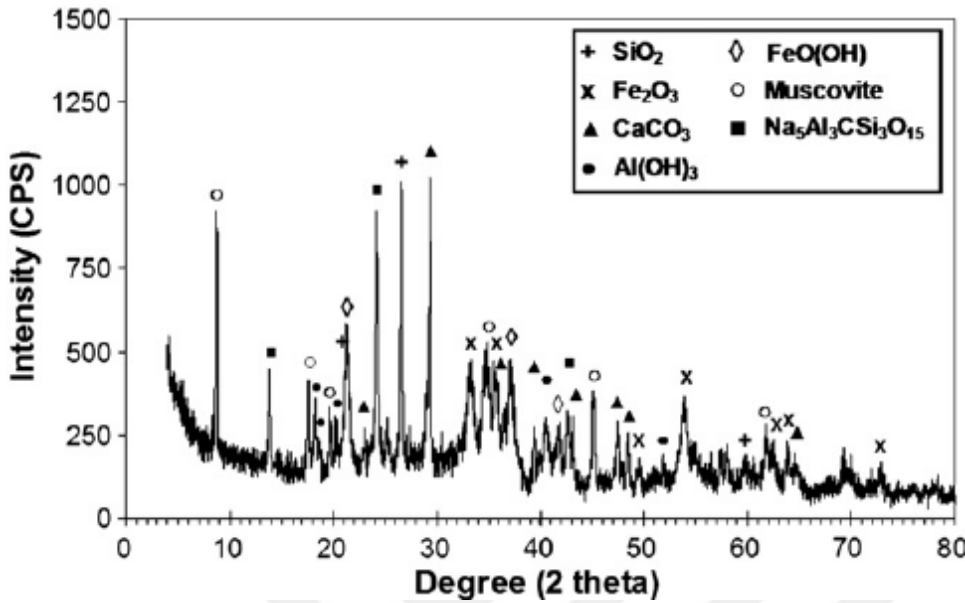


Figure 5-61. X-ray diffraction (XRD) pattern of dry red mud (Ribeiro et al. 2012)

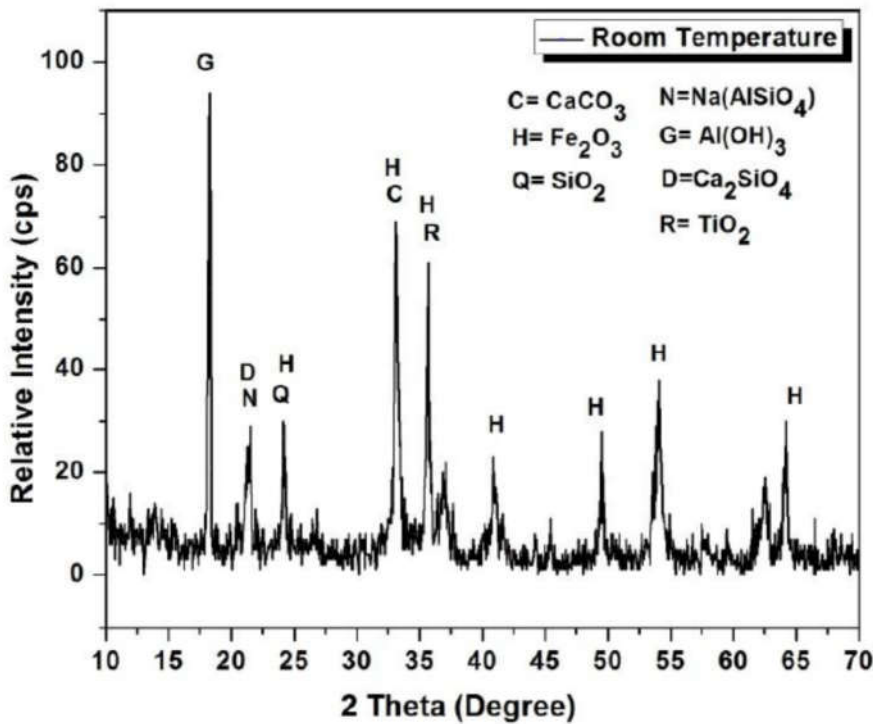


Figure 5-62. X-ray pattern of red mud (Nath and Sahoo 2014)

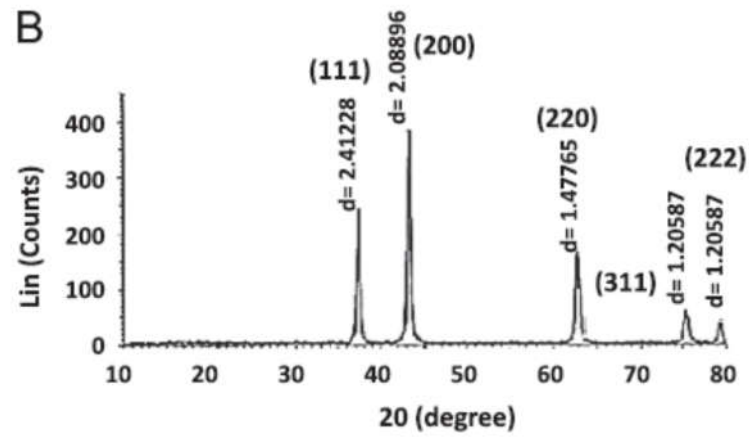


Figure 5-63. Nickel oxide nanoparticles XRD pattern (El-Kemary et al. 2013)

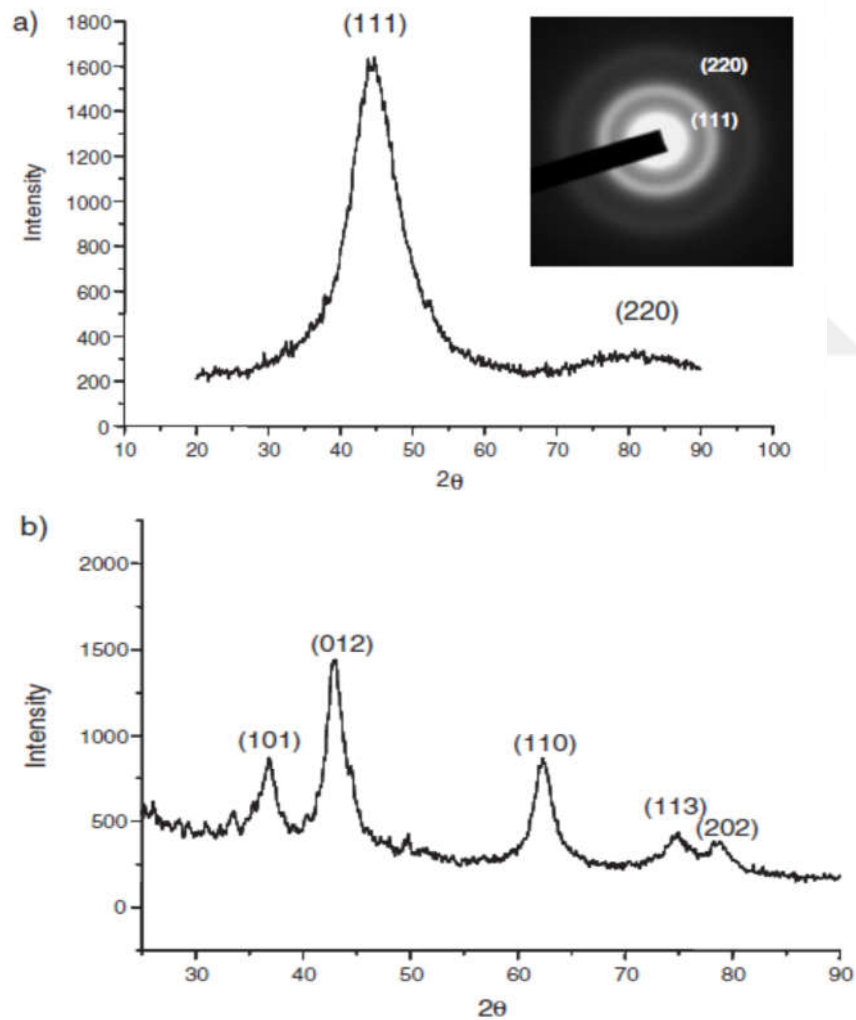


Figure 5-64. Nickel nanoparticles (a) and NiO (b) structures (Park et al. 2005)

The mean size of crystallites from pattern data by means of Origin software was done and given below in Figs 5-65 and 5-66. By applying Scherrer equation on the XRD pattern, the particle size can be calculated as:

$$D = K\lambda / (\beta \cos \theta)$$

Where D is the mean size of crystallites (nm), K is crystallite shape factor a good approximation is 0.9, λ is the X-ray wavelength, β is the full width at half the maximum (FWHM) in radians of the X-ray diffraction peak and θ is the Bragg's angle (deg.)

For B2 catalyst the β is found as 0.40 degree and converted to 0.00698 radian from the XRD pattern for Nickel Oxide particles which have a maximum intensity of 177.34 counts and FWHM is calculated at half (88.67 counts). 2θ is found as 43.38 and θ is $43.38/2 = 21.68$ degree and 0.378 radian.

The mean size of NiO crystallites is calculated as:

$$\lambda = 1.54060 \text{ \AA} \text{ (in the case of CuK}\alpha\text{1)}$$

$$D = 0.94 * 1.54 / (0.00698 * \cos(21.68)) \text{ [nm]}$$

$$D = 223.14 \text{ \AA} \text{ or } 22.3 \text{ nm}$$

For A21 catalyst the β is found as 0.401 degree and converted to 0.00700 radian from the XRD pattern for Nickel Oxide particles which have a maximum intensity of 345 counts and FWHM is calculated at half (172.5 counts). 2θ is found as 43.29 and θ is $43.29/2 = 21.645$ degree and 0.38 radian.

The mean size of NiO crystallites is calculated as:

$$\lambda = 1.54060 \text{ \AA} \text{ (in the case of CuK}\alpha\text{1)}$$

$$D = 0.94 * 1.54 / (0.00700 * \cos(21.645)) \text{ [nm]}$$

$$D = 292.46 \text{ \AA} \text{ or } 29.2 \text{ nm.}$$

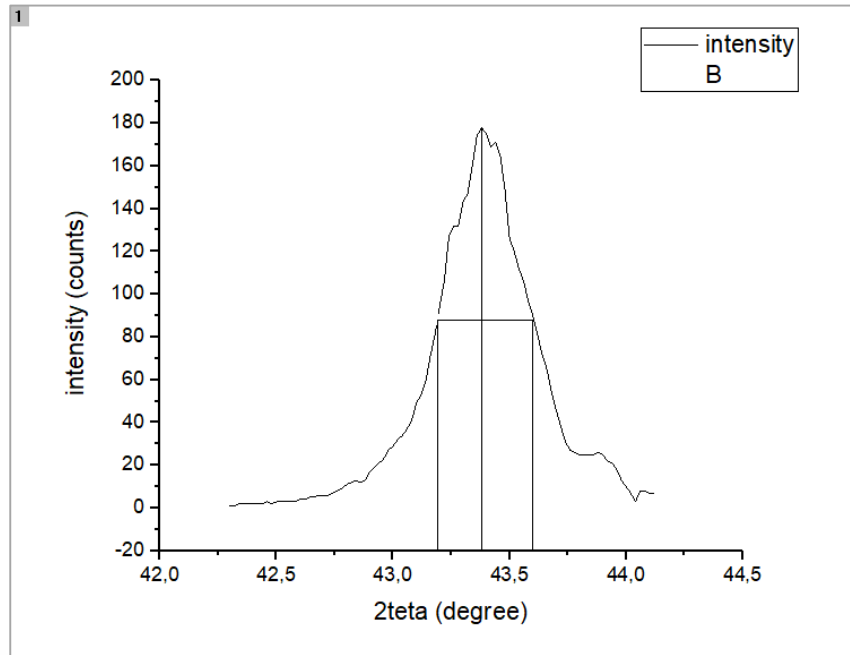


Figure 5-65. Plot of intensity versus degree (2θ) within NiO peak in XRD pattern of B2 catalyst for FWHM calculation with Origin software.

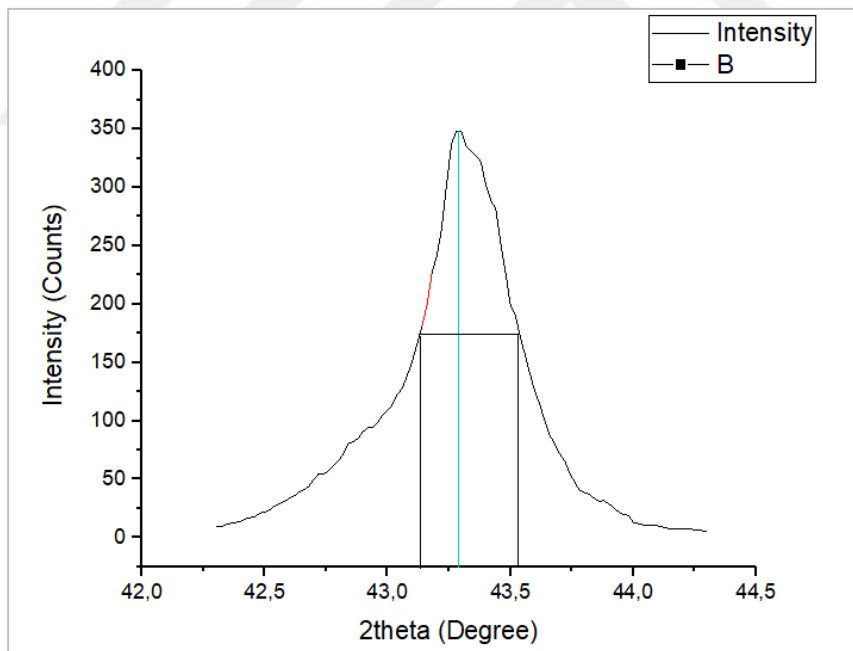


Figure 5-66. Plot of intensity versus degree (2θ) within NiO peak in XRD pattern of A21 catalyst for FWHM calculation with Origin software.

BET ANALYSIS RESULTS

Table 5-37 Experimental conditions of BET analysis.

Outgas Time	3.0 hrs
Analysis gas	NITROGEN
X sect. area	16.2 Å ² /molecule
Adsbate (DRP)	Nitrogen
Non-ideality	6.58 x 10 ⁻⁵
Outgas Temp	200.0 °C
Analysis Time	71.2 min
P/Po tolerance	3
Equil. time	2
Bath Temp.	77.40

Table 5-38 Multipoint BET results

<i>Sample Code</i>	Area, m²/g	Slope	Y - Intercept	Correlation Coefficient	C
A2	48.8	70.8	0.64	0.999917	112
A21	24.5	140.4	1.82	0.999946	78.3
B2	44.8	77.3	0.49	0.999901	157.1
B21	24.0	142.6	2.43	0.999919	59.7

❖ A2 BET Results in details

Table 5-39 Multipoint BET results of catalyst A2

P/Po	Volume, [cc/g] STP	1/(W((Po/P)-1))
5.9386×10^{-2}	10.4249	4.846×10^0
8.3292×10^{-2}	11.0484	6.580×10^0
1.0850×10^{-1}	11.6384	8.367×10^0
1.5456×10^{-1}	12.6919	1.152×10^1
2.0496×10^{-1}	13.7195	1.503×10^1
2.5499×10^{-1}	14.7180	1.861×10^1
3.049×10^{-1}	15.7065	2.235×10^1

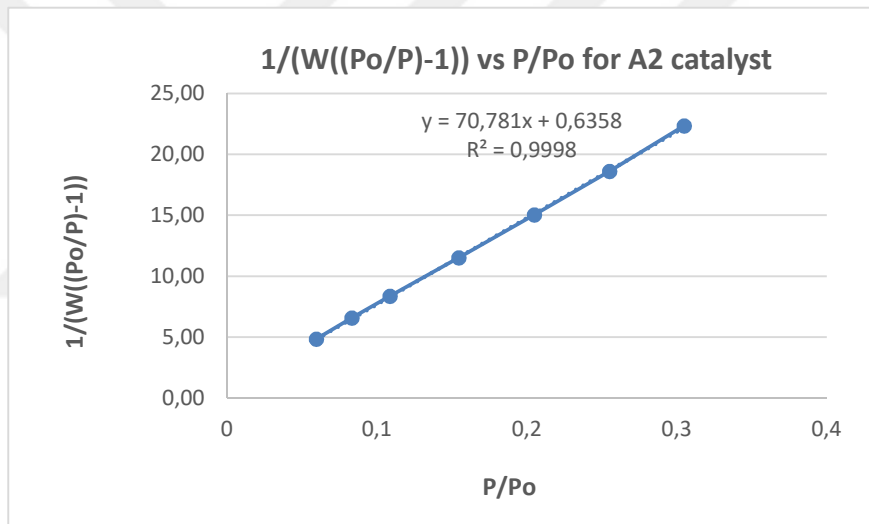


Figure 5-67. Multipoint BET plot for surface area determination for A2.

❖ A21 BET Results in details

Table 5-40 Multipoint BET results of catalyst A21

P/Po	Volume, [cc/g] STP	1/(W((Po/P)-1))
5.9994×10^{-2}	5.0971	1.002×10^1
8.5780×10^{-2}	5.4007	1.390×10^1
1.1050×10^{-1}	5.7110	1.740×10^1
1.5932×10^{-1}	6.2286	2.434×10^1
2.0910×10^{-1}	6.7595	3.129×10^1
2.5872×10^{-1}	7.3312	3.809×10^1
3.0838×10^{-1}	7.9266	4.501×10^1

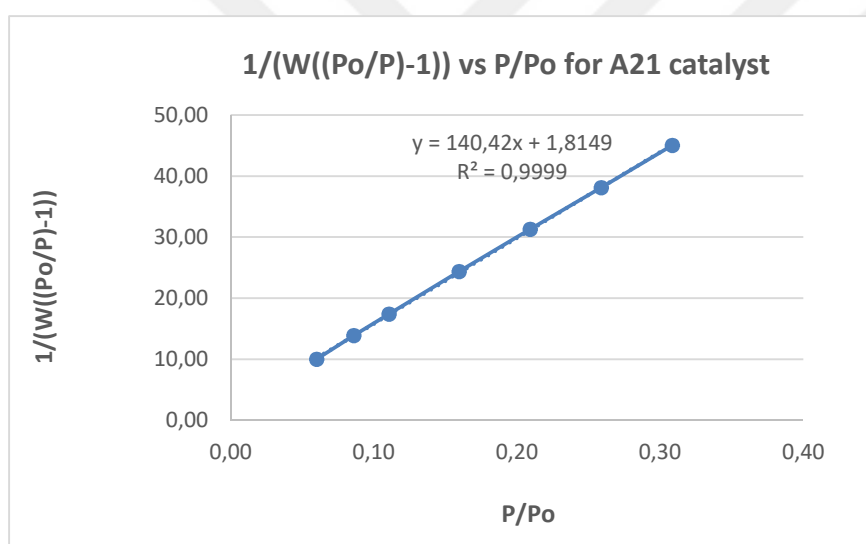


Figure 5-68. Multipoint BET plot for surface area determination for A21.

❖ **B2 BET Results in details**

Table 5-41 Multipoint BET results of catalyst B2

P/Po	Volume, [cc/g] STP	1/(W((Po/P)-1))
4.9845×10^{-2}	9.5693	4.386×10^0
8.2813×10^{-2}	10.3782	6.961×10^0
1.0928×10^{-1}	10.9455	8.969×10^0
1.5697×10^{-1}	11.8616	1.256×10^0
2.0699×10^{-1}	12.7624	1.636×10^0
2.5683×10^{-1}	13.6414	2.027×10^0
3.0670×10^{-1}	14.5220	2.437×10^0

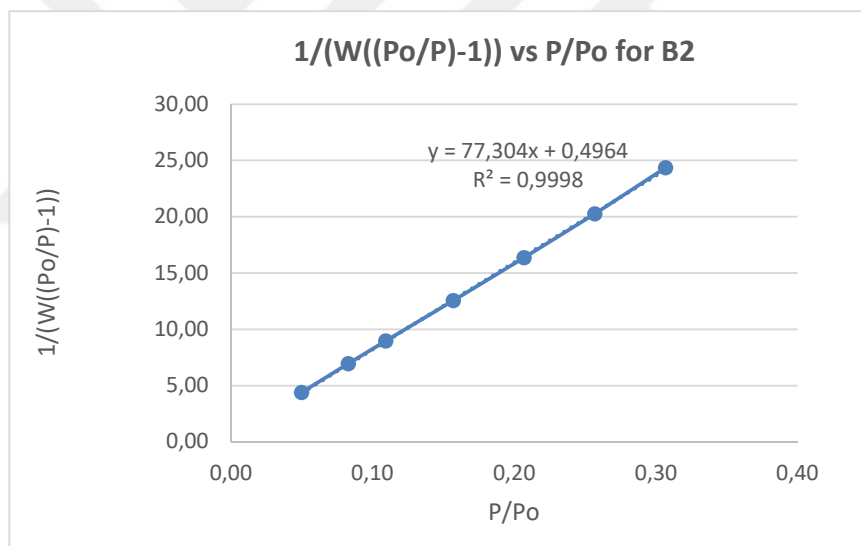


Figure 5-69. Multipoint BET plot for surface area determination for B2.

❖ B21 BET Results in details

Table 5-42 Multipoint BET results of catalyst B21

P/Po	Volume, [cc/g] STP	1/(W((Po/P)-1))
8.6032×10^{-2}	5.2045	1.447×10^1
1.1123×10^{-1}	5.4542	1.836×10^1
1.5901×10^{-1}	5.9832	2.528×10^1
2.0895×10^{-1}	6.5288	3.237×10^1
2.5871×10^{-1}	7.1066	3.929×10^1
3.0842×10^{-1}	7.7064	4.630×10^1

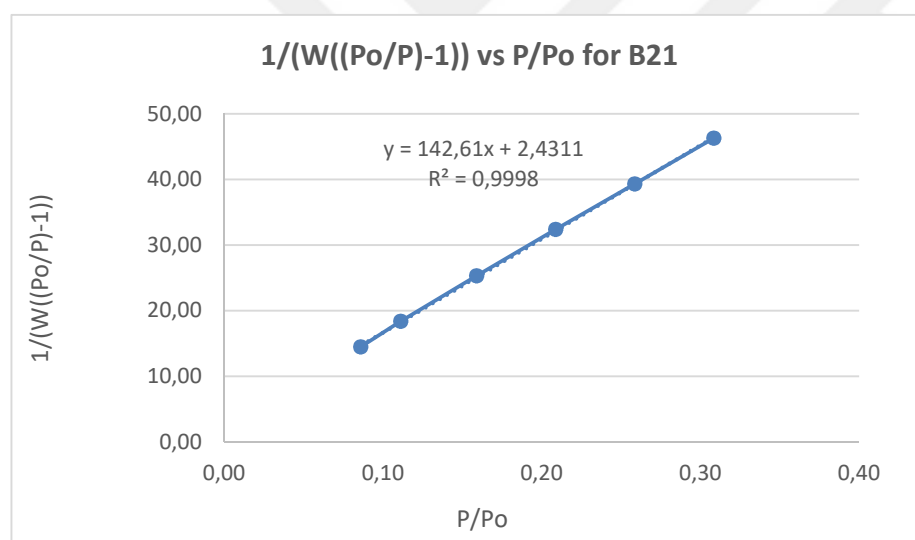


Figure 5-70. Multipoint BET plot for surface area determination for B21.

The BET results shows that reduction decreased the BET area and precipitation with NH₃ slightly increased BET area.

❖ Evaluation of BET results

Experimental conditions of BET analysis were given in Table 5-54 and the summarized results were given in Table 5-53. The detailed results were shown for A2, A21, B2 and B21 in Tables 5-54 to 5-57. For evaluation of the results better, plots of volume versus P/P_0 were drawn and given in Figs 5-55 and 5-56. The plots were compared isotherms if they fit an isotherm type is investigated. But the range of P/P_0 is not wide and it may be the reason that they seems does not fit any of classified isotherm for catalyst surface evaluation. Surface areas are calculated by using volume versus P/P_0 graphs and so plots were drawn for A2, A21, B2 and B21 catalysts.

Calculation Total Surface Area by using Multipoint BET plot:

In either the single point or multipoint method, the isotherm points are transformed with the BET equation:

$$\frac{1}{W[(P_0/P) - 1]} = \frac{1}{W_m C} + \frac{(C-1)}{W_m C} \frac{P}{P_0}$$

where W is the weight of nitrogen adsorbed at a given P/P_0 , and W_m the weight of gas to give monolayer coverage and C , a constant that is related to the heat of adsorption. A linear relationship between $1/W[(P_0/P)-1]$ and P/P_0 is required to obtain the quantity of nitrogen adsorbed. This linear portion of the curve is restricted to a limited portion of the isotherm, generally between 0.05-0.30. The slope and intercept are used to determine the quantity of nitrogen adsorbed in the monolayer and used to calculate the surface area.

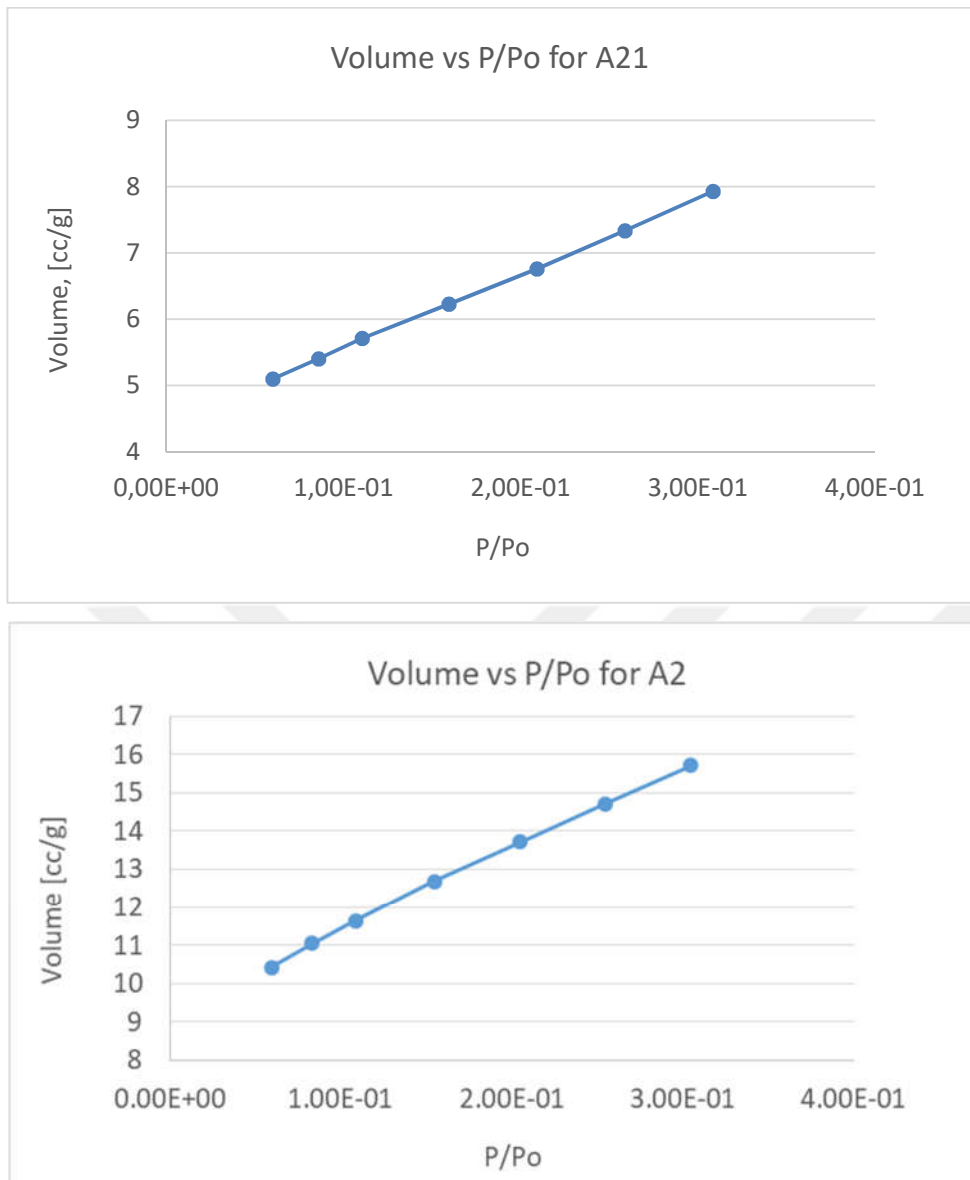


Figure 5-71. Volume versus P/Po graph of A2 and A21 catalysts

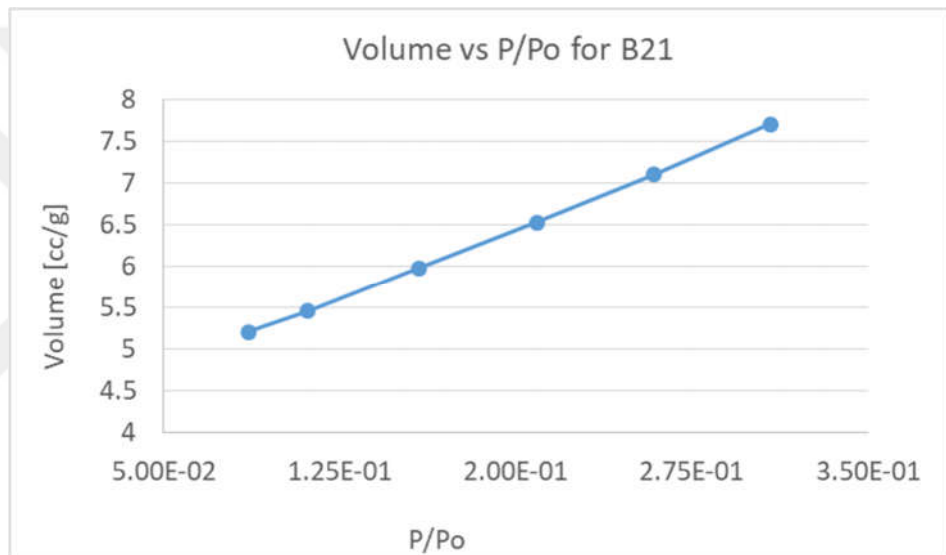
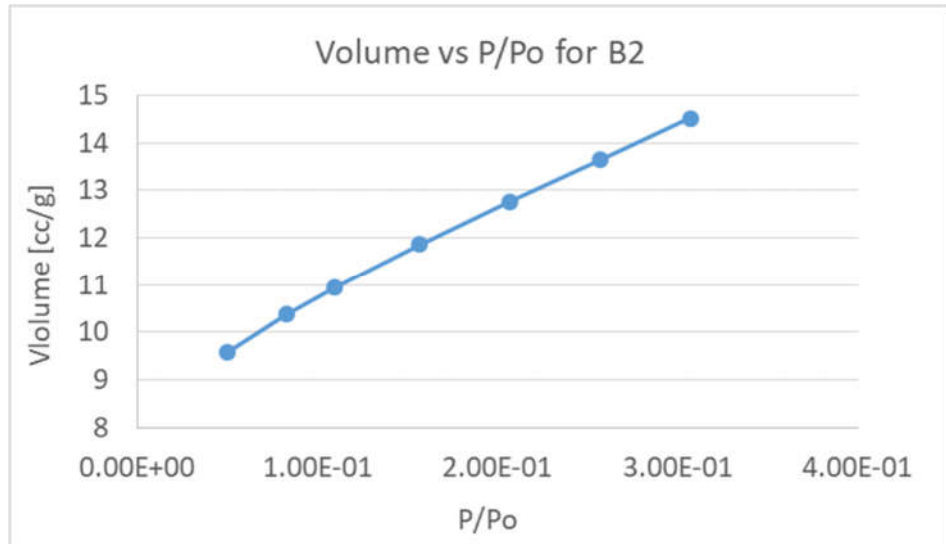


Figure 5-72. Volume versus P/Po graph of B2 and B21 catalysts

5.3.2 Influence of Alkali Catalysts on Gasification of Opium Alkaloid Wastewater

Table 5-43. Reaction conditions, and results of HTG of alkaloid wastewater in the absence of catalyst and in the presence of 0.5 g NaOH at various reaction temperatures with 15 mL of wastewater (T:temperature, NO:NaOH, and 3:300°C, 4:400°C, 5:500°C, 6:600°C)

	Reaction Temp. (°C)	Reaction Pressure (bar)	CGE (%)	CLE (%)	TOC (mg/L)	Produced gas amount (mmol/L ww.)
AF-T3	300	80	14.6	73.8	8505	144.8
AF-T4	400	240	23.7	59.1	6815	352.5
AF-T5	500	365	47.9	25.6	2950	672.5
AF-T6	600	440	68.5	14.4	1665	982.2
AF-T3-NO	300	110	28.9	51.0	5860	350.4
AF-T4-NO	400	250	35.9	40.3	4628	616.8
AF-T5-NO	500	375	69.3	11.3	1298	1072.8
AF-T6-NO	600	440	85.1	7.2	832	1403.2

Table 5-44. Reaction conditions, and results of HTG of alkaloid wastewater in the absence of catalyst and in the presence of 0.5 g KOH at various reaction temperatures with 15 mL of wastewater (T:temperature, KO:KOH and 3:300°C, 4:400°C, 5:500°C, 6:600°C)

	Reaction Temp. (°C)	Reaction Pressure (bar)	CGE (%)	CLE (%)	TOC (mg/L)	Produced gas amount (mmol/L ww.)
AF-T3	300	80	14.6	73.8	8505	144.8
AF-T4	400	240	23.7	59.1	6815	352.5
AF-T5	500	365	47.9	25.6	2950	672.5
AF-T6	600	440	68.5	14.4	1665	982.2
AF-T3-KO	300	98	31.8	50.4	5794	527.2
AF-T4-KO	400	240	48.4	34.2	3929	831.5
AF-T5-KO	500	370	78.2	8.0	919	1184.8
AF-T6-KO	600	415	90.9	4.9	566	1388.4

Table 5-45. Reaction conditions, and results of HTG of alkaloid wastewater in the absence of catalyst and in the presence of 0.5 g Na_2CO_3 at various reaction temperatures with 15 mL of wastewater. (T:temperature, 3:300°C, 4:400°C, 5:500°C, 6:600°C, and NC: Na_2CO_3)

	Reaction Temp. (°C)	Reaction Pressure (bar)	CGE (%)	CLE (%)	TOC (mg/L)	Produced gas amount (mmol/L ww)
AF-T3	300	80	14.6	73.8	8505	144.8
AF-T4	400	240	23.7	59.1	6815	352.5
AF-T5	500	365	47.9	25.6	2950	672.5
AF-T6	600	440	68.5	14.4	1665	982.2
AF-T3-NC	300	105	27.9	51.9	5961	1388.4
AF-T4- NC	400	230	35.2	45.1	5181	333.5
AF-T5- NC	500	362	68.6	13.9	1598	527.6
AF-T6- NC	600	460	82.8	9.9	1132	1027.6

Table 5-46. Reaction conditions, and results of HTG of alkaloid wastewater in the absence of catalyst and in the presence of 0.5 g K_2CO_3 at various reaction temperatures with 15 mL of wastewater (T:temperature, 3:300°C, 4:400°C, 5:500°C, 6:600°C, and KC: K_2CO_3)

	Reaction Temp. (°C)	Reaction Pressure (bar)	CGE (%)	CLE (%)	TOC (mg/L)	Produced gas amount (mmol/L ww)
AF-T3	300	80	14.6	73.8	8505	144.8
AF-T4	400	240	23.7	59.1	6815	352.5
AF-T5	500	365	47.9	25.6	2950	672.5
AF-T6	600	440	68.5	14.4	1665	982.2
AF-T3-KC	300	110	29.4	50.8	5834	271.8
AF-T4- KC	400	235	36.3	39.4	4585	666.5
AF-T5- KC	500	355	70.6	9.2	946	1081.9
AF-T6- KC	600	455	86.5	6.4	732	1330.1

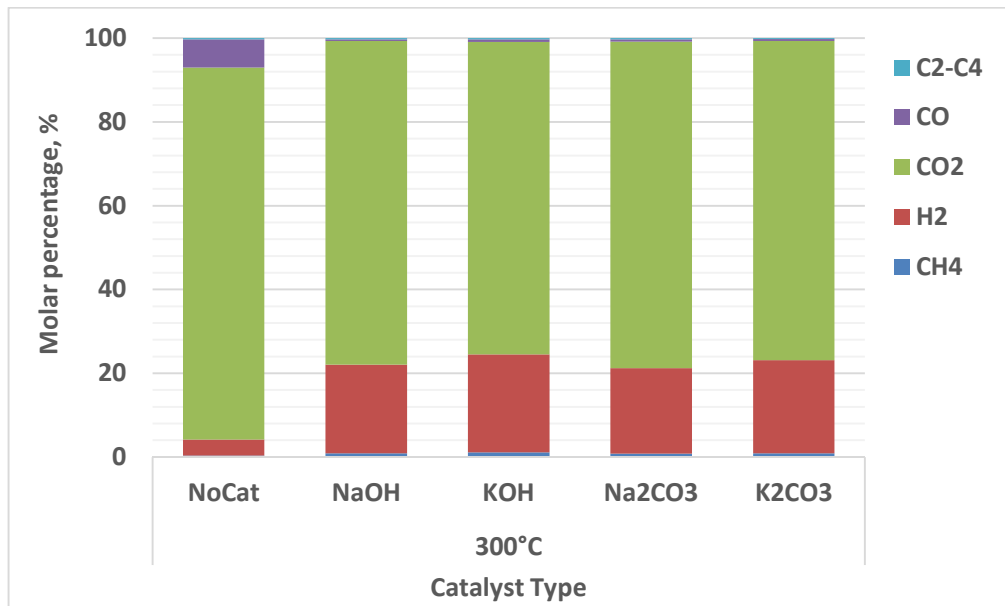


Figure 5-73. Effect of various catalysts on gaseous product distribution in hydrothermal gasification of alkaloid wastewater at 300°C

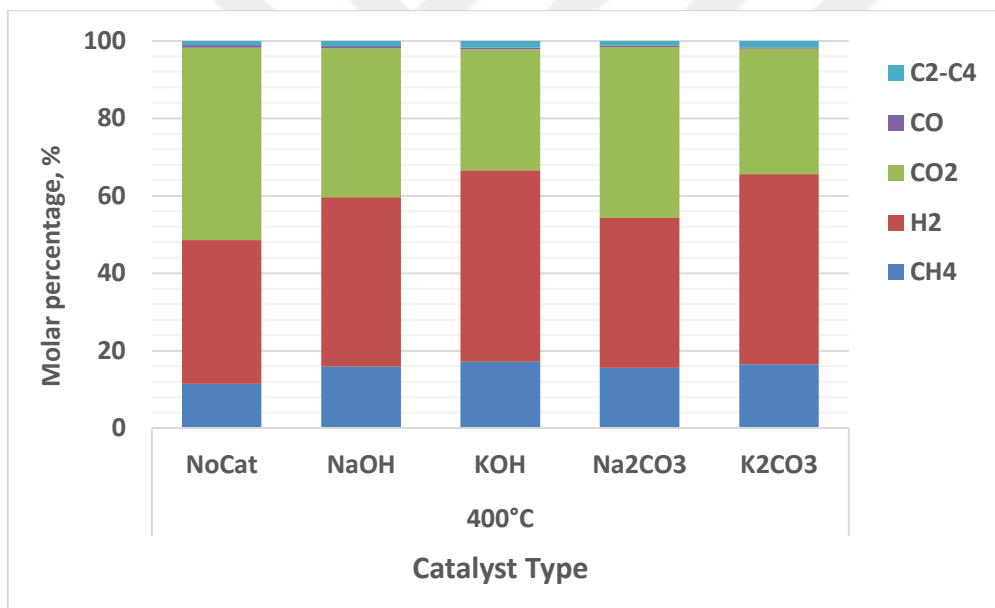


Figure 5-74. Effect of various catalysts on gaseous product distribution in hydrothermal gasification of alkaloid wastewater at 400°C

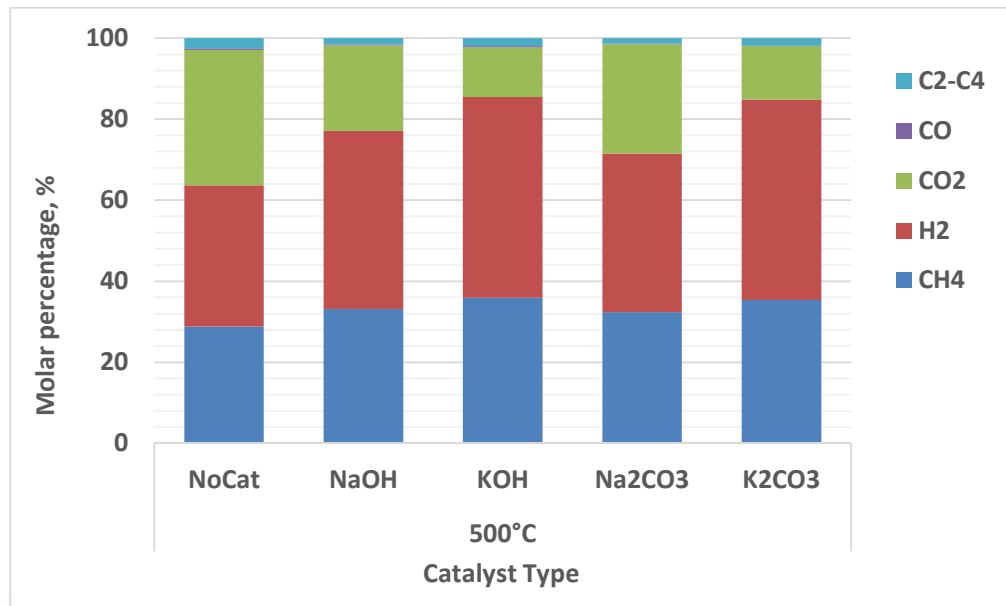


Figure 5-75. Effect of various alkali catalysts on gaseous product distribution in hydrothermal gasification of alkaloid wastewater at 500°C

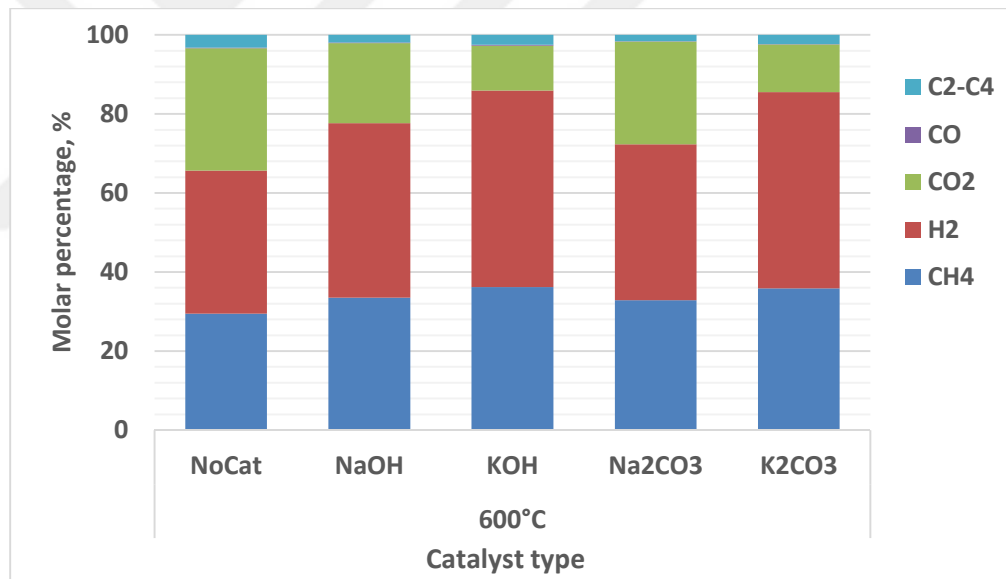


Figure 5-76. Effect of various alkali catalysts on gaseous product distribution in hydrothermal gasification of alkaloid wastewater at 600°C.

Table 5-47. The effect of catalyst type on gaseous product yields [mole gas/kg C in wastewater] in the detailed form in hydrothermal gasification of alkaloid wastewater in the presence of NaOH, KOH, Na₂CO₃, K₂CO₃ at 300 °C.

Mol/kg C in ww	<i>No catalysyt</i>	<i>NaOH</i>	<i>KOH</i>	<i>Na₂CO₃</i>	<i>K₂CO₃</i>
CH₄	0.04	0.2	0.4	0.17	0.17
H₂	0.31	4.9	8.2	4.5	4.2
CO₂	8.62	18	26.2	17.3	13.5
C₂-C₄	0.62	0.1	0.2	0.09	0.09
CO	0.03	0.07	0.1	0.07	0.03
Total	9.6	23.27	35.1	22.13	17.99

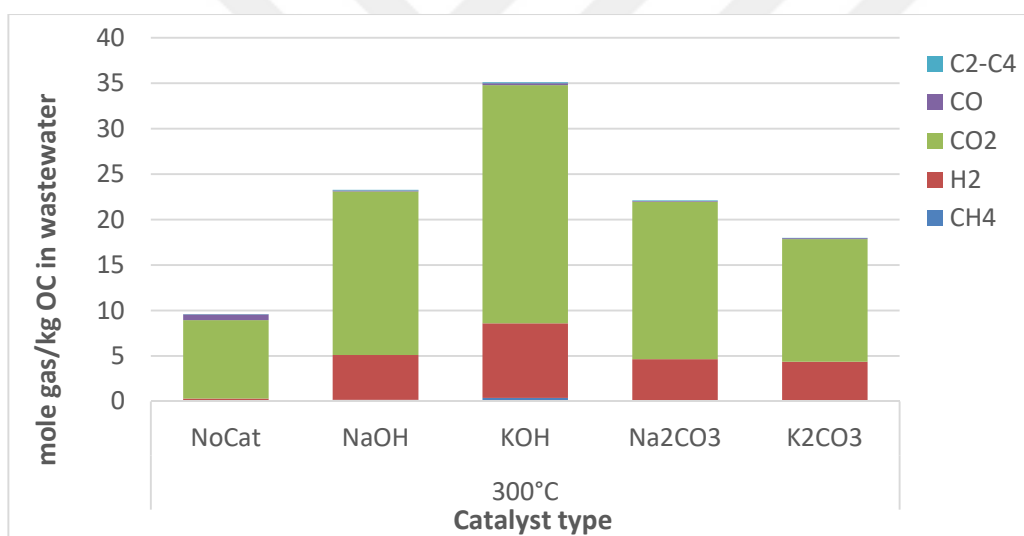


Figure 5-77. Effect of various alkali catalysts on gaseous product yields [mole/kg Organic Carbon] in hydrothermal gasification of alkaloid wastewater at 300°C.

Table 5-48. The effect of catalyst type on gaseous product yields [mole gas/kg C in wastewater] in the detailed form in hydrothermal gasification of alkaloid wastewater in the presence of NaOH, KOH, Na₂CO₃, K₂CO₃ at 400°C.

Mol/kg C in ww	No catalysyt	NaOH	KOH	Na ₂ CO ₃	K ₂ CO ₃
CH ₄	2.69	6.5	7.6	5.4	7.3
H ₂	8.69	18	24.7	13.6	21.8
CO ₂	11.69	15.8	22.2	15.5	14.4
C ₂ -C ₄	0.15	0.2	0.3	0.1	0.1
CO	0.23	0.6	0.7	0.4	0.7
Total	23.5	41.1	55.5	35.0	44.3

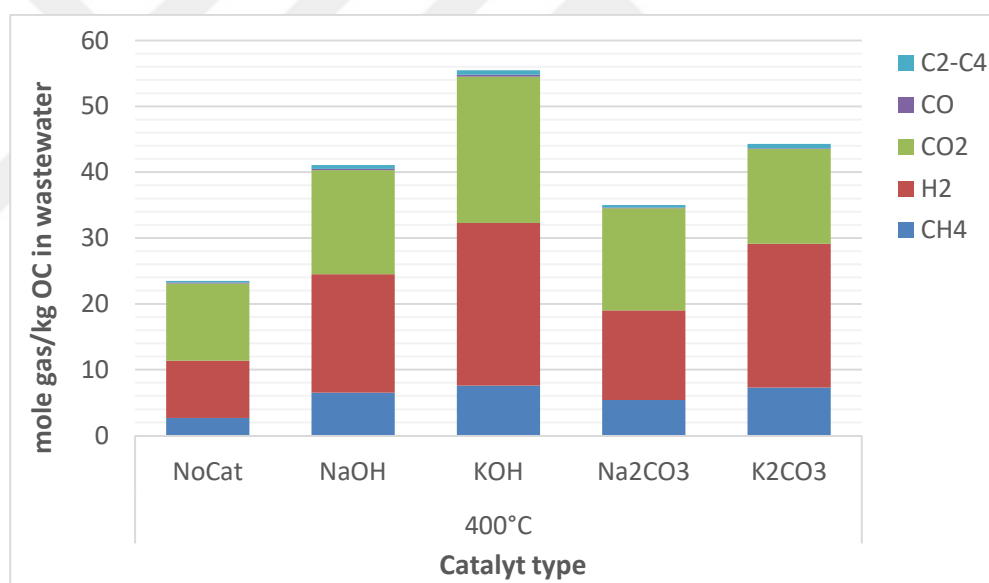


Figure 5-78. Effect of various catalysts on gaseous product yields [mole/kg Organic Carbon] in hydrothermal gasification of alkaloid wastewater at 400°C.

Table 5-49. The effect of catalyst type on gaseous product yields [mole gas/kg C in wastewater] in the detailed form in hydrothermal gasification of alkaloid wastewater in the presence of NaOH, KOH, Na₂CO₃, K₂CO₃ at 500°C.

Mol/kg C in ww	No catalysyt	NaOH	KOH	Na ₂ CO ₃	K ₂ CO ₃
CH ₄	12.92	22.7	28.6	22.2	25.6
H ₂	15.62	30	39.5	26.8	35.6
CO ₂	14.92	17.5	9.1	18.5	9.5
C ₂ -C ₄	0.15	0.13	0.24	0.1	0.08
CO	1.15	1.1	1.6	0.9	1.4
Total	44.8	71.43	79.04	68.5	72.18

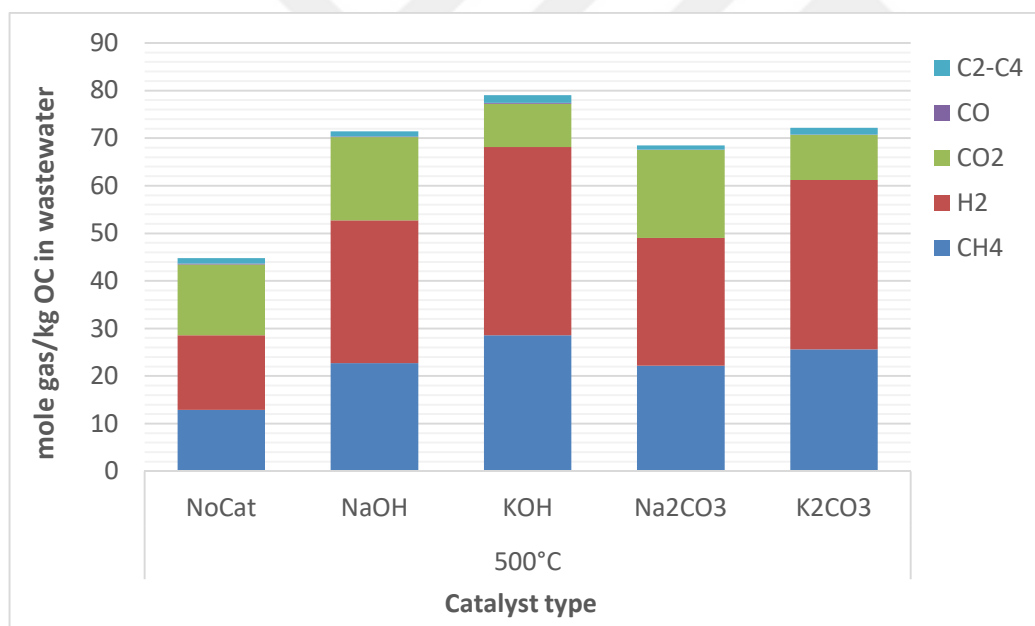


Figure 5-79. Effect of various catalysts on gaseous product yields [mole/kg Organic Carbon] in hydrothermal gasification of alkaloid wastewater at 500°C.

Table 5-50. The effect of catalyst type on gaseous product yields [mole gas/kg C in wastewater] in the detailed form in hydrothermal gasification of alkaloid wastewater in the presence of NaOH, KOH, Na₂CO₃, K₂CO₃ at 600 °C.

Mol/kg C in ww	<i>No catalyst</i>	<i>NaOH</i>	<i>KOH</i>	<i>Na₂CO₃</i>	<i>K₂CO₃</i>
CH₄	19.3	31.3	33.5	26.2	31.8
H₂	25.6	41.4	46.0	31.4	44.0
CO₂	17.6	18.9	10.5	20.7	10.7
C₂-C₄	0.15	0.20	0.18	0.08	0.08
CO	2.85	1.80	2.30	1.30	2.00
Total	65.5	93.6	92.5	79.7	88.6

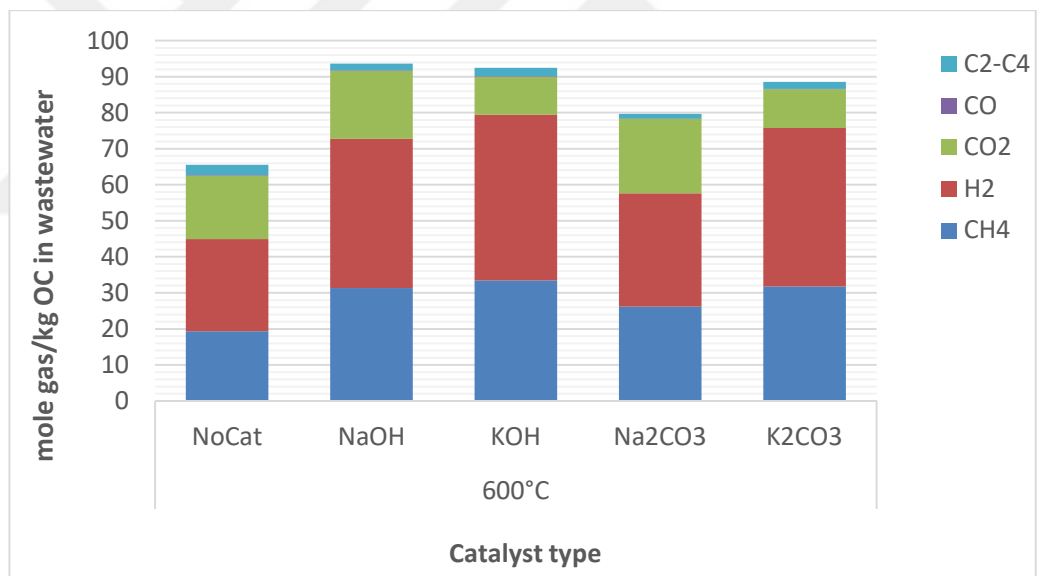


Figure 5-80. Effect of various catalysts on gaseous product yields [mole/kg Organic Carbon] in hydrothermal gasification of alkaloid wastewater at 600°C.

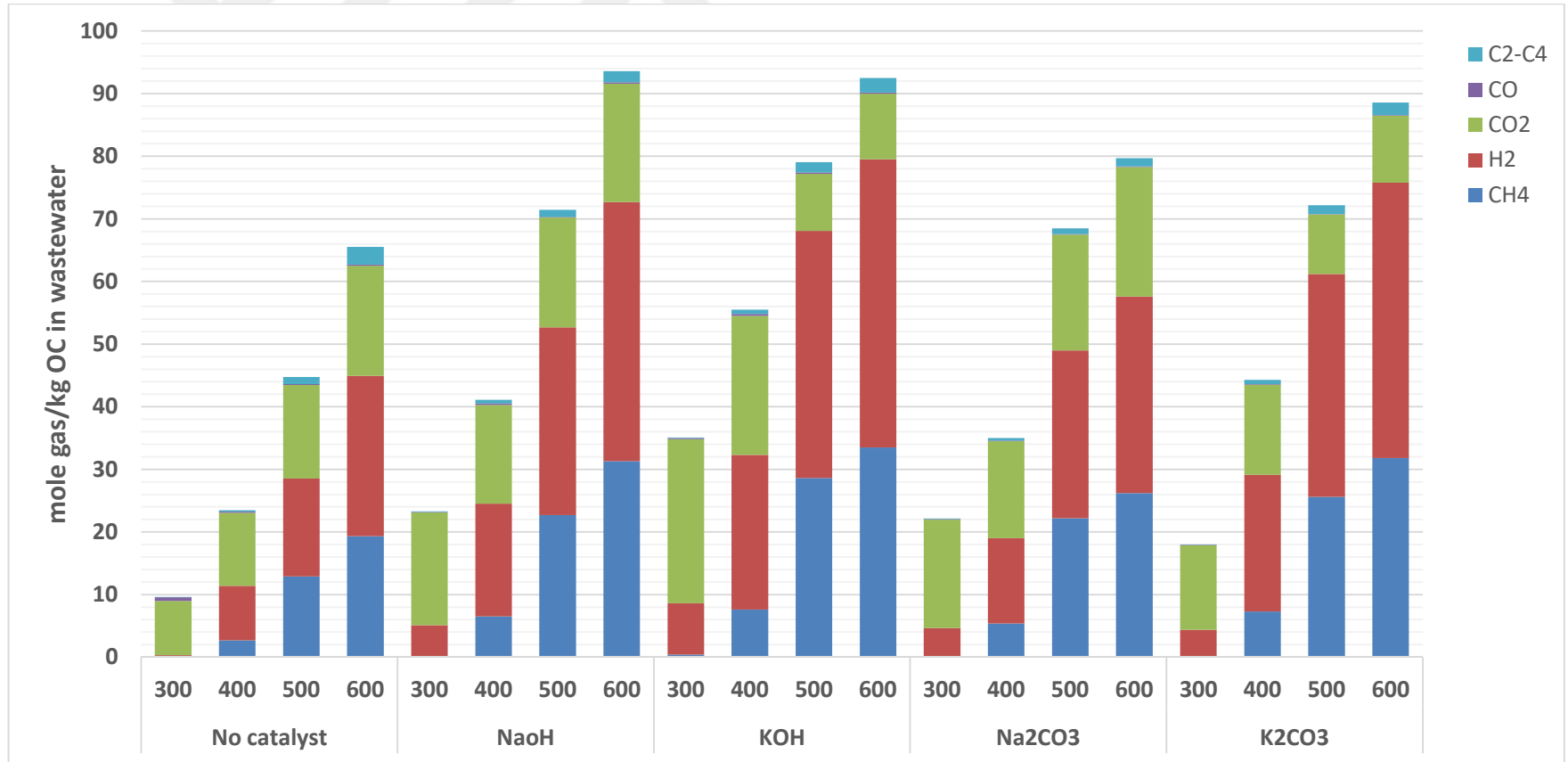


Figure 5-81. Effect of various catalysts and temperatures on gaseous product yields [mole/kg Organic Carbon] in hydrothermal gasification of alkaloid wastewater at all studied conditions.

Table 5-51. COD analysis results and COD removal efficiencies of the SCWG of Alkaloid wastewater absence of catalyst and in the presence of NaOH (NO), KOH (KO), Na₂CO₃ (NC), K₂CO₃ (KC) catalysts.

Experiment Code	Temp (°C)	Catalyst	COD Reactor Effluent [mg/L]	COD Removal Efficiency [%]
Raw wastewater		-	32050	-
AF-T3	300	-	29085	9.3
AF-T4	400	-	23380	27.1
AF-T5	500	-	8470	73.6
AF-T6	600	-	3045	90.5
AF-T3-NO	300	NaOH	27900	12.9
AF-T4-NO	400	NaOH	22550	29.6
AF-T5-NO	500	NaOH	6925	78.4
AF-T6-NO	600	NaOH	2875	91.0
AF-T3-KO	300	KOH	28700	10.5
AF-T4-KO	400	KOH	22625	29.4
AF-T5-KO	500	KOH	6340	80.2
AF-T6-KO	600	KOH	4725	85.3
AF-T3-NC	300	Na ₂ CO ₃	26975	15.8
AF-T4-NC	400	Na ₂ CO ₃	17575	45.2
AF-T5-NC	500	Na ₂ CO ₃	6370	80.1
AF-T6-NC	600	Na ₂ CO ₃	3230	89.9
AF-T3-KC	300	K ₂ CO ₃	28180	19.5
AF-T4-KC	400	K ₂ CO ₃	22710	29.1
AF-T5-KC	500	K ₂ CO ₃	4435	86.2
AF-T6-KC	600	K ₂ CO ₃	2835	91.2

Table 5-52. TOC analysis results and TOC removal efficiencies of the SCWG of Alkaloid wastewater absence of catalyst and in the presence of NaOH (NO), KOH (KO), Na₂CO₃ (NC), K₂CO₃ (KC) catalysts.

<i>Experiment Code</i>	<i>Temperature, °C</i>	<i>Catalyst</i>	<i>TOC Reactor Effluent [ppm]</i>	<i>TOC Removal Efficiency [%]</i>
Raw wastewater		-	11500	-
AF-T3	300	-	8505	26.0
AF-T4	400	-	6815	40.8
AF-T5	500	-	2950	74.4
AF-T6	600	-	1665	85.5
AF-T3-NO	300	NaOH	5860	49.0
AF-T4-NO	400	NaOH	4630	59.8
AF-T5-NO	500	NaOH	1300	88.7
AF-T6-NO	600	NaOH	830	92.8
AF-T3-KO	300	KOH	5795	49.6
AF-T4-KO	400	KOH	3930	65.8
AF-T5-KO	500	KOH	920	92.0
AF-T6-KO	600	KOH	565	95.1
AF-T3-NC	300	Na ₂ CO ₃	5960	48.2
AF-T4-NC	400	Na ₂ CO ₃	5180	54.9
AF-T5-NC	500	Na ₂ CO ₃	1600	86.1
AF-T6-NC	600	Na ₂ CO ₃	1130	90.2
AF-T3-KC	300	K ₂ CO ₃	5835	49.3
AF-T4-KC	400	K ₂ CO ₃	4585	60.1
AF-T5-KC	500	K ₂ CO ₃	950	91.8
AF-T6-KC	600	K ₂ CO ₃	730	93.6

5.3.2.1 Effect of reaction temperature

The reaction temperature is the most effective parameter on CGE and CLE in the studied range of temperature and pressure for both catalytic and non-catalytic experiments. At 300°C, carbon gasification efficiency is increased from 14.6 to 68.5% as the temperature goes up to 600°C without catalyst. The total produced gas amount is also promoted with high temperatures from 144.8 to 982.3 mmol/liter. On the contrary the liquefaction efficiency is decreased from 73.8 to 14.4% as the temperature is increasing from 300 to 600°C in the absence of catalyst. These tendency is valid in catalytic runs and is observed in Tables 4-7 clearly. In the case gaseous product yields, temperature increment accelerate CH₄, H₂ yields very strongly while CO₂ yields increases slightly in non-catalytic runs. In catalytic runs, increasing temperature promoted CH₄ and H₂ but CO₂ yields increased a little or decreased depends on the catalyst type from 300 to 600°C. The yields of C₂-C₄ compounds increased by temperature increment for all runs while CO yields increased in non-catalytic runs only. CO has the lowest amount in the gaseous product and in the presence of catalyst, produced CO amounts does not change considerably.

TOC and COD content in aqueous product decreased by elevating temperatures rapidly as a result removal efficiencies rised from approximately 10% to 90%'s from 300 to 600°C.

5.3.2.2 The effect of catalyst type

Carbon gasification efficiencies go up with the catalyst addition while the carbon liquefaction efficiencies lessening in all studied reaction temperatures. In the absence of catalyst CGE is maximized at 600°C with 68.5% and in the presence of catalyst, this ratio rise to the levels of 85-90% as shown in Tables 4-7. This uptrend is seen at 300, 400 and 500 °C. The liquefaction efficiency is minimized at 600°C as 14.4% and decreased to 4-10% with the catalyst use. The highest CLE was observed at 300°C with 73.8 % in the absence of catalyst and diminished to the levels of 50% by catalyst effect. At the other reaction temperatures operated, CLE is decreased by catalyst similarly for all catalyst types. The gaseous product

distribution within the range of 300-600°C changed with temperature and catalyst at all runs. The molar percentage of H₂ increases from 300 to 400°C but above 400°C, it remains almost constant at while the molar percentage of CH₄ is increased rapidly up to 500°C and does not change up to 600°C for both non-catalytic and catalytic cases. The highest percentage of H₂ is reached at 49.6 and 49.7% and the highest percentage of CH₄ is obtained at 35.9 and 36.2 % with K₂CO₃ and KOH respectively at 600°C. The CO₂ ratio in the product gas decreased from 88.8% to 30.9% as the temperature increasing from 300 to 600°C without catalyst. In catalytic runs CO₂ ratio is changed from 75-78 % levels to 20-26% with Na₂CO₃ and NaOH, from 74-76% levels to 11-12% levels with KOH and K₂CO₃. The yields of gaseous products in unit of mol/kg OC are promoted by the effect of catalyst generally except CO₂ and C₂-C₄. The yields of H₂ reached to 46 as maximum with KOH while it is 25.62 without catalyst at 600°C. The obtained CH₄ yields are 19.31 and 33.5 in the absence of catalyst and presence of KOH respectively. TOC and COD removal efficiencies slightly increased with catalyst effect.

A comparison may be done for studied catalysts in the case of CGE, TOC removal and H₂ and CH₄ yields as: Na₂CO₃ < NaOH < K₂CO₃ < KOH.

5.3.3 Influence of Nickel based Catalysts on Gasification of Opium

Alkaloid Wastewater

Table 5-53. Reaction conditions, CGE, produced gas amount and TOC values of hydrothermal gasification of alkaloid wastewater with various catalysts at 500°C.

	Catalyst	T (°C)	P (bar)	CGE (%)	CLE (%)	TOC (mg/L)	Produced gas amount (mmol/L ww)
No catalyst	-	500	365	47.9	25.6	2950	672.5
AF-T5-RN1	Raney Nickel 4200	500	350	74.4	9.8	1130	1208
AF-T5-RN2	Raney Nickel 2800	500	355	72.1	11.1	1275	1104
AF-T5-AN	Activated Nickel	500	385	72.4	8.6	985	1250
AF-T5-NSA	Nickel-Silica/Alumina	500	348	70.7	12.9	1480	1073

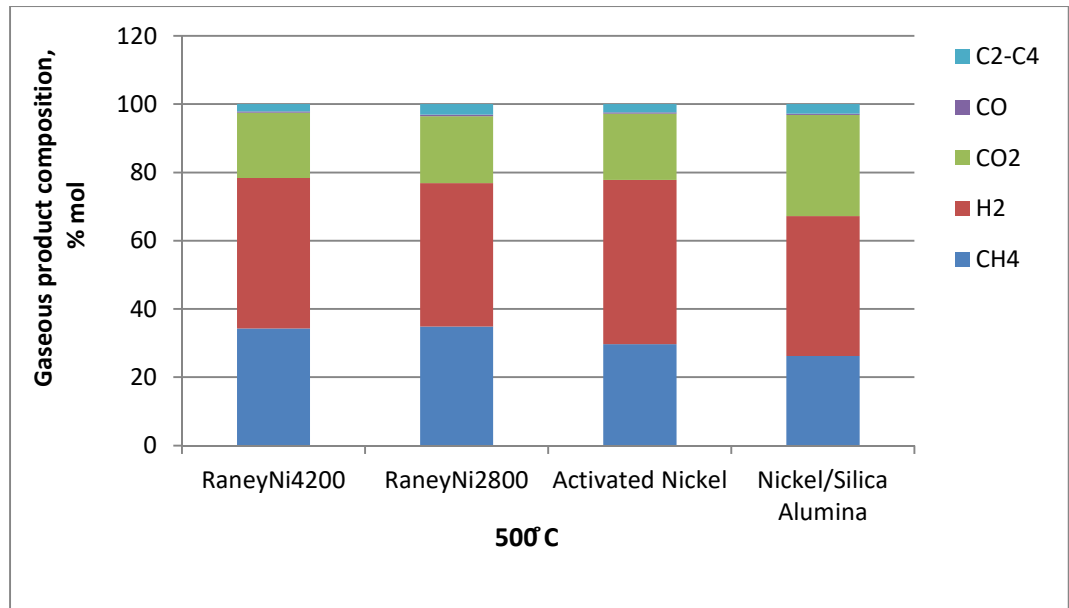


Figure 5-82. Comparison of the gaseous product composition in hydrothermal gasification of alkaloid wastewater with various catalysts at 500°C.

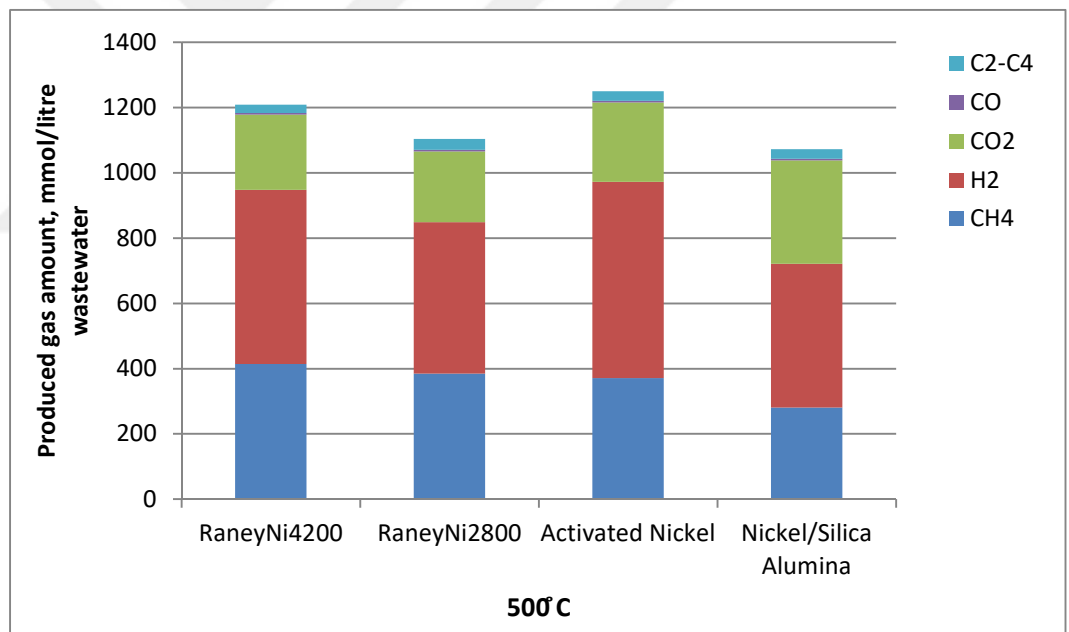


Figure 5-83. Comparison of the gaseous product yields [mole/kg Organic Carbon] in hydrothermal gasification of alkaloid wastewater with various catalysts at 500°C.

Table 5-54. COD analysis results and COD removal efficiencies of the SCWG of Alkaloid wastewater wastewater in the presence of Nickel based various catalysts at 500°C.

Mol/kg C in ww	AF-T5-RN2	AF-T5-RN1	AF-T5-AN	AF-T5-NS
CH ₄	36.0	33.5	32.3	24.4
H ₂	46.3	40.3	52.3	38.3
CO ₂	20.0	18.8	21.1	27.6
C ₂ -C ₄	0.4	0.38	0.4	0.37
CO	2.2	3.0	2.6	2.6
Total	36.0	33.5	32.3	24.4

Table 5-55. COD analysis results and COD removal efficiencies of the SCWG of Alkaloid wastewater wastewater in the presence of Nickel based various catalysts at 500°C.

Experiment Code	Catalyst type	Volume of ww (mL) and Catalyst amount (g)	COD Reactor Effluent (mg/L)	COD Removal Efficiency (%)
Raw wastewater	-	-	32050	-
No catalyst	-	-	8470	73.6
AF-T5-RN1	Raney Nickel 4200	15 mL/0.5 g	2250	92.3
AF-T5- RN2	Raney Nickel 2800	15 mL/0.5 g	2180	93.1
AF-T5-AN	Activated Nickel	15 mL/0.5 g	2510	92.1
AF-T5-NSA	Nickel- Silica/Alumina	15 mL/0.5 g	2725	91.5

Table 5-56. TOC analysis results and TOC removal efficiencies of the SCWG of Alkaloid wastewater in the presence of Nickel based various catalysts at 500°C.

Experiment Code	Catalyst type	Volume of ww (mL) and Catalyst amount (g)	COD Reactor Effluent (mg/L)	COD Removal Efficiency (%)
Raw wastewater	-	-	11500	-
No catalyst	-	-	2950	74.4
AF-T5-RN1	Raney Nickel 4200	15 mL/0.5 g	1130	90.2
AF-T5- RN2	Raney Nickel 2800	15 mL/0.5 g	1275	89.9
AF-T5-AN	Activated Nickel	15 mL/0.5 g	985	91.4
AF-T5-NSA	Nickel-Silica/Alumina	15 mL/0.5 g	1480	87.1

The studied catalyst types in this section are Raney Nickel 2800, Raney Nickel 4200, Activated Nickel, Nickel/Silica-Alumina, reaction temperature of 500°C. The results were given in Tables 5-77 to 5-80 and Figures 5-63 and 5.64.

Carbon gasification efficiencies go up with the catalyst addition while the carbon liquefaction efficiencies lessening with all studied catalysts. In the absence of catalyst CGE was 47.9% and accelerated from this level to within the range of 70.7-74.4% at 500°C in the presence of catalyst.

The gaseous product distribution with the studied Nickel based catalysts at 500°C changed with catalyst type significantly. The major gaseous products are CO₂, H₂ and CH₄ for all as expected while the distribution is varied depending on the catalyst type. Molar percentages of C₂-C₄ and CO are about 2-3% and 0.4%, respectively. The molar percentage of H₂ is found as highest with Activated Nickel as 48.1% and with Raney Nickel 4200 as 44.1% that is followed by other catalyst at slightly lower percentages. Raney Nickel 4200 and 2800 are the catalysts that enhanced the methanation reaction most and the percentage of CH₄ is reached levels of 34%. The sum of the H₂ and CH₄ is approximately 77% for Raney Nickel 4200 and 2800 and Activated Nickel while it is lower with Nickel/Silica-Alumina since

CO₂ percentage is higher with this catalyst. The yield of H₂ (52.3 mol/kg organic carbon) is highest and a high yield of CH₄ (32.3 mol/kg organic carbon) is obtained with Activated Nickel. The yield of CH₄ (36.0 mol/kg organic carbon) is highest and a high yield of H₂ (46.3 mol/kg organic carbon) were obtained with Raney Nickel 4200. When we evaluate both high H₂ and CH₄ yields, these two catalysts should be suggested as best. In terms of COD and TOC removal efficiencies, similar results were obtained. They decreased organic carbon content and oxygen demand successfully at a ratio about 90%.

5.4 Characterization analysis of raw alkaloid wastewater

Table 5-57. Opium Alkaloid Wastewater characteristics

Parameter	Unit	Sample
TOC	mg/L	11500
COD	mg/L	32050
Color	Pt/Co	16800
Conductivity	mS/cm	31.4
TDS	g/L	18.95
TSS	mg/L	1576
NH₄-N	mg/L	350.4
Turbidity	ntu	575.6
Resistance	Ω/cm	31.8
Salinity	‰	19.57
pH	-	4.73
Protein	%	0.0392
Na	mg/L	25.2
K	mg/L	2175
Mg	mg/L	3100
Ca	mg/L	54.1

Table 5-58. LC/MS-MS analysis results of raw alkaloid wastewater and aqueous product obtained in HTG of wastewater at various reaction temperatures without catalyst

<i>Compound Name</i>	<i>Retention time, min</i>	<i>Area</i>			
		<i>Raw wastewater</i>	<i>AF-T4</i>	<i>AF-T5</i>	<i>AF-T6</i>
7					
aminoclonazepam m/z:286.10>121.05	5.242	6362983	-	-	-
Diltiazem m/z:415.20>178.05	9.838	54838	-	-	-
Morphine m/z:286.10>165.10	5.249	28077786	18366	16108	12537
Codeine m/z:300.20>165.20	7.347	3941206	-	-	-
THCCOOH m/z:345.30>299.20	10.064	419648	-	-	-

❖ LC/MS-MS analysis of raw wastewater and aqueous product

Liquid chromatography-tandem mass spectrometry was used to analyze the wastewater samples for 136 chemicals, but only 5 were detected in the aqueous samples. The following: 7 aminoclonazepam, Diltiazem, Morphine, Codeine, and THCCOOH were detected in the raw wastewater. These detected chemicals other than the alkaloid types of Morphine and Codeine are the metabolite of some types of drugs or pharmaceutically active compounds. After the hydrothermal treatment of raw wastewater in the absence of a catalyst and at 400, 500, and 600 °C, morphine was only detected in the aqueous product. As it is seen in Table 5-82, even at 400°C reaction temperature, the compounds detected in the raw wastewater were destroyed completely except for the morphine. The area value of the morphine peak obtained in the raw wastewater analysis is reduced by 99.95 % in the aqueous products of gasification. To show the effect of gamma radiation on alkaloid wastewater proposed as a pretreatment method, Bural et al. (Cavit B. Bural) presented a visual comparison of the overlaid chromatograms of raw wastewater and irradiated samples from GC/MS. The peaks were diminished by irradiation to a certain extent. Similarly, the decreasing area values obtained in our study shows that compounds present in raw wastewater were destroyed with the superior

supercritical water properties in degrading organics with no need any other operation.

❖ HPLC Analysis Results of isolated raw wastewater samples supplied in 2013 (Sample 1) and 2015 (Sample 2)

Isolated wastewater samples were analyzed HPLC-RI in two different columns (Biorad and Macherey Nagel), since there are some separation obstacles of the compounds in due to very similar structures of them. Doing analysis in two different column gives a chance to evaluate results better. As you see in Tables in Appendix III, cellobiose, sucrose, glucose, mannose, xylose, galactose, rhamnose, arabinose and fructose were identified and analyzed in BIORAD column. The chromatogram was given in Figs. 5-84 and 85. There are some multiple peaks (mannose+xylose+galactose and arabinose+fructose) and they integrated manually to obtain more reliable results.

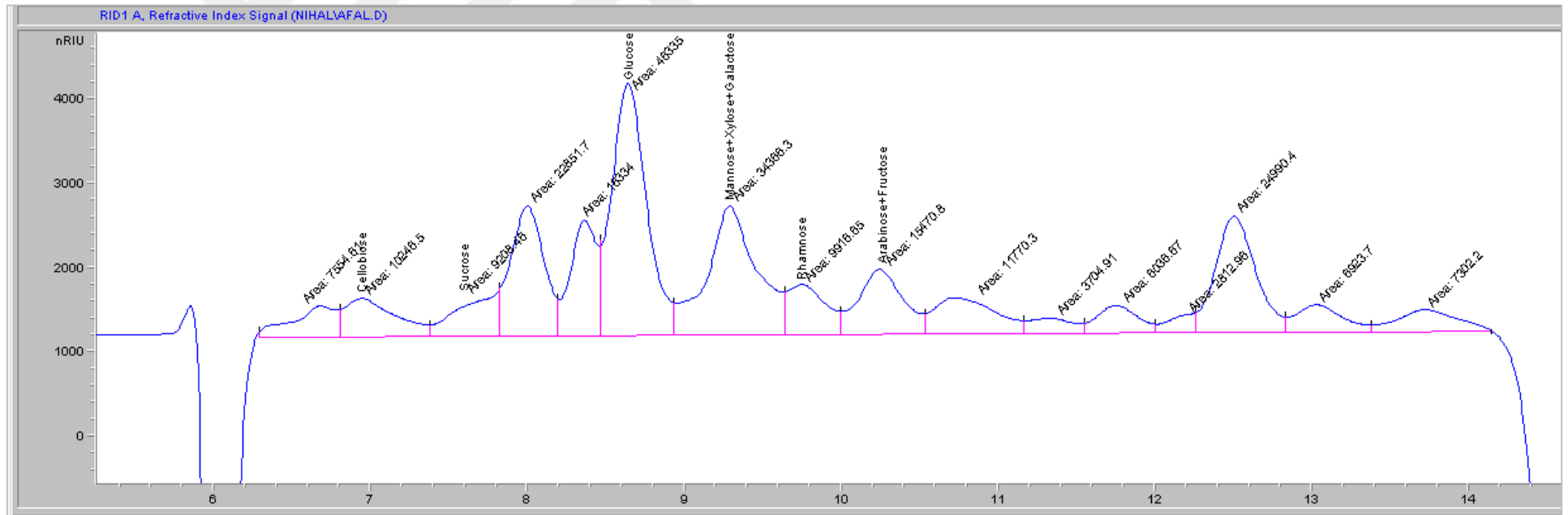


Figure 5-84. HPLC chromatogram of raw wastewater “Sample 1” in BIORAD column.

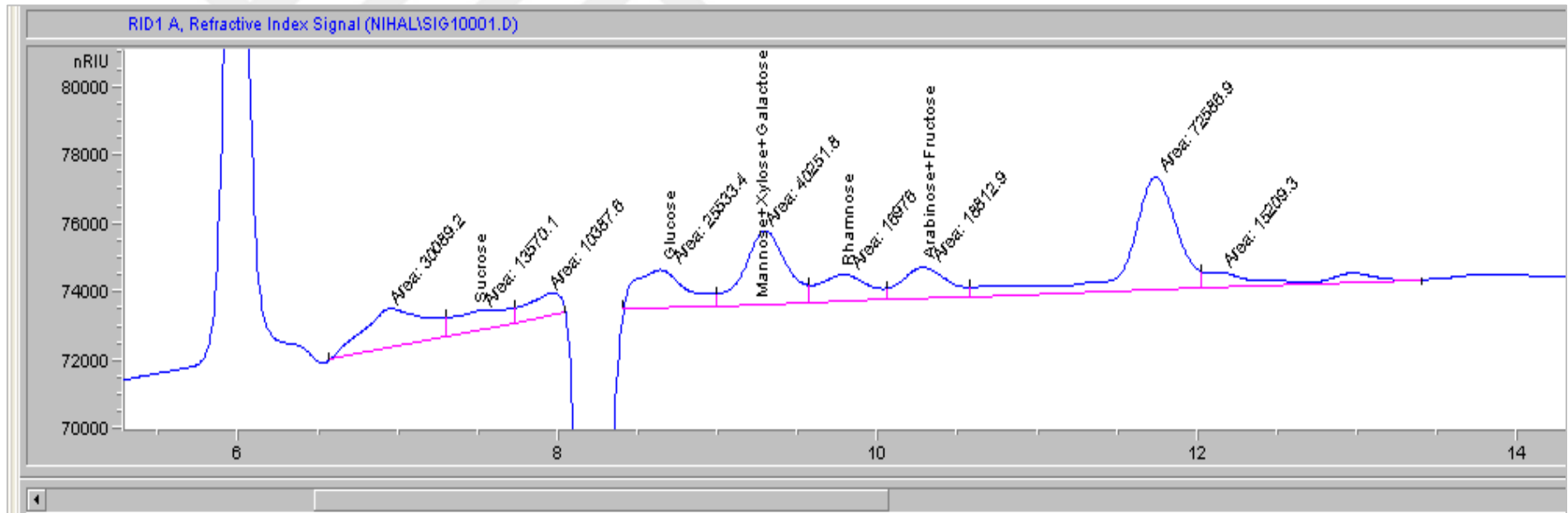


Figure 5-85. HPLC chromatogram of raw wastewater “Sample 2” in BIORAD column.

Wastewater supplied in 2015 have a HPLC chromatogram as in Figure 5-85 and integration results are given in Table 5-60. According to analysis results obtained with BIORAD column, carbohydrate contents were determined as 568 and 493 ppm for sample 1 and 2, respectively. Carbohydrate analysis were done with Bural (Cavit B. Bural) and by using the Dubois method and found the concentration of carbohydrate as 10000 ppm which is much more than in our analysis results. The difference may be generated we have used isolated samples instead of raw wastewater and the method is different.

Analysis in Macherey Nagel column provide better separation of the carbohydrate monomers as seen in Table 5-61 and 5-62. According to analysis results, carbohydrate amounts were quantified as 1294 and 776 ppm for “Sample 1” and “Sample 2” respectively. In this columns, the carbohydrate amount were found as higher comparing to Biorad. The reason may be better separation of the mannose, xylose, and galactose. Rhamnose contents are seen as higher in Macherey Nagel than Biorad. The baseline is not very straight in Sample 1 analysis in this column and this may lead difference between two samples results.

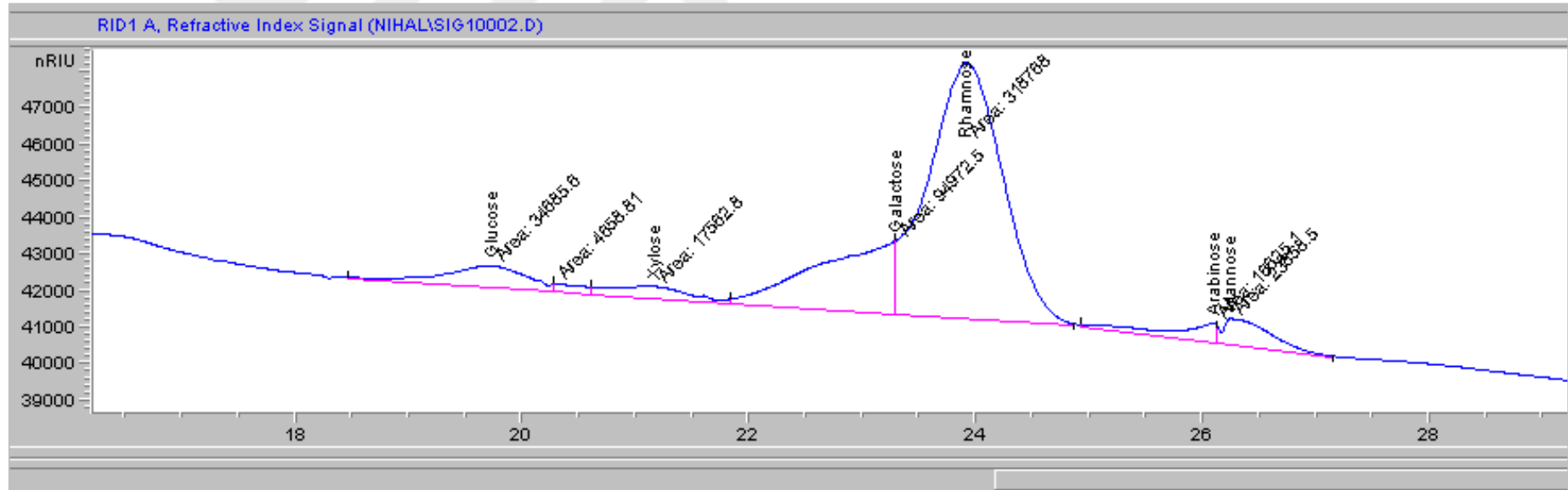


Figure 5-86. HPLC chromatogram of raw wastewater "Sample 1" in MACHEREY NAGEL COLUMN column.

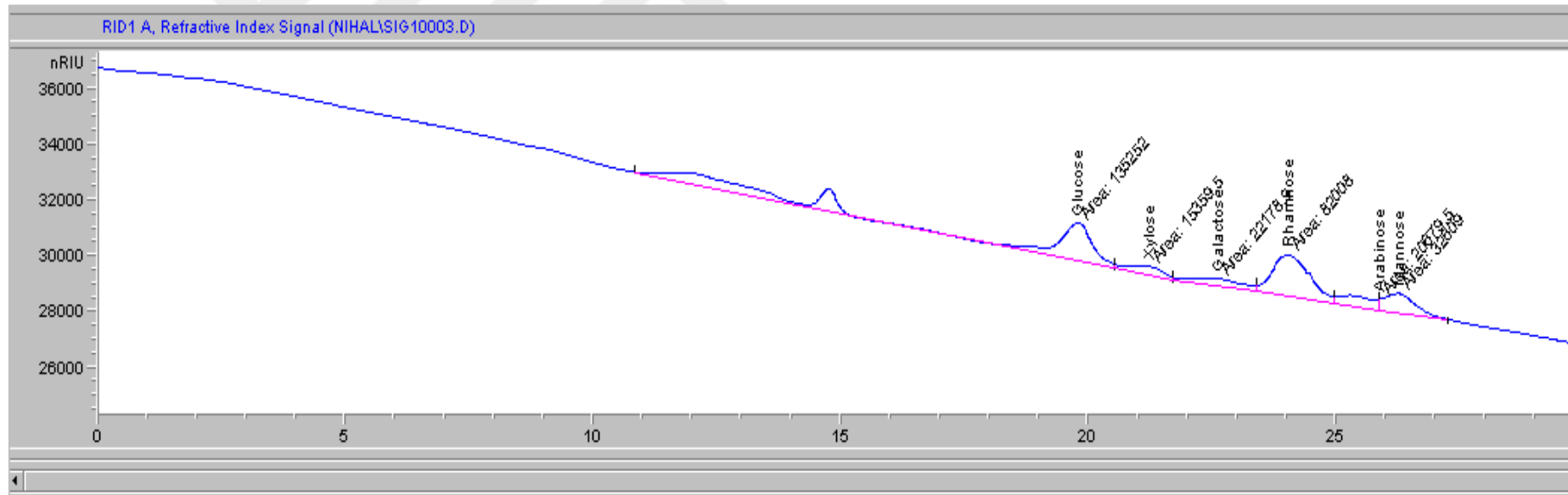


Figure 5-87. HPLC chromatogram of raw wastewater “Sample 2” in MACHEREY NAGEL COLUMN column.

6. CONCLUSIONS

In this study, wastewater from opium processing industry was gasified in sub, near and supercritical water conditions at various temperatures, pressures and in the absence of catalyst and presence of wide variety of catalysts. The optimization of the catalyst amount was done at all reaction temperatures.

The experimental studies are summarized in three main category and some sub-categories as:

❖ **The effect of temperature and catalyst amount** were evaluated by altering reaction temperature as 300, 400 500 and 600°C without catalyst firstly. Then the addition of various amounts of catalyst was studied using 0.125, 0.250, 0.375, 0.500, and 0.625 g of K_2CO_3 between 300-600°C.

❖ **The effect of reaction pressures** of 200 , 275, 350, 425 bar were investigated by adjusting wastewater and catalyst amount to maintain these pressures. Pre-experiments were done to provide the pressures specified. Both non-catalytic and catalytic pressure effect experimens were carried out at 500 and 600°C. The effect of K_2CO_3 in pressure effect experiments was examined.

❖ The **catalyst type** was investigated by using red mud and activated derivatives of it (precipitation with NH_3 or K_2CO_3 , nickel impregnation in varying ratios of 10, 20 and 30%, and reduction by $NaBH_4$), alkali catalysts (Na_2CO_3 , K_2CO_3 , $NaOH$, KOH), nickel based catalysts (Raney Nickel 4200, Raney Nickel 2800, Activated Nickel, Nickel/Silica-Alumina) at 500°C of reaction temperature.

The results obtained in HTG of alkaloid wastewater in terms of all studied parameters are concluded briefly as:

In temperature effect and catalyst amount optimization:

❖ The dominant parameter of the gasification of alkaloid wastewater is found as temperature, which is similar in the HTG of a biomass given in literature. As the reaction temperature increase from 300 to 600°C, carbon gasification efficiencies and the total number of gaseous products increased greatly: CGE

is risen from 14.5 to 68.5% and the amount of produced gas went up from 12.6 to 85.2 mol/kg C without catalyst.

❖ The addition of K_2CO_3 promotes CGE and produced gas amounts generally in the most favorable catalyst amount determination experiments. The most favorable amount of catalyst was found as 0.500 g of K_2CO_3 which effects the CGE, since no increase was observed with

0.625 g of K_2CO_3 compared with 0.500 g. The reason should be that the equilibrium was provided at the specified reaction temperatures with catalyst and so the increase in amount of catalyst did not make an enhancement.

❖ K_2CO_3 (0.5g) promoted CGE with varying ratios at different reaction temperatures as 15 % at 300°C, 6% at 400°C, 18 % at 500°C, and 5.5% at 600°C approximately. Increasing the amount of K_2CO_3 does not affect the CGE substantially at constant temperature, except 300°C and the total gas amount is increased slightly.

❖ The produced gas amount and CGE reached maximum as 106.3 mol/kg C and 74.0%, respectively, with the addition of 0.5 g of K_2CO_3 at 600°C.

❖ The organic carbon content of the wastewater is converted to gaseous product consist of CH_4 , H_2 , CO_2 , and CO and C_2 - C_4 hydrocarbons. Gaseous product distribution and yields are highly affected by temperature and catalyst.

❖ The yields of CH_4 increased from 0.5 to 25.1 mol/kg C with increasing temperature from 300 to 600°C without a catalyst. Methane formation is almost zero at 300°C even higher amount of catalyst. In the presence of 0.5g of K_2CO_3 , the yields of methane promoted with a higher ratio at 400 and 500°C (125% and 68%, respectively) than 600°C (37%).

❖ The highest CH_4 and H_2 amounts were achieved at 600°C and with 0.5 g K_2CO_3 as 34.3 and 47.7 mol/kg C, respectively.

❖ The molar percentage of H_2 rised with an increase in the amount of catalyst generally. The molar fraction of CH_4 in the gaseous product mixture is not affected with a change in the catalyst amount directly.

- ❖ The hydrogen yields are strongly enhanced with 0.5 g of K_2CO_3 by 113, 68, and 43% compared to the case without catalyst at 400, 500 and 600°C, respectively.
- ❖ In terms of COD removal efficiency, maximum ratios were reached obtained in our work is at 600°C about 92-95 % with K_2CO_3 in the range of 0.375 - 0.625 g at the end of of 1h HTG operation.
- ❖ As the temperature increased from 300 to 600°C, the COD and TOC removal ratios accelerated in both catalytic and non-catalytic runs. The increase in catalyst amount makes a slight increase in removal efficiencies.

In pressure effect experiments:

- ❖ CGE is slightly decreased as the pressure increasing from 200-425 bar at 500°C and 600°C, and both in non-catalytic and catalytic runs which are carried out in the presence of K_2CO_3 .
- ❖ Temperature increment in pressure effect experiments from 500 to 600°C and catalyst addition enhanced gasification and the highest CGE value is reached as 87.5% at 600°C and 200 bar with K_2CO_3 .
- ❖ The pressure promoted methanation reactions while affect H_2 formation negatively. H_2 yield decreases with increasing pressure, but using catalyst increases amount of H_2 produced at 500°C and 600°C.
- ❖ For maximum H_2 yield, 500°C, 200 bars and K_2CO_3 addition should be chosen while to maximize CH_4 , 600°C, 425 bar and non-catalytic run should be selected.
- ❖ Carbon dioxide yields are lower at lower pressures and increased slightly as increasing temperature. K_2CO_3 addition has also reduced the CO_2 yield at 600°C while the effect of catalyst at 500°C is not clear.
- ❖ CO and C_2 - C_4 hydrocarbons yields are very low comparing to H_2 , CH_4 and CO_2 . The yields of CO are slightly increased by increasing pressure and catalyst addition while the yields of C_2 - C_4 hydrocarbons are decreased at high pressures. Temperature is not much effective on C_2 - C_4 hydrocarbons yields.

- ❖ Chemical oxygen demand of the aqueous product lessens at high temperatures and pressures while the effect of temperature is stronger on COD removal.
- ❖ Catalyst use has a substantial effect since COD is reduced from 9000 to 5225 ppm at 500°C and 200 bars with addition of K_2CO_3 , but this effect is less at 600°C.
- ❖ In terms of operation cost, catalyst (K_2CO_3) addition provides COD removals at 500°C as high as in 600°C non-catalytic runs. Catalyst addition should be chosen instead of temperature increase to obtain similar treatment efficiency.

In various catalyst type experiments:

Activated Red Mud

- ❖ The produced gas amount promoted by activation of red mud in group A, since all the activated forms increased gas amount. Nickel impregnation enhanced gasification while the effect of reduction by $NaBH_4$ is not so effective.
- ❖ The original red mud increased the CH_4 amount (mmol/L wastewater) by 32% while enhancing the H_2 formation by 17%. It makes not a considerable effect on gasification but reduced TOC value of the aqueous product by 25%.
- ❖ A group activated red mud catalysts show good catalytic activity in hydrogen production and the yields of H_2 reached 34.1 and 34.3 as the highest with A3 and A31 catalyst while the yield of H_2 was only 20.3 mol/kg C in non-catalytic run.
- ❖ CH_4 yields are significantly enhanced by changing ratios of 52-74% with activated red muds in group A.
- ❖ The catalyst use (A group) improved COD_{RE} and TOC_{RE} by 10 and 15%, respectively at 500°C. The amount of nickel impregnated did not make a sensible change in COD_{RE} and TOC_{RE} while the reduction with $NaBH_4$ made a slightly negative effect in Group A.
- ❖ B group catalysts promoted CGE and produced gas amounts the highest gasification ratios were obtained as 68.6, 72.6, 70.8% with reduced forms of

them: with B21, B31, B41 respectively. Nickel impregnation was slightly increased gasification, while the amount of impregnated nickel did not a significant effect.

- ❖ The highest gaseous product amounts were reached with B3 and B31 (1000 and 1010 mmol/L wastewater) while the others give similar catalytic activity in terms of produced gas quantities.
- ❖ COD of the wastewater lowered to 4940-6240 ppm levels by a removal range of 81-85 % approximately while TOC content decreased around to 1200-1760 ppm by removal efficiencies of 85-90% with Group B.
- ❖ The effect of catalyst type within the activated state of red mud in B group can not be seen clearly since the effectiveness are alike.
- ❖ Addition of K_2CO_3 to A group catalyst give higher yields in case of hydrogen and AK accelerated methane formation up to the levels of 34-35 mol CH_4 /kg C. In terms of methane production, AK group is also the best group in activated red mud catalysts.
- ❖ CO_2 yields are generally increased while reduced catalysts give slightly lower CO_2 than other.

Alkali Group

- ❖ The highest percentage of H_2 is reached at 49.6 and 49.7% and the highest percentage of CH_4 is obtained at 35.9 and 36.2% with K_2CO_3 and KOH respectively at 600°C.
- ❖ A comparison may be done for studied catalysts in the case of CGE, TOC removal and H_2 and CH_4 yields as: $Na_2CO_3 < NaOH < K_2CO_3 < KOH$.
- ❖ In catalytic runs CO_2 ratio is changed from 75-78 % levels to 20-26% with Na_2CO_3 and NaOH, from 74-76% levels to 11-12% levels with KOH and K_2CO_3 .

Raney Nickel

- ❖ CGE was 47.9 and accelerated from this level to within the range of 70.7-74.4 % at 500°C in the presence of catalyst

- ❖ The major gaseous products are CO₂, H₂ and CH₄ for all as expected while the distribution is varied depending on the catalyst type.
- ❖ The molar percentage of H₂ is found as highest with Activated Nickel as 48.1% and with Raney Nickel 4200 as 44.1% that is followed by other catalyst at slightly lower percentages.
- ❖ In terms of COD and TOC removal efficiencies, similar results were obtained. They decreased organic carbon content and oxygen demand successfully at a ratio about 90%.

Characterization analysis

- ❖ In characterization study, wastewater samples were analyzed for 136 chemicals, but only 5 were detected in the aqueous samples. The following: 7 aminoclonazepam, Diltiazem, Morphine, Codeine, and THCCOOH were detected in the raw wastewater by LC/MS-MS analysis equipment.
- ❖ After the hydrothermal treatment of raw wastewater in the absence of a catalyst and at 400, 500, and 600 °C, morphine was only detected in the aqueous product.
- ❖ As a conclusion hydrothermal gasification of alkaloid wastewater was achieved with high COD removal efficiencies in terms of treatment resulting high yields of hydrogen and methane as product.

REFERENCES

- Alturkmani A., 2013, Industrial Wastewater, Environmental Engineering Consultant Technical Report, Syria, 1-15.
- A.F. Aydın, H. Z. S., 2002, Biyolojik Proseslerle Arıtılmış Afyon Alkaloidleri Endüstrisi Atıksularının Fenton Oksidasyonu ile İleri Arıtımı, *İTÜ Dergisi/d Mühendislik*, **1**(1).
- A.F. Aydın, M. Altınbaş, M.F. Sevimli, I. O. and H. Z. S., Advanced treatment of high strength opium alkaloid industry effluents, *Water Science & Technology*, **46**(9), 323–330.
- Afif, E., Azadi, P., and Farnood, R., 2011, Catalytic hydrothermal gasification of activated sludge, *Applied Catalysis B: Environmental*, **105**(1–2), 136–43.
- Akgül, G., and Kruse, A., 2012, Influence of salts on the subcritical water-gas shift reaction, *The Journal of Supercritical Fluids*, **66**, 207–14.
- Akgül, G., Madenoğlu, T. G., Cengiz, N. Ü., Gökkaya, D., Sağlam, M., Yüksel, M., and Damascena, R., 2014, The Journal of Supercritical Fluids Hydrothermal gasification of Rosa Damascena residues : Gaseous and aqueous yields Gökc, **85**, 135–42.
- Akiya, N., and Savage, P. E., 2002, Roles of water for chemical reactions in high-temperature water, *Chemical Reviews*, **102**(8), 2725–50.
- Akizuki, M., Fujii, T., Hayashi, R., and Oshima, Y., 2014, Effects of water on reactions for waste treatment, organic synthesis, and bio-refinery in sub- and supercritical water, *Journal of Bioscience and Bioengineering*.

REFERENCES (CONTINUED)

- Ali Sinag, Andrea Kruse, and J. R., 2004, Influence of the Heating Rate and the Type of Catalyst on the Formation of Key Intermediates and on the Generation of Gases During Hydrolysis of Glucose in Supercritical Water in a Batch, *Ind. Eng. Chem. Res.*, **43**(Figure 1), 502–8.
- Ali Sinag, Kruse, A., and Schwarzkopf, V., 2003, Key Compounds of the Hydrolysis of Glucose in Supercritical Water in the Presence of K_2CO_3 , *Ind. Eng. Chem. Res.*, **42**, 3516–21.
- Aydin, A. F., Ersahin, M. E., Dereli, R. K., Sarikaya, H. Z., and Ozturk, I., 2010, Long-term anaerobic treatability studies on opium alkaloids industry effluents., *Journal of Environmental Science and Health. Part A, Toxic/Hazardous Substances & Environmental Engineering*, **45**(2), 192–200.
- Aytimur, G., and Atalay, S., 2004, Treatment of an Alkaloid Industry Wastewater by Biological Oxidation and/or Chemical Oxidation, *Energy Sources*, **26:7**(April 2013), 661–70.
- Azadi, P., Khan, S., Strobel, F., Azadi, F., and Farnood, R., 2012, Applied Catalysis B: Environmental Hydrogen production from cellulose, lignin, bark and model carbohydrates in supercritical water using nickel and ruthenium catalysts, *Applied Catalysis B, Environmental*, **117–118**, 330–8.
- Basu, P., and Mettanan, V., 2009, Biomass Gasification in Supercritical Water -- A Review, *International Journal of Chemical Reactor Engineering*.
- Breinl, J., 2015, Report of "Hydrothermal Gasification of HTL wastewater, Vienna-Austria.
- Brown, K., 2010, The Drying Of Foods Using Supercritical Carbon Dioxide, A Thesis Submitted to The University of Birmingham for the Degree of Doctor of Engineering.

REFERENCES (CONTINUED)

- Brunner, G., 2010, Applications of Supercritical Fluids, *Annual Review of Chemical and Biomolecular Engineering*, **1**(1), 321–42.
- Brunner, G., 2014, *Hydrothermal and Supercritical Water Processes*, Vol. 5, Supercritical Fluid Science and Technology, Elsevier.
- Bu, W., Dinjus, E., Ederer, H. J., Kruse, A., and Mas, C., 2002, Ionic reactions and pyrolysis of glycerol as competing reaction pathways in near- and supercritical water, *Journal of Supercritical Fluids*, **22**, 37–53.
- Buffoni, I. N., Pompeo, F., Santori, G. F., and Nichio, N. N., 2009, Nickel catalysts applied in steam reforming of glycerol for hydrogen production, *Catalysis Communications*, **10**(13), 1656–60.
- Bural, C. B., Demirer, G. N., Kantoğlu, O., and Dilek, F. B., 2010, Treatment of opium alkaloid containing wastewater in sequencing batch reactor (SBR) — Effect of gamma irradiation, *Radiation Physics and Chemistry*, **79**(4), 519–26.
- Cao, C., Guo, L., Chen, Y., Guo, S., and Lu, Y., 2011, Hydrogen production from supercritical water gasification of alkaline wheat straw pulping black liquor in continuous flow system, *International Journal of Hydrogen Energy*, **36**(21), 13528–35.
- Castello, D., Kruse, A., and Fiori, L., 2014, Supercritical water gasification of glucose/phenol mixtures as model compounds for ligno-cellulosic biomass, *Chemical Engineering Transactions*, **37**, 193–8.
- Cavit B. Bural, 2006, Aerobic Biological Treatment of Opium Alkaloid Wastewater - Effect Of Gamma Radiation And Fenton's Oxidation As Pretreatment, *The Graduate School Of Natural And Applied Sciences Of Middle East Technical University*.

REFERENCES (CONTINUED)

- Chakinala, A. G., Brilman, D. W. F., Van Swaaij, W. P. M., and Kersten, S. R. a, 2010, Catalytic and non-catalytic supercritical water gasification of microalgae and glycerol, *Industrial and Engineering Chemistry Research*, **49**(3), 1113–22.
- Cocero, M. J., Alonso, E., Tori, R., Vallelado, D., and Sanz, T., 2000, Supercritical Water Oxidation (SCWO) for Poly (ethylene terephthalate) (PET) Industry Effluents, *Ind. Eng. Chem. Res.*, **39**, 4652–7.
- Di Blasi, C., Branca, C., Galgano, A., Meier, D., Brodzinski, I., and Malmros, O., 2007, Supercritical gasification of wastewater from updraft wood gasifiers, *Biomass and Bioenergy*, **31**, 802–11.
- De Blasio, C., Lucca, G., Özdenkci, K., Mulas, M., Lundqvist, K., Koskinen, J., Santarelli, M., Westerlund, T., and Järvinen, M., 2016, A study on supercritical water gasification of black liquor conducted in stainless steel and nickel-chromium-molybdenum reactors, *Journal of Chemical Technology and Biotechnology*, **91**(10), 2664–78.
- D'Jesús, P., Boukis, N., Kraushaar-Czarnetzki, B., and Dinjus, E., 2006, Influence of Process Variables on Gasification of Corn Silage in Supercritical Water, *Industrial & Engineering Chemistry Research*, **45**(5), 1622–30.
- Demirbas, A., 2004, Hydrogen-rich gas from fruit shells via supercritical water extraction, *International Journal of Hydrogen Energy*, **29**, 1237–43.
- Dereli, R. K., Ersahin, M. E., Ozgun, H., Ozturk, I., and Aydin, A. F., 2010, Applicability of Anaerobic Digestion Model No. 1 (ADM1) for a specific industrial wastewater: Opium alkaloid effluents, *Chemical Engineering Journal*, **165**(1), 89–94.

REFERENCES (CONTINUED)

- Dietrich, M. J., Randall, T. L., and Canney, P. J., 1985, Wet air oxidation of hazardous organics in wastewater, *Environmental Progress*, **4**(3), 171–7.
- Dinjus, E., and Kruse, A., 2004, Hot compressed water—a suitable and sustainable solvent and reaction medium?, *Journal of Physics: Condensed Matter*.
- Du, X., Zhang, R., Gan, Z., and Bi, J., 2010, Treatment of high strength coking wastewater by supercritical water oxidation, *Fuel*.
- Esfandiari, N., 2015, Production of micro and nano particles of pharmaceutical by supercritical carbon dioxide, *The Journal of Supercritical Fluids*, **100**, 129–41.
- Falamarzian, S., Tavakoli, O., Zarghami, R., and Faramarzi, M. A., 2014, Catalytic hydrothermal treatment of pharmaceutical wastewater using sub- and supercritical water reactions, *The Journal of Supercritical Fluids*, **95**, 265–72.
- Gahr, F., Hermanutz, F., and Oppermann, W., 1994, Ozonation - An important technique to comply with new German laws for textile wastewater treatment, In *Water Science and Technology*, **30**, 255–63.
- García Jarana, M. B., Sánchez-Oneto, J., Portela, J. R., Nebot Sanz, E., and Martínez de la Ossa, E. J., 2008, Supercritical water gasification of industrial organic wastes, *Journal of Supercritical Fluids*, **46**, 329–34.
- General Directorate of Turkish Grain Board (TMO) Poppy And Alkaloid Affairs Department, 2013, Technical Report, Ankara - TURKEY.
- Girotra, P., Singh, S. K., and Nagpal, K., 2013, Supercritical fluid technology: a promising approach in pharmaceutical research., *Pharmaceutical development and technology*, **18**(1), 22–38.

REFERENCES (CONTINUED)

- Guo, L., Cao, C., and Lu, Y., 2010, Supercritical Water Gasification of Biomass and Organic Wastes, *Chapter 9, "Biomass" edited by Momba and Bux*, 113–8.
- Guo, S., Guo, L., Cao, C., Yin, J., Lu, Y., and Zhang, X., 2012, Hydrogen production from glycerol by supercritical water gasification in a continuous flow tubular reactor, *International Journal of Hydrogen Energy*, **37**(7), 5559–68.
- Guo, Y., Wang, S. Z., Xu, D. H., Gong, Y. M., Ma, H. H., and Tang, X. Y., 2010b, Review of catalytic supercritical water gasification for hydrogen production from biomass, **14**, 334–43.
- Guolin Jing, Mingming Luan, T. C., 2016, Progress of catalytic wet air oxidation technology, *Arabian Journal of Chemistry*, **9**, S1208–13.
- Gutiérrez Ortiz, F. J., Serrera, A., Galera, S., and Ollero, P., 2013, Experimental study of the supercritical water reforming of glycerol without the addition of a catalyst, *Energy*, **56**, 193–206.
- Güngören Madenoğlu, T., Sağlam, M., Yüksel, M., and Ballice, L., 2013, Simultaneous effect of temperature and pressure on catalytic hydrothermal gasification of glucose, *The Journal of Supercritical Fluids*, **73**, 151–60.
- Gürkök, T., Parmaksız İ., Boztepe G., ve K. E., 2010, Haşhaş (Papaver somniferum L.) Bitkisinde Alkaloid Biyosentez Mekanizması, *Biyoteknoloji Elektronik Dergisi.*, **1**(2), 31–45.
- H. Kınılı, 1994, The report of treatability studies of biological wastewater treatment plant effluent of TMO Opium Alkaloids Plant, Gebze, Türkiye.

REFERENCES (CONTINUED)

- Hakuta, Y., Hayashi, H., and Arai, K., 2003, Fine particle formation using supercritical fluids, *Current Opinion in Solid State and Materials Science*, **7**(4–5), 341–51.
- Hao, X. H., Guo, L. J., Mao, X., Zhang, X. M., and Chen, X. J., 2003, Hydrogen production from glucose used as a model compound of biomass gasified in supercritical water, **28**, 55–64.
- He, C., Chen, C.-L., Giannis, A., Yang, Y., and Wang, J.-Y., 2014, Hydrothermal gasification of sewage sludge and model compounds for renewable hydrogen production: A review, *Renewable and Sustainable Energy Reviews*, **39**, 1127–42.
- Holliday, R. L., King, J. W., and List, G. R., 1997, Hydrolysis of Vegetable Oils in Sub- and Supercritical Water, *Ind. Eng. Chem. Res.*, **36**(Edko 76), 932–5.
- I. G. Lee, 2010, Hydrogen Production by Supercritical Water Gasification of Wastewater from Food Waste Treatment Processes, In *18th World Hydrogen Energy Conference*, 425–9, Essen.
- INGB, N. D. T. R., 2014, Estimated World Requirements for 2015 - Statistics for
- Iwamura, H., Sato, T., Okada, M., Sue, K., and Hiaki, T., 2016, Organic Reactions in Sub- and Supercritical Water in the Absence of Any Added Catalyst(January 2014), 0–9.
- Kaçar, Y., Alpay, E., and Ceylan, V. K., 2003, Pretreatment of Afyon alcaolide factory's wastewater by wet air oxidation (WAO), *Water Research*, **37**(5), 1170–6.

REFERENCES (CONTINUED)

- Kalinichev, A. G., 1993, Molecular dynamics and self-diffusion in supercritical water, *Berichte der Bunsengesellschaft/Physical Chemistry Chemical Physics*, **97**(7), 872–6.
- Kang, K., Azargohar, R., Dalai, A. K., and Wang, H., 2016, Hydrogen production from lignin, cellulose and waste biomass via supercritical water gasification: Catalyst activity and process optimization study, *Energy Conversion and Management*, **117**, 528–37.
- Kazemi, N., Tavakoli, O., Seif, S., and Nahangi, M., 2015, High-strength distillery wastewater treatment using catalytic sub- and supercritical water, *The Journal of Supercritical Fluids*, **97**, 74–80.
- Kıpçak, E., and Akgün, M., 2017, Biofuel production from olive mill wastewater through its Ni/Al₂O₃ and Ru/Al₂O₃ catalyzed supercritical water gasification, *Renewable Energy*, 1–10.
- Klingler, D., and Vogel, H., 2010, Influence of process parameters on the hydrothermal decomposition and oxidation of glucose in sub- and supercritical water, *The Journal of Supercritical Fluids*, **55** (1), 259–70.
- Knez, Markočič, E., Leitgeb, M., Primožič, M., Knez Hrnčič, M., and Škerget, M., 2014, Industrial applications of supercritical fluids: A review, *Energy*, **77**, 235–43.
- Koyuncu, I., 2003, An advanced treatment of high-strength opium alkaloid processing industry wastewaters with membrane technology: pretreatment, fouling and retention characteristics of membranes, *Desalination*, **155** (3), 265–75.
- Krammer P. and Vogel H., 2000, Hydrolysis of esters in subcritical and supercritical water, *The Journal of Supercritical Fluids*, **16** (3), 189-206.

REFERENCES (CONTINUED)

- Kritzer, P., 2004, Corrosion in high-temperature and supercritical water and aqueous solutions: A review, *Journal of Supercritical Fluids*.
- Kronholm, J., Kuosmanen, T., Hartonen, K., and Riekkola, M., 2003, Destruction of PAH s from soil by using pressurized hot water extraction coupled with supercritical water oxidation, *Waste Management*, **23**, 253–60.
- Kruse, A., and Ebert, K. H., 1996, Chemical Reactions in Supercritical Water 1. Pyrolysis, **83(I)**, 80–3.
- Kruse, A., Meier, D., Rimbrecht, P., and Schacht, M., 2000, Gasification of Pyrocatechol in Supercritical Water in the Presence of Potassium Hydroxide, *Industrial & Engineering Chemistry Research*, **39**, 4842–8.
- Kruse, A., and Dinjus, E., 2007, Hot compressed water as reaction medium and reactant 2 . Degradation reactions, **41**, 361–79.
- Kruse, A., 2008, Supercritical water gasification, *Biofuels, Bioproducts and Biorefining(2)*, 415–37.
- Kuhlmann, B., Arnett, E. M., and Siskin, M., 1994, Classical Organic-Reactions in Pure Superheated Water, *Journal of Organic Chemistry*, **59(11)**, 3098–101.
- Kunukcu, Y. K., and Wiesmann, U., 2004, Activated Sludge Treatment and Anaerobic Digestion of Opium Alkaloid Factory, *World Water Congress 2004*.
- Larsen, U., Pierobon, L., Haglind, F., and Gabriellii, C., 2013, Design and optimisation of organic Rankine cycles for waste heat recovery in marine applications using the principles of natural selection, *Energy*, **55**, 803–12.

REFERENCES (CONTINUED)

- Lee, I., 2010, Hydrogen Production by Supercritical Water Gasification of Wastewater from Food Waste Treatment Processes, *18th World Hydrogen Energy Conference*, **78**, 425–9.
- Lee, I.-G., Kim, M.-S., and Ihm, S.-K., 2002, Gasification of Glucose in Supercritical Water, *Industrial & Engineering Chemistry Research*, **41**(5), 1182–8.
- Lee, I. G., and Ihm, S. K., 2010, Hydrogen Production by SCWG Treatment of Wastewater from Amino Acid Production Process, *Industrial & Engineering Chemistry Research*, **49**, 10974–80.
- Liao, S.-K., and Chang, P.-S., 2012, “Special Issue—Supercritical Fluids” Literatures on Dyeing Technique of Supercritical Fluid Carbon Dioxide, *American Journal of Analytical Chemistry*, **3**(12), 923–30.
- Long, J. J., Xu, H. M., Cui, C. L., Wei, X. C., Chen, F., and Cheng, A. K., 2014, A novel plant for fabric rope dyeing in supercritical carbon dioxide and its cleaner production, *Journal of Cleaner Production*, **65**, 574–82.
- Lu, Y., Guo, L., Zhang, X., and Yan, Q., 2007, Thermodynamic modeling and analysis of biomass gasification for hydrogen production in supercritical water, *Chemical Engineering Journal*, **131**(1–3), 233–44.
- Lu, Y., Guo, L., Zhang, X., and Ji, C., 2011, Hydrogen production by supercritical water gasification of biomass : Explore the way to maximum hydrogen yield and high carbon gasification efficiency, *International Journal of Hydrogen Energy*, **37**(4), 3177–85.
- Lu, Y. J., Guo, L. J., Ji, C. M., Zhang, X. M., Hao, X. H., and Yan, Q. H., 2006, Hydrogen production by biomass gasification in supercritical water : A parametric study, *International Journal of Hydrogen Energy*, **31**, 822–31.

REFERENCES (CONTINUED)

- M. Modell, R.C. Reid, S.I. Amin, Gasification process, *US Patent*, **4**, 113,446 (1978).
- Madenoglu, T. G., Kurt, S., Sađlam, M., Yüksel, M., Gökkaya, D., and Ballice, L., 2012, Hydrogen production from some agricultural residues by catalytic subcritical and supercritical water gasification, *The Journal of Supercritical Fluids*, **67**, 22–8.
- Madenoglu, 2011, Investigation of Hydrogen and/or Methane Production From Lignocellulosic Wet Biomasses By Supercritical Water Gasification, *Doctorate Thesis, Ege University, Graduate School of Natural and Applied Science*.
- Madenoglu, T. G., Üremek, N. C., Sađlam, M., Yüksel, M., and Ballice, L., 2015, Catalytic Gasification of Mannose for Hydrogen Production in Near- and Super-Critical Water, *The Journal of Supercritical Fluids*.
- Minowa, T., Zhen, F., and Ogi, T., 1998, Cellulose decomposition in hot-compressed water with alkali or nickel catalyst, **13**, 253–9.
- Mishra, V. S., Mahajani, V. V., and Joshi, J. B., 1995, Wet Air Oxidation, *Industrial & Engineering Chemistry Research*, **34** (1), 2–48.
- Muangrat, R., Onwudili, J. A., and Williams, P. T., 2010, Applied Catalysis B : Environmental Influence of alkali catalysts on the production of hydrogen-rich gas from the hydrothermal gasification of food processing waste, “*Applied Catalysis B, Environmental*,” **100** (3–4), 440–9.
- Nagai, Y., Wakai, C., Matubayasi, N., and Nakahara, M., 2003, Noncatalytic Cannizzaro-type reaction of acetaldehyde in supercritical water, *Chemistry Letters*, **32**(3), 310–1.

REFERENCES (CONTINUED)

- Nath, H., and Sahoo, A., 2014, a Study on the Characterization of Red Mud, *International Journal on Applied Bio-Engineering*, **8** (1), 1–4.
- Ogunsola, O. M., 2000, Decomposition of isoquinoline and quinoline by supercritical water, *Journal of Hazardous Materials*, **74** (3), 187–95.
- Onwudili, J. A., and Williams, P. T., 2013, Enhanced methane and hydrogen yields from catalytic supercritical water gasification of pine wood sawdust via pre-processing in subcritical water, *RSC Advances*, **3** (30), 12432.
- Önmez, H., 2007, Papaver somniferum Bitkisinden Elde Edilen Alkaloidlerin Ekstraksiyonunda Kullanılan, Çözücü ve Metodların Karşılaştırılması, Yüksek Lisans Tezi, *Selçuk University, Graduate School of Natural and Applied Science*.
- Özcan, A. S., Clifford, A. A., Bartle, K. D., and Lewis, D. M., 1998, Dyeing of cotton fibres with disperse dyes in supercritical carbon dioxide, *Dyes and Pigments*, **36**(2), 103–10.
- Özdemir, R. T., 2006, Anaerobic Treatment of Opium Alkaloid Wastewater and Effect of Gamma-Rays on Anaerobic Treatment, Doctorate Thesis, *Middle East Technical University, Graduate School of Natural and Applied Science*.
- Park, J., Kang, E., Son, S. U., Park, H. M., Lee, M. K., Kim, J., Kim, K. W., Noh, H. J., Park, J. H., Bae, C. J., Park, J. G., and Hyeon, T., 2005, Monodisperse nanoparticles of Ni and NiO: Synthesis, characterization, self-assembled superlattices, and catalytic applications in the Suzuki coupling reaction, *Advanced Materials*, **17**(4), 429–34.
- Park, K. C., and Tomiyasu, H., 2003, Gasification reaction of organic compounds catalyzed by RuO₂ in supercritical water., *Chemical communications (Cambridge, England)*(6), 694–5.

REFERENCES (CONTINUED)

- Penninger, J. M. L., Kersten, R. J. A., and Baur, H. C. L., 1999, Reactions of diphenylether in supercritical water - Mechanism and kinetics, *Journal of Supercritical Fluids*, **16**(2), 119–32.
- Pioro, I., and Mokry, S., 2011, Thermophysical Properties at Critical and Supercritical Conditions, *Heat Transfer - Theoretical Analysis, Experimental Investigations and Industrial Systems*, 573–92.
- Reddy, S. N., Nanda, S., Dalai, A. K., and Kozinski, J. A., 2014, Supercritical water gasification of biomass for hydrogen production, *International Journal of Hydrogen Energy*, **39** 6912-6926.
- Ribeiro, D. V., Labrincha, J. A., and Morelli, M. R., 2012, Effect of the addition of red mud on the corrosion parameters of reinforced concrete, *Cement and Concrete Research*, **42**(1), 124–33.
- Schmieder, H., Abeln, J., Boukis, N., Dinjus, E., Kruse, A., Kluth, M., Petrich, G., Sadri, E., and Schacht, M., 2000, Hydrothermal gasification of biomass and organic wastes, *Journal of Supercritical Fluids*, **17**(2), 145–53.
- Sevimli, M. F., Aydin, A. F., Sarikaya, H. Z., and Ozturk, I., 1999, Characterization and treatment of effluent from opium alkaloid processing wastewater, *Water Science and Technology*, **40**(1), 23–30.
- Sevimli, M. F., Aydin, A. F., Ozturk, I., and Sarikaya, H. Z., 2000, Evaluation of the alternative treatment processes to upgrade an Opium alkaloid wastewater treatment plant, *Water Science and Technology*, **41**(1), 223–30.
- Shanableh, A., 1996, Supercritical water-A useful medium for waste destruction, *Arab Gulf Journal of Scientific Research*, **14**(3), 543–56.

REFERENCES (CONTINUED)

- Shin, Y. H., Shin, N. C., Veriansyah, B., Kim, J., and Lee, Y. W., 2009, Supercritical water oxidation of wastewater from acrylonitrile manufacturing plant, *Journal of Hazardous Materials*, **163**(2–3), 1142–7.
- Sinag, A., Kruse, A., and Maniam, P., 2012, Hydrothermal conversion of biomass and different model compounds, *The Journal of Supercritical Fluids*, **71**, 80–5.
- Söğüt, O. Ö., and Akgün, M., 2011, The Journal of Supercritical Fluids Hydrothermal gasification of olive mill wastewater as a biomass source in supercritical water, *Journal of Supercritical Fluids*, **57**, 50–7.
- Sricharoenchaikul, V., 2009, Assessment of black liquor gasification in supercritical water, *Bioresource Technology*, **100**(2), 638–43.
- Susanti, R. F., Dianningrum, L. W., Yum, T., Kim, Y., Lee, B. G., and Kim, J., 2012, High-yield hydrogen production from glucose by supercritical water gasification without added catalyst, *International Journal of Hydrogen Energy*, **37**(16), 11677–90.
- Susanti, R. F., Dianningrum, L. W., Yum, T., Kim, Y., Lee, Y. W., and Kim, J., 2014, High-yield hydrogen production by supercritical water gasification of various feedstocks: Alcohols, glucose, glycerol and long-chain alkanes, *Chemical Engineering Research and Design*, **92**(10), 1834–44.
- Tan, K. T., and Lee, K. T., 2011, A review on supercritical fluids (SCF) technology in sustainable biodiesel production: Potential and challenges, *Renewable and Sustainable Energy Reviews*, **15**(5), 2452–6.
- Tsujino, Y., Wakai, C., Matubayashi, N., and Nakahara, M., 1999, Noncatalytic Cannizzaro-type Reaction of Formaldehyde in Hot Water, *Chemistry Letters*, **28**(4), 287–8.

REFERENCES (CONTINUED)

- Turkish Atomic Energy Authority, 2011, Türkiye atom enerjisi kurumu.
- Tülay Güngören, Mehmet Sağlam, Mithat Yüksel, Hakan Madenoğlu, Rahim İşler, İsmail H. Metecan, Ahmet R. Özkan, and L. B., 2007, Near-Critical and Supercritical Fluid Extraction of Industrial Sewage Sludge, *Ind. Eng. Chem. Res.*, 1051–7.
- Uremek Cengiz, N., Eren, S., Sağlam, M., Yüksel, M., and Ballice, L., 2016, Influence of temperature and pressure on hydrogen and methane production in the hydrothermal gasification of wood residues, *Journal of Supercritical Fluids*, **107**, 243–9.
- Vazquez da Silva, M., 2010, Supercritical fluids and its applications, *Current Trends in Chemical Engineering*, 293–312.
- Watanabe, M., Inomata, H., Osada, M., Sato, T., Adschiri, T., and Arai, K., 2003, Catalytic effects of NaOH and ZrO₂ for partial oxidative gasification of n-hexadecane and lignin in supercritical water, *Fuel*, **82**(5), 545–52.
- Water Pollution Control Regulation, 2004, Official Newspaper, Ankara-TURKEY.
- Wen, D., Jiang, H., and Zhang, K., 2009, Supercritical fluids technology for clean biofuel production, *Progress in Natural Science*, **19**(3), 273–84.
- Xu, X., Antal, M. J., and Anderson, D. G. M., 1997, Mechanism and Temperature-Dependent Kinetics of the Dehydration of tert-Butyl Alcohol in Hot Compressed Liquid Water, *Industrial & Engineering Chemistry Research*, **36**(1), 23–41.
- Yan, B., Wei, C. H., Hu, C. S., Xie, C., and Wu, J. Z., 2007, Hydrogen generation from polyvinyl alcohol-contaminated wastewater by a process of supercritical water gasification, *Journal of Environmental Sciences*, **19**, 1424–9.

REFERENCES (CONTINUED)

- Yan, Q., Guo, L., and Lu, Y., 2006, Thermodynamic analysis of hydrogen production from biomass gasification in supercritical water, *Energy Conversion and Management*, **47**(11–12), 1515–28.
- Yanik, J., Ebale, S., Kruse, A., Saglam, M., and Yu, M., 2007, Biomass gasification in supercritical water : Part 1 . Effect of the nature of biomass, *Fuel*, **86**, 2410–5.
- Yanik, J., Ebale, S., Kruse, A., Saglam, M., and Yu, M., 2008, Biomass gasification in supercritical water : II . Effect of catalyst, *international journal of hydrogen energy*, **33**, 4520–6.
- Yoshida, T., and Matsumura, Y., 2001, Gasification of Cellulose , Xylan , and Lignin Mixtures in Supercritical Water, *Industrial & Engineering Chemistry Research*, 5469–74.
- Zhiyong, Y., and Xiuyi, T., 2014, Hydrogen generation from oily wastewater via supercritical water gasification (SCWG), *Journal of Industrial and Engineering Chemistry*, **23**, 44–9.

CURRICULUM VITAE

GENERAL INFORMATION

Name-Surname : Nihal (ÜREMEK) CENGİZ
Date and Place of Birth : 22.05.1984 - İzmir
Office Phone : 0 232 3881489 **Mobile:** 0 5357049600
e-maiş : nihal.cengiz@ege.edu.tr **Fax** : 0 232 3887776

EDUCATION

Period	Degree	University	Field
2011-	PhD.	Ege University	Chemical Engineering
2009-2011	MsC.	Ege University	Chemical Engineering
2002-2006	Bachelor	Ege University	Chemical Engineering

ACADEMIC AND PROFESSIONAL EXPERIENCE

Period	Position	Work place
2007 / 2008	Chemical Engineer	Denizli Sanayi Gazları Üretim ve Dolun Tesisi
2008 / 2009	Research Project Student	Ege University, Chemical Engineering Dep.
Sep-Dec 2009	MSc. Student	Institute of Chemical Technology, Prague.
2010/2011	Research Project Student	Ege University, Chemical Engineering
2011-	Research Assistant	Ege University, Chemical Engineering

SCI ARTICLES

Nihal Üremek Cengiz, Mehmet Sağlam, Mithat Yüksel, Levent Ballice, Treatment of High-Strength Opium Alkaloid Wastewater by Hydrothermal Gasification, *Journal of Supercritical Fluids*, *Journal of Supercritical Fluids*, (130) 301-310 (2017).

Murat Sert, Dilek Selvi Gökkaya, Nihal Cengiz, Levent Ballice, Mithat Yüksel, Mehmet Sağlam, Hydrogen production from olive-pomace by catalytic hydrothermal gasification, *Journal of the Taiwan Institute of Chemical Engineers*, available online 11 December 2017.

Nihal Cengiz, Seda Eren, Mehmet Sağlam, Mithat Yüksel, Levent Ballice, Influence of Temperature and Pressure on Hydrogen and Methane Production in Hydrothermal Gasification of Wood Residues, *Journal of Supercritical Fluids*, 107, 243–249 (2016)

Tülay Güngören Madenoğlu, Nihal Cengiz Üremek, Mehmet Sağlam, Mithat Yüksel, Levent Ballice, Catalytic Gasification of Mannose for Hydrogen Production in Near- and Supercritical Water, *Journal of Supercritical Fluids*, 107, 153-162 (2016)

Nihal Cengiz, Güray Yıldız, Murat Sert, Dilek Gökkaya Mehmet Sağlam, Mithat Yüksel, Levent Ballice, Supercritical Water Gasification of Biodiesel By-Product Crude Glycerol In The Presence of Phosphate Based Catalysts, *International Journal of Hydrogen Energy*, 40, 14806-14815 (2015)

Gökçen Akgül, Tülay G Madenoğlu, Nihal Ü Cengiz; Mehmet Sağlam, Mithat Yüksel, Hydrothermal Gasification of Rosa Damascena Residues. Gaseous and aqueous yields, *Journal of Supercritical Fluids*, 85, 135–142 (2014)

ARTICLES SUBMITTED FOR PUBLICATION

Nihal Üremek Cengiz, Mehmet Sağlam, Mithat Yüksel, Levent Ballice, Treatment of Opium Alkaloid Wastewater via Hydrothermal Gasification, Water Science and Technology, Under Review

OTHER ARTICLES PUBLISHED IN INTERNATIONAL PEER-REVIEWED JOURNAL

Nihal Cengiz Üremek, Mehmet Sağlam, Mithat Yüksel, Levent Ballice, Application Of Hydrothermal Gasification Method In The Treatment Of Wastewater Generated From Afyonkarahisar-Alkaloid Plant, Journal of the Turkish Chemical Society, Section B, (2016)

N. Cengiz, T. Madenoğlu M. Sağlam, M.Yüksel, L. Ballice, Hydrothermal Gasification of Corn-cob Hemicellulose to Produce Hydrogen and Methane, The international Conference on Environmental Science and Technology, Journal of Selçuk University Natural and Applied Science, ICOEST Conf. (Special Issue-1) 705-714 (2013)

D. Selvi Gökkaya, M. Yüksel, M. Sağlam, T. Güngören Madenoğlu, N. Cengiz, T. Çokkuvvetli, and L. Ballice, Wine Grape Residues Gasification in Supercritical Water, World Academy of Science, Engineering and Technology, International Journal of Chemical, Molecular, Nuclear, Materials and Metallurgical Engineering Vol:7, No:5, 2013 p 245-250.

PROCEEDINGS**Full Papers Submitted To International Scientific Meetings - Oral Presentations and Published in Proceedings Book**

Nihal Üremek Cengiz Mehmet Sağlam, Mithat Yüksel, Levent Ballice, Supercritical water gasification of opium alkaloid wastewater with KOH and NaOH catalysts, International Porous & Powder Materials, September 12-15, 2017, Kuşadası / Turkey.

Nihal Üremek Cengiz, Tülay G. Madenoğlu, Mehmet Sağlam, Mithat Yüksel, Levent Ballice, Supercritical Water Gasification of Biodiesel By-Product Crude Glycerin In The Presence Of KOH Catalyst, 6th International Ege Energy Symposium & Exhibition, June 28-30, 2012, Izmir, Turkey.

Nihal Üremek Cengiz Mehmet Sağlam, Mithat Yüksel, Levent Ballice, Catalytic Treatment of Opium Alkaloid Wastewater by Utilizing in Energy (CH_4/H_2) Production via Hydrothermal Gasification, EurAsia Waste Management Symposium, 2-4 Mayıs 2016 İstanbul /Turkey.

Nihal Üremek Cengiz Mehmet Sağlam, Mithat Yüksel, Levent Ballice, Supercritical Water Gasification of Biodiesel By-Product Crude Glycerol In The Presence of Phosphate Based Catalysts, The Second International Conference on Water, Energy and Environment, September 21-24, 2013, Kuşadası / Turkey.

Abstracts Submitted To International Scientific Meetings - Oral Presentations and Published in Proceedings Book

Nihal Üremek Cengiz Mehmet Sağlam, Mithat Yüksel, Levent Ballice, Treatment of Industrial Wastewaters by Utilizing in Energy (CH_4/H_2) Production via Hydrothermal Gasification, GCSTI, September 30-October 3, 2015, Çeşme /İzmir/TURKEY

Full Papers Submitted To International Scientific Meetings - Poster Presentations and Published in Proceedings Book

Nihal Ü. Cengiz, Tülay G. Madenoğlu, Murat Sert, Tuğçe Çokkuvvetli, Mehmet Sağlam, Mithat Yüksel, Levent Ballice, Supercritical Water Gasification of Mannose as a Model Compound for Hemicellulose, 6th International Ege Energy Symposium & Exhibition, June 28-30, 2012, Izmir, Turkey

N. Cengiz, T. Madenoğlu M. Sağlam, M.Yüksel, L. Ballice, Hydrothermal Gasification of Corn-cob Hemicellulose to Produce Hydrogen and Methane, The international Conference on Environmental Science and Technology – ICOEST'2013 – Cappadocia, Nevsehir, Turkey, June 18 - 21, 2013.

Abstracts Submitted To International Scientific Meetings - Poster Presentations and Published in Proceedings Book

Nihal Üremek Cengiz*, Seda Eren, A. Tuğçe Çokkuvvetli, Murat Sert, Dilek Gökkaya, Mehmet Sağlam, Mithat Yüksel, Levent Ballice, Hydrothermal Gasification of Galactose In The Presence of KOH, GCSTI, September 30-October 3, 2015 Çeşme / İzmir/TURKEY.

Full Papers Submitted To National Scientific Meetings - Oral Presentations and Published in Proceedings Book

Nihal Üremek Cengiz Mehmet Sağlam, Mithat Yüksel, Levent Ballice, Afyonkarahisar Alkaloid Fabrikası Atık Suyunun Arıtılmasında Katalitik Hidrotermal Gazlaştırma Yönteminin Uygulanması, Ulusal Kimya Mühendisliği Kongresi, UKMK 2016, İzmir.

Nihal C. Üremek, Tülay G. Madenoğlu, Mehmet Sağlam, Mithat Yüksel, Levent Ballice Hemiselüloz Model Bileşiği Mannozyun K_2CO_3 ve aktif Karbon Katalizörleri Varlığında Süperkritik Su Ortamında Gazlaştırılması, 10'ncü Ulusal Kimya Mühendisliği Kongresi, UKMK-10 Koç Üniversitesi, İstanbul-Türkiye, 3-6 Eylül 2012.

Ayşe Tuğçe Çokkuvvetli, Tülay G. Madenoğlu, Nihal C. Üremek, Mehmet Sağlam, Mithat Yüksel, Levent Ballice, Kavak Ağacı Talaşının Suyun Kritikaltı/Kritiküstü Koşullarda Gazlaştırmasıyla H_2 ve CH_4 üretimi, 10'ncü Ulusal Kimya Mühendisliği Kongresi, UKMK-10, Koç Üniversitesi, İstanbul-Türkiye, 3-6 Eylül 2012.

Abstracts Submitted To National Scientific Meetings - Oral Presentations and Published in Proceedings Book

Nihal Üremek Cengiz Mehmet Sağlam, Mithat Yüksel, Levent Ballice, Biyodizel Yan Ürünü Gliserinin Süperkritik Su Yöntemiyle Gazlaştırılması, Yenilenebilir Enerji Kaynağı Biyokütle Çalıştayı ve Sergisi, 7-8 Ekim 2011, Bursa, Türkiye.

Full Paper Submitted To National Scientific Meetings – Poster Presentations and Published in Proceedings Book

Seda Eren, T. Tülay G. Madenoğlu, Nihal C. Üremek, Mehmet Sağlam, Mithat Yüksel, Levent Ballice, Çam Ağacı Talaşının Kritikaltı-Kritiküstü Su Gazlaştırmasında Rutenyum Emdirilmiş Aktif Karbon Katalizörünün Hidrojen ve Metan Oluşumuna Etkisinin İncelenmesi, 10'ncu Ulusal Kimya Mühendisliği Kongresi, UKMK-10, Koç Üniversitesi, İstanbul-Türkiye, 3-6 Eylül 2012

Abstracts Submitted To National Scientific Meetings – Poster Presentations and Published in Proceedings Book

Gökçen Akgül, Mehmet Sağlam, Mithat Yüksel, Nihal Üremek Cengiz, Tülay G. Madenoğlu, Dilek Gökkaya, İbrahim Üçgül, Isparta Gül Yağı Üretim Atıklarının, Hidrotermal Gazlaştırılması, Yenilenebilir Enerji Kaynağı Biyokütle Çalıştayı ve Sergisi, 7-8 Ekim 2011, Bursa, Türkiye.

T.G. Madenoğlu, N. J. Falizi, M. Soylu, N.Ü. Cengiz, Y. Kukul, K. Meriç, E. Özçakal, N. Kabay, L. Ballice, S. Ötleş, T.Pek, M.Yüksel, M.Sağlam: MBR Yöntemiyle Artırılmış Atık Su Kullanılarak Yetiştirilen Aspir Bitkisinden Yağ ve Biyodizel Üretiminin İncelenmesi, Ulusal Kimya Mühendisliği Kongresi, UKMK 2016, İzmir

APPENDICES

Appendix I Carbon Gasification Efficiency (CGE, %) and Gaseous Product Yield Calculations

Appendix II Experimental results tables

Appendix III HPLC Results of Wastewater Samples in BIORAD and Macherey Nagel columns.



APPENDIX I

CARBON GASIFICATION EFFICIENCY (CGE) AND GASEOUS PRODUCT YIELD CALCULATIONS

A sample Calculation for the Experiment with the code of AF- A1- R1 (in the presence of A1 catalyst and first repetition) Carbon gasification efficiency (CGE,

$$\%) = \frac{\sum_i n_i C_i \frac{PV_{gas}}{RT} M}{V_{feed} TOC_{ww}} \times 100$$

The amount of organic carbon fed to the reactor ($V_{feed} * TOC_{ww}$):

$$TOC = 11500 \text{ ppm} = 11500 \text{ mg/L}; \quad V_{feed} = 15 \text{ mL}$$

$$15 \text{ mL feed} \times 11500 \frac{\text{mg}}{\text{L}} \times \frac{1 \text{ L}}{1000 \text{ mL}} = 172.5 \text{ mg feed to the reactor}$$

$$\text{Total organic carbon in the feed} = 172.5 \text{ mg} * \frac{1 \text{ g}}{1000 \text{ mg}} = 0.173 \text{ g}$$

Concentration of component 'i' in the gas product (vol. %) C_i values are taken from GC analysis results and are shown in the Table A1-1.

Table A1-1 GC analysis results and calculation for gaseous product of A1 catalyst

Molecules	C_i	C_i without N₂	m mol	n_i	m mol C
CH ₄	30.95	32.78	6.14	1	6.14
C ₂ H ₆	2.05	2.17	0.41	2	0.82
C ₂ H ₄	0.30	0.32	0.06	2	0.12
C ₃ H ₈	0.87	0.93	0.17	3	0.52
C ₄ H ₁₀	0.08	0.09	0.02	4	0.07
CO ₂	23.70	25.10	4.70	1	4.70
N ₂	5.60	-	-	-	-
CO	0.50	0.53	0.10	1	0.10
H ₂	35.95	38.08	7.13	-	-
Total	100.01	100.00	18.73		12.46

Calculation of mol % of CH₄ in the mixture without N₂ :

$$\text{Total amount (\%)} - \text{mol \% N}_2 = 100 - 5.60 = 94.4 \%$$

$$\text{Mol \% CH}_4 \text{ in the mixture without N}_2 = 30.95 \times \frac{100}{94.4} = 32.8 \%$$

Calculations of mol % of C₂H₆ in the mixture without N₂ :

$$\text{Mol \% of C}_2\text{H}_6 \text{ in the mixture without N}_2 = 2.05 \times \frac{100}{94.4} = 2.17 \%$$

Molar percentage values of the other compounds in the mixture without N₂ are calculated in the same way and shown in Table A1-1

Conditions of the gaseous product mixture taken from reactor:

$$P = 1 \text{ atm}$$

$$T = 298 \text{ K}$$

$$R = 0.082 \text{ (L.atm)/(mol.K)}$$

Note: The product gas mixture is assumed as ideal gas. Total gas amount is calculated from ideal gas equation:

$$P \times V = n \times R \times T$$

$$n = \frac{1 \text{ atm} \times 0.33 \text{ L}}{0.08206 \frac{\text{L.atm}}{\text{mol.K}} \times 298 \text{ K}} = 0.0135 \text{ mol}$$

Conversions from % mol to mmol:

For CH₄:

$$0.0135 \text{ mol} \times \frac{32.8 \text{ (mol \% no N}_2\text{)}}{100} \times \frac{1000 \text{ mmol}}{1 \text{ mol}} = 4.41 \text{ mmol}$$

For C₂H₆:

$$0.0135 \text{ mol} \times \frac{2.17}{100} \times \frac{1000 \text{ mmol}}{1 \text{ mol}} = 0.29 \text{ mmol}$$

Amounts of the other produced gases in the mixture in unit of mmol are calculated similarly and shown in Table A1-1.

Carbon contents in the molecules (mmol C) :

For CH₄:

$$4.41 \text{ mmol} \times 1 \text{ Carbon atom} = 4.41 \text{ mmol C}$$

For C₂H₆:

$$0.29 \times 2 \text{ Carbon atoms} = 0.58 \text{ mmol C}$$

Organic gas yield calculations in different units:

Volume of waste water fed to the reactor = 0.015 L

$$\text{CH}_4: \quad 4.41 \text{ mmol} \times \frac{1}{0.015 \text{ L waste water}} = 294.2 \frac{\text{mmol}}{\text{Lww}} \text{ for CH}_4$$

$$\left(4.41 \text{ mmol} \times \frac{16 \text{ g}}{\text{mol methane}} \right) \div (0.015 \text{ L feed ww} \times 1000) \\ = 4.71 \text{ g gas /Lww}$$

$$(4.41 \text{ mmol}) \div \left(0.173 \text{ g total organic carbon} \times \frac{1}{1000} \right) \\ = 25.5 \frac{\text{mmol CH}_4}{\text{g Organic Carbon}} = 25.5 \frac{\text{mol CH}_4}{\text{kg Organic Carbon}}$$

This calculation is done for every species.

Table A-2. Organic gas yield calculations in various units

Molecules	m mol /L ww	g gas/L ww	mol gas/kg C biomass	mg C
CH ₄	294.23	4.71	25.55	52.96
C ₂ H ₆	19.49	0.55	1.69	7.02
C ₂ H ₄	2.86	0.09	0.25	1.03
C ₃ H ₈	8.31	0.35	0.72	4.49
C ₄ H ₁₀	0.79	0.04	0.07	0.57
CO ₂	225.31	9.91	19.59	40.55
N ₂	-	-	-	-
CO	4.75	0.13	0.41	0.86
H ₂	341.76	0.68	29.72	-
Total	897.50	16.46	78.04	107.47

Firstly, organic carbon contents of *each product gas component* are determined by using the formula given below:

Amount of C in product gas molecule = Amount of compound in product gas in mmol x Number of C atoms in the molecule x Molecular weight of Carbon atom

Amount of C in product gas molecule:

$$\left(4.41 \text{ mmol } CH_4 \times \frac{1 \text{ mol}}{1000 \text{ mmol}} \times \frac{1 \text{ mol } C}{1 \text{ mol } CH_4} \times \frac{12 \text{ g } C}{1 \text{ mol } C} \times \frac{1000 \text{ mg}}{1 \text{ g}} \right) \\ = 52.9 \text{ mg } C \text{ in } CH_4$$

This calculations are done for every species in the product gas composition and finally a summation is obtained. The ratio of this summation to the organic carbon fed to the reactor gives the organic gas yield (CGE):

$$\text{Total Amount of C in product gas molecule} = \sum_i n_i C_i \frac{PV_{gas}}{RT} M$$

$$\text{CGE, \%} = \frac{\sum_i n_i C_i \frac{PV_{gas}}{RT} M}{V_{feed} TOC_{ww}} \times 100$$

$$= \frac{\text{Total amount of C in the product gas}}{\text{Organic C amount fed to the reactor}} = \frac{107.5 \text{ mg}}{0.173 \text{ g}} \times \frac{1 \text{ g}}{1000 \text{ mg}} * 100 \\ = 62.2 \%$$

CARBON LIQUEFICATION EFFICIENCY (CLE) CALCULATIONS

$$\text{Carbon liquefaction efficiency (CLE, \%)} = \frac{TOC_{aq} V_{aq}}{V_{feed} TOC_{ww}} \times 100$$

$$V_{feed} = 15 \text{ mL}$$

$V_{aq} = 100 \text{ mL}$ (total volume after washing the reactor with pure water including aqueous product and pure water, diluted form)

$$TOC_{ww} = 11500 \text{ ppm}$$

$$TOC_{aq} = 315 \text{ ppm (measurement of the diluted product)}$$

$$\begin{aligned}\text{Carbon amount in the aqueous product} &= TOC_{aq} V_{aq} = \frac{315.6 \text{ ppm} \times 100 \text{ mL liquid}}{15 \text{ mL feed ww}} \\ &= 2100 \text{ mg C in liquid}\end{aligned}$$

$$\text{CLE, \%} = \frac{\text{mg C in the liquid product}}{\text{mg organic carbon fed to the reactor}} \times 100 = \frac{2100}{11500} \times 100 = 18.3 \%$$

RESIDUE CALCULATION

$$\text{Residue (RE, \%)} = \frac{TOC_R \kappa}{V_{feed} TOC_{ww}} \times 100$$

$\kappa = 0.02 \text{ g} = 20 \text{ mg}$ (residue on filter paper weighed after drying in oven for 1 day)

SSM-TOC result of residue in this experiment, $TOC_{\kappa} = 1.452 \%$

$$\text{Carbon amount in residue} = \kappa TOC_{\kappa} = 0.02 \times \frac{1.452}{100} = 0.029 \text{ g Carbon}$$

$$\text{Residue (RE, \%)} = \frac{\text{mg C in the residue}}{\text{mg organic carbon fed to the reactor}} = \frac{0.029 \text{ g C}}{0.173 \text{ g}} \times 100 = 16.7 \%$$

TOC REMOVAL EFFICENCY CALCULATION, $TOC_{RE} \%$

$$\text{Total Organic Carbon Removal Efficiency (TOC}_{RE}, \%) = \frac{TOC_{ww} - TOC_{aq}}{TOC_{ww}} \times 100$$

$$TOC_{aq} = TOC_{avg} = TOC, avg * \text{Dilution factor} = 315 \text{ ppm} * 6.7 = 2100 \text{ ppm}$$

$$TOC_{RE} \% = \frac{11500 - 2100}{11500} \times 100 = 82$$

COD REMOVAL EFFICENCY CALCULATION, $COD_{RE} \%$

$$\begin{aligned}\text{Chemical Oxygen Demand Removal Efficiency (COD}_{RE}, \%) &= \\ &= \frac{COD_{ww} - COD_{aq}}{COD_{ww}} \times 100\end{aligned}$$

$$COD_{aq} = COD_{avg} = COD, avg * \text{Dilution factor} = 1126 \text{ ppm} * 5 = 5630 \text{ ppm}$$

$$COD_{RE} \% = \frac{32050 - 5630}{32050} \times 100 = 82.4 \%$$

APPENDIX II

Experiment Number	1	2	3	4
Experiment Code	AF-T3	AF-T4	AF-T5	AF-T6
Reaction Temperature, °C	300	400	500	600
Reaction Pressure, atm	80	240	365	440
Catalyst type	-	-	-	
Catalyst, g	-	-	-	-
Volume of wastewater, mL	15	15	15	15
Wastewater TOC, mg/L	11500	11500	11500	11500
Wastewater COD, mg O₂/L	32050	32050	32050	32050

Gaseous product composition, % mol

CH₄	0.4	11.5	28.8	29.5
H₂	3.8	37.1	34.9	36.2
CO₂	88.8	49.6	33.0	30.9
CO	6.7	0.7	0.4	0.9
C₂-C₄	0.3	1.1	2.9	3.2

Produced gas amount, mmol/litre wastewater

CH₄	0.6	40.6	220.8	283.5
H₂	5.5	130.8	267.5	347.9
CO₂	128.3	175.0	252.9	297.0
CO	9.7	2.4	3.1	1.9
C₂-C₄	0.4	3.4	22.2	30.7

Produced gas amount mol/kg organic carbon in wastewater

CH₄	0.05	3.5	19.2	24.7
H₂	0.5	11.4	23.2	30.2
CO₂	11.2	15.2	22.0	25.8
CO	0.8	0.2	0.3	0.2
C₂-C₄	0.04	0.3	1.9	2.7

CGE, %	14.5	23.7	55.5	68.7
CLE, %	74.0	59.3	25.6	14.4
Residue (tar, coke, and loss) %	9.3	12.9	15.6	15.8
TOC mg/L	8504	6819	2943	1665
COD mg O₂/L	29085	20150	8470	3620
TOC RE, %	26	41	74	86
COD RE %	9.3	37.1	75.8	88.7

Experiment Number/Code	5	6	7	8	9
Reaction Temperature, °C	300	300	300	300	300
Reaction Pressure, atm	115	95	95	110	120
Catalyst type	K ₂ CO ₃	K ₂ CO ₃	K ₂ CO ₃	K ₂ CO ₃	K ₂ CO ₃
Catalyst, g	0.125	0.250	0.375	0.500	0.625
Volume of wastewater, mL	15	15	15	15	15
Wastewater TOC, mg/L	11500	11500	11500	11500	11500
Wastewater COD, mg O₂/L	35000	35000	35000	35000	35000

Gaseous product composition, % mol

CH₄	0.5	0.6	0.8	0.9	1.0
H₂	6.3	8.2	14.2	22.2	23.3
CO₂	92.2	90.6	84.3	76.2	75.1
CO	0.6	0.4	0.5	0.5	0.4
C₂-C₄	0.4	0.2	0.2	0.2	0.2

Produced gas amount, mmol/litre wastewater

CH₄	0.9	1.3	2.2	3.3	3.6
H₂	11.7	18.4	39.0	81.3	82.8
CO₂	170.7	203.8	233.0	280.0	266.6
CO	1.1	0.9	1.3	1.8	1.1
C₂-C₄	0.7	0.4	0.5	0.7	0.7

Produced gas amount mol/kg organic carbon in wastewater

CH₄	0.08	0.1	0.2	0.3	0.3
H₂	1.0	1.6	3.4	7.1	7.2
CO₂	14.8	17.7	20.2	24.3	23.2
CO	0.1	0.07	0.1	0.16	0.1
C₂-C₄	0.06	0.04	0.04	0.06	0.06

CGE, %	17.7	21.6	23.9	29.8	29.0
CLE, %	66.9	64.2	58.8	50.8	50.7
Residue (tar, coke, and loss) %	13.4	14.6	16.2	17.8	18.2
TOC mg/L	7685	7372	6760	5834	5828
COD mg O₂/L	31915	28900	28620	28180	28310
TOC RE, %	33.2	35.9	41.2	49.2	49.3
COD RE %	8.81	17.4	18.2	19.5	19.1

Experiment Number	10	11	12	13	14
Reaction Temperature, °C	400	400	400	400	400
Reaction Pressure, atm	255	260	240	235	230
Catalyst type	K ₂ CO ₃	K ₂ CO ₃	K ₂ CO ₃	K ₂ CO ₃	K ₂ CO ₃
Catalyst, g	0.125	0.250	0.375	0.500	0.625
Volume of wastewater, mL	15	15	15	15	15
Wastewater TOC, mg/L	11500	11500	11500	11500	11500
Wastewater COD, mg O₂/L	35000	35000	35000	35000	35000

Gaseous product composition, % mol

CH₄	14.9	15.6	16.2	16.5	16.4
H₂	42.9	44.6	46.8	49.1	49.4
CO₂	41.0	38.5	35.1	32.4	32.3
CO	0.4	0.3	0.3	0.3	0.2
C₂-C₄	0.8	1.0	1.6	1.7	1.7

Produced gas amount, mmol/litre wastewater

CH₄	68.2	75.4	85.5	105.4	107.0
H₂	196.6	215.6	247.0	307.3	322.4
CO₂	187.9	185.4	185.3	207.0	210.8
CO	1.8	1.4	1.6	1.9	1.3
C₂-C₄	3.7	4.8	8.5	10.9	11.1

Produced gas amount mol/kg organic carbon in wastewater

CH₄	5.9	6.6	7.4	9.2	9.3
H₂	17.1	18.7	21.5	26.7	28.0
CO₂	16.3	16.1	16.1	18.0	18.3
CO	0.16	0.1	0.13	0.16	0.1
C₂-C₄	0.3	0.4	0.7	0.9	1.0

CGE, %	27.9	28.8	30.1	35.7	36.2
CLE, %	52.0	50.4	43.7	39.5	39.7
Residue (tar, coke, and loss) %	15.7	16.4	22.9	23.2	22.9
TOC mg/L	6071	5789	5020	4535	4562
COD mg O₂/L	20710	18940	19710	18445	17000
TOC RE, %	47.2	50.3	56.3	60.6	60.3
COD RE %	40.8	45.9	43.7	47.3	51.4

Experiment Number	15	16	17	18	19
Reaction Temperature, °C	500	500	500	500	500
Reaction Pressure, atm	360	355	350	355	345
Catalyst type	K ₂ CO ₃	K ₂ CO ₃	K ₂ CO ₃	K ₂ CO ₃	K ₂ CO ₃
Catalyst, g	0.125	0.250	0.375	0.500	0.625
Volume of wastewater, mL	15	15	15	15	15
Wastewater TOC, mg/L	11500	11500	11500	11500	11500
Wastewater COD, mg O₂/L	35000	35000	35000	35000	35000

Gaseous product composition, % mol

CH₄	29.6	30.5	31.2	35.4	35.6
H₂	35.3	37.8	38.6	43.4	42.8
CO₂	33.3	29.8	28.2	19.2	19.6
CO	0.3	0.2	0.2	0.1	0.1
C₂-C₄	1.5	1.7	1.8	1.9	1.9

Produced gas amount, mmol/litre wastewater

CH₄	271.3	313.5	329.3	427.7	420.3
H₂	323.5	388.4	407.4	524.4	505.2
CO₂	305.2	306.2	297.7	232.0	231.4
CO	2.7	2.1	2.1	1.2	1.2
C₂-C₄	13.7	17.4	19.0	22.9	22.4

Produced gas amount mol/kg organic carbon in wastewater

CH₄	23.6	27.3	28.6	37.2	36.5
H₂	28.1	33.8	35.4	45.6	43.9
CO₂	26.5	26.6	25.9	20.2	20.1
CO	0.2	0.18	0.18	0.1	0.1
C₂-C₄	1.2	1.5	1.7	2.0	2.0

CGE, %	64.0	69.4	70.6	74.9	74.5
CLE, %	15.2	12.1	9.9	8.4	8.6
Residue (tar, coke, and loss) %	17.9	17.1	16.9	15.7	15.5
TOC mg/L	1740	1480	1320	1230	970
COD mg O₂/L	4435	4200	4600	3870	3710
TOC RE, %	85	87	88	89	92
COD RE %	87	88	85	89	89

Experiment Number	20	21	22	23	24
Reaction Temperature, °C	600	600	600	600	600
Reaction Pressure, atm	425	445	450	425	442
Catalyst type	K ₂ CO ₃	K ₂ CO ₃	K ₂ CO ₃	K ₂ CO ₃	K ₂ CO ₃
Catalyst, g	0.125	0.250	0.375	0.500	0.625
Volume of wastewater, mL	15	15	15	15	15
Wastewater TOC, mg/L	11500	11500	11500	11500	11500
Wastewater COD, mg O₂/L	32050	32050	32050	32050	32050

Gaseous product composition, % mol

CH₄	27.9	28.1	28.5	35.9	36.0
H₂	38.0	38.9	39.2	49.4	49.5
CO₂	32.0	30.8	30.0	12.1	12.1
CO	0.1	0.1	0.1	0.1	0.1
C₂-C₄	2.0	2.1	2.2	2.3	2.3

Produced gas amount, mmol/litre wastewater

CH₄	313.8	331.7	360.1	548.4	545.0
H₂	427.5	459.2	495.4	757.7	749.4
CO₂	360.0	363.6	379.2	184.8	183.1
CO	1.1	1.2	1.3	1.5	1.5
C₂-C₄	22.5	24.8	27.8	35.1	34.8

Produced gas amount mol/kg organic carbon in wastewater

CH₄	27.3	28.8	31.3	47.7	47.4
H₂	37.2	39.9	43.1	65.9	65.2
CO₂	31.3	31.6	33.0	16.1	15.9
CO	0.1	0.1	0.1	0.13	0.12
C₂-C₄	1.9	2.1	2.4	3.1	3.0

CGE, %	76.2	79.2	84.5	85.8	85.3
CLE, %	11.1	9.8	7.8	7.1	7.4
Residue (tar, coke, and loss) %	9.5	7.6	6.8	5.8	5.9
TOC mg/L	1200	1050	890	830	540
COD mg O₂/L	2855	2670	1575	1835	1715
TOC RE, %	91	91	92	93	96
COD RE %	92	92	96	95	95

Experiment Number	25	26	27	28
Reaction Temperature, °C	500	500	500	500
Reaction Pressure, atm	198	270	345	420
Catalyst type	-	-	-	-
Catalyst, g	-	-	-	-
Volume of wastewater, mL	10	12.5	15	20
Wastewater TOC, mg/L	11500	11500	11500	11500
Wastewater COD, mg O₂/L	32050	32050	32050	32050

Gaseous product composition, % mol

CH₄	23.1	25.8	28.8	31.3
H₂	40.0	38.3	34.9	34.4
CO₂	34.3	33.0	33.0	30.7
CO	0.5	0.5	0.4	0.3
C₂-C₄	2.1	2.4	2.9	3.3

Produced gas amount, mmol/litre wastewater

CH₄	202.1	211.4	220.8	234.7
H₂	350.0	313.8	267.5	258.0
CO₂	300.1	270.4	252.9	230.2
CO	4.4	4.1	3.1	2.2
C₂-C₄	18.4	19.7	22.2	24.7

Produced gas amount mol/kg organic carbon in wastewater

CH₄	17.6	18.4	19.2	20.4
H₂	30.4	27.3	23.2	22.4
CO₂	26.1	23.5	22.0	20.0
CO	0.38	0.36	0.3	0.19
C₂-C₄	1.6	1.7	1.9	2.2

CGE, %	57.7	55.9	55.5	55.1
CLE, %	24.0	24.9	25.6	28.6
Residue (tar, coke, and loss) %	14.6	15.1	15.6	16.2
TOC mg/L	2766	2866	2943	3296
COD mg O₂/L	9000	7400	6370	5400
TOC RE, %	75.9	75.1	74.4	71.3
COD RE %	71.9	76.7	80.1	83.1

Experiment Number	29	30	31	32
Reaction Temperature, °C	600	600	600	600
Reaction Pressure, atm	209	270	372	430
Catalyst type	-	-	-	-
Catalyst, g	-	-	-	-
Volume of wastewater, mL	8	10	12.5	15
Wastewater TOC, mg/L	11500	11500	11500	11500
Wastewater COD, mg O₂/L	32050	32050	32050	32050

Gaseous product composition, % mol

CH₄	24.4	26.1	27.1	29.5
H₂	43.0	41.5	38.6	36.2
CO₂	30.0	29.6	31.3	30.9
CO	0.4	0.3	0.2	0.2
C₂-C₄	2.2	2.5	2.8	3.2

Produced gas amount, mmol/litre wastewater

CH₄	274.5	282.7	274.8	283.5
H₂	483.7	449.6	391.4	347.9
CO₂	337.5	320.7	317.3	297.0
CO	4.5	3.2	2.0	1.9
C₂-C₄	24.7	27.1	28.4	30.7

Produced gas amount mol/kg organic carbon in wastewater

CH₄	23.9	24.6	23.9	24.7
H₂	42.1	39.1	34.0	30.2
CO₂	29.3	27.9	27.6	25.8
CO	0.4	0.28	0.18	0.16
C₂-C₄	2.1	2.4	2.5	2.7

CGE, %	70.8	70.3	69.4	68.7
CLE, %	11.9	12.2	12.8	14.4
Residue (tar, coke, and loss) %	12.3	12.6	12.9	13.2
TOC mg/L	1367	1406	1466	1665
COD mg O₂/L	4875	3100	3490	3950
TOC RE, %	88.1	87.8	87.2	85.6
COD RE %	84.8	90.3	89.1	87.7

Experiment Number	33	34	35	36
Reaction Temperature, °C	500	500	500	500
Reaction Pressure, atm	198	270	345	420
Catalyst type	K ₂ CO ₃	K ₂ CO ₃	K ₂ CO ₃	K ₂ CO ₃
Catalyst, g	0.333	0.416	0.500	0.666
Volume of wastewater, mL	10	12.5	15	20
Wastewater TOC, mg/L	11500	11500	11500	11500
Wastewater COD, mg O₂/L	32050	32050	32050	32050

Gaseous product composition, % mol

CH₄	25.6	31.9	35.4	39.7
H₂	46.9	45.4	43.4	40.3
CO₂	25.5	20.7	19.2	17.6
CO	0.4	0.3	0.1	0.1
C₂-C₄	1.6	1.7	1.9	2.3

Produced gas amount, mmol/litre wastewater

CH₄	344.9	412.0	427.7	441.1
H₂	631.8	586.4	524.4	447.7
CO₂	343.5	267.3	232.0	195.6
CO	5.4	3.9	1.2	1.1
C₂-C₄	21.5	22.0	22.9	25.5

Produced gas amount mol/kg organic carbon in wastewater

CH₄	30.0	35.8	37.2	38.4
H₂	54.9	50.9	45.6	38.9
CO₂	29.9	23.2	20.2	17.0
CO	0.5	0.3	0.1	0.1
C₂-C₄	1.9	1.9	2.0	2.2

CGE, %	78.0	77.0	74.9	73.1
CLE, %	7.0	7.5	8.4	10.1
Residue (tar, coke, and loss) %	10.4	12.8	15.7	15.9
TOC mg/L	799	866	966	1165
COD mg O₂/L	5225	5960	3650	3425
TOC RE, %	93.1	92.5	91.6	89.9
COD RE %	83.7	81.4	88.6	89.3

Experiment Number	37	38	39	40
Reaction Temperature, °C	600	600	600	600
Reaction Pressure, atm	197	270	355	425
Catalyst type	K ₂ CO ₃	K ₂ CO ₃	K ₂ CO ₃	K ₂ CO ₃
Catalyst, g	0.266	0.333	0.416	0.500
Volume of wastewater, mL	8	10	12.5	15
Wastewater TOC, mg/L	11500	11500	11500	11500
Wastewater COD, mg O₂/L	32050	32050	32050	32050

Gaseous product composition, % mol

CH₄	28.0	29.6	31.2	35.9
H₂	50.6	50.2	49.7	49.6
CO₂	19.2	17.9	16.8	12.1
CO	0.4	0.3	0.2	0.1
C₂-C₄	1.8	2.0	2.1	2.3

Produced gas amount, mmol/litre wastewater

CH₄	450.3	468.7	485.3	548.7
H₂	813.8	794.8	773.1	757.7
CO₂	308.8	283.4	261.3	184.8
CO	6.4	4.7	3.1	1.5
C₂-C₄	28.9	31.7	32.7	35.1

Produced gas amount mol/kg organic carbon in wastewater

CH₄	39.2	40.7	42.2	47.7
H₂	70.8	69.1	67.2	65.9
CO₂	26.9	24.6	22.7	16.1
CO	0.6	0.41	0.27	0.13
C₂-C₄	2.5	2.7	2.8	3.1

CGE, %	87.5	87.2	86.8	85.8
CLE, %	5.7	6.0	6.6	7.1
Residue (tar, coke, and loss) %	4.0	4.2	4.7	5.8
TOC mg/L	652	686	759	826
COD mg O₂/L	4190	2600	2240	1330
TOC RE, %	94.3	94.0	93.4	92.8
COD RE %	86.9	91.9	93	95.8

Experiment Number	41	42	43	44	45
Reaction Temperature, °C	500	500	500	500	500
Reaction Pressure, atm	355	360	370	360	355
Catalyst type	ORM	A1	A2	A3	A4
Catalyst, g	0.5	0.5	0.5	0.5	0.5
Volume of wastewater, mL	15	15	15	15	15
Wastewater TOC, mg/L	11500	11500	11500	11500	11500
Wastewater COD, mg O₂/L	32050	32050	32050	32050	32050

Gaseous product composition, % mol

CH₄	31.7	32.8	33.8	33.7	33.6
H₂	36.6	38.1	39.4	39.3	38.9
CO₂	28.3	25.1	22.7	22.8	23.5
CO	0.4	0.5	0.4	0.3	0.4
C₂-C₄	3.0	3.5	3.7	3.9	3.6

Produced gas amount, mmol/litre wastewater

CH₄	254.2	293.8	320.4	337.0	325.5
H₂	273.5	341.3	373.4	393.0	376.8
CO₂	217.7	224.8	215.0	228.0	227.5
CO	3.2	4.5	3.8	3.0	4.0
C₂-C₄	24.1	31.3	35.1	39.0	34.9

Produced gas amount mol/kg organic carbon in wastewater

CH₄	22.1	25.6	27.8	29.3	28.3
H₂	23.8	29.7	32.5	34.1	32.8
CO₂	18.9	19.5	18.7	19.8	19.8
CO	0.3	0.4	0.3	0.3	0.3
C₂-C₄	3.1	2.7	3.0	3.4	3.0

CGE, %	57.6	62.7	65.3	69.4	67.1
CLE, %	20.2	18.3	10.9	9.2	10.4
Residue (tar, coke, and loss) %	19.1	16.7	20.3	16.7	17.9
TOC mg/L	2125	2000	1250	1065	1201
COD mg O₂/L	7610	5630	5325	5025	5100
TOC RE, %	79.9	82.6	89.1	90.7	89.5
COD RE %	76.3	82.4	83.4	84.3	84.1

Experiment Number	46	47	48
Reaction Temperature, °C	500	500	500
Reaction Pressure, atm	365	380	360
Catalyst type	A2-1	A3-1	A4-1
Catalyst, g	0.5	0.5	0.5
Volume of wastewater, mL	15	15	15
Wastewater TOC, mg/L	11500	11500	11500
Wastewater COD, mg O₂/L	32050	32050	32050

Gaseous product composition, % mol

CH₄	32.9	31.7	31.5
H₂	38.9	39.1	38.2
CO₂	23.6	24.4	25.8
CO	0.3	0.3	0.2
C₂-C₄	4.3	4.5	4.3

Produced gas amount, mmol/litre wastewater

CH₄	318.7	320.0	311.7
H₂	376.8	395.1	378.0
CO₂	228.4	246.5	255.2
CO	2.9	3.0	2.0
C₂-C₄	41.7	45.5	42.6

Produced gas amount mol/kg organic carbon in wastewater

CH₄	27.7	27.8	27.1
H₂	32.8	34.3	32.8
CO₂	19.9	21.4	22.2
CO	0.3	0.3	0.2
C₂-C₄	3.6	3.9	3.7

CGE, %	68.3	71.3	70.5
CLE, %	13.9	14.7	17.2
Residue (tar, coke, and loss) %	15.5	11.9	11.4
TOC mg/L	1595	1685	1975
COD mg O₂/L	6550	6475	5625
TOC RE, %	86.1	85.3	82.8
COD RE %	79.6	79.8	82.4

Experiment Number	49	50	51	52
Reaction Temperature, °C	500	500	500	500
Reaction Pressure, atm	380	365	385	380
Catalyst type	B1	B2	B3	B4
Catalyst, g	0.500	0.500	0.500	0.500
Volume of wastewater, mL	15	15	15	15
Wastewater TOC, mg/L	11500	11500	11500	11500
Wastewater COD, mg O₂/L	32050	32050	32050	32050

Gaseous product composition, % mol

CH₄	32.3	32.5	32.4	32.8
H₂	38.9	39.4	39.7	38.3
CO₂	24.6	24.3	24.4	25.2
CO	0.5	0.4	0.4	0.4
C₂-C₄	3.7	3.4	3.1	3.3

Produced gas amount, mmol/litre wastewater

CH₄	289.3	297.9	307.1	304.1
H₂	348.5	361.2	376.3	355.1
CO₂	220.3	222.8	231.3	233.6
CO	4.5	3.7	3.8	3.7
C₂-C₄	32.4	31.2	29.4	30.6

Produced gas amount mol/kg organic carbon in wastewater

CH₄	25.1	25.9	26.7	26.4
H₂	30.3	31.4	32.7	30.9
CO₂	19.1	19.3	20.1	20.3
CO	0.4	0.3	0.3	0.3
C₂-C₄	2.8	2.7	2.6	2.6

CGE, %	62.3	62.9	64.2	64.5
CLE, %	12.1	11.5	10.4	13.0
Residue (tar, coke, and loss) %	24.0	22.0	22.7	21.3
TOC mg/L	1675	1325	1200	1504
COD mg O₂/L	5800	4940	5860	6240
TOC RE, %	85.4	88.5	89.6	86.9
COD RE %	81.9	84.6	81.7	80.5

Experiment Number	53	54	55
Reaction Temperature, °C	500	500	500
Reaction Pressure, atm	370	375	370
Catalyst type	B2-1	B3-1	B4-1
Catalyst, g	0.5	0.5	0.5
Volume of wastewater, mL	15	15	15
Wastewater TOC, mg/L	11500	11500	11500
Wastewater COD, mg O₂/L	32050	32050	32050

Gaseous product composition, % mol

CH₄	33.6	32.8	32.4
H₂	39.2	36.5	36.9
CO₂	22.6	26.4	26.8
CO	0.4	0.4	0.3
C₂-C₄	4.2	3.9	3.6

Produced gas amount, mmol/litre wastewater

CH₄	329.0	329.3	320.6
H₂	383.8	366.5	365.2
CO₂	221.3	265.1	265.2
CO	3.9	4.0	3.0
C₂-C₄	41.1	39.2	35.6

Produced gas amount mol/kg organic carbon in wastewater

CH₄	28.6	28.6	27.9
H₂	33.3	31.8	31.8
CO₂	19.2	23.0	23.1
CO	0.3	0.4	0.3
C₂-C₄	3.6	3.4	3.1

CGE, %	68.6	72.6	70.8
CLE, %	14.6	13.0	15.3
Residue (tar, coke, and loss) %	14.2	13.6	12.4
TOC mg/L	1675	1500	1760
COD mg O₂/L	5950	6050	5230
TOC RE, %	85.4	86.9	84.7
COD RE %	81.4	81.1	83.7

Experiment Number	56	57	58	59
Reaction Temperature, °C	500	500	500	500
Reaction Pressure, atm	365	355	355	380
Catalyst type	A1-K	A2-K	A3-K	A4-K
Catalyst, g	0.5+0.5 K ₂ CO ₃	0.5+0.5 K ₂ CO ₃	0.5+0.5 K ₂ CO ₃	0.5+0.5 K ₂ CO ₃
Volume of wastewater, mL	15	15	15	15
Wastewater TOC, mg/L	11500	11500	11500	11500
Wastewater COD, mg O₂/L	32050	32050	32050	32050

Gaseous product composition, % mol

CH₄	32.8	33.8	34.6	34.7
H₂	38.7	37.6	37.1	36.7
CO₂	25.8	26.2	25.9	26.0
CO	0.4	0.3	0.3	0.4
C₂-C₄	2.3	2.1	2.1	2.2

Produced gas amount, mmol/litre wastewater

CH₄	359.4	376.7	383.5	383.1
H₂	424.1	419.1	411.1	405.2
CO₂	282.7	292.0	287.1	287.1
CO	4.4	3.3	3.3	4.4
C₂-C₄	25.2	23.4	23.3	24.3

Produced gas amount mol/kg organic carbon in wastewater

CH₄	31.3	32.0	33.3	33.3
H₂	36.9	36.4	35.8	35.2
CO₂	24.6	25.4	24.9	24.9
CO	0.4	0.3	0.3	0.4
C₂-C₄	2.2	2.0	2.0	2.1

CGE, %	74.0	76.2	76.4	76.8
CLE, %	8.3	13.2	13.5	13.3
Residue (tar, coke, and loss) %	14.3	9.5	9.2	8.3
TOC mg/L	950	1514	1550	1539
COD mg O₂/L	6150	6390	7210	6325
TOC RE, %	91.7	86.8	86.5	86.8
COD RE %	80.8	80.1	77.5	80.3

Experiment Number	60	61	62
Reaction Temperature, °C	500	500	500
Reaction Pressure, atm	372	365	360
Catalyst type	A21-K	A31-K	A41-K
Catalyst, g	0.5+0.5 K ₂ CO ₃	0.5+0.5 K ₂ CO ₃	0.5+0.5 K ₂ CO ₃
Volume of wastewater, mL	15	15	15
Wastewater TOC, mg/L	11500	11500	11500
Wastewater COD, mg O₂/L	32050	32050	32050

Gaseous product composition, % mol

CH₄	33.9	34.5	35.5
H₂	38.7	39.6	38.9
CO₂	24.6	23.6	23.0
CO	0.4	0.3	0.3
C₂-C₄	2.4	2.0	2.3

Produced gas amount, mmol/litre wastewater

CH₄	384.9	383.8	390.5
H₂	439.4	440.5	427.9
CO₂	279.3	262.5	253.0
CO	4.5	3.3	3.3
C₂-C₄	27.2	22.2	25.3

Produced gas amount mol/kg organic carbon in wastewater

CH₄	33.4	33.3	33.9
H₂	38.2	38.3	37.2
CO₂	24.3	22.8	22.0
CO	0.4	0.3	0.3
C₂-C₄	2.3	1.9	2.2

CGE, %	76.9	73.6	74.1
CLE, %	14.0	14.4	15.8
Residue (tar, coke, and loss) %	7.9	10.0	9.8
TOC mg/L	1610	1660	1815
COD mg O₂/L	6800	5400	6875
TOC RE, %	86.0	85.6	84.2
COD RE %	78.8	83.2	78.5

Experiment Number	63	64	65	66
Reaction Temperature, °C	300	400	500	600
Reaction Pressure, atm	105	230	362	460
Catalyst type	Na ₂ CO ₃	Na ₂ CO ₃	Na ₂ CO ₃	Na ₂ CO ₃
Catalyst, g	0.5	0.5	0.5	0.5
Volume of wastewater, mL	15	15	15	15
Wastewater TOC, mg/L	11500	11500	11500	11500
Wastewater COD, mg O₂/L	32050	32050	32050	32050

Gaseous product composition, % mol

CH₄	0.8	15.6	32.4	32.9
H₂	20.4	38.7	39.1	39.4
CO₂	78.0	44.1	27.0	26.0
CO	0.5	0.4	0.2	0.1
C₂-C₄	0.3	1.2	1.3	1.6

Produced gas amount, mmol/litre wastewater

CH₄	2.7	82.3	332.9	392.0
H₂	68.0	204.2	401.8	470.6
CO₂	260.3	232.7	277.5	310.5
CO	1.3	2.1	2.1	1.2
C₂-C₄	1.0	6.3	13.4	19.1

Produced gas amount mol/kg organic carbon in wastewater

CH₄	0.2	7.2	28.9	34.2
H₂	5.9	17.8	34.9	40.2
CO₂	22.6	20.2	24.1	27.0
CO	0.1	0.1	0.1	0.1
C₂-C₄	0.08	0.6	1.2	1.7

CGE, %	27.9	35.2	67.4	78.5
CLE, %	51.9	4.1	13.9	10.1
Residue (tar, coke, and loss) %	17.8	17.1	16.5	7.7
TOC mg/L	5961	5186	1598	1165
COD mg O₂/L	26975	17575	6370	3230
TOC RE, %	48.1	54.9	86.1	89.8
COD RE %	15.8	45.2	80.1	89.9

Experiment Number	67	68	69	70
Reaction Temperature, °C	300	400	500	600
Reaction Pressure, atm	110	250	375	440
Catalyst type	NaOH	NaOH	NaOH	NaOH
Catalyst, g	0.5	0.5	0.5	0.5
Volume of wastewater, mL	15	15	15	15
Wastewater TOC, mg/L	11500	11500	11500	11500
Wastewater COD, mg O₂/L	32050	32050	32050	32050

Gaseous product composition, % mol

CH₄	0.9	15.9	33.2	33.5
H₂	21.2	43.7	44.2	44.9
CO₂	77.2	38.5	20.8	19.5
CO	0.4	0.5	0.2	0.2
C₂-C₄	0.3	1.4	1.6	1.9

Produced gas amount, mmol/litre wastewater

CH₄	3.1	99.3	378.1	474.5
H₂	74.2	273.1	503.4	636.1
CO₂	270.3	239.9	235.5	276.2
CO	1.8	3.1	2.3	2.8
C₂-C₄	1.0	8.7	18.2	26.9

Produced gas amount mol/kg organic carbon in wastewater

CH₄	0.27	8.6	32.9	41.3
H₂	6.4	23.7	43.8	55.3
CO₂	23.5	20.8	20.5	24.0
CO	0.2	0.2	0.2	0.2
C₂-C₄	0.1	0.8	1.6	2.3

CGE, %	28.9	38.0	69.2	8.6
CLE, %	50.4	41.3	12.2	7.2
Residue (tar, coke, and loss) %	18.5	18.1	17.4	6.1
TOC mg/L	5794	4741	1399	832
COD mg O₂/L	27900	22550	6925	2875
TOC RE, %	49.6	58.8	87.8	92.8
COD RE %	12.9	29.6	78.4	91

Experiment Number	71	72	73	74
Reaction Temperature, °C	300	400	500	600
Reaction Pressure, atm	110	235	355	425
Catalyst type	K ₂ CO ₃	K ₂ CO ₃	K ₂ CO ₃	K ₂ CO ₃
Catalyst, g	0.5	0.5	0.5	0.5
Volume of wastewater, mL	15	15	15	15
Wastewater TOC, mg/L	11500	11500	11500	11500
Wastewater COD, mg O₂/L	32050	32050	32050	32050

Gaseous product composition, % mol

CH₄	0.9	16.5	35.4	35.9
H₂	22.2	49.1	49.4	49.6
CO₂	76.2	32.4	13.2	12.1
CO	0.5	0.3	0.1	0.1
C₂-C₄	0.2	1.7	1.9	2.3

Produced gas amount, mmol/litre wastewater

CH₄	2.6	114.5	452.3	548.7
H₂	64.0	341.0	631.2	757.7
CO₂	203.4	225.0	168.7	184.8
CO	1.3	2.1	1.3	1.5
C₂-C₄	0.5	11.8	24.2	35.1

Produced gas amount mol/kg organic carbon in wastewater

CH₄	0.2	9.9	39.3	47.7
H₂	5.6	29.6	54.9	65.9
CO₂	17.7	19.6	14.7	16.1
CO	0.1	0.18	0.1	0.13
C₂-C₄	0.04	1.0	2.1	3.1

CGE, %	29.4	38.7	71.2	85.8
CLE, %	50.8	39.4	9.2	7.1
Residue (tar, coke, and loss) %	18.5	18.4	18.2	5.8
TOC mg/L	5834	4528	1066	826
COD mg O₂/L	28180	22710	4435	2835
TOC RE, %	49.2	60.6	90.7	92.8
COD RE %	19.5	29.1	86.2	91.2

Experiment Number	75	76	77	78
Reaction Temperature, °C	300	400	500	600
Reaction Pressure, atm	98	240	370	415
Catalyst type	KOH	KOH	KOH	KOH
Catalyst, g	0.5	0.5	0.5	0.5
Volume of wastewater, mL	15	15	15	15
Wastewater TOC, mg/L	11500	11500	11500	11500
Wastewater COD, mg O₂/L	32050	32050	32050	32050

Gaseous product composition, % mol

CH₄	1.1	17.2	35.9	36.2
H₂	23.4	49.4	49.6	49.7
CO₂	74.6	31.2	12.4	11.5
CO	0.6	0.4	0.1	0.1
C₂-C₄	0.3	1.8	2.0	2.5

Produced gas amount, mmol/litre wastewater

CH₄	5.8	155.0	509.5	573.2
H₂	123.4	445.9	704.0	786.9
CO₂	393.3	281.7	176.0	182.1
CO	3.2	3.6	1.4	1.6
C₂-C₄	1.5	16.2	28.4	39.6

Produced gas amount mol/kg organic carbon in wastewater

CH₄	0.5	13.5	44.3	49.8
H₂	10.7	38.8	61.2	68.4
CO₂	34.2	24.5	15.3	15.8
CO	0.2	0.3	0.1	0.1
C₂-C₄	0.1	1.4	2.5	3.4

CGE, %	31.8	50.2	79.1	89.3
CLE, %	50.4	34.2	8.0	4.9
Residue (tar, coke, and loss) %	17.4	12.4	9.8	3.9
TOC mg/L	5794	3933	920	566
COD mg O₂/L	28700	22625	6340	4725
TOC RE, %	49.6	65.8	92.0	95.1
COD RE %	10.5	29.4	80.2	85.3

Experiment Number	79	80	81	82
Reaction Temperature, °C	500	500	500	500
Reaction Pressure, atm	350	355	385	348
Catalyst type	Raney Ni 4200	Raney Ni 2800	Activated Nickel	Nickel/Silica-Alumina
Catalyst, g	0.5	0.5	0.5	0.5
Volume of wastewater, mL	15	15	15	15
Wastewater TOC, mg/L	11500	11500	11500	11500
Wastewater COD, mg O₂/L	32050	32050	32050	32050

Gaseous product composition, % mol

CH₄	34.3	34.9	29.7	26.2
H₂	44.1	42.0	48.1	41.0
CO₂	19.1	19.6	19.4	29.6
CO	0.4	0.4	0.4	0.4
C₂-C₄	2.1	3.1	2.4	2.8

Produced gas amount, mmol/litre wastewater

CH₄	414.5	385.3	371.3	281.1
H₂	532.8	463.8	601.2	439.8
CO₂	230.8	216.4	242.5	317.5
CO	4.8	4.4	5.0	4.3
C₂-C₄	25.3	34.2	30.0	30.0

Produced gas amount mol/kg organic carbon in wastewater

CH₄	36.0	33.5	32.3	24.4
H₂	46.3	40.3	52.3	38.3
CO₂	20.0	18.8	21.1	27.6
CO	0.4	0.38	0.4	0.37
C₂-C₄	2.2	3.0	2.6	2.6

CGE, %	74.4	72.1	72.4	70.7
CLE, %	9.8	11.1	8.6	12.9
Residue (tar, coke, and loss) %	13.9	14.6	15.7	15.1
TOC mg/L	1130	1275	985	1480
COD mg O₂/L	2250	2180	2510	2725
TOC RE, %	90.2	89.9	91.4	87.1
COD RE %	92.3	93.1	92.1	91.5

APPENDIX III

The results of Wastewater "Sample 1" in BIORAD column.

Signal 1: RID1 A, Refractive Index Signal						
RetTime [min]	Type	Area [nRIU*s]	Amt/Area	Amount [ppm]	Grp	Name
6.941	MF	1.42947e4	4.84800e-3	69.30074		Cellobiose
7.586	MF	7774.59766	4.28769e-3	33.33510		Sucrose
8.726	MF	4.58904e4	5.25062e-3	240.95262		Glucose
9.307	MF	3.18179e4	3.17922e-3	101.15610		Mannose+Xylose+Galactose
9.824	MF	9882.57910	2.91233e-3	28.78135		Rhamnose
10.277	MF	1.44509e4	6.59815e-3	95.34884		Arabinose+Fructose
Totals :				568.87475		

The results of Wastewater "Sample 2" in BIORAD column

Signal 1: RID1 A, Refractive Index Signal						
RetTime [min]	Type	Area [nRIU*s]	Amt/Area	Amount [ppm]	Grp	Name
7.136		-	-	-		Cellobiose
7.507	MF	1.35701e4	4.28769e-3	58.18458		Sucrose
8.696	MF	2.55334e4	5.25062e-3	134.06593		Glucose
9.278	MF	4.02518e4	3.17922e-3	127.96932		Mannose+Xylose+Galactose
9.811	MF	1.69760e4	2.91233e-3	49.43981		Rhamnose
10.315	MF	1.88129e4	6.59815e-3	124.13007		Arabinose+Fructose
Totals :				493.78971		

The results of Wastewater "Sample 1" in MACHEREY NAGEL column

Signal 1: RID1 A, Refractive Index Signal						
RetTime [min]	Type	Area [nRIU*s]	Amt/Area	Amount [ppm]	Grp	Name
16.898		-	-	-		Sucrose+Cellobiose
19.706	MM	2.50360e4	2.35361e-3	58.92490		Glucose
21.190	MM	1.25134e4	2.34109e-3	29.29505		Xylose
23.263	MF	8.75842e4	2.24812e-3	196.90018		Galactose
23.911	FM	3.14952e5	3.04045e-3	957.59552		Rhamnose
26.100	MF	6259.18799	1.93034e-3	12.08235		Arabinose
26.244	FM	1.57269e4	2.54782e-3	40.06930		Mannose
27.919		-	-	-		Fructose
Totals :				1294.86730		

The results of Wastewater "Sample 1" in MACHEREY NAGEL column

Signal 1: RID1 A, Refractive Index Signal						
RetTime [min]	Type	Area [nRIU*s]	Amt/Area	Amount [ppm]	Grp	Name
16.898		-	-	-		Sucrose+Cellobiose
19.778	MF	1.35252e5	2.35361e-3	318.33050		Glucose
21.233	FM	1.53595e4	2.34109e-3	35.95810		Xylose
22.615	MF	2.21789e4	2.24812e-3	49.86099		Galactose
24.019	MF	8.20080e4	3.04045e-3	249.34080		Rhamnose
25.877	MF	2.06795e4	1.93034e-3	39.91836		Arabinose
26.251	FM	3.26090e4	2.54782e-3	83.08173		Mannose
27.919		-	-	-		Fructose
Totals :				776.49048		

